evaluated. The program staff is using both raster and vector-based geographic information systems in the work.

Data layers which are currently included in the GIS include:

- A land-use and land-cover dataset (generated from manual interpretation of Landsat TM imagery and inputted to the database by coordinate digitizing);
- Topography in the form of digital elevation model (DEM) data acquired in standard 1-degree-by-1-degree blocks from the USGS; and
- Paved roads, approximate urban area boundaries, county boundaries, national forest areas and wildlife preserve areas. These themes were coordinate-digitized from the 1:250,000 clear plastic topographic sheets which are used as the base maps for the database.

The results of the initial work on the project demonstrate that a geographic information system is an efficient and effective tool for compiling and analyzing the large amount of disparate environmental data that is relevant to condor habitat. An interactive GIS is the only method currently available that can be used for predictive habitat modeling for the condor and for other rare, threatened, and endangered species within California.

12.7 Municipal GIS

San Bernardino Country, California, has developed a centralized facility for geographic information and processing. The following was kindly provided by Craig Gooch, manager of the Geographic Information Management System (GIMS), County of San Bernardino. A core group of GIS experts in GIMS, supported by staff from the County Office of Management Services, provides applications support, product generation, facilities management, and trouble shooting for a wide range of users. This centralized service is the result of a number of recent trends, including the need for improved productivity and service to the public, increasing demands for geographic information and analysis, and a desire to minimize redundancy and cost.

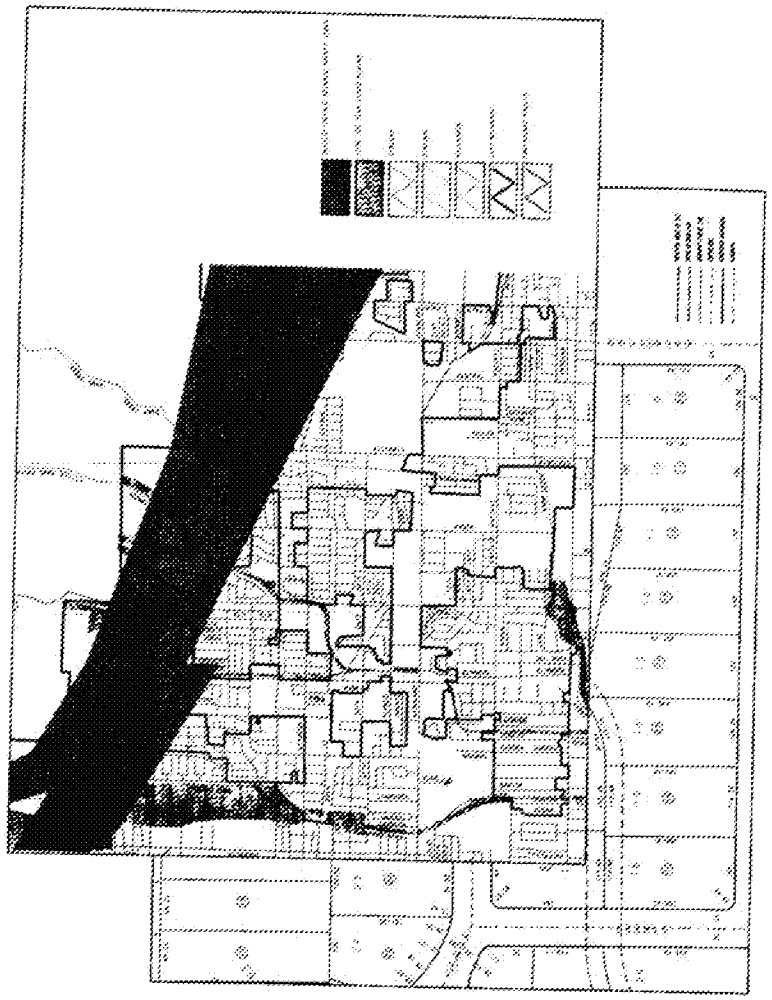


Figure 12.2 Centralized Municipal GIS.

1541
Pictometry EX2002 (Part 7 of 13)
Roofr v. Pictometry
IPR2023-00436

The heart of the centralized repository of geographic information for the county is composed of three parts: survey control throughout the county, parcel boundaries, and a comprehensive street network. The primary survey network was developed from satellite positioning techniques, which are supplemented by photogrammetric methods and conventional survey records. The California State Plane coordinate system, based on the 1983 North American Datum, is the plane of reference for position information.

Manual assessor maps are the second element, and they have been digitized and corrected for errors. Standards are used so that placement and size of text as well as line symbology is consistent. Finally, the street network is stored as a set of street centerlines, with attached attributes to identify the street name, range of addresses for each street segment, and city and zip code. These two components, storing the parcel and street base for the county, form the basis for all subsequent GIS applications.

The GIMS users cover a wide range of municipal services and agencies. The Assessor office uses GIMS for parcel map production. The Registrar of Voters will use GIMS for voter and precinct management. County schools have active systems for analyzing attendance and developing pupil transportation plans. The county's Environmental Health agency has hazardous waste management and groundwater analysis applications. New applications are being developed for pavement management. In addition, a number of cities within the counties have cooperative data and analysis programs with GIMS.

To supplement these kinds of applications, a number of services are provided through GIMS, including applications development, training, system and user documentation, and database management (such as the development of access policies, development and administration of database standards, and quality control functions). Figure 12.2 shows examples of the some of the output products which are available from GIMS, including parcel maps and thematic maps showing flood and earthquake hazards.

12.3 Agricultural Production Modeling

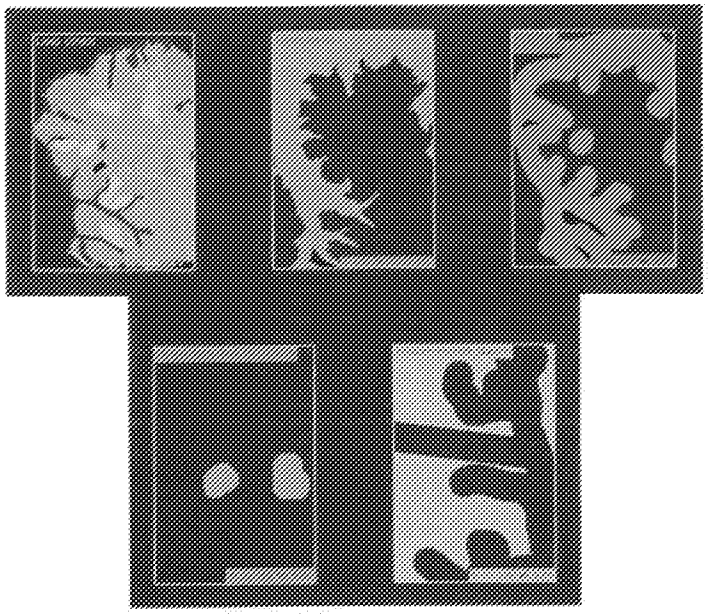
The administrative bodies of Regione del Veneto in northern Italy has instituted a cooperative research program with the University of California. The goal of this program is to develop regional crop determination procedures and production and yield estimation techniques to support agricultural



PLATE 1
Color infrared aerial photograph. (Courtesy of author.)

PLATE 3
Proposed dam site placement. This graphic demonstrates the use of three-dimensional graphics for site selection and analysis. (Image analysis by ERDAS, Inc., Atlanta, Georgia.)

PLATE 4
Master planning. This graphic shows the data layers and routes of exclusion for a proposed hospital development. (Courtesy of Intergraph Corporation, Huntsville, Alabama.)



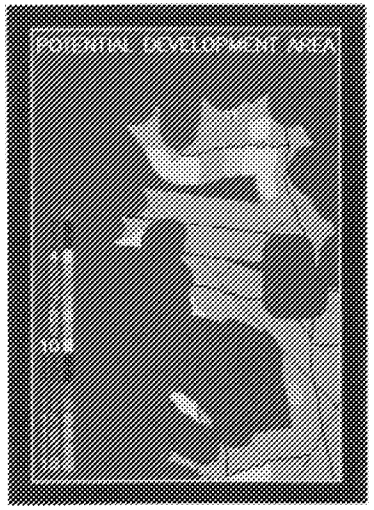


PLATE 4
Waste site selection. The important characteristics for selecting a site for waste disposal are joined with Boolean operators to create a map of appropriate locations for the site. (Courtesy of John R. Jensen.)

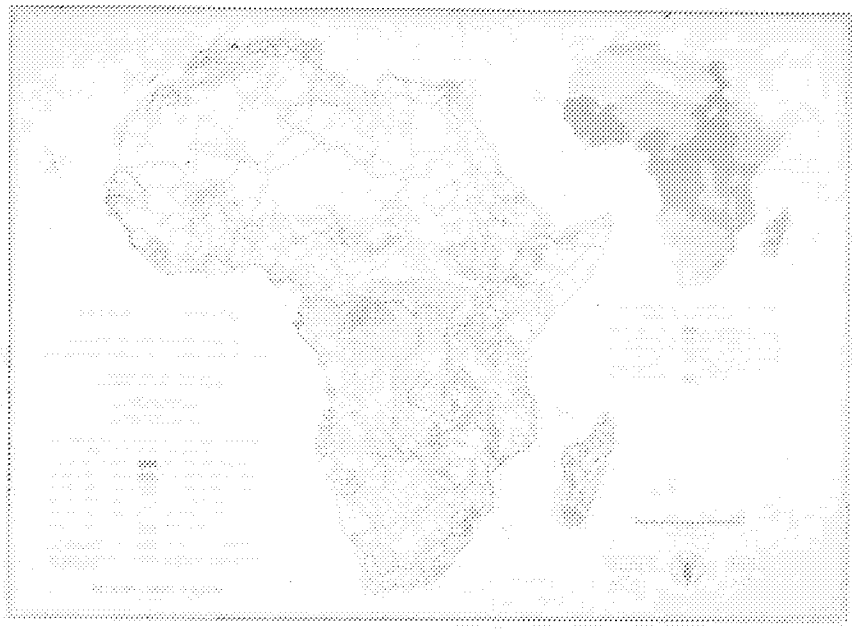


PLATE 5
African water resources. Many data sources were fused to create thematic maps of irrigation and water resource potential. (© Copyright 1992, Environmental Systems Research Institute, Inc. Used with permission.)



PLATE 6
Raster/vector data for map update. Raster datasets from satellite observations are merged to update vector map data. (Image analysis by ERDAS, Inc., Atlanta, Georgia.)

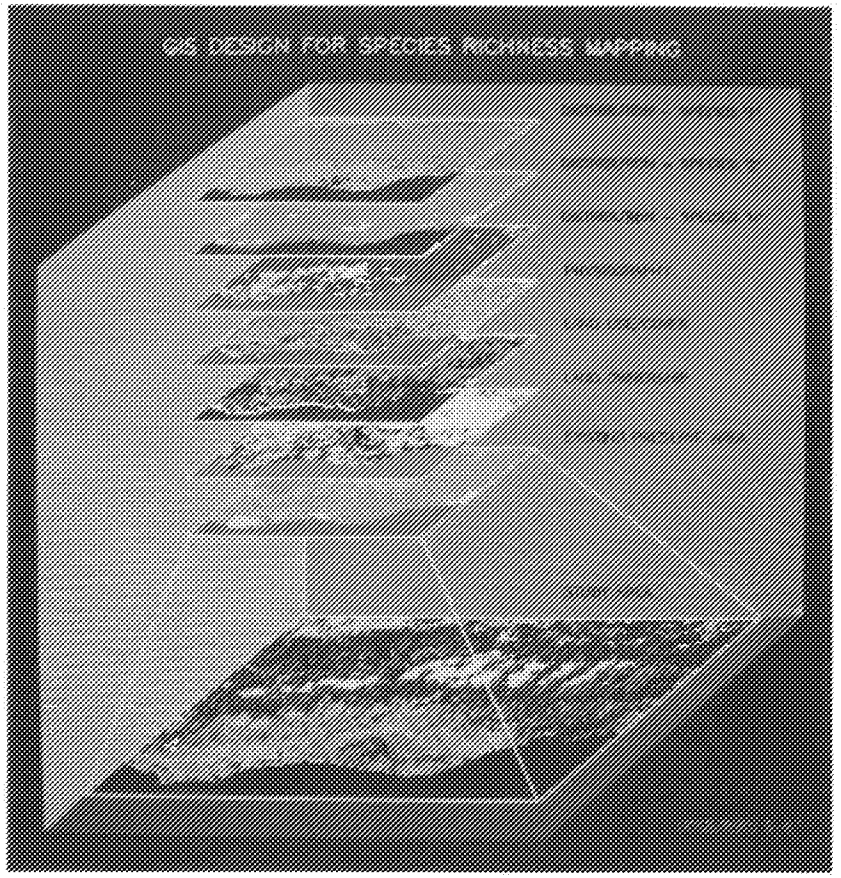


PLATE 7
California Condor database. This graphic comes from an analysis of observations of Condor activities as compared to site characteristics. (Courtesy of author.)

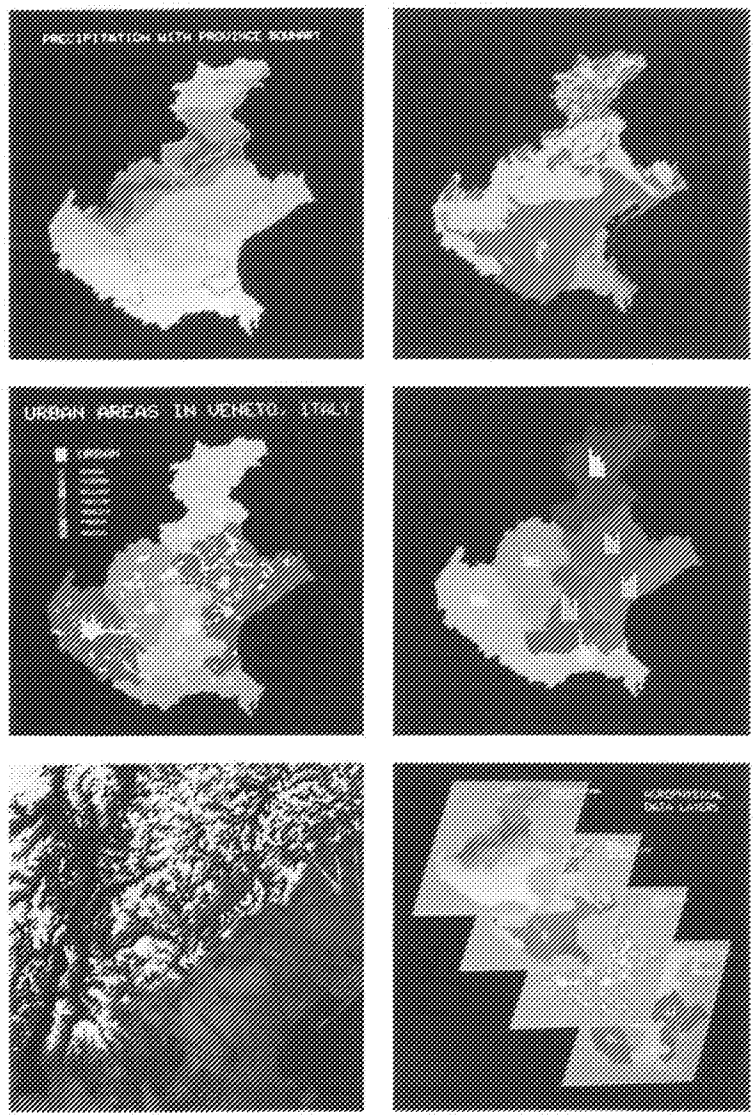


PLATE 8
Agricultural production modeling. Information about local characteristics, climate, and farming practices are used along with satellite observations to predict crop yield throughout the growing season. (Courtesy of author.)

resource management (Plate 8). This project is a part of an integrated environmental monitoring program being implemented for the Regione. Accurate crop yield prediction capabilities can increase the efficiency of agriculture in the Regione as well provide useful environmental data on the use of water resources and the use of chemical fertilizers and pesticides. Accurate, systematic crop inventory and yield and production estimation techniques are being developed for six principal crops grown within the Regione: small grains (wheat and barley), soybeans, sugar beets, corn, wine grapes, and orchard fruit.

Developing a system of crop inventory in this area presents some particular challenges. The Regione del Veneto contains an extremely complex mix of land uses and land covers. In addition, agricultural production in the Regione is characterized by small field sizes, a diverse crop mix, and multiple cropping in some areas.

A geographic information system format has been selected for use in compiling the large amount of environmental, economic, and agronomic data that is required for accurate crop production estimation and economic modeling. It is necessary to compile several layers of spatially referenced data for these purposes. These layers include:

- Crop classification and crop-class area maps. These will be generated yearly using multidate Landsat Thematic Mapper (TM) multispectral data and a suite of digital image-processing techniques.

- Meteorological data, including precipitation and temperature. This data is acquired in the Regione using a combination of digital and analog procedures. The data will be transferred from the Regione, reformatted (including coordinate digitizing if necessary), and inputted to the GIS. As some of this data is routinely received as point data (acquired by a group of irregularly distributed weather stations), processing is required to transform it into georeferenced area maps.

- Soils maps produced by the Regione.

- Maps of agricultural potentialities for various parts of the Regione del Veneto are produced by the Regione by combining soils, weather, and historic yield data.

Initial work in this study has demonstrated that both crop identification and crop yield modeling are data dependent. Accurate crop identification requires careful selection and timely acquisition of satellite data. Agrometeorological-based crop yield modeling is dependent upon complete and accurate historical yield and weather datasets. At this time, several efforts are proceeding in parallel. Economists are building databases of crop sales and prices. Agronomists are monitoring a series of test sites in the region to provide ground truth for crop practices such as planting and harvest dates and irrigation practices. Remote sensing specialists are developing numerical models of crop growth, to be able to identify crop types and predict yield at the end of the season based on multi-temporal satellite observations. A raster-based geographic information system forms the core of the analysis software.

12.9 KBGIS: Artificial Intelligence and Geographic Information Systems

The development of a geographic information system based on principles of artificial intelligence and data structures has been a part of ongoing research activities at the University of California, Santa Barbara. The system is called the *knowledge based geographic information system*, or KBGIS. The essence of the system is described in Smith et al. (1987b). We will briefly outline the key components of the system and will describe one or two applications.

KBGIS contains two principal databases. One, the **object database**, contains information about discrete spatial objects. It is implemented by means of *frames*, a powerful structure that allows for inheritance. For example, we may define the object *well*, which has among its attributes location and depth. When we later define a new object *water well* as a particular class of *wells*, it "inherits" characteristics of the parent. This can be a useful way to structure knowledge about spatial objects.

The second database in KBGIS is a **quad-tree**, as discussed in Chapter 4. Separate quad-trees are maintained for each thematic layer in the database. Continuous data, such as elevation, may be kept in nodes of a tree, as may categorical data, such as classes of land use. For continuous data, at coarse resolution levels of the tree, minimum and maximum values in addition to mean values may be stored, aiding search. For categorical data, at higher levels of the quad-tree, the complete list of all categories included at the

relevant smaller cells is maintained.

The system characterizes spatial objects in terms of three classes. The first class consists of pixel properties, that is, the kinds of properties stored at a single pixel in an equivalent raster GIS data layer. These include such things as the land-cover class at a location, or the elevation there. The second class of properties consists of groups of pixels. The most natural of these group properties are such things as the area, perimeter, and shape of a homogeneous area. The third class of properties involves relationships between areas. This final class includes the distance between two areas, or the direction, relative to true north, of the line connecting two areas at their closest approach.

The system is able to learn in several ways. New object definitions may be created by explicitly teaching the new object definition to the system, via a menu system. For example, the object "good place for an airport" might be defined as complex object with the following characteristics:

- a contiguous area of greater than a specified size,
- an area having a certain class of permissible land uses,
- an area located within a certain distance of a principal road, and
- an area within a predefined distance of a population center.

Of course, the relevant data layers must be loaded into the system for the system to be able to use such a definition. The definition is created at one time, and then the system may be told to **learn** examples of such a complex object by searching the quad-tree database.

Search may be guided heuristically, to minimize the costs of search. In the example above, the system can exclude all areas in the database that are not within a specified annular region around a population center, and thus can avoid searching all of the spatial data. Such a capability can make tremendous differences in the performance of a geographic information system.

Inductive learning is also implemented in the system. By inductive learning, we mean that the system can determine the general characteristics of a class of objects by studying a number of specific examples. In KBGIS, the analyst enters coordinate locations that correspond to places of interest. The system then characterizes each location in terms of the information it has about these places. The key step occurs when the system generalizes a new

object description from these known examples, and the description is consistent with the examples. Finally, the system can be asked to locate new examples of the object.

As an illustration of the inductive learning capability, the U.S. Geological Survey provided a raster dataset over the Black Hills of South Dakota and Wyoming. Layers in the dataset included surficial geology, elevation, slope, and categories of land cover. The geologists specified four coordinate locations in the dataset and a spatial window around these locations to consider as part of the site. The system was instructed to consider the four data layers above, as well as the derived characteristics of size of spatial objects, distance between objects, direction of one object from another, and containment.

After determining the specified characteristics of the spatial objects at the four sites, the system generalized the properties at the sites to determine the common characteristics of the four. In this specific example, the generalized description derived by the system was based on three spatial objects. In the vocabulary we have used in this text, these spatial objects would be (possibly complex) polygons. One object was characterized by its land cover of forests, while the other two were characterized by their surficial geologies. The system also determined size constraints on the three objects: the forest-covered region covered the entire window around the site, while the other two objects had derived minimum and maximum areas. Finally, the system determined that the two polygons characterized by their surface geology were oriented east/west of each other, and that the forest-covered region contained one of the polygons defined by surface geology (in other words, the boundaries of one were contained within the boundary of the other). This complex object description is automatically added to the system's knowledge base, and the system can then be asked to find other examples of this new object.

1548

Chapter 13

Looking Toward the Future

Applications of geographic information systems are increasing rapidly, as city, regional and environmental planners, resource managers, and the scientific community become aware of the full potential of these systems. Both science-oriented and applied-oriented users of GISs are learning that these systems can help them in many ways. They assist in focusing user's data-acquisition activities, provide a framework for improving data storage, and provide tools that can facilitate data management. GISs also provide these users with analytic and reporting capabilities (including graphic production tools) that were unheard of 20 years ago. Systems outputs in text, tabular, and graphic forms can be used to present the results of research and operational programs in a positive, easy to understand form.

Most users involved in geographic analyses want to see a map that contains information relevant to their application. Along with significant federal and state requirements for thematic products, the business community has definite thematic mapping requirements. In particular, private concerns that supply information derived from remotely sensed data have found that almost all client requirements are, to a large extent, cartographic in nature (Simonett, 1976).

To a very real extent, map accuracy is an important and unresolved issue. Assessing the accuracy of thematic maps is a difficult issue in its own right. A number of publications deal specifically with this subject (Rosenfeld et al., 1981; Rosenfeld, 1982; and Estes et al., 1984, among others). The problem is compounded in GIS applications, where data layers with differing accuracies are combined to produce a new product. Under very limited circumstances, it is possible to derive the accuracy of a resulting data layer from statements of accuracy in the original input data. In the vast majority of cases, we cannot ascertain the accuracy of the resulting data layer.

For many practical reasons, the data input to a geographic information system are simply the "best available", particularly when dealing with thematic maps as source data. The way in which errors propagate through a spatial data analysis task is an important research topic. In addition, because monitoring inherently involves change detection, and because modeling can involve the analysis of processes that can add their own variance to data, a user can readily see the importance of knowing the accuracy associated with various GIS data inputs.

Monitoring is central to environmental planning and management applications. It is of direct interest not only to federal agencies, such as the Environmental Protection Agency in the United States, but to local agencies as well. This is also true on the international level, as we move towards the era of the International Council of Scientific Unions Global Change Program, and NASA's Mission to Planet Earth. Monitoring is also central to a variety of other applications in such areas as agriculture, hydrology, and urban and regional analysis. Modeling has become increasingly important as computer technology has advanced. Advances in processing power and techniques have facilitated the use of models for the analysis of a variety of spatially distributed phenomena, from atmospheric and ocean circulation to the migration of materials through soil and groundwater.

An example of the operational use of geographic information system technology is found in a paper by Tinney and Ezra (1986). The authors bridge from use of GIS technology in the Department of Energy's Comprehensive Integrated Remote Sensing Program to a discussion of specific programmatic goals. These programmatic goals include the production of reports, maps, charts, and other visuals and computer generated products. Datasets produced by this program may be used in a wide variety of studies from site development planning to emergency response and disaster control planning. One major emphasis in this paper is the use of remotely sensed data for providing input to the Department of Energy databases.

Many of the difficult and expensive problems arising in the design and use of a GIS come from the very large and rapidly increasing volumes of data that users demand. Resource managers, scientists, city planners, and other users of digital geographic data are acquiring information from a broad range of sources. Both practical and theoretical problems develop when users attempt to integrate these datasets.

More data is also becoming available in digital formats. This will help to expand the use of GIS technology, by reducing the cost of data access and

1549

preprocessing. Agencies such as the Departments of the Interior and Commerce in the United States, as well as international organizations such as the United Nations GEMS (Global Environmental Monitoring System) and UNEP/GRID (United Nations Environment Program Global Resources Information Database) programs continue to increase the volume of their annual output of data in coded digital formats. With this increase in the volume of digital data, from a wide variety of agencies around the world, the issue of standard data formats becomes important.

The National Aeronautics and Space Administration has been a significant provider of digital datasets. Satellite digital data volume is projected to increase dramatically in the late 1990s with the launch of the Earth Observing Satellite (EOS) system. This planned polar orbiting system has projected data production volumes on the order of 1 terabyte per day. To illustrate this incredible data volume, 1 terabyte of digital data, if stored on standard IBM-format 5.25-inch floppy disks, would require 2.7 million disks, and require a shelf almost 7 kilometers long. Alternatively, using standard 1600 BPI magnetic tapes, hung on ordinary tape racks, EOS would fill a room of 900 square feet each day, for the 40,000 magnetic tapes the system may produce. Intelligent acquisition, selective storage, manipulation, and analysis of these data will require advanced geographic information systems if we are not to drown in this sea of environmental data.

NASA is of course not the only U.S. Federal agency that is creating large volumes of digital data, and is interested in facilitating the use of these datasets. At this time, an Interagency Working Group for Data on Global Change has been established within the government. One of the objectives of this group is to plan for a virtual national database by the mid-1990s. Such a data system has important implications for both current and future users of GIS technology. The implementation of such a system would provide a single point of contact for such diverse spatial datasets as demographic data from the Department of Commerce, bathymetric data from the National Oceanic and Atmospheric Administration, topographic data from the U.S. Geological Survey, and remotely sensed data from NASA sensors. Research will be needed in a number of areas to be able to develop such a system, including heterogeneous database management, network communications, security, and distributed processing.

Computer and geoprocessing technologies that support GIS operations are evolving to higher levels of capability. Computer technology, particularly in terms of hardware for data processing and storage, is advancing at a

tremendous pace. New algorithms and data structures are being developed. Overall, we have moved from an environment in which only large institutions could support GIS activities to one in which researchers and resource managers can have useful analytic, data storage, and display capabilities in the personal computer on their desk. In addition to advances in traditional computer technology, research groups around the world are looking at fields of artificial intelligence (e.g., expert systems, natural language understanding and image understanding) to make geographic information systems more efficient and more friendly to users with limited computer literacy.

Based on our work with geographic information systems, we see that growing knowledge and practical experience is providing greater capabilities, at the expense of greater complexity. This directly affects the costs of software (in terms of programming for new functions), database development, and maintenance. This complexity must be balanced against preserving flexibility to being able to incorporate new analytic models as well as new hardware over time. The underlying data models and structures in a practical system determine the efficiency of different processing functions. In addition, with the cost of data-processing systems generally decreasing (or from another perspective, the price/performance ratio decreasing), new applications are becoming economically feasible.

For those still looking for aid in selecting and implementing a GIS, Streich (1986) will be helpful. Streich states that with the basic GIS procurement process becoming more routine, environmental resource managers can pay more attention to customizing GISs to solve specific applications problems. He discusses potential problems that may arise when bringing a digital GIS into an organization. He concludes that with proper planning and good communication channels with institutions engaged in similar areas, management personnel charged with environmental protection responsibilities will be able to maximize their return on GIS technology investment. Indeed, papers such as this by Streich and another by Star, Cosentino and Foresman (1984) should be required reading for prospective developers and purchasers of GISs.

Another important lesson to remember is that as a GIS becomes an established element of the way an organization conducts its operations, it often happens that the system is found by a wider user community, with broader ranges of needs, than originally intended. As with the example of the Canadian Geographic Information System discussed in Chapter 2, care must be taken that systems do not become overwhelmed with users and find that

1550

they cannot adequately respond to the original requirements. In a sense, this problem is no different for the managers of any other data-processing or information system. Management must also face the continuous need for technology upgrades. Hardware and software improvements through time must be a specific part of system life-cycle management practice. These last comments imply that geographic information systems are not static.

By way of further general observations, we see that there are still few commercial vendors marketing fully integrated geographic information systems. The reasons for this are not all that clear. The overall complexity of the development of such systems is of a course a hindrance. A perceived lack of a current market that is sufficient to support a major development effort is also a key factor. The domain, discipline, and application-specific nature of many GISs tends to encourage the development of in-house systems, and this may also play a role. The presence of established commercials firms that already have a large market share and already provide user support in the form of systematic upgrades and documentation and training is yet another possible inhibiting factor.

Finally, the practical design and application of digital geographic information systems is a young field, and as we hope we have shown, an interdisciplinary one. Smith et al. (1987a) discuss what should be required of a GIS. A GIS should:

- be able to work with large, heterogeneous spatial databases;
- be able to query the databases about the existence, location, and characteristics of a wide variety of objects;
- operate efficiently, so that the user can work interactively with the underlying data and the required data analysis models;
- be easy to tailor to a variety of applications, as well as to many kinds of users;
- be able to "learn" in significant ways about the data and the user's objectives; and
- be able to supply a readily interpretable output product for the ultimate users of the system.

We look on this list as an entry into research topics rich in complexity and interest for a wide range of disciplines, as a set of objectives that a user might try to levee on a system's developers, and as a set of goals that a developer may strive to attain.

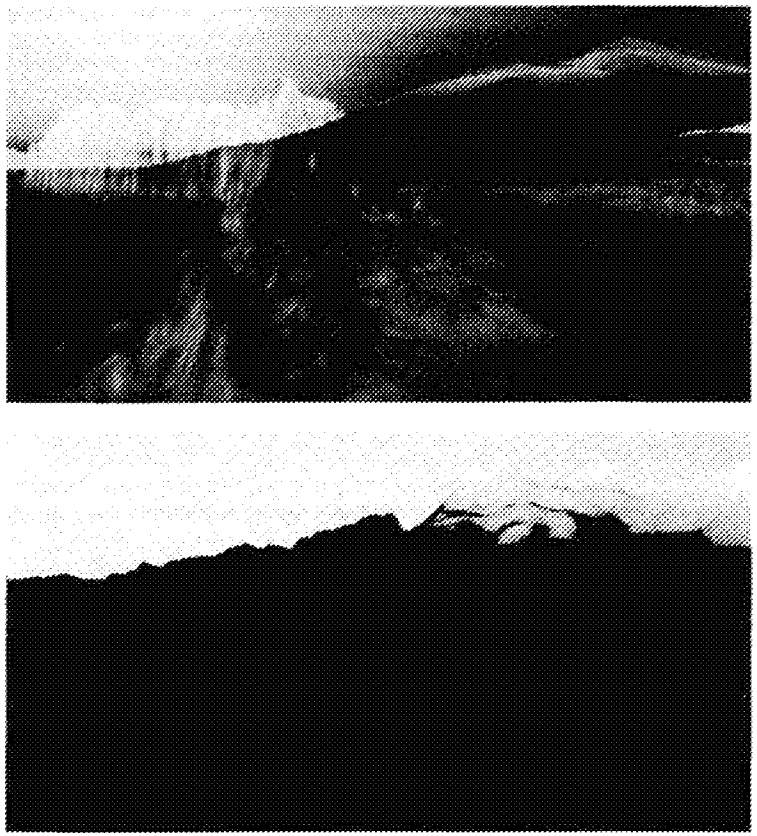


Figure 13.1 The upper figure shows a three-dimensional representation of the South American Continent, with clouds above the land surface (Courtesy J. Hall and B. Mortenson, Image Processing Laboratory, Jet Propulsion Laboratory). The lower figure is an enhanced image from a Photon Scanning Tunneling Microscope (Courtesy Biomedical and Environmental Sciences Division, Oak Ridge National Laboratory).

As we mentioned in section 1.6, scientists are interested in objects and phenomena at both the smallest and largest of scales. The images in Figure 13.1 provide a good example of these extremes. The upper part of the figure is a composite of two three-dimensional databases, to form this perspective representation looking north from Antarctica to the South American continent. The cloud data, which depicts the base of the cloud layer, is from the High Resolution Infrared Sounder on the NOAA 7 satellite. The terrain information is derived from ten-minute resolution digital elevation data from the National Center for Atmospheric Research. Total relief in this dataset is on the order of 20,000 meters. The lower part of the figure is a computer-enhanced view of a quartz microscope slide, taken by the Photon Scanning Tunneling Microscope. The mountainous structure is a residual of the polishing process; total relief in this dataset is only 200 nm. These images illustrate an important issue presented in this text: the search to discover new methods to visualize environmental elements and processes in space, from micro to macro scales.

Finally, geographic information systems technology is one more way in which we can improve our understanding of the Earth. Much recent discussion in the United States has emphasized our general lack of geographic understanding. From our admittedly biased point of view, we are convinced that an understanding of geography, in general, and processes distributed in space, in particular, is important in today's society. It is our hope that this text is a small step in the process of realizing the full potential of geographic information systems.

1551

Suggestions for Exercises

The follow are suggestions for classroom exercises. Some require access to an automated geographic information or image-processing system, while many others do not. Some require nothing more than paper and a pencil. This list is cross-referenced to the relevant chapter.

Chapter 2: Background and History

A. Inquire of your regional natural resource, forestry, or water resource agency:
What spatial datasets are kept? How are they storing this data? What base map projections and map scales are in common usage? Is there a systematic means of updating their spatial data? How long have they been doing it this way?

B. On a timeline, indicate the principal dates and accomplishments in the development of GISs. Then find key dates for the computer industry (for example, IBM's introduction of the System 360) and space exploration (for example, the U.S. Landsat program), and enter these dates and accomplishments as well.

Chapter 3: The Essential Elements of a GIS: An Overview

A. Contrast the five elements of a Geographic Information System with the equivalent elements of an employee records management system. Where are the similarities in staff roles, in hardware, and in software?

Chapter 4: Data Structures

A. With paper and pencil, roughly enlarge a local street map to a scale of approximately 1:1000.

(a) Develop a raster dataset of the transportation network:
On a light table, lay a sheet of millimeter graph paper over the enlarged street map, and mark off the cells corresponding to the center lines of the principal streets.

(b) Develop a vector dataset of the transportation network:
Lay a second sheet of millimeter graph paper over the map and draw the center lines of the roadway as a series of straight line segments. Use the cells at the end points of these straight vectors to indicate the points that might be termed nodes in a vector database.

(c) Compare the number of raster cells coded in (a) with the number of end cells required in (b).

B. Examine the arc-node data structure example in this chapter (Figure 4.12).

(a) How would you revise this example so that *all* the information in this example is stored in a raster data structure?

(b) Estimate the relative data volume of the arc-node example in comparison with your choice of raster representation.

C. If a relational or flat-file database management system is available, develop a single database which stores spatial objects. An example might be based on countries in Europe, with country name, population, and the x-y coordinates of the capital city stored in the database. Compare this simple system to the vector structures discussed in the chapter, in terms of the kinds of analysis that may be possible.

Chapter 5: Data Acquisition

A. When was the last time your national government updated the maps of your local area? (in the United States, for example, the relevant map would be a USGS 7.5-minute topographic quad sheet.)

B. Contact your local municipal planning agencies. When was the last time they revised the local land-use plans? Are aerial photographs a part of the revision process? Are automated systems in use?

C. Find an aerial photograph of a local housing development, preferably at a relatively large scale.

(a) Choose a set of land-cover classes that represent the majority of the area in this development (such as residences, gardens, roads, recreational areas, and so forth).

(b) Sample the data in the photograph by choosing random locations in the photo (via a random number table, or a computer program) and noting the apparent land-cover class at each location. Keep track of the proportions of the different classes as you increase the number of samples.

(c) How many samples seem necessary for a stable estimate of the fractional cover of the dominant land-cover classes? A plot of fractional cover versus the number of points is a good way to display the data.

(NOTE: If there are a large number of students, this exercise may be efficiently run in small groups, with the groups comparing answers at the end of the exercise.)

Chapter 6: Preprocessing

A. Programmers:

(a) Try coding a vector to raster conversion routine: read in an integer to indicate the number of points in the vector, followed by the sequence of formatted x-y data value pairs, and convert the data into a raster of specified size and scale. For an output raster of the order of a few hundred cells on a side, use an ordinary memory-based data array.

(b) What strategies might you use when the output raster is too large to contain in memory at once?

B. Everybody:

(a) Using an ordinary photocopy machine, duplicate two adjacent maps from a well-known small-scale map series (1:250000, for

example). Mechanically match the edges as well as you can, and tape the edges together.

(b) For ten of the features that span the boundary (such as contour lines, roads, water bodies and so forth), estimate the worst mismatch of the features along the boundary, in both millimeters on the map and in meters on the ground

(c) Try and quantify the size of the errors you have created at the boundary by calculating the *Root Mean Square Error*: estimate the mismatch, in terms of meters on the ground; then calculate the RMS error as follows:

$$\text{RMS Error} = \sqrt{\sum \text{of squared errors}/\text{number of measurements}}$$

C. Class project:

(a) Everybody together: from a map, determine the geodetic coordinates of a set of ten unambiguous locations: benchmarks, roadway intersections, etc. Write down the (northing-easting) tuples.

(b) Everybody separately: Set up a raster data array, each choosing different starting coordinates and cell sizes. Convert the point locations from the map to the relevant cell. Write down the list of cell locations of the objects, and convert these cell centers back to geodetic locations. Calculate the RMS error. This shows you the error inherent in converting between data structures.

(c) Everybody together: graph RMS error versus cell size. What patterns do you see?

D. If a GIS or image processing system is available:

(a) Take a small raster dataset with integer categories, such as a 100-by-100-cell array of land-cover classes, and rotate the orientation of the array clockwise by 30 degrees.

(b) Then, rotate the results counterclockwise back to the original orientation. Compare the results when using a nearest-neighbor algorithm versus a cubic convolution.

(c) Visually, how does the final dataset compare to the original? Numerically, how would you use the tools of the GIS to compare the original data to the rotated-and-then-counter-rotated data?

E. Interpolation: Obtain large scale (approximately 1:10000) topographic maps, that show areas of low relief and areas of high relief. For one low relief area and one high relief area:

(a) Locate five points, and estimate their elevations.
(b) Select a point which is in the midst of the others. Call the selected point the *test* point, and call the others *known* points.
(c) Average the elevation of the four *known* points; compare this simplest value to the elevation of the *test* point estimated from the map.
(d) Select two *known* points, that are roughly on either side of the *test* point. Using the map scale bar, estimate the distance between the *test* point and the selected *known* points.
(e) Add the distances between the *test* point and the two selected points together; call this sum *S*.
(d) For the two selected points, weight their elevation by (*S* minus the distance to the *test* point) / *S*).
(e) Add the two weighted elevations, to compute an interpolated elevation for the *test* point. Compare the resulting value to the elevation as estimated from the map.
(f) For another comparison, consider fitting a surface to the *known* data points to predict the *test* point. Use a statistics program to fit either a multiple linear regression or a second-order polynomial regression, to predict elevation as a function of *x* and *y* position. Use the *known* data points to calibrate the model, and then test its performance with the *test* point.

F. Digitizing reproducibility: A standard problem in the preprocessing phase is understanding the errors in the process of digitizing. If a GIS or CAD/CAM system is available, each student in the class may digitize a small set of features. Then each student should determine the area and perimeter of the features, the lengths of a few lines, and the relative positions of a pair of points (both displacement and direction). As a class project, plot the histograms of each of the measurements to develop a feeling for the reproducibility of the process.

Chapter 7: Data Management

A. With a ruler, measure the size of a box of ten standard personal computer floppy disks, an optical disk (a stereo CD is fine) in its case, and a standard 9-track magnetic tape. Find out the amount of data which may be stored on the floppy disks. Assume that the 9-track tape is 2400 feet long, with a useful linear data density of 2 kilobytes per inch. Assume that the optical disk holds 400 megabytes of data. Compare the volumetric data storage efficiency of the three storage mechanisms.

B. Inspect a copy of your local telephone directory.
(a) Estimate the number of bytes of data in the directory by noting the number of pages, the number of lines of text per page on a randomly selected page, and the number of characters per line from a few randomly selected lines. Assume 1 character on the page will require 1 byte for storage.
(b) How many floppy disks will it take to store the telephone directory? How many optical disks? How many magnetic tapes?

C. Find out the area of the county or municipality in which you live. Assume that we wish to store data about this geographic object in an uncompressed raster data structure with a 1-meter cell size. The themes to consider are elevation (requiring 4 bytes of storage per cell), plus one more byte each for land-use classes, population density classes, and municipal services codes. How many floppy disks would be required to store this data? How many magnetic tapes? How many optical disks?

D. Projections for NASA's Earth observing space platforms in the late 1990s suggest a data-production capability of approximately two terabytes of data per day. Calculate the length of the shelf required to hold a single day's data on floppy disks. Assume that magnetic tapes are stored reasonably efficiently, how many meters of wall space, 3 meters high, will be required to hold 1 year's data? How many meters of wall space will be required for optical disks?

Chapter 8: Manipulation and Analysis

A. Why doesn't it make sense to use a mean spatial filter on a nominal dataset? Why does it make sense to use a median filter on such data, at least in some circumstances?

B. Thematic data overlay:
- (a) Find a map of a local park or recreation area, with a map scale of approximately 1:5000 or 1:10000.
- (b) Lay a sheet of plastic over the map and sketch the trails on the plastic.
- (c) Sketch an impact boundary area around the trails on the plastic sheet, the impact area having a total width of 150 meters.
- (d) Estimate the total area affected by foot traffic on the trails, as sketched in part (c), in several ways:
  - using a random dot grid,
  - using an electronic planimeter, and
  - cutting the area out of the sheet and weighing it on a precision balance.
- (e) Compare your area estimates, and comment on sources of errors in each of the estimation techniques.

C. Examine one of the issues in interpolation.
- (a) Draw a 5-by-5 cell grid on a sheet of paper; number the cells 1 to 5 in the x and y directions.
- (b) Calculate the value of each grid cell -- call it Z -- by the following function:

$$Z = x/5 + \sin(y/2)$$

  where y is in radians.
- (c) Choose five random locations in the gridded area and estimate their locations to 1/10 of a grid unit. Either use a random number table, or a computer, or (literally) throw darts at the grid.
- (d) Using a nearest-neighbor rule, select the value from grid cell whose center is closest to each random location. Compare this value to one calculated from the equation above.
- (e) Subdivide one of the 5-by-5 grid cells into four equal smaller cells. Devise a rule for estimating the values of the four quadrants from the original large cell values, and compare them to the values calculated from the equation above.

Chapter 9: Product Generation

A. How fine a line can you create, using either a technical pen or computer plotter? Investigate the capabilities of the computer printers and plotting devices in terms of lines (or dots) per unit length and the total number of available colors or gray levels.

B. Estimate the resolving power of your eye:
- (a) On a sheet of paper, draw a set of six parallel lines 4 millimeters apart, approximately 20 to 30 mm long.
- (b) Hold the page at different distances from your eyes and estimate the distance at which you are unable to reliably distinguish the individual lines.
- (c) Based on this distance, calculate the minimum useful line spacing in terms of the angle subtended from one line, back to your eye, to the next line.
- (d) What does this tell you about a useful raster display size on a 50-by-50 centimeter sheet of paper at normal viewing distances?

C. At your local computer center, compare costs of line printer plot versus the available plotters, versus a color-film hardcopy device if available. Include in this survey the number of unique colors possible, the available sizes of finished product, and the amount of clock time required to produce an average graphic.

D. Aliased lines:
- (a) On a sheet of centimeter graph paper, draw two straight lines: one at approximately 45 degrees from the vertical, the other approximately 10 degrees from the vertical.
- (b) Darken the cells that either line crosses: thus we have converted these vectors to a raster representation, with no anti-aliasing.
- (c) On a second sheet of paper, draw the same vectors, but try and draw an anti-aliased raster, based on the discussion in Chapter 9.

(d) Attach each of these sketches to a wall. Carefully look at these two sketches from various distances from the wall, and comment on the quality of the raster-converted vectors as a function of viewing distance.

Chapter 10: Remote Sensing and GIS

A. Find out what air photographic coverage, at what scales, is available for your local area.

B. If a geographic information or image processing system is available:
   (a) Choose a single-channel raster image.
   (b) Rectify the original image to a different scale and orientation, and then rectify the image back to its original scale and orientation. For a class project, arrange that each of nearest-neighbor, bilinear, and cubic interpolations are all used for comparison.
   (c) Compare the original image to the doubly-rectified image, on a pixel-by-pixel basis, to try to detect change.
   (d) Alternatively, classify the original and doubly-rectified images separately, and perform a symbolic change detection. Comment on what differences you found in comparison to Step c.

C. If time and facilities permit, demonstrate the concept of multispectral imagery:
   (a) Mount a camera on a tripod overlooking a complex scene that includes vegetation, roads, buildings, clouds, etc. An oblique view from a window in a tall building is often good for this purpose.
   (b) Take a number of exposures of panchromatic film through a variety of different filters -- haze correcting filters, primary and secondary colors. If an infrared emulsion is available, expose this as well according to manufacturer specifications.
   (c) Print the various exposures, and try to develop spectral signatures for a variety of spatial objects in the scene.
   (d) For several types of objects, can you suggest an minimum set of spectral bands that reliably distinguish the objects?

1556

Glossary

Accuracy
Freedom from error, lack of bias, close to true values. Note that accuracy is distinct from precision.

Active System
In remote sensing, a system that provides its own source of the electromagnetic radiation to be reflected or scattered by the object being sensed. For example, radar is an *active* microwave system since the radar system emits energy which is later detected. In contrast to a *passive* system.

Algorithm
A procedure for performing a specific action. In computer software, an algorithm is a set of instructions to the computer.

Alphanumeric
Consisting of both letters and numbers.

Analog
The representation of continuous numerical quantities (voltage, current, brightness, etc.) as opposed to discrete or "digital" units.

Ancillary Data
Additional, supplemental data.

Angular Field of View
See *Field of View* (FOV).

Array Processor
A specialized computing device used with a general-purpose computer. An

array processor performs mathematical operations on rectangular arrays of data at great speed. Frequently used in image processing and signal analysis.

Automated Geographic Information System (AGIS)
A geographic information system based on digital computers.

Band
A range of wavelengths of electromagnetic radiation; synonym for the term *channel*.

Band Interleaved by Line (BIL)
A specific implementation of a multivariate raster dataset. For each line in the raster, the values of each of the variables or bands are stored in sequence, before the set for the succeeding line.

Band Interleaved by Pixel (BIP)
A specific implementation of a multivariate raster dataset. For each pixel, the values of each of the variables or bands are stored before moving on to the next pixel.

Band Sequential (BSQ)
A specific implementation of a multivariate raster dataset. The complete data array for each separate variable or band is stored independently of the other variables.

Batch Processing
A computer processing procedure that is run at one time, without operator intervention, in contrast to *interactive processing*.

Bit
In digital computing, a binary digit, the smallest element of information. Two states are possible: "one" and "zero", also called "on" and "off", or "true"and "false."

Bits Per Inch (BPI)
A measurement of linear data density on magnetic storage materials such as tape.

1557

Bits Per Second (BPS)
A measurement of the speed of data communications.

Byte
In a digital computer, a collection of 8 bits, and thus, 2^8 or 256 unique values. One byte can represent any of 256 discrete values; often as an integer between 0 and 255, or in a different system, any integer between -127 and +128.

Calibration
Determining the relationship between measurements with an instrument and standard or "known" values.

Camera
A device for recording images on a sensitized substrate, using one or more lenses to focus the light on the substrate, and a shutter to delimit the exposure.

Cartography
The science and practice of representing the features of the Earth's surface graphically.

Catalog
A collection of detailed information about whole datasets.

Cathode Ray Tube (CRT)
A device for displaying data electronically. The display surface is covered by a material that emits light when it is struck by an electron beam, which is steered by electrical signals. Used as the display device in direct-view televisions and many computer displays.

Census Tract
In the U.S., small areas averaging 4000 in population. They represent neighborhoods having similar socioeconomic characteristics and are defined in cooperation with the U.S. Bureau of the Census.

Central Processing Unit (CPU)
The part of a digital computer, that is responsible for numerical calculations and control.

Channel
In remote sensing, a specified spectral interval; also referred to as a *band*.

Coastal Zone Color Scanner (CZCS)
A multispectral sensor that flew on the Nimbus 7 satellite. The sensor was designed to register the color of ocean water as an indication of the amount of phytoplankton and other matter in the water.

Color Infrared Film (CIR)
A film emulsion with sensitivity from green through infrared. This emulsion is in common use, in part due to its sensitivity to different characteristics of live vegetation.

Computer Compatible Tape (CCT)
Magnetic tape containing data in computer-readable digital format. The most common format is termed *9-track*, for the number of parallel data recording tracks; frequently used linear data densities on the tracks are 1600 and 6250 bits per inch.

Contour Map
A topographic map that portrays relief by the use of lines indicating equal elevation. Such iso-elevation lines are termed *contour lines*.

Contrast
The differences in intensity (bright versus dark) of different parts of an image. The highest possible contrast is between black and white.

Contrast Enhancement
A procedure for artificially increasing the contrast in an image, often used to improve an analyst's ability to discern features.

Coordinate
A set of numerical quantities that designate position in a given reference system.

1558

Dataset
A collection of similarly formatted records having like information (from one or more data sources).

Dataset Granule
A segment of a dataset, such as a single image, or one or several records in some fixed time increment, or files on each of several tapes. Usually considered the smallest element of information of value to a user.

Data System
A composite of capabilities for managing data, combining functions for maintaining a data directory, catalog, and inventory, as well as accessing data.

Defense Mapping Agency (DMA)
An agency of the U.S. Department of Defense.

Digital Computer
An electronic calculating device that operates on discrete variable representations, rather than with continuous or analog values (compare with "analog computer").

Digital Elevation Model (DEM)
A raster array of elevation values.

Digital Line Graph (DLG)
A vector data type produced by the U.S. Geological Survey.

Digital Number (DN)
In remote sensing, the numerical value of a specific pixel.

Digital to Analog Converter (D/A)
A device used to convert digital computer values to analog voltages. Found in computer display systems, where the digital computer values are converted to analog signals to manipulate the electron beam in a video display.

Digitizer
A device that converts analog information into a digital form. For flat graphic material, a digitizer can be either *flatbed* or *scanning*. For analog signals, a

digitizer consists of a digital-to-analog converter plus associated control and interface devices.

Directory
A collection of high-level information about whole datasets, for example, a directory could consist of dataset name, location where it is stored, and sources of further information.

Disks
A kind of direct-access storage device. Data is stored as coded areas on the face of one or more platters. With magnetic materials, flux changes are used to code for bits; with optical materials, changes in the refraction or reflection of light are used. Platters may have a data surface on one or both sides. The concentric circles of data on a platter are called tracks. These platters rotate rapidly and each bit of data is available to the reading/writing head once per revolution, providing high-speed random data access.

Dual Independent Map Encoding (DIME)
A form of vector data structure.

Easement
A restriction on land use. For example, an easement may prohibit a landowner from construction that would prevent emergency vehicles from gaining access to the property.

Electromagnetic Radiation
Energy propagating through space or matter in the form of waves of interacting electric and magnetic fields. Radio waves and light are examples of electromagnetic radiation.

Electromagnetic Spectrum
The range of wavelengths of known electromagnetic radiations, including ultraviolet radiation, visible radiation, infrared radiation, and microwaves.

End of File (EOF)
A specific computer code used to indicate the end of a dataset.

1559

False Color Composite
An image formed by assigning colors arbitrarily to two or more black-and-white images of a single scene. The resulting image pinpoints differences and similarities between the original images; the input data frequently comes from the different wavelength bands of a multispectral sensor.

Field of View (FOV)
The solid angle through which an instrument is sensitive to radiation.

Footprint
The area on the surface being investigated by a remote sensing device; it is approximately given by the product of the beam width (in radians) times the altitude of the remote sensing platform.

Format
The physical organization of data elements within a dataset.

Fortran
A commonly used high-level algebraic language for coding computer algorithms; derived from FORmula TRANslation.

Geographic Information System (GIS)
The complete sequence of components for acquiring, processing, storing, and managing spatial data.

Geostationary Satellite
A satellite orbiting above the earth's equator at an altitude of approximately 36,000 km, such that its period of revolution about the Earth matches the Earth's rotational period. Thus, the satellite continuously views the same portion of the Earth's surface. Also called *geosynchronous satellite*.

Ground Truth
Information obtained on the ground, at the same time a remote sensing system is acquiring data from the same location. Ground truth is normally considered the most accurate available, and is used to interpret and calibrate remotely sensed observations.

Hardware
The physical components of a computer: central processing unit, memory, disk storage, tape drives, etc.

High-Density Digital Tape (HDDT)
An analog system for storing very high rate data that is not directly compatible with general-purpose computer systems.

High-Level Programming Language
A programming language (such as Fortran or Pascal) that is relatively close to written language or mathematics, and thus, relatively distant from the machine instructions executed by a computer.

Hotine Oblique Mercator (HOM)
A map projection, often used for data from spacecraft platforms.

Human Engineering
The design and implementation of automated and mechanical systems, taking human psychological concerns into consideration.

Image
A two-dimensional data representation. Examples include a photograph, a multispectral imaging sensor's data output, and the processed result of an aeromagnetic survey.

Image Classification
Analysis of digital image values, including one or more spatial, temporal, and spectral band relationships, to obtain categories of information about specific features.

Information
Data that has been processed for a particular use.

Instantaneous Field of View (IFOV)
For a sensing device, the area covered at a single moment, described either as the angle through which the sensor gathers radiation, or the area on the ground at a specified altitude.

1560

Integrated Geographic Information System (IGIS)
A geographic information system that includes facilities for working with remotely sensed data.

Interactive Processing
Operation of a computer system through continual, instantaneous communication between man and machine. In contrast to *batch processing*.

Interval
(1) The time between two events. (2) As a measurement scale, variables in which the distances between data values are meaningful but based on an arbitrary starting point (e.g., Celsius and Fahrenheit temperature scales).

Inter-record Gap (IRG)
The effectively empty distance between data records on magnetic tape storage.

Inventory
A collection of information about the granules of a dataset.

Land Cover
The materials covering a land surface, such as vegetation, exposed soils, and so forth.

Landsat
A series of Earth-observing satellites (originally named ERTS, for Earth Resources Technology Satellite), first launched in 1972 by NASA, that serve as platforms for several instruments, including the return beam vidicon, the multispectral scanner, and the thematic mapper.

Land Use
Human-imposed functions of a land area.

Latitude
A system for indicating location north or south of the equator, based on the minimum angle subtended between the location in question, the Earth's center, and the equator.

LIDAR
The abbreviation for *light detection and ranging*. A remote sensing system, using the interaction of light pulses with materials at a distance. Used for determining atmospheric constituents and range of distant surfaces, among other things.

Longitude
An arbitrary system for indicating location east or west, based on the angular distance around the Earth's surface from the half of a great circle passing between the north and south poles and through Greenwich, England.

Low-Level Programming Language
A programming language very close to a computer's actual instruction set, working with the essential electronic elements of the computer; in contrast to high-level language.

Magnetometer
A device for measuring magnetic fields.

Manual Classification
The manual identification of features on aerial or satellite photographs by tone, color, texture, pattern, shape, and size.

Map
Usually a two-dimensional representation of all or part of the Earth's surface, showing selected natural or man-made features or data, preferably constructed on a definite projection with a specified scale.

Maximum Likelihood Rule
A decision criterion for assisting in the assignment of features to different classes. Where there is confusion between classes, assignments are made to the class of the highest probability.

Measurement Scale
A system for quantifying observations according to predetermined rules, which define four successfully greater levels of data precision (nominal, ordinal, interval, and ratio).

1561

Medium
A physical device on which data is stored, such as a photographic product, map, or magnetic tape.

Multispectral Scanner (MSS)
Generally, a remote sensing device that records electromagnetic energy in several wavelength bands simultaneously. Specifically, a four-channel sensor carried by the Landsat series of satellites, first launched by NASA in 1972, with approximately an 80-meter IFOV.

Nadir
The point on the ground directly beneath the center of the remote sensing system.

National Science Foundation (NSF)
An independent agency of the U.S. federal government.

Nimbus
A series of Earth-observing experimental weather satellites carrying a variety of sensors. The Nimbus program was operated by the U.S. National Oceanic and Atmospheric Administration. The last of the series (Nimbus-7) was launched late in 1978.

Nominal
As a measurement scale, distinguishes things in terms of discrete categories, such as urban versus rural.

Oblique or Off-Nadir Viewing
A remote sensing system in which the observed electromagnetic radiation does not come from the vertical or nadir direction.

Operating System (OS)
The high-level administrative program running in a computer at all times. This program controls the overall operation of the computer and its tasks. Operating systems are usually hardware-specific, with the notable exception of the UNIX operating system.

Ordinal
As a measurement scale, distinguishes categories on the basis of rank by some quantitative measure (e.g., small, medium, large).

Orthophoto
A photograph that has been manipulated in such a way as to eliminate image displacement due to photographic tilt and relief.

Passive System
In remote sensing, a system that detects electromagnetic radiation that either has been emitted by the target object or has come from a natural source, such as the sun, and has been reflected or scattered by the target object. In contrast to an *active system*.

Photogrammetry
The techniques of obtaining precise measurements from images.

Pixel
Of a surface: the smallest unit whose characteristics may be uniquely determined. From *pic*ture *el*ement.

Planimetric Map
A map designed to portray the horizontal positions of features; vertical information is specifically ignored.

Platform
In remote sensing, the physical object (e.g., balloon, rocket, or satellite) that carries the instrument or sensor that makes the remote measurement.

Plotter
A device used to record information, such as graphs or maps, on paper or film. Frequently based on one or more pens that are moved over the medium under control of a computer.

Precision
The degrees of exactness with which a quantity is stated; this is directly related to the number of significant figures used in a description. A measurement that

1562

divides phenomena into 10 intervals has less precision than one that divides the same phenomena into 100 intervals.

Preprocessing
The manipulation of data to make it suitable for further analysis. Often includes geometric modifications to bring several sets of data into a common map projection and scale, as well as scaling and reclassification.

Principal Point
On an aerial photograph, the point that corresponds to the axis of the lens system; commonly taken as the exact center of the photograph.

Projection
A systematic construction of features on a plane surface to represent corresponding features on a spherical surface. These features include observable phenomena (e.g., physical and cultural features such as coastlines and highways) as well as constructs (e.g., lines to represent parallels and meridians, political boundaries, or statistical units).

Quality Assurance (QA)
Referring to procedures for ensuring that an activity meets specified accuracy and precision goals.

Radiance
The flux of radiant (electromagnetic) energy measured in power units (e.g., watts).

Radiometer
A passive device for intercepting and quantitatively measuring electromagnetic radiation in a band of wavelengths.

Ratio
As a measurement scale, distinguishes things on the basis of magnitudes, such as length or age, where the multiplication and division of values have meaning, since the starting location (or zero-point) is not arbitrary.

Rectification
The process of projecting data onto a plane to bring the geometric

characteristics of data into conformance with a known coordinate system. For example, an oblique photograph could be rectified so that the location of features on the photograph correspond with their locations on a planimetric map.

Registration
Superposition of locations on one image with the corresponding locations on a second image or map.

Remote Sensing
Obtaining information about an object or phenomenon without direct contact.

Resampling
A set of mathematical procedures for changing the geometric characteristics of spatial data. Used in the processes of rectification and registration.

Resolution
(1) An indication of the number of component parts or units in a measurement system. When considering spatially referenced data, sometimes the number of units is normalized per unit area. (2) The minimum size of a feature that can be reliably distinguished by a remote sensing system.

Scalar
A quantity with a numeric value.

Scale
The ratio of distance on a map, chart, or image to the equivalent distance on the Earth's surface.

Seasat
An Earth-observing satellite designed to gather information about the oceans. Seasat was launched by NASA in 1978, but died abruptly later in that year. Data from Seasat's synthetic aperture radar is still in common use.

Sensor
A device that gathers electromagnetic radiation or other physical data and presents it in a form suitable for obtaining information about the environment.

1563

Signal-to-Noise Ratio (S/N or SNR)
A determination that provides information about the quality of a measured value.

Signature
A set of spectral, tonal, temporal, or spatial characteristics that together serve to identify a class or feature by remote sensing.

Software
A computer program as written in a high- or low-level language.

Spatial Data
Data or information with implicit or explicit information about location.

Spatial Data Integration
The process of combining multiple spatial datasets and providing for their storage, retrieval, analysis, and display.

Spectrometer
A radiometer with a dispersive element (prism, grating, or circular interference filter) that enables characteristics of the incident radiation to be determined as a function of wavelength.

SPOT
Système Probatoire d'Observation de la Terre. A multispectral remote sensing satellite system with pointable sensors. The IFOV of the system is 20 meters in multispectral mode, and 10 meters in monochromatic mode. This French system was first launched in 1986.

Supervised Classification
Classification of data into discrete categories based on statistics developed from training sites.

Swath Width
The area on either side of a platform that is surveyed by a remote sensing instrument.

Synthetic Aperture Radar (SAR)
A radar system based on a series of elemental antenna units or sequences of observations from a single antenna, from which the effective antenna is mathematically constructed through signal processing. Such a system permits scanning of the signal through space without the need for moving antenna parts.

Tag
A descriptive element in a database. A database field such as "UPDATED=01/10/88" is composed of a tag to indicate the meaning of the data that follow, and the data itself (in this case, a date).

Thematic Mapper (TM)
A seven-channel, 30-meter IFOV multispectral scanner, designed for monitoring Earth resources. Flown by NASA on the Landsat 4 and 5 platforms.

Topography
The collective features of the surface of the Earth, including relief, hydrography, and cultural features.

Training Sites
Recognizable areas on an image with distinct spectral reflectance or other properties useful for identifying other similar areas.

Tuple
A data element composed of more than one value. For example, geographic locations are often specified by two values: latitude and longitude. The pair of latitude-longitude is called a tuple.

Ultraviolet (UV)
Electromagnetic radiation with wavelengths of 1.5 to 400 nanometers.

Unsupervised Classification
Automated classification of data into discrete categories by grouping together similar observations without the aid of training data. Also called *statistical clustering*.

1564

Universal Transverse Mercator (UTM)
A common system for locations on the Earth's surface, based upon ground distances. A series of north-south zones are established, and locations are designated in terms of distance in meters east of the western edge of the zone, and north (or south) of the equator.

Variable
An unknown quantity. There are four essential kinds of variables: nominal, ordinal, interval, and ratio.

Vector
Generally, a quantity possessing both numerical value and direction. In terms of GIS, typically representing a boundary between spatial objects.

Video Information Communication and Retrieval (VICAR)
An image processing and raster GIS system developed by NASA's Jet Propulsion Laboratory.

Zoom Transfer Scope (ZTS)
An optical device for superimposing photographs and graphics on top of maps or other graphics, often used to update maps rapidly by direct tracing.

Abbreviations

AGIS
Automated Geographic Information System

AID
Agency for International Development

BIL
Band Interleaved by Line

BIP
Band Interleaved by Pixel

BPI
Bits Per Inch

BPS
Bits Per Second

BSQ
Band Sequential

B/W
Black and White

CBD
Central Business District

CCRS
Canada Centre for Remote Sensing

1565

CCT
Computer Compatible Tape

CIR
Color Infrared Film

CPU
Central Processing Unit

CRT
Cathode Ray Tube

CZCS
Coastal Zone Color Scanner

D/A
Digital to Analog Converter

DEM
Digital Elevation Model

DIME
Dual Independent Map Encoding

DLG
Digital Line Graph

DMA
Defense Mapping Agency

DN
Digital Number

EOF
End of File

EPA
Environmental Protection Agency

ESA
European Space Agency

FL
Focal Length

FOV
Field of View

GBIS
Geo-Based Information System

HDDT
High-Density Digital Tape

HOM
Hotine Oblique Mercator

IFOV
Instantaneous Field of View

IGIS
Integrated Geographic Information System

IRG
Inter-record Gap

MSS
Multispectral Scanner

NASA
National Aeronautics and Space Administration

NOAA
National Oceanic and Atmospheric Administration

1566

NSF
National Science Foundation

OS
Operating System

PI
Photo Interpretation or Photo Interpreter

QA
Quality Assurance

SAR
Synthetic Aperture Radar

SCA
Suitability/Capability Analysis

SNR or S/N
Signal to Noise Ratio

SPOT
Système Probatoire d'Observation de la Terre

TM
Thematic Mapper

UNESCO
United Nations Educational, Scientific, and Cultural Organization

UV
Ultraviolet

VICAR
Video Information Communication and Retrieval

ZTS
Zoom Transfer Scope

Bibliography

Allder, W.R., and A.A. Elasal, 1984. *Digital Line Graphs from 1:24,000-Scale Maps*. Circular 895-C, U.S. Geological Survey, Reston, Virginia.

Allder, W.R., A.J. Sziede, R.B. McEwen, and F.J. Beck, 1984. *USGS Digital Cartographic Data Standards: Digital Line Graph Attribute Coding Standards*. Circular 895-G, U.S. Geological Survey, Reston, Virginia.

Amidon, E.L., 1964. *A Computer-Oriented System for Assembling and Displaying Land Management Information*. U.S. Forest Service Research Paper PSW-17, Berkeley, California.

Anderson, J.M. and E.M. Mikhail, 1985. *Introduction to Surveying*. New York: McGraw-Hill Book Co.

Brooks, F.P. Jr., 1975. *The Mythical Man-Month: Essays on Software Engineering*. Reading, Massachusetts: Addison-Wesley Publishing Co.

Burgess, T.M. and R. Webster, 1980. "Optimal Interpolation and Isarithmic Mapping of Soil Properties: I. The Semi-Variogram and Punctual Kriging." *Journal of Soil Science*, Vol. 31, pp. 315-331.

Burrough, P.A., 1986. *Principles of Geographical Information Systems for Earth Resources Assessment*. Oxford: Clarendon Press.

Burt, P.J., 1980. "Tree and pyramid structures for coding Hexagonally Sampled Binary Images." *Computer Graphics and Image Processing*, Vol. 14, No. 3, pp. 271-280.

Calkins, H.W. and R.F. Tomlinson, 1977. *Geographic Information Systems: Methods and Equipment for Land Use Planning*. International Geographic Union Commission on Geographical Data Sensing and Processing. Resource and Land Investigations (RALI) Program, U.S. Geological Survey, Reston, Virginia.

Carson, R.L., 1962. *The Silent Spring*. Boston: Houghton-Mifflin Co.

Carter, J.R., 1984. *Computer Mapping: Progress in the 80's*. Washington, D.C.: Association of American Geographers.

Chang, Ning-San, 1981. *Image Analysis and Image Database Management*. Ann Arbor, Michigan: UMI Research Press.

Chin, R.T. and C.R. Dyer, 1986. "Model-based recognition in robot vision." *Computing Surveys*, Vol. 18, No. 1, pp. 67-108.

Cicone, R.C., 1977. Remote Sensing and Geographically Based Information Systems, *Proceedings of the 11th International Symposium on Remote Sensing of the Environment*, Vol. 2, p. 1130.

Colby, C.C., 1936. "Currents of Geographical Thought." *Annals AAG*, Vol. 26, pp. 1-36.

Colwell, R.N., ed., 1983. *The Manual of Remote Sensing*. Falls Church, Virginia: American Society of Photogrammetry.

Congalton, R.G., 1988. "A Comparison of Sampling Schemes Used in Generating Error Matrices for Assessing the Accuracy of MAps Generated from Remotely Sensed Data." *Photogrammetric Engineering and Remote Sensing*, Vol. 54, No. 5, pp. 593-600.

Cooke, D.F. and W.F. Maxfield, 1967. The Development of a Geographic Base File and its Uses for Mapping, *Urban and Regional Information System for Social Programs*, Proceedings of the 5th Annual Conference of the Urban and Regional Information Systems Association, pp. 207-218.

Cooke, D.F., 1987. "Map Storage on CD-ROM." *Byte Magazine*, Vol. 12, No. 8, pp. 129-138.

Coulson, R.N., L.J. Folse, and D.K. Loh, 1987. "Artificial Intelligence and Natural Resource Management." *Science*, Vol. 237, pp. 262-267.

Cowen, D.J., 1987. *GIS vs. CAD vs. DBMS: What are the Differences?* San Francisco: GIS '87, pp. 46-56.

Crapper, P.F., 1984. "An Estimate of the Number of Boundary Cells in a Mapped Landscape Coded to Grid Cells". *Photogrammetric Engineering and Remote Sensing*, Vol. 50, No. 10, pp. 1497-1503.

Dangermond, J., 1986. "CAD vs. GIS." *Computer Graphics World*, Vol. 9, No. 10, pp. 73-74.

Deuker, K.J., 1979. Land Resource Information Systems: Spatial and Attribute Resolution Issues, *Proceedings, Int. Symposium on Cartography and Computing: Auto-Carto IV*, Vol. 2, pp. 328-336.

Domaratz, M.A., C.A. Hallam, W.E. Schmidt and H.W. Calkins, 1983. *USGS Digital Cartographic Data Standards: Digital Line Graphs from 1:2,000,000-Scale Maps*. Circular 895-D, U.S. Geological Survey, Reston, Virginia.

Douglas, D.H. and A.R. Boyle, eds., 1982. *Computer Assisted Cartography and Information Processing: Hope and Realism*. Ottawa, Canada: Canadian Cartographic Association.

Doyle, F.J., 1985. "The Large Format Camera on Shuttle Mission 41-G." *Photogrammetric Engineering and Remote Sensing*, Vol. 51, No. 2, pp. 200-203.

Durfee, R.C., 1974. *ORRMIS: Oak Ridge Regional Modeling Information System*. Oak Ridge, Tennessee: Oak Ridge National Laboratory, p. 19.

Elassal, A.A. and V.M. Caruso, 1983. *USGS Digital Cartographic Data Standards: Digital Elevation Models*. Circular 895-B, U.S. Geological Survey, Reston, Virginia.

Enderle, G., K. Kansy and G. Pfaff, 1984. *Computer Graphics Programming:*

1568

GKS-The Graphics Standard. New York: Springer-Verlag.

Estes, J.E., 1984. Improved Information Systems: A Critical Need. *Proceedings 10th Int. Symp. Machine Processing of Remotely Sensed Data.* Purdue University Laboratory for Applications of Remote Sensing, pp. 2-8.

Estes, J.E., J. Scepan, L. Ritter, and H.M. Borella, 1980. *Evaluation of Low-Altitude Remote Sensing Techniques for Obtaining Site Information*. Washington, D.C.: Nuclear Regulatory Commission, NUREG/CR-3583, S-762-RE.

Fegeas, R.G., R.W. Claire, S.C. Guptill, K.E. Anderson and C.A. Hallam, 1983. *USGS Digital Cartographic Data Standards: Land Use and Land Cover Digital Data*. Circular 895-E, U.S. Geological Survey, Reston, Virginia.

Foley, J.D. and A. Van Dam, 1982. *Fundamentals of Interactive Computer Graphics*. Reading, Massachusetts: Addison-Wesley Publishing Co.

Ford, G.E. and C.I. Zanelli, 1985. "Analysis and Quantification of Errors in the Geometric Correction of Satellite Images." *Photogrammetric Engineering and Remote Sensing*, Vol. 51, No. 11, pp. 1725-1734.

Foresman, T.W., 1986. "Mapping, Monitoring and Modeling of Hazardous Waste Sites." *The Science of the Total Environment*. Vol. 56, pp. 255-264.

Freeman, H. and J. Ahn, 1984. Autonap: an Expert System for Automatic Map Name Placement. *Proc. International Symposium on Spatial Data Handling*. Zurich. Vol. 2, pp. 544-569.

Gaits, G.M., 1969. "Thematic Mapping by Computer." *Cartographic Journal*. Vol. 6, No. 1, pp. 50-68.

Gibson, L. and D. Lucas, 1982. Vector of Raster Images using Hierarchical Methods. *Computer Graphics and Image Processing*, Vol. 20, pp. 82-89.

Goetz, A.F.H., B.N. Rock, and L.C. Rowan, 1983. "Remote Sensing for Exploration: An Overview." *Economic Geology*, Vol. 78, No. 4, pp. 573-684.

Goetz, A.F.H., G. Vane, J.E. Solomon, and B.N. Rock, 1985. "Imaging Spectrometry for Earth Remote Sensing." *Science*, Vol. 228, No. 4704, pp. 1147-1153.

Goodchild, M.F., 1980. "Fractals and the Accuracy of Geographic Measures." *Mathematical Geology*. Vol. 12, No. 2, pp. 85-98.

Goodchild, M.F., 1987. "A Spatial Analytical Perspective on Geographical Information Systems." *Int. J. Geographical Information Systems*, Vol. 1, No. 4, pp. 327-334.

Goodchild, M.F. and B.R. Rizzo, 1987. "Performance Evaluation and Work-load Estimation for Geographic Information Systems". *Int. J. Geographical Information Systems*, Vol. 1, No. 1, pp. 67-76.

Green, R., 1964. *The Storage and Retrieval of Data for Water Quality Control*. Public Health Service Publication No. 1263, U.S. Department of Health, Education, and Welfare, Public Health Service. Washington, D.C.

Hansen, H., 1987. *Justification for a Management Information System*. San Francisco: GIS '87, pp. 19-28.

Hardisky, M.A., R.M. Smart, and V. Klemas, 1983. "Seasonal Spectral Characteristics and Aboveground Biomass of the Tidal Marsh Plant Spartina alterniflora. *Photogrammetric Engineering and Remote Sensing*, Vol. 49, No. 1, pp. 85-92.

Harley, J.B., B.B. Petchenik, and L.W. Towner, 1978. *Mapping the American Revolutionary War*. Urbana, Illinois: University of Illinois Press.

Hewitt, M.J. III and E.N. Koglin, 1987. *A Planning Strategy for using GIS in the assessment of Environmental Problems: A Customer's Guide*. San Francisco: GIS '87, pp. 128-147.

Jarvenpaa, S.L. and G.W. Dickson, 1988. "Graphics and Managerial Decision Making: Research Based Guidelines." *Communications of the ACM*, Vol. 31, No. 6, pp. 764-774.

1569

Jensen, J.R. and E.J. Christensen, 1986. "Solid and Hazardous Waste Disposal Site Selection using Digital Geographic Information System Techniques." *The Science of the Total Environment*, Vol. 56, pp. 265-276.

Jensen, J.R., E.W. Ramsey, H.E. Mackey Jr., E.J. Christensen, and R. R. Sharitz, 1987. "Inland Wetland Change Detection using Aircraft MSS Data." *Photogrammetric Engineering and Remote Sensing*, Vol. 53, No. 5, pp. 521-529.

Kemper, A. and M. Wallrath, 1987. "An Analysis of Geometric Modeling in Database Systems." *ACM Computing Surveys*, Vol. 19, No. 1, pp. 47-91.

Kennedy, M. and C. Guinn, 1975. *Automated Spatial Data Information Systems: Avoiding Failure*. Louisville, Kentucky: Urban Studies Center.

Kennedy, M. and C.R. Meyers, 1977. *Spatial Information Systems: Introduction*, Louisville, Kentucky: Urban Studies Center.

Knapp, E., 1978. *Landsat and Ancillary Data Inputs to an Automated Geographic Information System*, Report No. CSC/tr-78/6019. Silver Springs, MD: Computer Science Corp.

Kok, A.L., J.A.R. Blais and R.M. Rangayyan, 1987. "Filtering of Digitally Corrected Gestalt Elevation Data." *Photogrammetric Engineering and Remote Sensing*, Vol. 53, No. 5, pp. 535-538.

LeDrew, E.F. and S.E. Franklin, 1985. "The Use of Thermal Infrared Imagery in Surface Current Analysis of a Small Lake." *Photogrammetric Engineering and Remote Sensing*, Vol. 51, No. 5, pp. 565-573.

Lemmon, H., 1986. "Comax: An Expert System for Cotton Crop Management." *Science*, Vol. 233, pp. 29-33.

Lewis, J., 1985. "The Birth of EPA." *EPA Journal*, Vol. II, No. 9, United States Environmental Protection Agency, pp. 6-11.

Light, D.L., 1983. "Mass Storage Estimates for the Digital Mapping Era." *Technical Papers of the 43rd Annual Meeting of the American Congress on Surveying and Mapping*, Washington, D.C., March 1983.

Lillesand, T.M. and R.W. Kiefer, 1987. *Remote Sensing and Image Interpretation*, 2nd edition. New York: John Wiley and Sons.

Lorie, R.A. and A. Meier, 1984. "Using a Relational Database for Geographical Databases." *Geo-Processing*, Vol. 2, pp. 243-257.

MacDonald, R.B. and F.G. Hall, 1981, "Global Crop Forecasting," *Science*, Vol. 208, pp. 670-679.

MacDonald, R.B., A.G. Houston, R.P. Heydorn, D.B. Botkin, J.E. Estes and A. H. Strahler, 1981. *Monitoring Global Vegetation*, Reprint of Paper for 7th International Symposium on Machine Processing of Remotely Sensed Data. Houston, Texas: Earth Resources Sensing Division, Space and Life Science Directorate, NASA.

Males, R.M., 1977. *ADAPT-A Spatial Data Structure for Use with Planning and Design Models*, Working Papers from the Advanced Study Symposium on Topological Data Structures for Geographic Information Systems, Vol. 2, pp. 1-35.

Marble, D.F. and D.J. Peuquet, 1977. *Computer Software for Spatial Data Handling: Current Status and Future Development Needs*. Buffalo, New York: Geographic Information Systems Laboratory, State University of New York.

Marble, D.F., H.W. Calkins, and D.J. Peuquet, 1984. *Basic Readings in Geographic Information Systems*. Williamsville, New York: Spad Systems, Ltd.

Mark, D.M. and P.B. Aronson, 1984. "Scale-Dependent Fractal Dimensions of Topographic Surfaces: An Empirical Investigation, with Applications in Geomorphology and Computer Mapping." *Mathematical Geology*, Vol. 16, No. 7, pp. 671-683.

Martin, J. 1975. *Computer Data-Base Organization*. Englewood Cliffs, New Jersey: Prentice-Hall, Inc.

Martin, D. 1986. *Advanced Database Techniques*. Cambridge, Massachusetts: MIT Press.

McEwen, R.B., H.W. Calkins, and B.S. Ramey, 1983. *USGS Digital Cartographic Data Standards: Overview and USGS Activities*. Circular 895-A. U.S. Geological Survey, Reston, Virginia.

McHarg, I., 1969. *Design With Nature*. Garden City, New Jersey: Doubleday and Co.

Meynen, E., 1973. *Multilingual Dictionary of Technical Terms in Cartography*. International Cartographic Association, Commission II. Wiesbaden, West Germany: Franz Steiner Verlag GBMH.

Moik, J.G., 1980. *Digital Processing of Remotely Sensed Images*. Houston, Texas: National Aeronautics and Space Administration NASA SP431.

Monmonier, M. and G.A. Schnell, 1988. *Map Appreciation*. Englewood Cliffs, New Jersey: Prentice Hall.

Nagy, G. and S. Wagle, 1979. "Geographic Data Processing." *Computing Surveys*, Vol. 11, No. 2, pp. 139-181.

Naisbitt, J., 1984. *Megatrends*. New York: Warner Books, Inc.

Noyt-Meir, I. and R.H. Whittaker, 1977. "Continuous Multivariate Methods in Community Analysis: Some Problems and Developments." *Vegetatio*, Vol. 33, pp. 79-98.

Parent P. and R. Church, 1988. *Evolution of Geographic Information Systems as Decision Making Tools*. San Francisco: GIS '87. pp. 63-71.

Peucker, T.K. and N. Chrisman, 1975. "Cartographic Data Structures". *The American Cartographer*, Vol. 2, No. 1, pp. 55-69.

Peuquet, D.J., 1977. *Raster Data Handling in Geographic Information Systems*. Buffalo, New York: Geographic Information Systems Laboratory, State University of New York.

Peuquet, D.J., 1981a. "An Examination of Techniques for Reformatting Digital Cartographic Data. Part 1: The Raster-to-Vector Process."

Cartographica, Vol. 18, No. 1, pp. 34-48.

Peuquet, D.J., 1981b. "An Examination of Techniques for Reformatting Digital Cartographic Data. Part 2: The Vector-to-Raster Process." *Cartographica*, Vol. 18, No. 3, pp. 21-33.

Pountain, D., 1987. "Vector-To-Raster Algorithms." *Byte Magazine*, Sept. 1987, pp. 177-184.

Rice, H.C. Jr. and A.S.K. Brown (eds. and translators), 1972. *The American Campaigns of Rochambeau's Army*. Princeton, New Jersey: Princeton University Press.

Robinson, A., R. Sale and J. Morrison, 1978. *Elements of Cartography*. 4th ed. New York: John Wiley and Sons.

Robinson, B.F. and D.P. DeWitt, 1983. "Electro-Optical Non-Imaging Sensors." In *The Manual of Remote Sensing*. R.N. Colwell, ed. Falls Church, Virginia: American Society of Photogrammetry, pp. 293-333.

Rosenfeld, G.H., 1982. "Sample Design for Estimating Change in Land Use and Cover," *Photogrammetric Engineering and Remote Sensing*, Vol. 48, No.5, pp. 793-801.

Rosenfeld, G.H., K. Fitzpatrick-Lins, and H.S. Ling, 1981. "Sampling for Thematic Map Accuracy Testing." *Photogrammetric Engineering and Remote Sensing*, Vol. 48, No. 1, pp. 131-137.

Rowe, J.S., 1959. *Forest Regions of Canada*. Bulletin 123. Ottowa, Canada: Dept. Northern Affairs and Natural Resources, Forestry Branch.

Salmen, L., D.L. Mutter, and K. Burnham, 1977. *A General Design Schema for an Operational Geographic Information System for the U.S. Fish and Wildlife Service Region Six*. Fort Collins, Colorado: Western Governors Policy Office, p. 27.

Samet, H., 1985. "Data Structures for Quadtree Approximation and Compression." *Communications ACM*, Vol. 28, No. 9, pp. 973-993.

1571

Samet, H., 1984. "The Quadtree and Relate Hierarchical Data Structures." *ACM Computing Surv.*, Vol. 16, No. 2, pp. 187-260.

Sauer, C.O., 1919. "Mapping Utilization of Land." *Geographical Review*. Vol. 8., pp. 47-54.

Scott, D.S. and S. S. Iyengar, 1986. "TID: A Translation Invariant Data Structure for Storing Images." *Communications ACM*, Vol. 29, No. 5, pp. 418-429.

Shelton, R.L. and J.E. Estes, 1979. "Integration of Remote Sensing and Geographic Information Systems," *Proceedings, 13th International Symposium on Remote Sensing of Environment*. Ann Arbor, Michigan: Environmental Research Institute of Michigan, pp. 675-692.

Short, N.M., 1982. *The Landsat Tutorial Workbook: Basics of Satellite Remote Sensing*. NASA Remote Sensing Pub. 1078. Washington, D.C.: U.S. Government Printing Office.

Simonett, D.S., ed., 1976. *Applications Review for a Space Program Imaging Radar*. Santa Barbara Remote Sensing Unit, Technical Report No. 1, NASA Contract No. NAS9-14816, Johnson Space Center, pp. 6-18.

Slater, P.N., 1983. "Photographic Systems for Remote Sensing." In *The Manual of Remote Sensing*, R.N. Colwell, ed. American Society of Photogrammetry, pp. 231-291.

Smith, B. and J. Wellington, 1986. *Initial Graphics Exchange Specifications (IGES), Version 3.0*. U.S. Department of Commerce NBSIR 86-3359.

Smith, T.R., 1984. *Knowledge-Based Approaches to Spatial Data Handling Systems-Background Materials to Workshop 3*, International Geographical Union, International Symposium on Spatial Data Handling. Zurich, Switzerland.

Smith, T.R., S. Menon, J.L. Star and J.E. Estes, 1987a. "Requirements and Principles for the implementation and construction of Large-scale Geographic

Information Systems." *Int. J. Geographical Information Systems*, Vol. 1, No. 1, pp. 13-32.

Smith, T.R., D.J. Peuquet, S. Menon and P. Agarwal, 1987b. "KBGIS II: A Knowledge Based Geographic Information System." *Int. J. Geographical Information Systems*, Vol. 1, No. 2, pp. 149-172.

Snyder, J.P., 1985. *Computer-Assisted Map Projection Research*. U.S. Department of the Interior, U.S. Geological Survey Bulletin 1629. Washington, D.C.: U.S. Government Printing Office, 157 pp.

Spanner, M.A., A.H. Strahler, and J.E. Estes, 1982. "Soil Loss Prediction in a Geographic Information System Format." *16th Int. Symposium on Remote Sensing of the Environment*, Buenos Aires, Argentina.

Star, J.L., M.J. Cosentino and T.W. Foresman, 1984. "Geographic Information Systems: Questions to Ask Before It's Too Late." *Proceedings 10th Int. Symp. on Machine Processing of Remotely Sensed Data*. Lafayette, Indiana: Purdue University Lab. for Applications of Remote Sensing, pp. 194-197.

Steinitz, C.F., P. Parker and L. Jordan, 1976. "Hand Drawn Overlays: Their History and Prospective Uses." *Landscape Architecture*, Vol. 66, pp. 444-455.

Streich, T.A., 1986. *Geographic Data Processing: A Contemporary Overview*. Master's thesis, University of California, Santa Barbara, Department of Geography.

System Development Corp., 1968. *Urban and Regional Information Systems: Support for Planning in Metropolitan Areas*. Washington, D.C.

Tailor, A., A. Cross, D.C. Hogg, and D.C. Mason, 1986. "Knowledge-based Interpretation of Remotely Sensed Images." *Image and Vision Computing*, Vol. 4, No. 2, pp. 67-83.

Thompson, M.M., ed., 1966. *Manual of Photogrammetry*, 3rd edition. Falls Church, Virginia: American Society of Photogrammetry.

1572

Tinney, L.R. and C.E. Ezra, 1986. "Geographic Information Systems Applications for the United States Department of Energy's Comprehensive Integrated Remote Sensing Program." *Proc. Workshop on Geographic Information Systems for Environmental Protection*, Las Vegas, Nevada: Environmental Research Center, University of Nevada, Las Vegas, pp. 24-33.

Tobler, W.R., 1979. *Cellular Geography*, In S. Gale and G. Olsson, eds. *Philosophy in Geography*, Dordrecht, Holland: D. Riedel Publishing Company, pp. 379-386.

Tobler, W.R., 1987. "Measuring Spatial Resolution." *Proc. International Workshop on Geographic Information Systems*, in Chen, Shupeng, et al., eds. Beijing, pp. 42-48.

Tobler, W.R. and Z. Chen, 1986. "A Quadtree for Global Information Storage." *Geographical Analysis*, Vol. 18, No. 4, pp. 360-371.

Tomlinson, R.F., 1982. "Panel Discussion: Technology Alternatives and Technology Transfer." In *Computer Assisted Cartography and Geographic Information Processing, Hope, and Realism*, Douglas and Boyle, eds. Canadian Cartographic Association, Dept. of Geography, University of Ottawa, pp. 65-71.

Tucker, C.J., B.N. Holben and T.E. Goff, 1984. "Intensive Forest Clearing in Rondonia, Brazil as Detected by Satellite Remote Sensing." *Remote Sensing of Environment*, Vol. 15, pp. 255-261.

Tucker, C.J. and J.A. Gatlin, 1984. "Monitoring Vegetation in the Nile Delta with NOAA-6 and NOAA-7 AVHRR Imagery," *Photogrammetric Engineering and Remote Sensing*, Vol. 50, No. 1, pp. 53-61.

Tucker, C.J., J.R.G. Townshend and T.E. Goff, 1985. "African Land-Cover Classification Using Satellite Data." *Science*, Vol. 227, pp. 369-374.

Tufte, E.R., 1983. *The Visual Display of Quantitative Information*, Cheshire, Connecticut: Graphics Press.

Ullman, J.D., 1982. *Principles of Database Systems*, 2nd ed. Rockville, Maryland: Computer Science Press.

U.S. Department of Commerce, Bureau of the Census, 1970. *The DIME Geocoding System*, Report #4, Census Use Study. Washington, D.C.

U.S. Department of the Interior, 1984. *Map Projections for use with the Geographic Information System*. Fish and Wildlife Service FWS/OBS-84/17, Washington, D.C.: U.S. Government Printing Office.

U.S. Fish and Wildlife Service, 1977. *Comparison of Selected Operational Capabilities of Fifty-four Geographic Information Systems*. FWS/OBS 77/54, Biological Services Program. Washington, D.C.: Government Printing Office.

Van Roessel, J.W., 1987. "Design of a Spatial Data Structure using Relational Normal Forms." *Int. J. Geographical Information Systems*, Vol. 1, No. 1, pp. 33-50.

Vlcek, J. and D. King, 1983. "Detection of Subsurface Soil Moisture by Thermal Sensing: Results of Laboratory, Close Range, and Aerial Studies." *Photogrammetric Engineering and Remote Sensing*, Vol. 49, No. 11, pp. 1593-1597.

Waldrop, M.M., 1984. "Natural Language Understanding." *Science*, Vol. 224, pp. 372-374.

Webster, R. and T.M. Burgess, 1980. "Optimal Interpolation and Isarithmic Mapping of Soil Properties: III. Changing Drift and Universal Kriging." *Journal of Soil Science*, Vol. 31, pp. 505-524.

Welch, R., T.R. Jordan, and M. Ehlers, 1985. "Comparative Evaluations of the Geodetic Accuracy and Cartographic Potential of Landsat-4 and Landsat-5 Thematic Mapper Image Data." *Photogrammetric Engineering and Remote Sensing*, Vol. 51, No. 9, pp. 1249-1262.

Winkler, R.L. and W.L. Hays, 1975. *Statistics: Probability, Inference and Decision*, 2nd ed. New York: Holt, Rinehart, and Winston.

Wolfe, P.R., 1983. *Elements of Photogrammetry*, 2nd ed. New York: McGraw-Hill Book Co.

Index

Aberrations, 200
Absolute, 29, 98, 112, 120, 124
Accuracy, 16, 22, 25, 28, 57, 62, 70, 85, 88, 96, 100, 123, 124, 151, 172, 191, 207, 210, 215, 222, 225, 235, 237, 245, 246
Acquisition, 24, 27, 61, 70, 78, 120, 126, 199, 205, 217, 225, 235, 242, 247
Across-track, 203, 204
Address, 19, 51, 61, 131, 201, 219
Adjacency, 90, 142
Aerial, 2, 6, 24, 43, 62, 66, 69, 75, 96, 98, 105, 111, 114, 118, 179, 191, 193, 197, 201, 209, 211, 221, 234
Aggregation, 68, 93, 114, 144, 146, 151, 152, 153
Aircraft, 77, 106, 118, 120, 124, 145, 156, 173, 192, 198, 201, 202, 231
Albers, 101, 102
Algorithms, 31, 41, 62, 82, 84, 96, 109, 143, 151, 161, 183, 210, 211, 215, 229, 248
Aliasing, 81, 186
Altitude, 63, 105, 199, 202, 205, 208, 232
Analog, 3, 17, 20, 66, 188, 193, 211, 241
Ancillary, 22, 33, 63, 82, 107, 119, 122, 191, 192, 205, 218, 227
Animation, 179
Anti-aliasing, 187
Aperture, 123, 209
Approximation, 104, 115, 235
Arc, 52, 80, 129, 147, 164, 234
Archive, 27, 50, 63, 69, 183, 224, 229
Arc-node, 49, 52, 59, 80, 94, 129, 136, 147
Arrays, 34, 47, 77, 107, 112, 137, 147, 199, 214
Aspect, 123, 163
Astigmatism, 200
Attribute, 17, 29, 33, 41, 45, 51, 80, 93, 107, 113, 132, 143, 151, 161, 164, 175, 184, 215, 227
Autocorrelation, 71
Averaging, 42, 93, 109, 114, 116, 152
Axis, 67, 84, 88, 90, 99, 154, 197, 200, 202
Azimuthal, 99, 101

Backup, 132, 140, 170, 223
Band, 77, 196, 201, 211
Bathymetry, 168, 226, 247
Benchmark, 30, 80, 143
Bias, 59, 70, 110, 251
BIL, 78, 79
Bilinear, 107, 108, 109
Binary, 41, 46, 81, 173, 214, 234
BIP, 78
Bit, 47, 130, 186, 204, 209, 215
Bit-per-pixel, 214
Black-and-white, 67, 186, 193, 209
Boolean, 148, 170, 234
Boundaries, 4, 7, 27, 32, 39, 47, 49, 55, 58, 62, 65, 68, 80, 83, 88, 91, 93, 98, 120, 141, 145, 156, 161, 164, 175, 177, 215, 218, 230, 236, 238, 240, 244
BPI, 224, 247
Bresenham's algorithm, 186
Brightness, 77, 88, 90, 107, 114, 119, 186, 207, 213, 232
Browse, 133
BSQ, 78
Buffer, 132, 158
Byte, 186, 204

Cache, 131
Calibrate, 71, 89, 101, 116, 119, 205, 226

Caliper, 124
Camera, 63, 67, 101, 105, 118, 124, 193, 202
Campaign, 75
Cardinal, 42
Cartesian, 34, 112
Cartogram, 179
Cartography, 15, 17, 19, 22
Cell, 33, 68, 80, 93, 107, 113, 147, 151, 156, 160, 167, 170, 178, 186, 202, 222, 224, 227
Census, 18, 50, 57, 65, 68, 72, 169, 175, 182
Centroid, 141, 156, 165
Chain, 2, 10, 40, 41, 49, 90
Chart, 180, 181
Choropleth, 175, 176, 177
Chromatic, 200
Circumference, 91, 98
Classification, 16, 62, 100, 149, 171, 192, 210, 217, 227, 237, 241
Clumped, 71
Cluster, 139, 151
Collateral, 122, 192
Color, 9, 30, 67, 88, 119, 121, 175, 183, 190, 193, 196, 210, 232
Coma, 200
Compression, 41, 213, 224
Concurrency, 137
Confidence, 150, 225
Conformal, 100, 103
Conic, 99
Containment, 90, 142, 244
Contextual, 210
Contiguous, 52, 230, 243
Continuous-tone, 209
Contour, 4, 27, 33, 35, 58, 67, 164, 176, 214, 231
Convolution, 108, 160
Coordinate, 7, 15, 34, 48, 52, 57, 64, 68, 80, 89, 98, 139, 154, 236
Correlation, 118, 125, 168
Corridor, 7, 157
Cost, 42, 54, 66, 82, 86, 123, 148, 172, 201, 238, 246
Covariance, 168
Covariate, 208
Coverage, 96
Cross-tabulation, 168, 169
Cubic interpolation, 108
Cursor, 86, 88
Curvature, 106, 154
Curvilinear, 182
Cylindrical, 100

Dasymetric, 177
Database, 2, 7, 26, 49, 68, 76, 91, 110, 115, 126, 157, 165, 181, 191, 222
Datum, 33, 240
Decision-making, 2, 61, 221
Deflection, 198
Deformation, 99
Demographic, 19, 26, 50, 61, 114, 168, 182, 226, 247
Densitometer, 88
Derivative, 162
Detection, 57, 76, 93, 122, 210, 246
Dichotomous key, 122
Digital Line Graph, 55
Digitize, 86, 95, 125, 191, 212, 236
DIME, 49, 50, 51, 52, 57, 58, 142
Dimensionality, 217
Discontinuities, 97, 120
Discriminate, 186, 213
Dispersed, 71, 200
Display, 15, 57, 97, 101, 156, 170, 210, 213, 221, 248
Distance, 11, 15, 28, 34, 66, 71, 75, 99, 100, 110, 115, 116, 124, 131, 150, 158, 164, 172, 177, 187, 197, 243
Distance-weighted, 118
Distortion, 6, 81, 96, 106, 154, 186, 199
Distributions, 63, 69, 74, 121, 161, 178, 207
Dynamic-range, 17

Easement, 4, 39, 157
Easting, 111
Edge-detection, 161, 211
Efficiencies, 224
Electrostatic, 86, 183, 188
Elevation, 4, 8, 11, 27, 32, 35, 42, 58, 62, 64, 68, 70, 77, 80, 88, 93, 114, 121, 133, 139, 143, 152, 162, 172, 177, 192, 197, 200, 217, 222, 232, 238, 242, 251
Emission, 206
Emulsion, 63, 195

Encoding, 41, 49, 57, 62, 90, 93, 133, 142
Endpoints, 51, 72
Energy, 65, 160, 196, 197, 204, 208, 209, 246
Enhance, 161, 207, 212
Equal-area, 101
Equivalence, 101
Estimation, 114, 240, 241
Exclusive-OR, 149
Expectations, 211
Exponential, 128
Exposure, 188, 197, 201
Extract, 62, 65, 79, 82, 96, 169, 181, 191, 211, 218
Extrapolate, 73, 96, 228

Far-infrared, 208
Fieldwork, 191
Film, 6, 27, 63, 77, 86, 106, 118, 183, 196
Filtering, 152, 160, 207, 236
Fine-grained, 120
Fixed-length, 126

Generalization, 17, 76, 91, 151, 244
Geocoding, 20, 97, 103
Geodetic, 7, 9, 33, 43, 88, 98, 103, 107, 113, 205
Geographers, 1, 18
Geography, 1, 19, 24, 119, 251
Geometry, 30, 33, 53, 67, 103, 119, 123, 149, 198, 202, 205, 217
Geoprocessing, 19, 22, 27, 247
Georeferencing, 34, 62, 76, 88, 96, 98, 104, 109
Geostationary, 12, 202
Gradient, 171, 177
Granules, 182
Gray-scale, 183

Half-tones, 67
Hardcopy, 229
Heuristics, 167, 183
Hexagon, 38
Hierarchical, 42, 52, 59, 95, 137, 142
Higher-resolution, 46
High-pass, 161, 236
Histogram, 167, 168, 181
Homogeneity, 77
Hypotheses, 24, 75, 122, 151, 168, 182, 206
Hypsography, 55, 68, 224

Illumination, 210, 216
Imagery, 62, 85, 118, 122, 154, 183, 186, 196, 201, 206, 210, 216, 231, 238
Image-processing, 207, 211, 214, 218, 241
Independence, 130, 140
Indexing, 141
Inductive, 243
Inferences, 70, 101, 121
Infrared, 121, 160, 193, 208, 214, 251
Integer, 81, 93, 128, 152, 178
Integration, 153, 191
Integrity, 129, 140, 224
Intensity, 119, 205
Interleaved, 78
Interpolation, 76, 107, 114, 152, 156, 164, 177, 218, 226
Interpretation, 2, 4, 22, 37, 66, 119, 151, 192, 207, 210, 217, 238
Intersection, 52, 99, 147, 164
Interval, 28, 42, 74, 148, 160, 168, 177, 202, 216
Isarithmic, 177
Isolines, 172, 214

Kernel, 160
Keywords, 166
Knowledge-based, 211
Kriging, 117
Kurtosis, 167

Lambert, 101
Landcover, 156
Landform, 179
Landuse, 21
Large-format, 86
Latitude, 7, 29, 34, 63, 88, 98, 103, 106, 128, 207
Layers, 4, 7, 17, 20, 32, 42, 55, 68, 76, 143, 146, 154, 157, 168, 180, 196, 213, 222, 225, 230, 233

1575

Least-cost, 172
Least-squares, 92
Length, 7, 10, 37, 53, 67, 93, 103, 111, 118, 124, 130, 159, 165, 171, 180, 190, 197, 202, 226, 229
Lens, 67, 106, 118, 193, 200, 203
Life-cycle, 249
Light, 88, 99, 121, 150, 188, 195, 200, 216, 223, 232
Location, 7, 15, 26, 29, 33, 45, 48, 50, 55, 62, 69, 78, 80, 86, 88, 93, 103, 106, 110, 113, 119, 139, 149, 156, 165, 171, 177, 188, 203, 214, 218, 222, 242, 249
Logical, 29, 63, 126, 129, 148, 205, 217
Longitude, 7, 29, 88, 98, 103, 106, 128, 202
Look-up, 178
Lower-resolution, 46, 93
Low-altitude, 200
Low-frequency, 160
Low-order, 116, 123
Low-pass, 160, 161

Machine-assisted, 191, 196, 209
Magnetic-tape, 132
Magnification, 197
Mainframe, 142
Majority, 37, 39, 66, 93, 152, 245
Manipulation, 24, 58, 76, 130, 141, 148, 161, 163, 169, 223, 247
Manuscript, 130, 223
Man-machine, 95
Man-Month, 229
Map, 2, 11, 15, 20, 27, 30, 49, 55, 62, 85, 95, 109, 123, 129, 137, 145, 154, 172, 184, 211, 215, 223, 231, 240, 245
Map-guided, 217
Matrix, 110, 146, 217
Maximize, 72, 114, 230, 248
Mean, 11, 33, 44, 70, 115, 142, 151, 160, 167, 202, 242
Measurement, 12, 28, 72, 100, 119, 122, 164, 192, 210, 226
Media, 77, 130, 139, 174
Medial, 84
Median, 121, 161, 167
Memory, 126, 131,
Mercator, 34, 68, 99, 110, 236
Merging, 59, 76, 95, 146, 153, 191, 232, 235
Meridian, 34, 103
Metadata, 128
Microfilm, 183
Microwave, 208
Middle-infrared, 208
Milestones, 228
Minicomputer, 142
Minimization, 130
Model, 12, 20, 24, 27, 32, 36, 54, 58, 65, 68, 99, 106, 114, 124, 134, 136, 165, 172, 222, 226, 231, 234, 238
Monitoring, 8, 12, 26, 74, 192, 215, 228, 241, 246
Monochrome, 186, 188
Mosaic, 96
Multispectral, 75, 77, 107, 145, 150, 172, 183, 191, 201, 203, 206, 210, 214, 227, 241
Multivariate, 77, 149, 215

Nadir, 199
Navigational, 137, 138
Nearest-neighbor, 107
Near-infrared, 208
Neighborhood, 36, 83, 93, 115, 157
Network, 8, 33, 55, 62, 133, 158, 171, 179, 230, 233, 236, 240, 247
Nodes, 9, 43, 47, 50, 80, 95, 107, 110, 113, 129, 147, 164, 242
Nominal, 28, 41, 93, 109, 114, 134, 145, 168, 202, 205, 218
Non-parametric, 161, 168
Non-procedural, 136
Northing, 131

Oblateness, 98
Oblique, 105, 179
Off-nadir, 106
Optimizing, 79, 130, 133
Orbit, 199, 202, 203
Ordinal, 28, 93, 109, 114, 145, 160, 163, 168
Orthographic, 106
Orthophoto, 67

Output, 13, 27, 44, 60, 77, 83, 101, 107, 123, 136, 147, 156, 169, 171, 174, 177, 183, 187, 190, 217, 235, 240, 247
Overlay, 6, 20, 37, 57, 98, 123, 146, 149, 191, 231, 236
Overpass, 203

Paging, 141
Panchromatic, 206, 224, 236
Parallax, 125
Parcel, 4, 150, 159, 165, 240
Partitioned, 230
Path, 30, 83, 92, 163, 170, 198
Patterns, 2, 4, 16, 71, 90, 99, 103, 121, 151, 161, 173, 175, 177, 179, 184, 203, 207, 217, 231
Perimeter, 140, 142, 164, 180, 243
Perspective, 6, 29, 101, 106, 152, 156, 182, 199, 209, 232, 248, 251
Phosphor, 190
Photodetector, 90, 198
Photogrammetry, 19, 66, 91, 101, 119, 195
Photograph, 4, 6, 11, 67, 75, 85, 96, 105, 114, 119, 120, 124, 199
Photointerpretation, 62, 76, 118, 122, 124, 214, 234
Physiography, 114, 226, 227
Pigments, 208
Pixel, 41, 46, 78, 80, 93, 109, 150, 154, 160, 164, 172, 184, 186, 203, 207, 213, 216, 227, 236, 243
Pixel-interleaved, 78
Planar, 33
Plane, 15, 32, 38, 48, 98, 101, 116, 162, 197, 200, 240
Planimeter, 7
Planimetric, 6, 30, 67, 101, 124, 156, 234
Plot, 148, 181
Pointers, 54, 79, 80, 129
Polar, 199, 202, 247
Polyconic, 99
Polygon, 10, 33, 49, 50, 53, 57, 80, 84, 93, 140, 147, 150, 156, 159, 164, 175, 227
Polynomial, 92, 108, 115
Postclassifier, 217
Precision, 25, 48, 58, 62, 64, 70, 86, 88, 124, 151, 164, 198, 215, 216, 222, 225,
Preprocessing, 24, 76, 118, 124, 144, 154, 157, 167, 183, 211, 223, 235, 247
Probability, 122, 169, 227
Programmers, 62, 229
Propagation, 231
Proximal, 177
Proximity, 7, 15, 57, 157, 165, 172, 231, 234
Pyramid, 42

Quadrant, 44, 205
Quadrat, 72
Quadtree, 42, 59, 242
Quality-assurance, 182
Quantization, 209
Query-by-example, 136

Radar, 123, 193, 206, 209, 231
Radiation, 195
Radiometer, 202
Raster, 33, 58, 68, 77, 88, 90, 93, 106, 113, 143, 159, 178, 184, 192, 198, 202, 214, 217, 222, 243
Rasterize, 81, 83
Reclassification, 144
Rectification, 62, 76, 93, 97, 101, 103, 154
Recursively, 38
Redundancy, 46, 53, 84, 90, 130, 140, 238
Red-green-blue, 213
Reflectance, 150, 160, 188, 193, 196, 206
Refresh, 188
Regression, 106, 168, 182, 223
Relational, 49, 53, 59, 80, 134, 147, 169
Relief, 67, 232, 251
Remote-sensing, 194
Resampling, 42, 93, 153
Reset, 12, 37
Residual, 216, 251
Rhumb, 100
Root-mean-square, 226
Rotation, 47, 88, 99, 107, 131, 199, 201
Rubber sheet, 106
Run-length, 41, 90, 91

1576

Sample, 29, 36, 69, 72, 135
Satellite, 39, 66, 96, 124, 145, 160, 172, 183, 186, 192, 202, 211, 218, 236, 240, 242, 247, 251
Scale, 4, 6, 11, 15, 34, 44, 55, 62, 86, 89, 91, 99, 110, 119, 124, 137, 145, 153, 174, 197, 209, 212, 218, 223, 234, 237
Scan, 88, 90, 96, 151, 188, 199, 203
Scan-digitizing, 212
Security, 26, 64, 128, 137, 140, 247
Sensor, 66, 77, 123, 150, 160, 193, 199, 217
Sequential, 78, 132, 142, 147, 204
Shadow, 120, 217
Shrinkage, 86, 96
Shutter, 197
Signatures, 145, 196, 206
Significance, 122, 222, 226
Simulate, 113, 156, 209
Skeletonizing, 81, 84, 90, 215
Skewed, 199
Skewness, 167
Slivers, 94, 96
Slope, 27, 78, 114, 146, 162, 171, 217, 226, 235, 244
Small-scale, 11
Snapping, 95
Sonar, 226
Sorting, 80, 166, 177, 217, 218
Spaghetti, 58
Spatially-referenced, 3
Specifications, 63, 99, 127, 145, 201, 225
Spectrum, 80, 193, 195, 203
Standards, 49, 55, 62, 68, 133, 225, 240
Statistics, 151, 161, 167, 170, 182
Stereoplotter, 125
Stereoscopes, 124
Stratification, 75, 141, 217
Subsets, 139
Supervised, 149, 218
Survey, 2, 21, 33, 54, 65, 67, 110, 154, 222, 226, 240, 244, 247
Synchronization, 129
Synergism, 215
Syntax, 80

Tabular, 61, 123, 174, 235, 245
Tags, 127
Taxonomy, 120, 144
Television, 186, 188
Temporal, 29, 188, 195, 202, 207, 225, 236
Terrain, 4, 9, 63, 70, 114, 146, 159, 163, 177, 198, 217, 222, 231, 234, 251
Tessellation, 38
Texture, 91, 120, 161, 210, 235
Theme, 4, 32, 78, 214, 222, 224, 234
Thermal-infrared, 193
Thinning, 84, 93
Three-dimensional, 30, 32, 91, 103, 110, 117, 124, 156, 179, 232, 250
Throughput, 221
Tiles, 141, 195
Tilt, 67, 198
Timeliness, 191
Tolerance, 92, 95, 172
Tone, 119, 210
Topographic, 4, 33, 55, 67, 124, 154, 177, 200, 201, 223, 238, 247
Topology, 30, 49, 55, 80
Tract, 65, 114, 216
Trafficability, 146
Transaction, 129
Transect, 72
Transformations, 15, 106, 161, 215
Traverse, 9, 97, 137, 147, 188
Trend-surface, 115, 118
Triangular, 38, 116
Triangulate, 86
Trigonometric, 197
Tuple, 41, 134, 138, 147
Typewriter-like, 184

Ultraviolet, 193, 195
Unaligned sampling, 74
Union, 164, 246
Univariate, 170
Unsupervised, 149, 151, 213, 214
Update, 26, 57, 69, 124, 139, 215, 225, 235
Universal Transverse Mercator, 89, 99, 109

Validation, 28
Variable, 28, 79, 114, 138, 146, 160, 169, 182, 218, 235

Variable-length, 127
Variance, 150, 167, 168, 246
Vector, 48, 53, 77, 80, 86, 102, 107, 113, 129, 136, 140, 154, 163, 170, 184, 186, 215, 223, 230, 234
Verify, 70, 122, 227, 231
Vernier, 124
Video, 156, 185, 188, 190
Viewpoint, 119, 144, 153
Viewshed, 164, 167, 171
Visibility, 164, 171
Visualize, 251
Volume, 29, 32, 41, 58, 91, 133, 141, 165, 179, 183, 223, 229, 235, 247

Watershed, 156, 159, 235
Wavelength, 77, 152, 193, 196, 200
Weighting, 115, 116
Whisk-broom, 203
Window, 141, 160, 170, 244
Wireframe, 231

Yaw, 199
Yield, 181, 240, 241, 242

Zones, 99, 158, 218, 231, 233
Zoom transfer scope, 124

1577

Geographic Information Systems

AN INTRODUCTION

JEFFREY STAR
JOHN ESTES

Geographic Information Systems: An Introduction represents a timely new resource for students and professionals alike.

The authors' main objective is to emphasize data integration as a philosophical basis for modern GIS, wherein a geographic information system is the appropriate tool for integrating the technologies used in gathering, analyzing, and assessing spatial data.

The book begins with an introduction to the vocabulary, history, and essential components of geographic information systems. Following is an exploration of the five important parts of a GIS: data acquisition, preprocessing, database management, analysis and manipulation, and producing the final output. The later chapters introduce practical applications ranging from the design and management of large facilities to research on the global carbon cycle. A final chapter examines future trends and research developments in the field of geographic information systems.

PRENTICE HALL
Englewood Cliffs, N.J. 07632

ISBN 0-13-350123-5

Shape and Motion from Image Streams: a Factorization Method

2. Point Features in 3D Motion

Carlo Tomasi Takeo Kanade

January 1991
CMU-CS-91-105

School of Computer Science
Carnegie Mellon University
Pittsburgh, PA 15213

This research was sponsored by the Avionics Laboratory, Wright Research and Development Center, Aeronautical Systems Division (AFSC), U.S. Air Force, Wright-Patterson AFB, Ohio 45433-6543 under Contract F33615-90-C-1465, ARPA Order No. 7597.

The views and conclusions contained in this document are those of the authors and should not be interpreted as representing the official policies, either expressed or implied, of the U.S. government.

OFEK07611

Keywords: computer vision, motion, shape, time-varying imagery

OFEK07612

Abstract

In principle, three orthographic images of four points are sufficient to recover the positions of the points relative to each other (shape), and the viewpoints from which the images were taken (motion).

In practice, however, the solution to this structure-from-motion problem is reliable only when the viewing direction changes considerably between images. This conflicts with the difficulty of establishing correspondence between images over long-range camera motions.

Image streams, long sequences of images covering a wide motion in small steps, allow solving this conflict by using tracking for correspondence and redundancy for increased reliability in the structure-from-motion computation.

This report is the second of a series on a new factorization method for the computation of shape and camera motion from a stream of images. While the first report considered a camera moving on a plane, we now extend theory, analysis and experiments to general, three-dimensional motion.

In our method, we represent feature points in an image stream by a $2F \times P$ measurement matrix, which gathers the horizontal and vertical coordinates of the P points tracked through F frames. If coordinates are measured with respect to their centroid, we show that under orthography the measurement matrix is of rank 3.

Using this fact, we cast structure-from-motion as a matrix factorization problem, which we solve with an algorithm based on Singular Value Decomposition. Our algorithm gives accurate results, without relying on any smoothness assumption for either shape or motion.

OFEK07613

OFEK07614

Preface

In principle, the stream of images produced by a moving camera allows the recovery of both the shape of the objects in the field of view, and the motion of the camera. Traditional algorithms recover depth by triangulation, and compute shape by taking differences between depth values. This process, however, becomes very sensitive to noise as soon as the scene is more than a few focal lengths away from the camera. Furthermore, if the camera displacements are small, it is hard to distinguish the effects of rotation from those of translation: motion estimates are unreliable, and the quality of the shape results deteriorates even further.

To overcome these problems, we have developed a factorization method to decompose an image stream directly into object shape and camera motion, without computing depth as an intermediate step. The method uses a large number of frames and feature points to reduce sensitivity to noise. It is based on the fact that the incidence relations among projection rays can be expressed as the degeneracy of a matrix that gathers all the image measurements.

To explore this new method, we designed a series of eleven technical reports, as shown in figure 1, going from basic theory to implementation.

The first report, already published as CMU-CS-90-166, illustrates the idea in the case of planar motion, in which images are single scanlines.

The present report, number 2, extends the idea to three-dimensional camera motion and full image streams. It also carries out a somewhat more systematic error analysis, and discusses an experiment with a real stream. The method used to track points from frame to frame is described in detail in report number 3.

If point features are too sparse to give sufficient shape information, line features can be used either instead or in addition, as discussed in report

OFEK07615

number 4. Report number 5 shows how to extract and track line features.

The performance of our shape-and-motion algorithm is rather atypical. Because it does away with depth and capitalizes on the diversity of viewpoints made possible by long image streams, it performs best when the scene is distant and the motion of the camera is complex. Report number 6 examines what happens when objects are close to the camera, and perspective foreshortening occurs. Report number 7 shows how to deal with degenerate types of motion.

Occlusion can be handled by our method, and is treated in report number 8.

A basic assumption of our shape-and-motion algorithm is that only the camera moves. In some cases, however, a few points move in space with respect to the others, for instance, due to reflections from a shiny surface. Report number 9 examines how to detect these cases of spurious motion.

Our factorization algorithm deals with the whole stream of images at once. For some applications this is undesirable. Report number 10 proposes an implementation that can work with an indefinitely long stream of images.

Report number 11 considers a more radical departure from the assumption of a static scene than spurious motion. If several bodies are moving independently in the field of view of the camera, our factorization method can be used to count the number of moving bodies.

OFEK07616

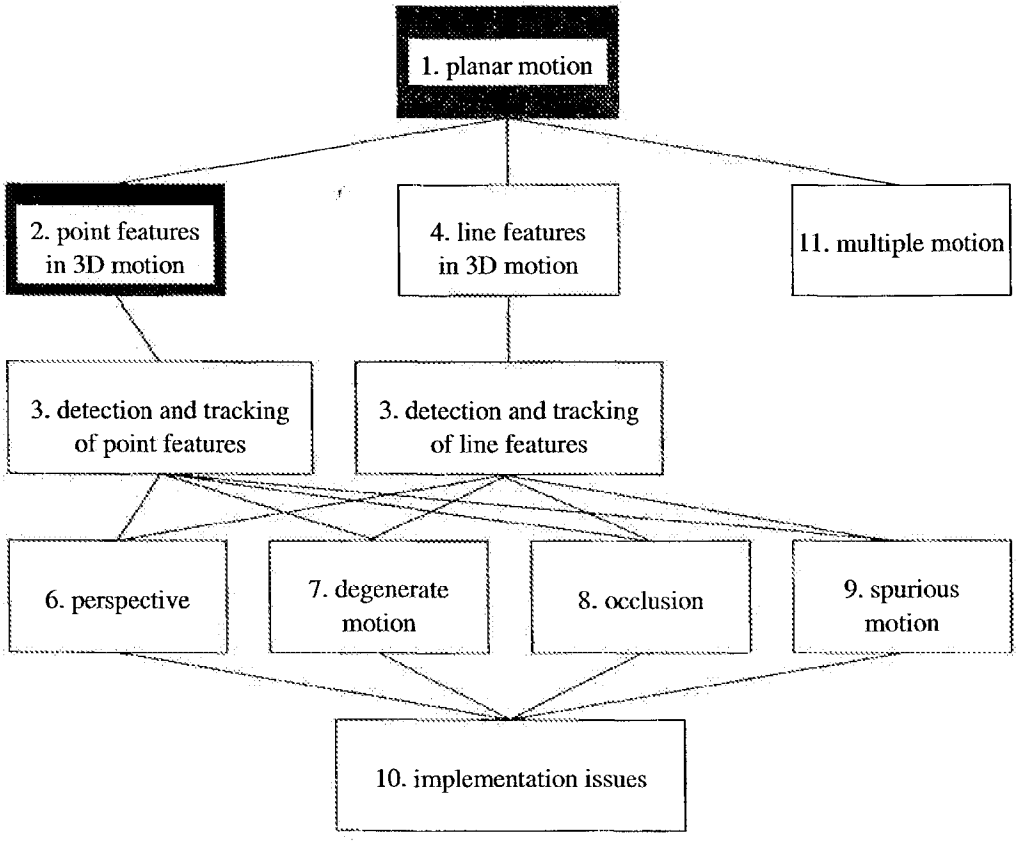


Figure 0.1: The reports in the series. Number 1 was published as CMU-CS-90-166.

OFEK07617

Chapter 1

Introduction

In principle, three orthographic images of four points are sufficient to recover *shape* and *motion*, that is, the positions of the points relative to each other and the viewpoints from which the images were taken.

In practice, however, the solution to this structure-from-motion problem is reliable only when the viewing direction changes considerably from image to image. For a given level of image noise and scene distance, this implies a substantial camera motion to achieve good performance.

Too wide a camera motion, on the other hand, poses two fundamental problems which limit the range of acceptable motions from above: establishing correspondence between images and avoiding occlusion of features from image to image.

To summarize, correspondence and occlusion are lesser problems with short-range motions, while reliability calls for long-range motion. Typically, for the classical structure-from-motion problem, characterized by few frames and points, these requirements are not compatible.

Image streams, that is, long sequences of image frames covering a wide motion in small steps, allow bridging the gap between short and long range motion. On the one hand, features can be, thus establishing correspondence between distant frames through the solution of many, simple correspondence problems between consecutive frames. On the other hand, the redundancy of information intrinsic in a stream improves the resiliency to noise, and allows dealing with streams spanning a shorter range of viewing angles.

A successful attack to the structure-from-motion problem based on image streams depends on our ability to deal with the great mass of data in an image

1586

OFEK07618

stream in a systematic and computationally efficient way for the recovery of shape and motion.

In [Tomasi and Kanade, 1990a] (also presented at ICCV90, [Tomasi and Kanade, 1990b]), we showed that, under the assumption of orthographic projection, we can directly *factor* the information contained in an image stream into shape and motion. However, we made the assumption that the camera move on a plane, in order to simplify the mathematical treatment. In the present report, we remove this assumption.

More specifically, we show that an image stream can be represented by a $2F \times P$ measurement matrix, which gathers the horizontal and vertical coordinates of P points tracked through F frames. If image coordinates are measured with respect to their centroid, we prove the following *rank principle*: under orthography, the measurement matrix is of rank 3. As a consequence of this principle, we show that measurement matrix can be factored into the product of two slender matrices of size $2F \times 3$ and $3 \times P$, respectively, where the first matrix encodes motion, the second shape.

The extension from planar to arbitrary camera motion is relatively straightforward, as far as the computation of shape and motion is concerned. The measurement matrix becomes twice as large, and one must incorporate the constraint that the columns and the rows in every image are mutually orthogonal.

Outline of the Report

In the next chapter we examine how our work relates with relevant results in the literature. This review extends somewhat the one given in [Tomasi and Kanade, 1990a].

We then show how to build the measurement matrix from a stream of full images (chapter 3), prove that the measurement matrix is of rank 3 (chapter 4), and show how to use this result to factor the measurement matrix into shape and camera rotation (chapter 5).

Chapter 6 describes some experiments on synthetic and real image streams, and chapter 7 summarizes the differences with respect to the planar case.

Chapter 2

Relations with Previous Work

In this chapter, we place our algorithm within the context of the literature on structure-from-motion, by pointing out papers which pursue closely related approaches, and by stating our major contributions to the field.

Some shape-from-motion algorithms address the most general problem, others only part of it. Approaches differ in the assumptions they make about the world, the imaging model, and the motion. They require different types of input primitives, work on varying numbers of images, and produce different forms of output.

We address the problem of shape-from-motion in its entirety, in that we make no assumption on either shape or motion. In this regard, our work can be compared with that of Thompson [Thompson, 1959], one of the earliest solutions to the two-frame problem, and Ullman [Ullman, 1979], who proposed an automated solution for four points and three frames. Our work can be contrasted to that of Baker et al. [Bolles *et al.*, 1987], and that of Matthies et al. [Matthies *et al.*, 1989], in that they recover depth from known motion.

Heel [Heel, 1989] produces dense maps and recovers both depth and motion, but he restricts the latter to pure translation. Both Heel and Matthies use incremental methods, where new images are processed as they become available, while we process a whole sequence at once. This is a disadvantage of our method, which deserves future investigation.

The only restrictions we make are the static (rigid) world and the orthographic imaging model. Ullman [Ullman, 1984] considers a less restrictive world model, allowing for non-rigid and rubbery motion, but is more inter-

1588

OFEK07620

ested in understanding biological systems than in achieving high precision. With Ullman [Ullman, 1979] we use an orthographic projection model, while Prazdny [Prazdny, 1980], Bruss and Horn [Bruss and Horn, 1983], Adiv [Adiv, 1985], Waxman and Wohn [Waxman and Wohn, 1985], and more recently Heeger and Jepson [Heeger and Jepson, 1989] and [Spetsakis and Aloimonos, 1989] assume a perspective model. On the other hand, Pradzny, Bruss and Horn, and Adiv cast the solution as a general search in the space of possible motions, which is computationally expensive, Waxman and Wohn use second order derivatives of image intensity, which are sensitive to noise, and Spetsakis and Aloimonos need a two-frame algorithm to initialize the search. The work by Heeger and Jepson is discussed below.

We make no assumption about the motion, except that it must contain a sufficiently large rotation component around the scene. Frequent limitations in the literature are to pure translation [Lawton, 1983], [Jain, 1983], [Matthies *et al.*, 1989], cases where one of the motion components is known [Horn and Weldon, 1988], smooth motion [Broida *et al.*, 1990], or constant motion [Debrunner and Ahuja, 1990]. On the other hand, Lawton, Jain, Matthies et al., Horn, Broida et al. propose solutions for the perspective model, and Matthies et al. and Broida et al. have incremental algorithms.

Our solution is multi-frame, and can therefore achieve a lesser sensitivity to noise than other approaches. Ullman works with three frames in [Ullman, 1979], but extends it to an arbitrary number in [Ullman, 1984]. Tsai and Huang [Tsai and Huang, 1984] work on two frames at a time, and Heeger and Jepson [Heeger and Jepson, 1989] use instantaneous image velocities.

The results by Heeger and Jepson [Heeger and Jepson, 1989] and Debrunner and Ahuja [Debrunner and Ahuja, 1990] are similar to ours at a conceptual level, in that they are also based on the bilinear nature of the projection equation. Heeger and Jepson, on the other hand, use essentially two frames at a time, and the perspective imaging model. Debrunner and Ahuja limit the type of motion, as said above, and use a different mathematical formalism.

We use Singular Value Decomposition as our major tool for solution. Also Tsai and Huang [Tsai and Huang, 1981], [Tsai *et al.*, 1982] use SVD, but only as an intermediate technical step to decompose their "essential parameter matrix". In contrast, we use SVD to decompose the measurement matrix, corresponding to an image stream, into shape and motion. Thus, SVD is the fundamental core of our method, and is the computational counterpart

to the rank principle proven in chapter 4. Thus, the relation with Tsai and Huang is only superficial.

To summarize, our algorithm is general, in that it does not assume *a priori* knowledge of either shape or motion, and makes no assumptions on the latter. It assumes rigid shape, and an orthographic projection model. It requires features to be extracted from images and tracked over time in the image stream. The algorithm produces motion and relative shape (the 3D coordinates of the tracked feature points relative to each other).

The major contributions of our approach are two. One is the conceptual result of the rank principle, described in chapter 4, which captures precisely and simply the nature of the redundancy of an image stream. The other contribution is the computational efficiency and simplicity of our matrix factorization method, which is based on the well-behaved algorithm of Singular Value Decomposition [Golub and Reinsch, 1971].

Chapter 3

The Measurement Matrix

In this chapter we show how to transform an image stream into a matrix collecting the feature coordinates to be fed to the algorithm that computes shape and motion. This assumes the existence of a method for tracking features from frame to frame, which will be described in detail in report number 3 in our series.

Suppose that we track P feature points over F frames in the image stream, resulting in a sequence of image coordinates $\{(u'_{fp}, v'_{fp}) \,|\, f = 1, \ldots, F, p = 1, \ldots, P\}$.

The horizontal coordinates u'_{fp} of those features are written into an $F \times P$ matrix U': there is one row per frame, and one column per feature point. Similarly, an $F \times P$ matrix V' is built from the vertical coordinates v'_{fp}.

The rows of the matrices U' and V' are then registered by subtracting from each entry the centroid of the entries in the same row:

$$\begin{aligned} u_{fp} &= u'_{fp} - \overline{u}_f \\ v_{fp} &= v'_{fp} - \overline{v}_f \,, \end{aligned} \tag{3.1}$$

where

$$\begin{aligned} \overline{u}_f &= \frac{1}{P} \sum_{p=1}^{P} u'_{fp} \\ \overline{v}_f &= \frac{1}{P} \sum_{p=1}^{P} v'_{fp} \,. \end{aligned}$$

1591

OFEK07623

This produces two new $F \times P$ matrices $U = [u_{fp}]$ and $V = [v_{fp}]$. The matrix

$$W = \left[\frac{U}{V}\right]$$

is called the *measurement matrix*. This is the input to our shape-and-motion algorithm.

Some of the features disappear during tracking, because of occlusion. Some others change in appearance so much that they are discarded as unreliable. Only the features that survive from the first to the last frame are used in the shape and motion recovery stage. In the future, we plan to investigate how to modify our algorithm to deal with a variable number of feature points over the image stream.

OFEK07624

Chapter 4

The Rank of the Measurement Matrix

This chapter introduces the fundamental principle on which our shape-and-motion algorithm is based: the $2F \times P$ matrix W of the registered image coordinates of P points tracked through F frames is higly rank-deficient.

The orientation of the camera reference system corresponding to frame number f is determined by a pair of unit vectors, $\mathbf{i}_f$and $\mathbf{j}_f$, pointing along the scanlines and the columns of the image respectively, and defined with respect to a world reference system with coordinates x, y, and z (see figure 7.1). Under orthography, all projection rays are then parallel to the cross product of $\mathbf{i}_f$and $\mathbf{j}_f$:

$$\mathbf{k}_f = \mathbf{i}_f \times \mathbf{j}_f \ .$$

The position of the camera reference system is determined by the position of the *image center*, defined as the point on the image plane with respect to which all image coordinates are measured.

The projection (u'_{fp}, v'_{fp}) of point $\mathbf{s}'_p = (x'_p, y'_p, z'_p)^T$ onto frame f is then given by the equations

$$\begin{aligned} u'_{fp} &= \mathbf{i}_f \cdot (\mathbf{s}'_p - \mathbf{t}_f) \\ v'_{fp} &= \mathbf{j}_f \cdot (\mathbf{s}'_p - \mathbf{t}_f) \ , \end{aligned}$$

where $\mathbf{t}_f$is the vector from the world origin to the image center of frame f.

We can now write expressions for the entries u_{fp} and v_{fp} of the measurement matrix by substituting the projection equations above into the

OFEK07625

registration equations (3.1). For the horizontal coordinates we have

$$\begin{aligned} u_{fp} &= u'_{fp} - \overline{u}_f \\ &= \mathbf{i}_f \cdot (\mathbf{s}'_p - \mathbf{t}_f) - \frac{1}{P}\sum_{p=1}^{P} \mathbf{i}_f \cdot (\mathbf{s}'_p - \mathbf{t}_f) \\ &= \mathbf{i}_f \cdot \left(\mathbf{s}'_p - \frac{1}{P}\sum_{p=1}^{P} \mathbf{s}'_p\right) \\ &= \mathbf{i}_f \cdot \mathbf{s}_p \ , \end{aligned}$$

where

$$\mathbf{s}_p = \frac{1}{P}\sum_{p=1}^{P} \mathbf{s}'_p$$

is the centroid of the scene points in space. Thus, the fact that the projection of the centroid is the centroid of the projections allows us to remove translation from the projection equations.

We can write a similar equation for the registered vertical image projection v_{fp}. To summarize,

$$\begin{aligned} u_{fp} &= \mathbf{i}_f \cdot \mathbf{s}_p \\ v_{fp} &= \mathbf{j}_f \cdot \mathbf{s}_p \ , \end{aligned} \tag{4.1}$$

where $\mathbf{s}_p = (x_p, y_p, z_p)$ gathers the coordinates of scene point number p with respect to the centroid of all the points being tracked.

Notice that, in our formulation, translation and rotation are referred to a world-centered system of reference. This is different from the camera-centered reference system usually used for the perspective projection equations. Also, while camera rotation in a camera-centered system supplies no shape information under perspective, translation (in either frame) is useless for shape recovery under orthography. This should come to no surprise: a set of images contains shape information only if the images are taken from different viewpoints, that is, when the center of projection moves betwen images. Under perspective, motion of the center of projection means translation of the camera. Under orthography, the center of projection is at infinity, and moving the center of projection means changing the direction of the projection rays.

OFEK07626

Because of the two sets of $F \times P$ equations (4.1), the measurement matrix W can be expressed in a matrix form:

$$W = MS \tag{4.2}$$

where

$$M = \begin{bmatrix} \mathbf{i}_1^T \\ \vdots \\ \mathbf{i}_F^T \\ \mathbf{j}_1^T \\ \vdots \\ \mathbf{j}_F^T \end{bmatrix} \tag{4.3}$$

represents the camera motion, and

$$S = \begin{bmatrix} \mathbf{s}_1 & \cdots & \mathbf{s}_P \end{bmatrix} \tag{4.4}$$

is the shape matrix. In fact, the rows of M represent the orientations of the horizontal and vertical camera reference axes throughout the sequence, while the columns of S are the coordinates of the P feature points with respect to their centroid.

Since M is $2F \times 3$ and S is $3 \times P$, the matrix projection equation (4.2) implies the following fact.

The Rank Principle

> *Without noise, the measurement matrix W is at most of rank three.*

The rank principle expresses the simple fact that the $2F \times P$ image measurements are highly redundant. Indeed, they could all be described concisely by giving F frame reference systems and P point coordinate vectors, if only these were known.

Geometrically, the rank principle expresses an incidence property. In fact, we can view the projection of point p onto frame f as the intersection of three planes: a "vertical" plane through $\mathbf{s}_p$ and orthogonal to the unit vector $\mathbf{i}_f$, a "horizontal" plane through $\mathbf{s}_p$ and orthogonal to the unit vector $\mathbf{j}_f$, and

OFEK07627

the image plane. The two projection equations (4.1) say that the "vertical" planes through point p belong to a star [1] of planes, and so do the "horizontal" planes.

In the next chapter, we show how to use the rank principle to determine the motion and shape matrices M and S, given the measurement matrix W.

[1] A star of planes is the set of planes passing through a fixed point.

OFEK07628

Chapter 5

The Factorization Method

When noise corrupts the images, the measurement matrix W will not be exactly of rank 3. However, the rank principle can be extended to the case of noisy measurements in a well-defined manner. The next section introduces this extension, using the concept of Singular Value Decomposition [Golub and Reinsch, 1971] to introduce the notion of approximate rank.

Section 5.2 then points out the properties of the motion matrix M in the projection equation (4.2) that must be enforced to uniquely determine the shape and motion solution. Finally, section 5.3 outlines the complete shape-and-motion algorithm.

5.1 Approximate Rank

Assuming [1] that $2F \geq P$, the matrix W can be decomposed [Golub and Reinsch, 1971] into a $2F \times P$ matrix L, a diagonal $P \times P$ matrix Σ, and a $P \times P$ matrix R,

$$W = L\Sigma R\,, \tag{5.1}$$

such that $L^T L = R^T R = RR^T = \mathcal{I}$, and $\sigma_1 \geq \ldots \geq \sigma_P$. Here, $\mathcal{I}$ is the $P \times P$ identity matrix, and the *singular values* $\sigma_1, \ldots, \sigma_P$ are the diagonal entries of Σ. This is the *Singular Value Decomposition* (SVD) of the matrix U.

[1] This assumption is not crucial: if $2F < P$, everything can be repeated for the transpose of W.

OFEK07629

If we now partition the matrices L, Σ, and R as follows:

$$
\begin{aligned}
L &= \underbrace{\left[\; L' \;\middle|\; L'' \;\right]}_{3 \quad P-3} \Big\}_{2F} \\
\Sigma &= \underbrace{\left[\begin{array}{c|c} \Sigma' & 0 \\ \hline 0 & \Sigma'' \end{array}\right]}_{3 \quad P-3} \begin{array}{l} \}_3 \\ \}_{P-3} \end{array} \\
R &= \underbrace{\left[\begin{array}{c} R' \\ \hline R'' \end{array}\right]}_{P} \begin{array}{l} \}_3 \\ \}_{P-3} \end{array} ,
\end{aligned}
\tag{5.2}
$$

we have

$$L\Sigma R = L'\Sigma' R' + L''\Sigma'' R'' .$$

Let W^* be the ideal measurement matrix, that is, the matrix we would obtain in the absence of noise. Because of the rank principle, the non-zero singular values of W^* are at most three. Since the singular values in Σ are sorted in non-increasing order, Σ' must contain all the singular values of W^* that exceed the noise level. As a consequence, the term $L''\Sigma''R''$ must be due entirely to noise, and the product $L'\Sigma'R'$ is the best possible rank-3 approximation to W^*.

We can now restate our key point.

The Rank Principle for Noisy Measurements

> *All the shape and motion information in W is contained in its three greatest singular values, together with the corresponding left and right eigenvectors.*

Thus, the best possible approximations to the ideal measurement matrix W^* is the product

$$\hat{W} = L'\Sigma'R'$$

OFEK07630

where the primes refer to the partition (5.2). With the definitions

$$\begin{aligned} \hat{M} &= L'[\Sigma']^{1/2} \\ \hat{S} &= [\Sigma']^{1/2} R' , \end{aligned}$$

we can also write

$$\hat{W} = \hat{M}\hat{S} . \tag{5.3}$$

The two matrices $\hat{M}$ and $\hat{S}$ are of the same size as the desired motion and shape matrices M and S: $\hat{M}$ is $2F \times 3$, and $\hat{S}$ is $3 \times P$. However, the decompositions (5.3) are not unique. In fact, if A is *any* invertible 3×3 matrix, the matrices $\hat{M}A$ and $A^{-1}\hat{S}$ are also a valid decomposition of W, since

$$(\hat{M}A)(A^{-1}\hat{S}) = \hat{M}(AA^{-1})\hat{S} = \hat{M}\hat{S} = \hat{W} .$$

Thus, $\hat{M}$ and $\hat{S}$ are in general different from M and S. A striking fact, however, is that, except for noise, the matrix $\hat{M}$ is a linear transformation of the true motion matrix M, and the matrix $\hat{S}$ is a linear transformation of the true shape matrix S. In fact, in the absence of noise, M and $\hat{M}$ both span the column space of the measurement matrix $W = W^* = \hat{W}$. Since that column space is three-dimensional, because of the rank principle, M and $\hat{M}$ are different bases for the same space, and there must be a linear transformation between them.

Whether the noise level is low enough that it can be ignored at this juncture depends also on the camera motion and on shape. Notice, however, that the singular value decomposition yields sufficient information to make this decision: the requirement is that the ratios between the third and the fourth largest singular values of W be sufficiently large.

5.2 The Metric Constraints

To summarize, the matrix $\hat{M}$ is a linear transformation of the true motion matrix M. Likewise, $\hat{S}$ is a linear transformation of the true shape matrix S. More specifically, there exists a 3×3 matrix A such that

$$\begin{aligned} M &= \hat{M}A \\ S &= A^{-1}\hat{S} . \end{aligned} \tag{5.4}$$

OFEK07631

In order to find A it is sufficient to observe that the rows of the true motion matrix M are unit vectors, and that the first F are orthogonal to corresponding F in the second half. These *metric constraints* yield the over-constrained, quadratic system

$$\begin{aligned} \hat{\mathbf{i}_f}^T AA^T \hat{\mathbf{i}_f} &= 1 \\ \hat{\mathbf{j}_f}^T AA^T \hat{\mathbf{j}_f} &= 1 \\ \hat{\mathbf{i}_f}^T AA^T \hat{\mathbf{j}_f} &= 0 \end{aligned} \tag{5.5}$$

in the entries of A. This is a simple data fitting problem which, though non-linear, can be solved efficiently and reliably.

A last ambiguity needs to be resolved: if A is a solution of the metric constraint problem, so is AR, where R is any orthonormal matrix. In fact,

$$\begin{aligned} \hat{\mathbf{i}_f}^T (AR)(R^T A^T) \hat{\mathbf{i}_f} &= \hat{\mathbf{i}_f}^T A(RR^T)A^T \hat{\mathbf{i}_f} \\ &= \hat{\mathbf{i}_f}^T AA^T \hat{\mathbf{i}_f} \\ &= 1 \,, \end{aligned}$$

and likewise for the remaining two constraint equations. Geometrically, this corresponds to the fact that the solution is determined up to a rotation, since the orientation of, say, the first camera reference system with respect to the world reference system is arbitrary. This arbitrariness can be removed, if desired, by rotating the solution so that the first frame is represented by the identity matrix.

5.3 Outline of the Complete Algorithm

Based on the development in the previous sections, we now have a complete algorithm for the computation of shape and rotation from the measurement matrix W derived from a stream of images. To summarize, the motion matrix M and the shape matrix S defined in equations (4.3) and (4.4) can be computed as follows.

1. Compute the singular-value decompositions of W:

$$W = L\Sigma R \,.$$

OFEK07632

2. Define

$$\begin{aligned} \hat{M} &= L'(\Sigma')^{1/2} \\ \hat{S} &= (\Sigma')^{1/2} R' \,, \end{aligned}$$

where the primes refer to the block partitioning defined in (5.2).

3. Compute the matrix A in equations (5.4) by imposing the metric constraints (equations (5.5)).

4. Compute the motion matrix M and the shape matrix S as

$$\begin{aligned} M &= \hat{M} A \\ S &= A^{-1} \hat{S} \,. \end{aligned}$$

5. If desired, align the first camera reference system with the world reference system by finding the rotation matrix R' that minimizes the residue

$$\left\| \begin{bmatrix} 1 & 0 & 0 \\ 0 & 1 & 0 \\ 0 & 0 & 1 \end{bmatrix} - R' \begin{bmatrix} \mathbf{i}_1 & \mathbf{j}_1 & \mathbf{k}_1 \end{bmatrix} \right\| ,$$

where the columns of the identity matrix on the left represent the axis unit vectors of the world reference system, $\mathbf{i}_1$ and $\mathbf{j}_1$ are the first and $F+1$-st row of M, and $\mathbf{k}_1 = \mathbf{i}_1 \times \mathbf{j}_1$. This is an absolute orientation problem, and can be solved by the procedure described in [Horn *et al.*, 1988].

OFEK07633

Chapter 6

Experiments

This chapter describes experiments on the computation of shape and motion.

First, the three-dimensional shape and motion computation is tested on simulations, in order to assess the ability of the algorithm to cope with varying levels of noise and with different numbers of frames and feature points.

Second, experiments on real images are presented. The complete shape and motion computation is demonstrated with general camera motion, for which accurate ground truth was measured with a mechanical positioning platform.

Simulations

In our simulations, we generated points in space randomly within a cube, with uniform distribution for each coordinate. We simulated camera motion with the camera always keeping those points in the field of view. Because of the assumption of orthographic projection, the distance between the camera and the object cannot be computed by the algorithm. Instead, the algorithm computes the remaining components of translation, along the image plane, in the registration phase (equations (3.1)) and the rotation of the camera around the centroid of the feature points. As discussed in chapter 4, under orthography, only the rotation component contains shape information. Consequently, we ignore the translation. In the simulations, rotation is characterized by equal amounts of pitch, yaw and roll. We added Gaussian noise to the images with various standard deviations, in order to test the

1602

OFEK07634

robustness of the algorithm.

Figures 7.2 through 7.4 show the simulation results. In each pair of graphs, the first shows the shape error and the second shows the rotation error.

The shape error is defined as the root-mean-squared error on the computed point coordinates, averaged over all points, and divided by the side-length of the cube.

We measured the angle distance between true and computed rotation as the smallest angle necessary to make the two rotations coincide. The rotation error is then defined as the root-mean-squared angle distance error, averaged over all frames, and divided by the total rotation angle.

The effect of image noise is shown in figure 7.2 for three different point-set sizes. For the curves in these two figures, the camera motion was 30 degrees. For the noise levels in the abscissas we assume a 512×512 image. Similar diagrams are shown in figure 7.3, but for varying stream lengths. The total camera rotation was kept at 30 degrees, so shorter streams correspond to greater motions between frames.

Figure 7.4 shows the effects of the total angle of rotation. Both the number of points and the number of frames were set to 50, and plots are given for a few different image noise levels.

Qualitatively, the diagrams show what we would expect: errors increase with more image noise, fewer points or frames, and a smaller range of viewing angles.

Quantitatively, we observe that even for noise values as high as three pixels standard deviation the shape and motion errors are less than one half of one percent. This is demonstrated again in the next section, which describes experiments on real image streams.

The noise we found in practice with real streams is on the order of a tenth of a pixel. The simulations show that for those noise levels we can expect good performance even with as few as ten points and viewing angles of five degrees.

Real Image Streams

In this section we describe an experiment on a real stream of images of a small plastic model of a building. The camera is a Sony CCD camera with a

1603

OFEK07635

200 mm lens, and is moved by means of a high-precision positioning platform. Figure 7.5 shows the setup. The motion of the camera is such as to keep the building withing the field of view throughout the stream. Some frames in the stream are shown in figure 7.6. Camera pitch, yaw, and roll around the model are all varied as shown by the dashed curves in figures 7.12 through 7.11.

Figure 7.7 shows the trajectories left by a subset of 50 features tracked through 150 frames. For feature tracking, we extended the method described in [Lucas and Kanade, 1981] to allow also for the automatic selection of image features. We will describe the method in report number 3 in our series. The entire set of 430 features is displayed in figure 7.8, overlayed on the first frame of the stream. Of these features, 42 were abandoned during tracking because their appearance changed too much. The remaining 388 features are displayed in figure 7.9, superimposed on the last frame of the sequence.

The solid curves in figures 7.10, 7.11, and 7.12 compare the rotation components computed by the algorithm with the values measured mechanically from the mobile platform. In each figure, the top diagram shows the computed and the measured rotation components, superimposed, while the bottom diagram shows the difference between the two.

The errors are everywhere less than 0.4 degrees. The computed motion follows closely also rotations with curved profiles, such as the roll profile between frames 1 and 20 (figure 7.11), and faithfully preserves all discontinuities in the rotational velocities. This is a consequence of the fact that no assumption was made on the camera motion: the algorithm does not smooth the results. If the rows of the measurement matrix were permuted, thus simulating a camera jumping back and forth, the computed yaw, roll, and pitch values would be permuted correspondingly, yielding discontinuous plots.

Between frames 60 and 80, yaw and pitch are nearly constant. This means that the image stream contains almost no shape information along the optical axis during that subsequence, since the camera is merely rotating about its optical axis. This demonstrates that it is sufficient for the stream *as a whole* to be taken during non-degenerate motion. The algorithm can deal without difficulty with streams that contain degenerate subsequences, because the information in the stream is used all at once in our method.

We are not yet able to account for the residue error of about 0.3 degrees in the yaw and pitch components. This might be due to lens distortion, errors in the determination of the camera's aspect ratio, poor calibration of

OFEK07636

the mechanical measurements of motion, or errors due to our algorithm.

The shape results are shown qualitatively in figure 7.13, which shows the computed shape viewed from above. The view in figure 7.13 is similar to that in figure 7.14, included for visual comparison. Notice that the walls, the windows on the roof, and the chimneys are recovered in their correct positions.

To evaluate the shape performance quantitatively, we measured some distances on the actual house model with a ruler, and compared them with the distances computed from the point coordinates in the shape results. Figure 7.15 shows the selected features superimposed on the first frame of the sequence, with the number assigned to them by our feature detection algorithm. The diagram in figure 7.16 shows the distances between pairs of features, both as measured on the actual model and as computed from the results of our algorithm. The results of the algorithm were scaled so as to make the computed distance between feature 117 and 282 equal to the distance measured on the model. Lengths are in millimeters. The measured distances between the steps along the right side of the roof (7.2 mm) were obtained by measuring five steps and dividing the total distance (36 mm) by five. The differences between computed and measured results are of the order of the resolution of our ruler measurements (one millimeter).

OFEK07637

Chapter 7

Conclusion

In this report, we extended our factorization method for the recovery of shape and motion from a stream of images to unrestricted camera motion.

We were initially surprised to observe that the algorithm performs better in three dimensions than in two, in the sense that its performance degrades more gracefully as the number of frames and/or feature points decreases, or as the range of viewing directions becomes smaller.

A posteriori, however, this fact is easy to explain. If the camera motion contains both pitch and yaw, then shape can be recovered from *either* the horizontal or the vertical image coordinates. Computing shape and motion from *both* sets of measurements at once is an additional source of redundancy, which improves the performance. In other words, the measurement matrix is of rank three, but only half of it is necessary in principle. In a related context, the learning of shapes from images, Poggio says it succintly: "1.5 snapshots are sufficient" [Poggio, 1990] to recover the structure.

In practice, going from two to three dimensions, the additional difficulties in the method are two. First of all, one has to know the aspect ratio of the camera pixels in order to write the measurement matrix. Of course, this was not necessary in the planar case. However, this is a simple calibration to perform.

Secondly, and much more importantly, features are harder to track in a full image than in a single scanline. Our tracking method, based on previous work by Lucas and Kanade [Lucas and Kanade, 1981] yielded accurate displacement measurements. Although there may be situations where the algorithm can fail, we did not encounter any in our experiments. We will

OFEK07638

discuss the features selection and tracking method in report number 3 of our series.

OFEK07639

Bibliography

[Adiv, 1985]
G. ADIV. Determining three-dimensional motion and structure from optical flow generated by several moving objects. *IEEE Pattern Analysis and Machine Intelligence*, 7:384–401, 1985.

[Bolles *et al.*, 1987]
R. C. BOLLES, H. H. BAKER, AND D. H. MARIMONT. Epipolar-plane image analysis: An approach to determining structure from motion. *International Journal of Computer Vision*, 1(1):7–55, 1987.

[Broida *et al.*, 1990]
T. BROIDA, S. CHANDRASHEKHAR, AND R. CHELLAPPA. Recursive 3-d motion estimation from a monocular image sequence. *IEEE Transactions on Aerospace and Electronic Systems*, 26(4):639–656, July 1990.

[Bruss and Horn, 1983]
A. R. BRUSS AND B. K. P. HORN. Passive navigation. *Computer Vision, Graphics, and Image Processing*, 21:3–20, 1983.

[Debrunner and Ahuja, 1990]
C. H. DEBRUNNER AND N. AHUJA. A direct data approximation based motion estimation algorithm. In *Proceedings of the 10th International Conference on Pattern Recognition*, pages 384–389, Atlantic City, NJ, June 1990.

[Golub and Reinsch, 1971]
G. H. GOLUB AND C. REINSCH. Singular value decomposition and least squares solutions, In *Handbook for Automatic Computation*, volume 2, chapter I/10, pages 134–151. Springer Verlag, New York, NY, 1971.

OFEK07640

[Heeger and Jepson, 1989]
D. J. HEEGER AND A. JEPSON. Visual perception of three-dimensional motion. Technical Report 124, MIT Media Laboratory, Cambridge, Ma, December 1989.

[Heel, 1989]
J. HEEL. Dynamic motion vision. In *Proceedings of the DARPA Image Understanding Workshop*, pages 702–713, Palo Alto, Ca, May 23-26 1989.

[Horn and Weldon, 1988]
B. K. P. HORN AND E. J. WELDON JR. Direct methods for recovering motion. *International Journal of Computer Vision*, 2:51–76, 1988.

[Horn *et al.*, 1988]
B. K. P. HORN, H. M. HILDEN, AND S. NEGAHDARIPOUR. Closed-form solution of absolute orientation using orthonormal matrices. *Journal of the Optical Society of America A*, 5(7):1127–1135, July 1988.

[Jain, 1983]
R. JAIN. Direct computation of the focus of expansion. *IEEE Pattern Analysis and Machine Intelligence*, 5:58–63, 1983.

[Lawton, 1983]
D. T. LAWTON. Processing translational motion sequences. *Computer Graphics and Image Processing*, 22:116–144, 1983.

[Lucas and Kanade, 1981]
B. D. LUCAS AND T. KANADE. An iterative image registration technique with an application to stereo vision. In *Proceedings of the 7th International Joint Conference on Artificial Intelligence*, 1981. More details can be found in B. D. LUCAS, *Generalized Image Matching by hte Method of Differences*, PhD thesis, Carnegie Mellon University, 1984.

[Matthies *et al.*, 1989]
L. MATTHIES, T. KANADE, AND R. SZELISKI. Kalman filter-based algorithms for estimating depth from image sequences. *International Journal of Computer Vision*, 3(3):209–236, September 1989.

OFEK0764

[Poggio, 1990]
T. POGGIO. 3d object recognition: on a result of Basri and Ullman. Technical report, IRST, Trento, Italy, March 1990.

[Prazdny, 1980]
K. PRAZDNY. Egomotion and relative depth from optical flow. *Biological Cybernetics*, 102:87–102, 1980.

[Spetsakis and Aloimonos, 1989]
M. E. SPETSAKIS AND J. Y. ALOIMONOS. Optimal motion estimation. In *Proceedings of the IEEE Workshop on Visual Motion*, pages 229–237, Irvine, California, March 1989.

[Thompson, 1959]
E. H. THOMPSON. A rational algebraic formulation of the problem of relative orientation. *Photogrammetric Record*, 3(14):152–159, 1959.

[Tomasi and Kanade, 1990a]
C. TOMASI AND T. KANADE. Shape and motion from image streams: a factorization method. Technical Report CMU-CS-90-166, Carnegie Mellon University, Pittsburgh, Pa, September 1990.

[Tomasi and Kanade, 1990b]
C. TOMASI AND T. KANADE. Shape and motion without depth. In *Proceedings of the Third International Conference in Computer Vision (ICCV)*, Osaka, Japan, December 1990.

[Tsai and Huang, 1981]
R. Y. TSAI AND T. S. HUANG. Estimating three-dimensional motion parameters of a rigid planar patch. *IEEE Transactions on Acoustics, Speech, and Signal Processing*, ASSP-29:1147–1152, December 1981.

[Tsai and Huang, 1984]
R. Y. TSAI AND T. S. HUANG. Uniqueness and estimation of three-dimensional motion parameters of rigid objects with curved surfaces. *IEEE Transactions on Pattern Analysis and Machine Intelligence*, PAMI-6(1):13–27, January 1984.

OFEK07642

[Tsai *et al.*, 1982]
R. Y. TSAI, T. S. HUANG, AND W. L. ZHU. Estimating three-dimensional motion parameters of a rigid planar patch, ii: Singular value decomposition. *IEEE Transactions on Acoustics, Speech, and Signal Processing*, ASSP-30:525–534, August 1982.

[Ullman, 1979]
S. ULLMAN. *The Interpretation of Visual Motion.* The MIT Press, Cambridge, Ma, 1979.

[Ullman, 1984]
S. ULLMAN. Maximizing rigidity: the incremental recovery of 3-d structure from rigid and rubbery motion. *Perception*, 13:255–274, 1984.

[Waxman and Wohn, 1985]
A. M. WAXMAN AND K. WOHN. Contour evolution, neighborhood deformation, and global image flow: planar surfaces in motion. *International Journal of Robotics Research*, 4:95–108, 1985.

OFEK07643

Figure 7.1: The image and world reference systems.

1612

OFEK07644

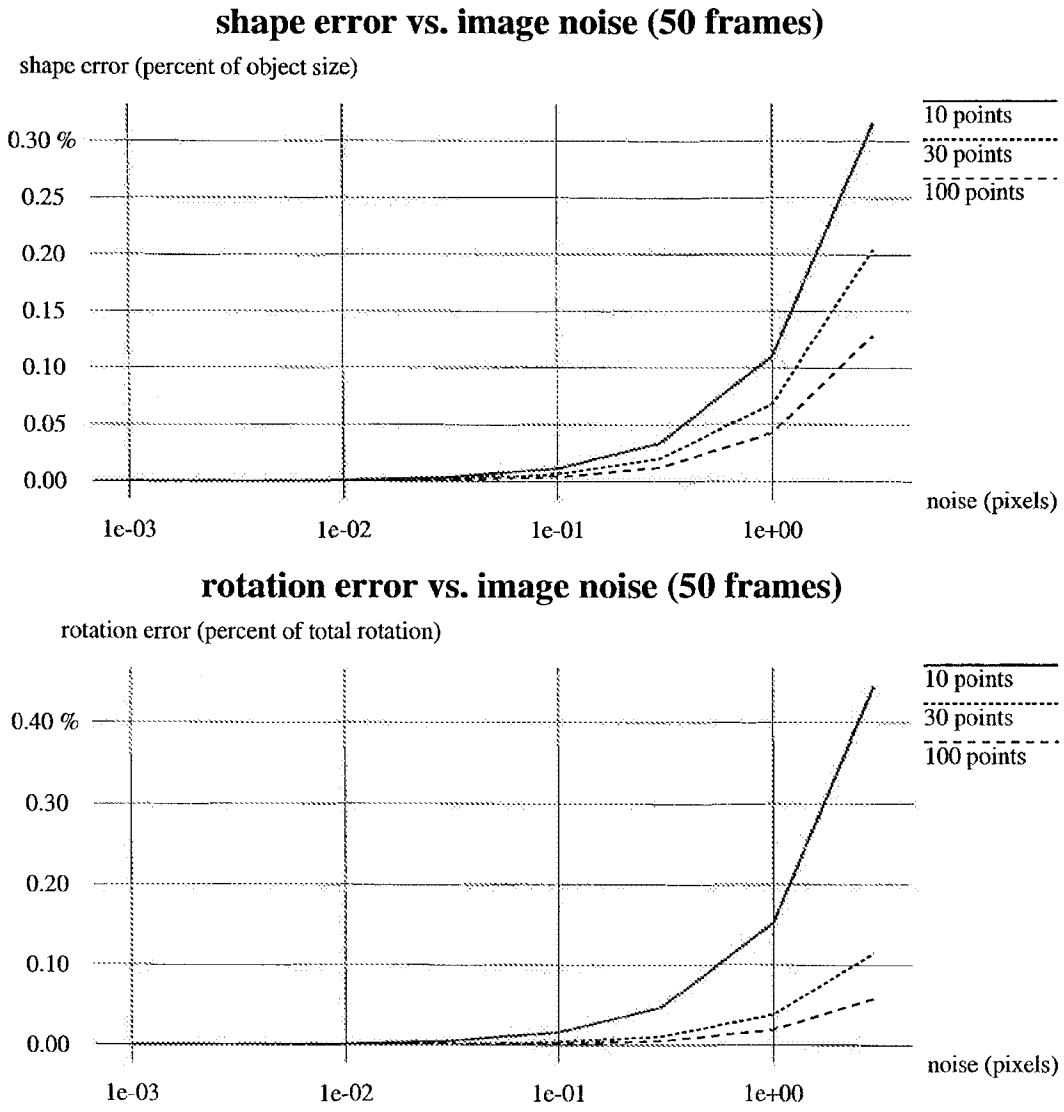


Figure 7.2: Relative shape and rotation error versus image noise for three different point-set sizes. Gaussian noise standard deviation figures assume a 512×512 image.

OFEK07645

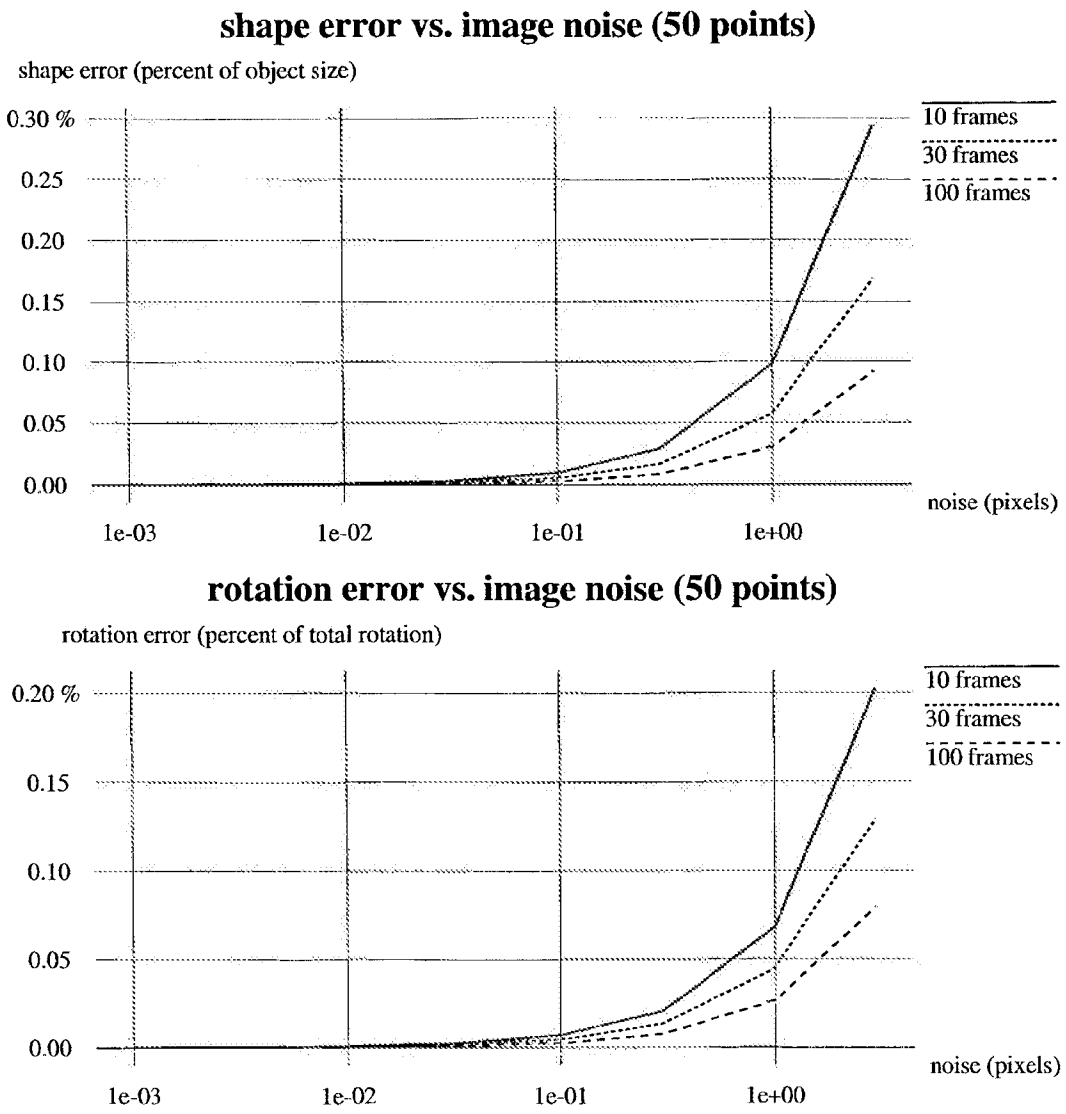


Figure 7.3: Relative shape and rotation error versus image noise for three different stream lengths. Gaussian noise standard deviation figures assume a 512×512 image. Shorter streams correspond to greater motions between frames. See text for details.

OFEK07646

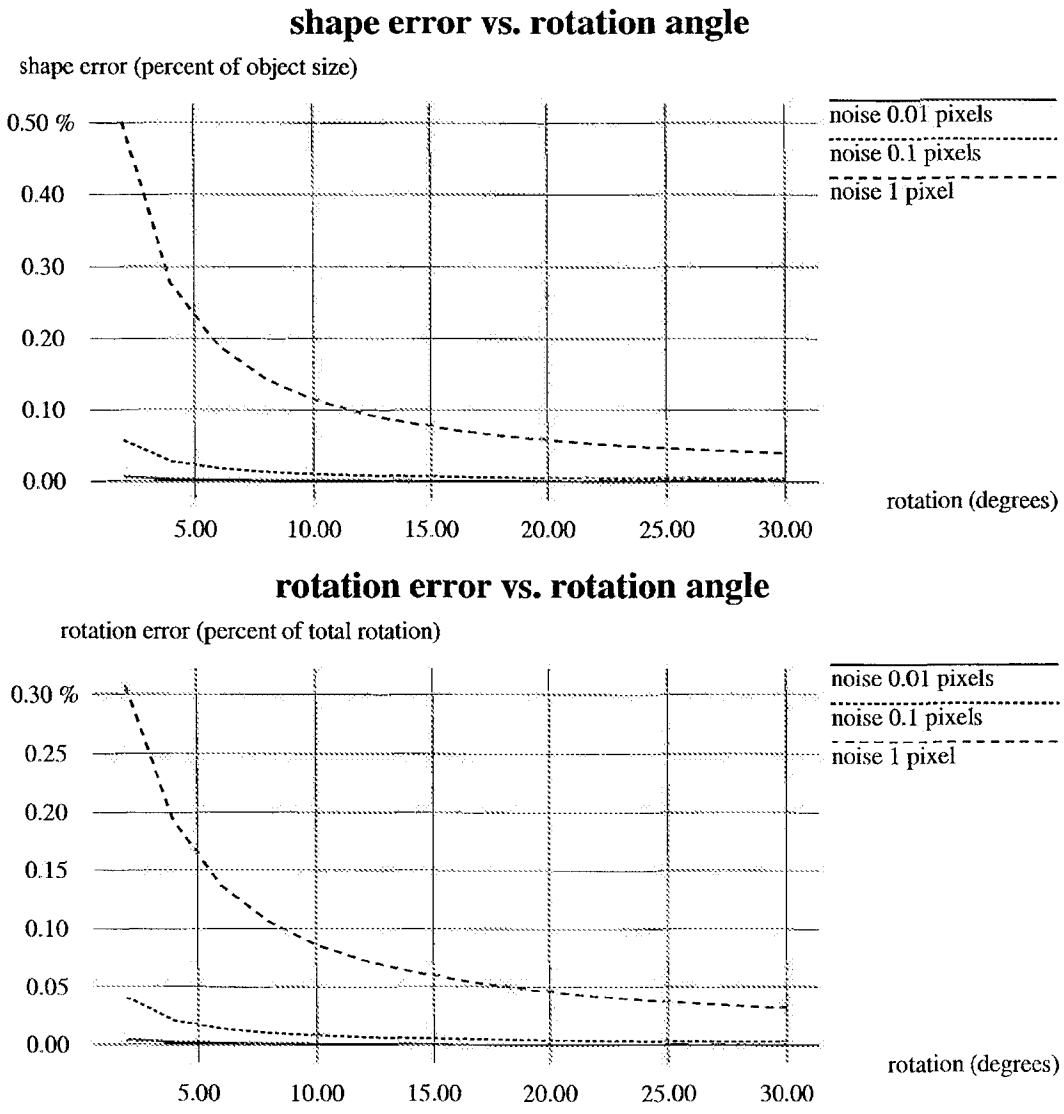


Figure 7.4: Relative shape and rotation error versus total camera rotation angle for various noise levels. Gaussian noise standard deviation figures assume a 512×512 image. See text for details.

OFEK07647

Figure 7.5: The setup used in the experiment. The drawing is not to scale.

1616

OFEK07648

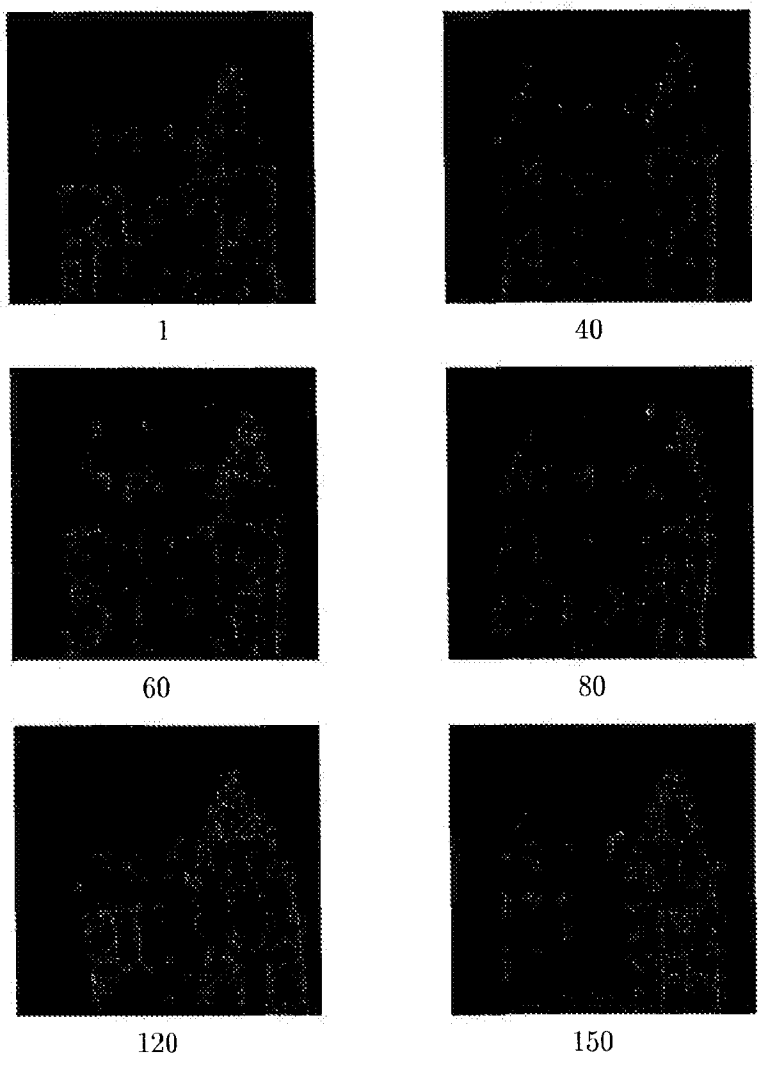


Figure 7.6: Some frames in the stream.

OFEK07649

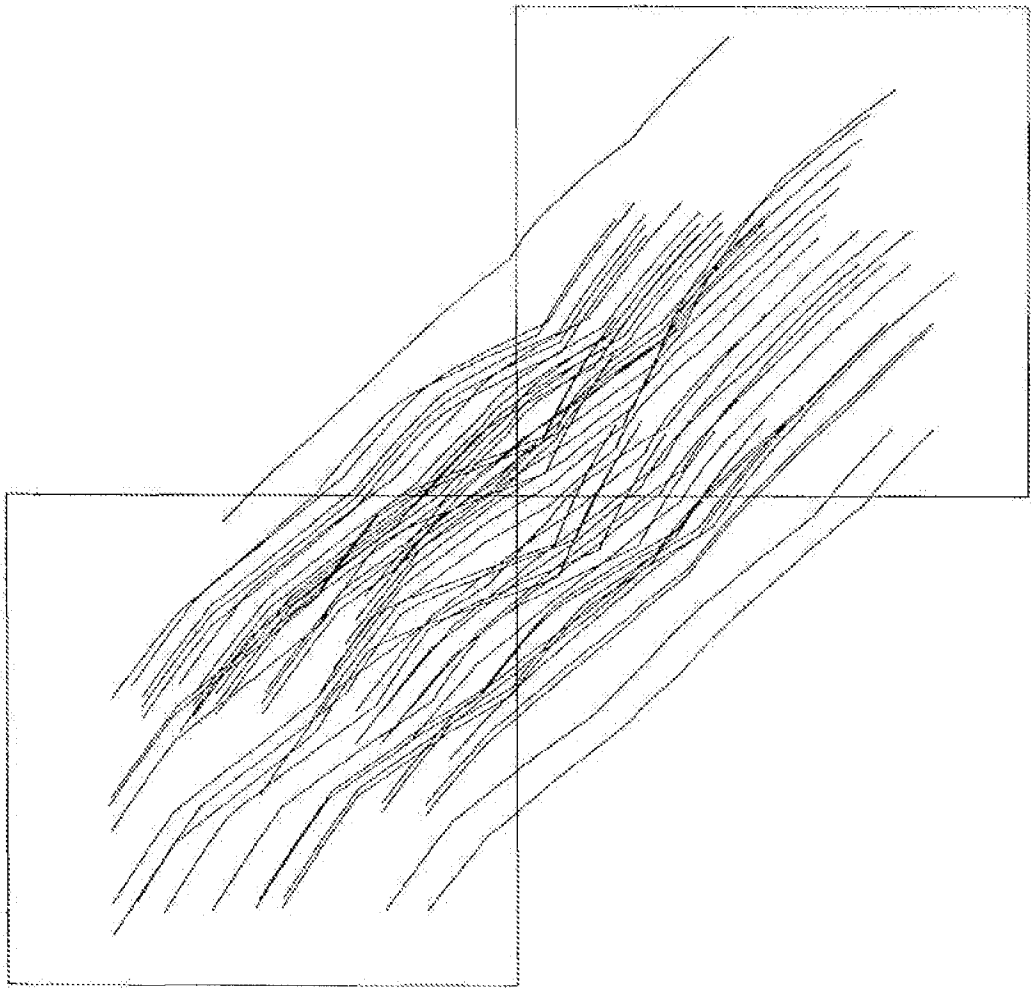


Figure 7.7: Tracks of 50 randomly selected features, from frame 1 to frame 151 of a real stream.

OFEK07650

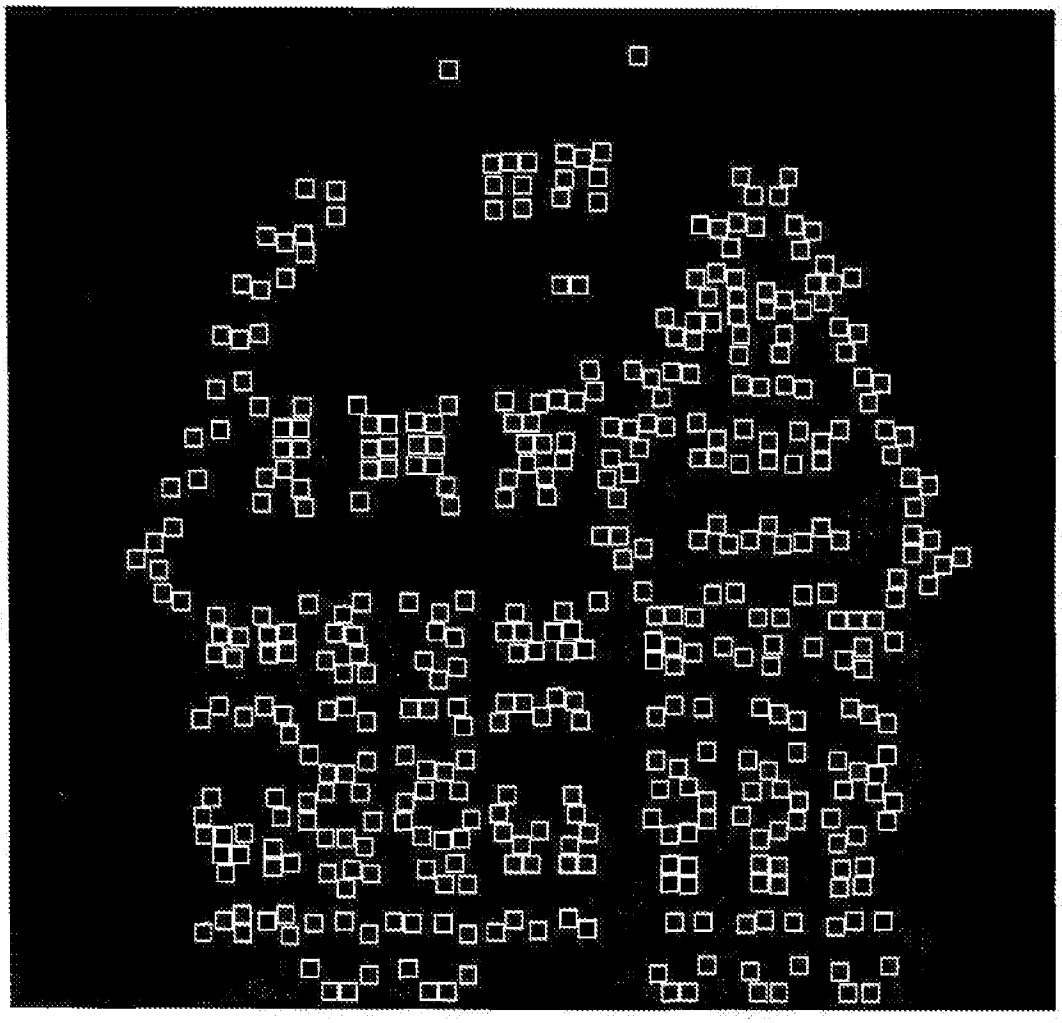


Figure 7.8: The 430 features selected by the automatic detection method, shown superimposed on the first frame of the stream.

OFEK07651

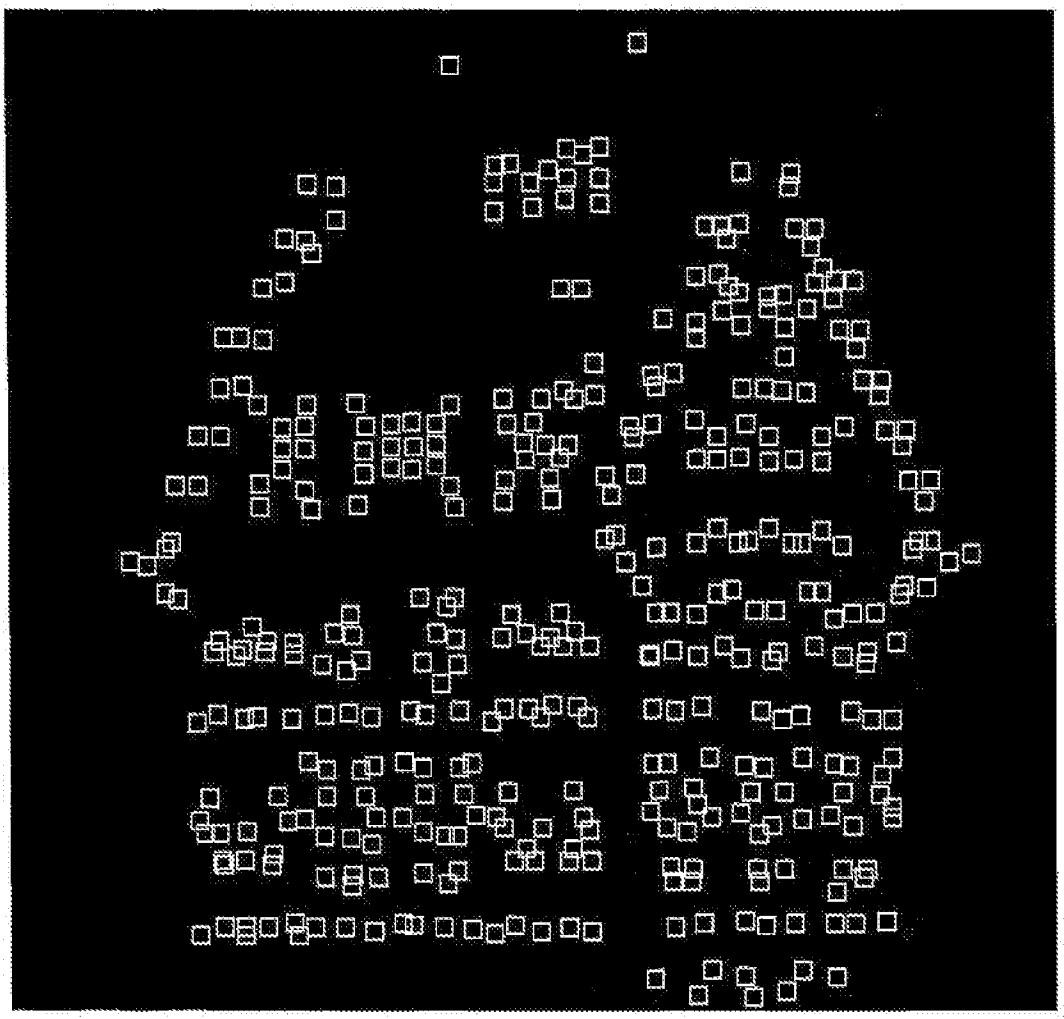


Figure 7.9: The 388 features surviving tracking through 150 frames, shown superimposed on the last frame of the stream.

OFEK07652

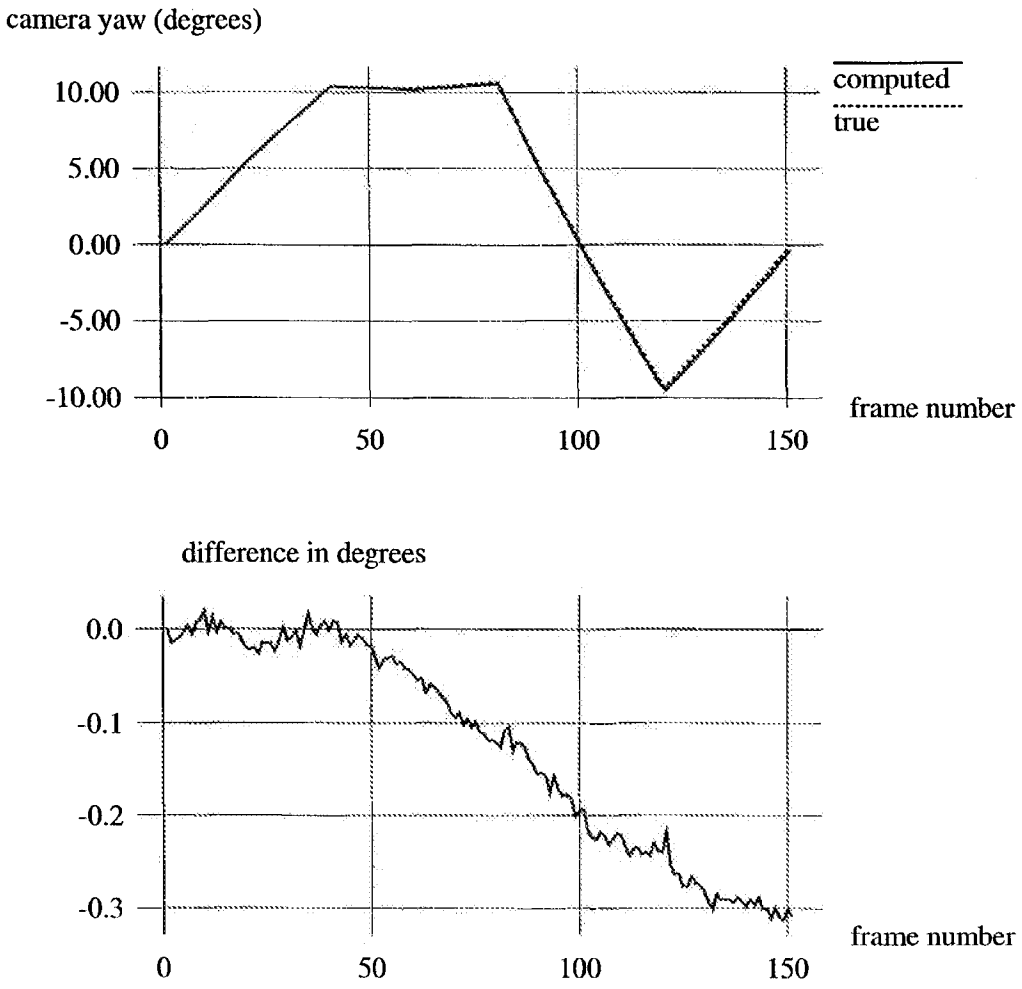


Figure 7.10: Results for the camera yaw. The top graph shows true and computed camera yaw, superimposed, versus the frame number. The bottom graph is a blow-up of the difference between the two plots. The rotation is around the centroid of the feature points.

OFEK07653

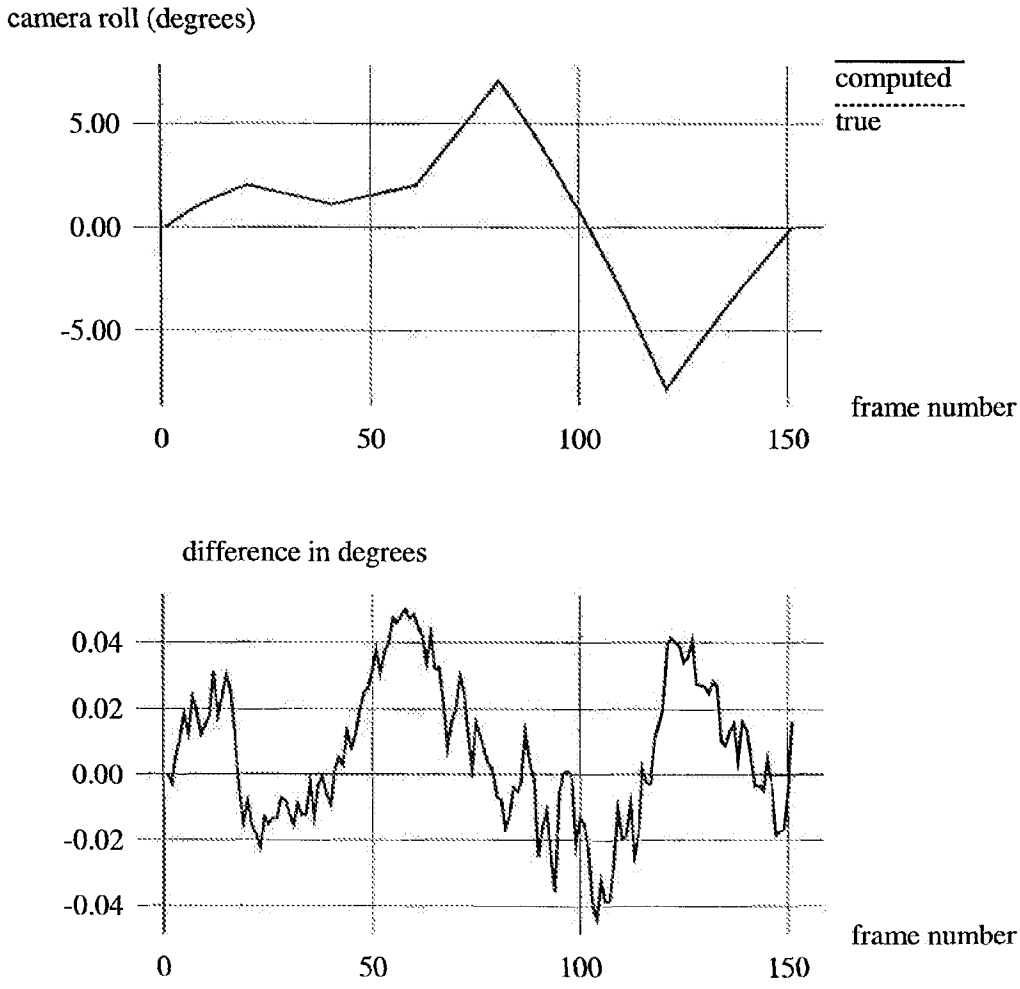


Figure 7.11: Results for the camera roll. The top graph shows true and computed camera roll, superimposed, versus the frame number. The bottom graph is a blow-up of the difference between the two plots. The rotation is around the centroid of the feature points.

OFEK07654

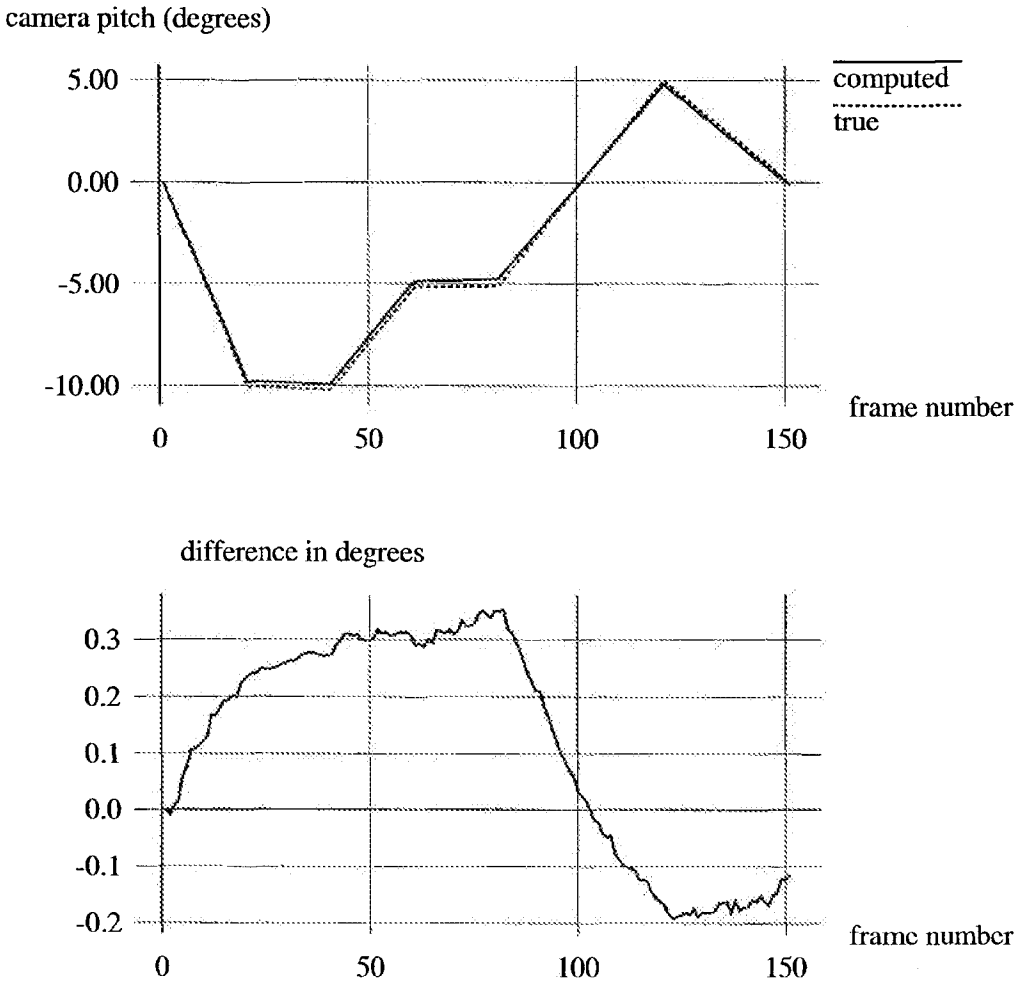


Figure 7.12: Results for the camera pitch. The top graph shows true and computed camera pitch, superimposed, versus the frame number. The bottom graph is a blow-up of the difference between the two plots. The rotation is around the centroid of the feature points.

OFEK07655

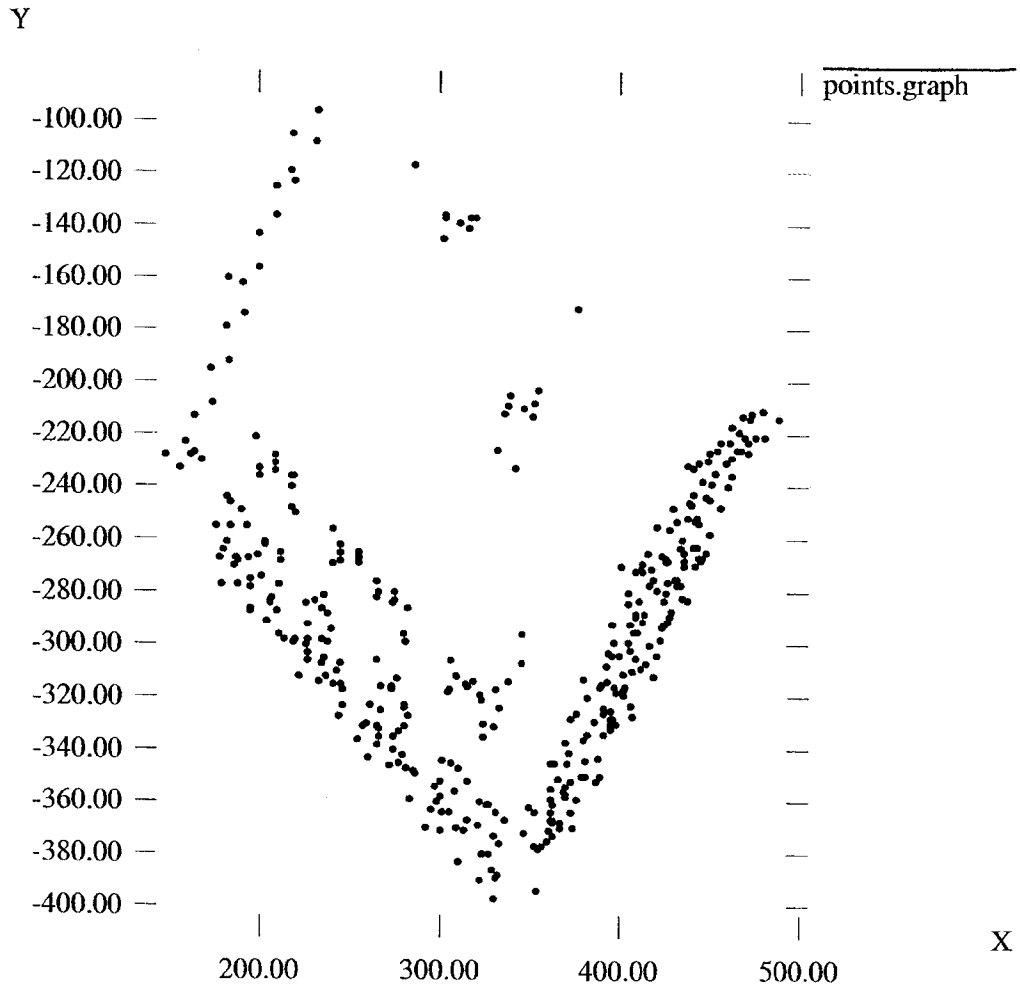


Figure 7.13: A view of the computed shape from approximately above the building (compare with figure 7.14). Notice the correct location of the walls, the windows on the roof, and the chimneys.

OFEK07656

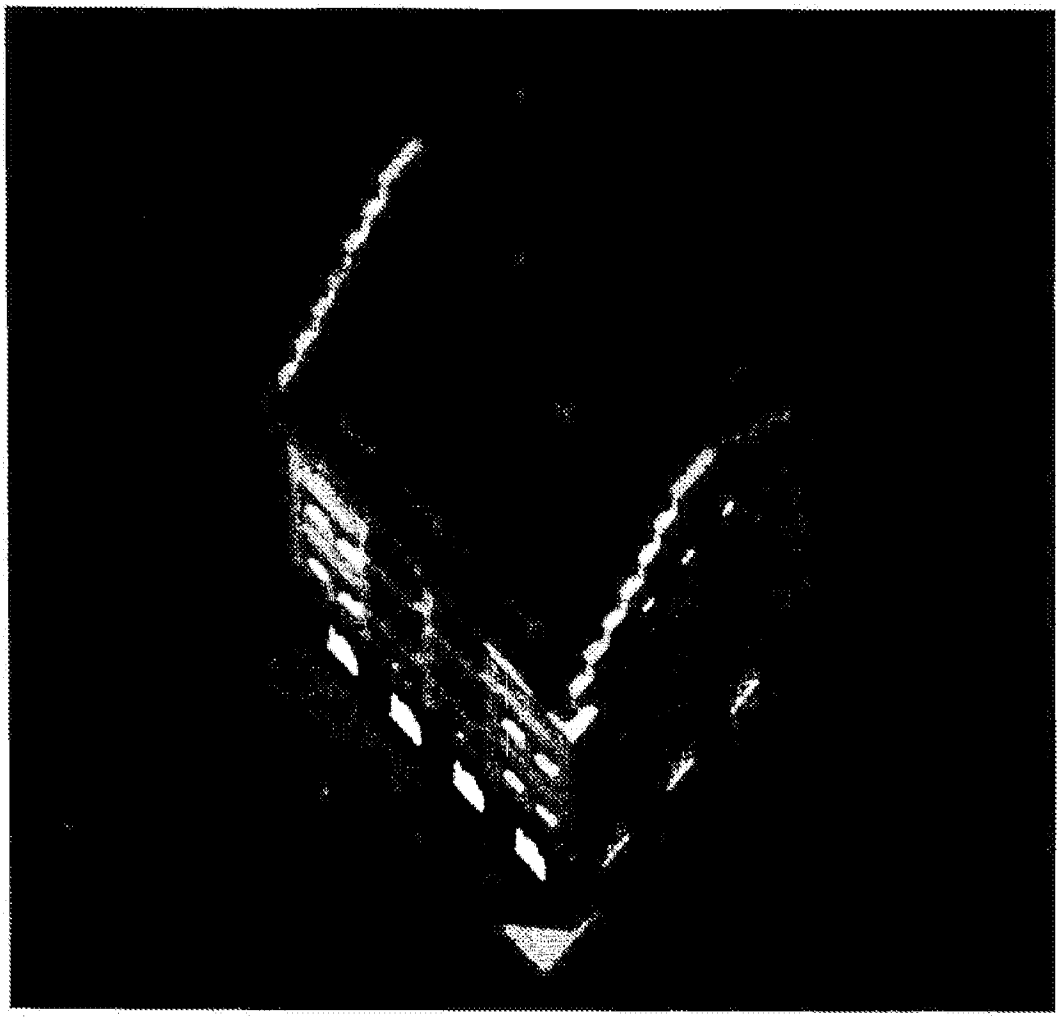


Figure 7.14: A real picture from above the building, similar to figure 7.13. This figure and figure 7.13 were not precisely aligned, but are intended for qualitative comparison.

OFEK07657

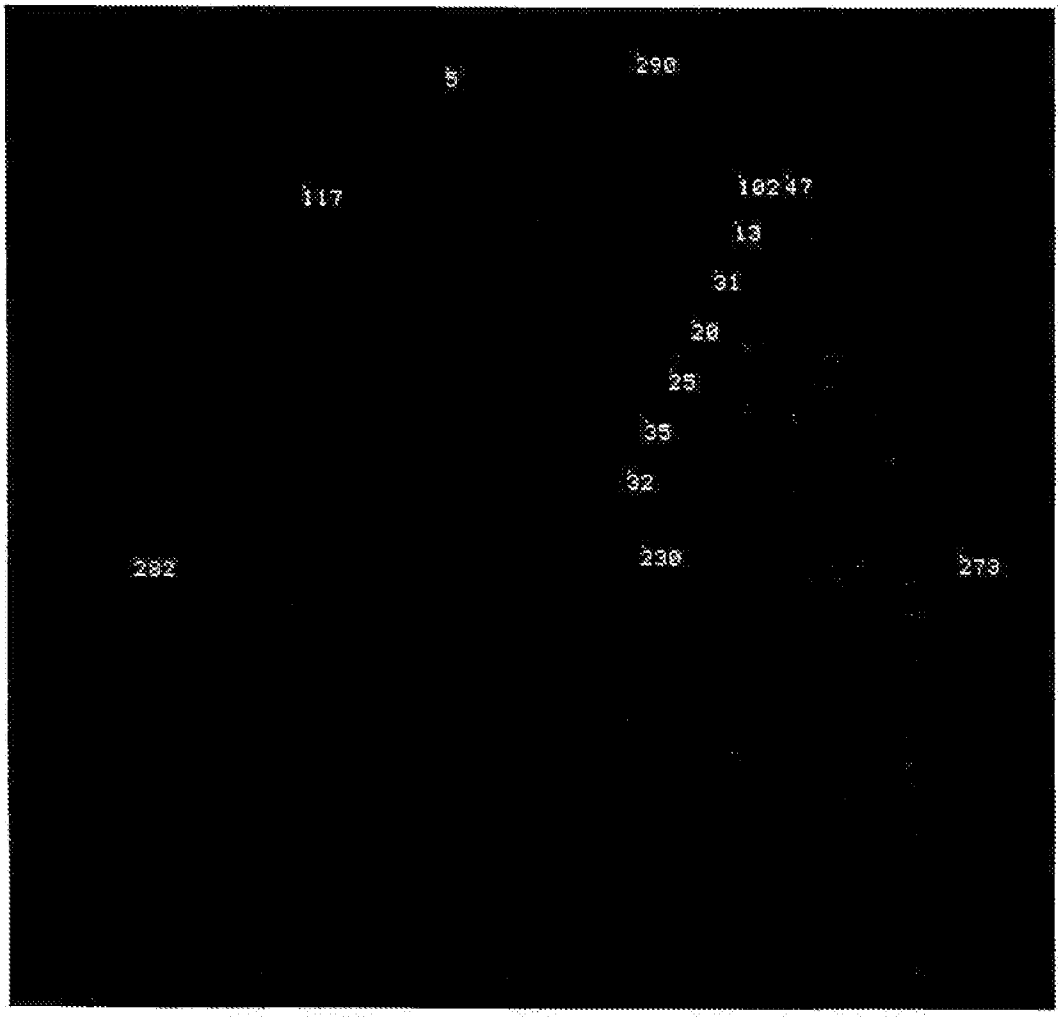


Figure 7.15: For a quantitative evaluation, distances between the features show in the picture were measured on the actual model, and compared with the computed results. The comparison is shown in figure 7.16.

OFEK07658

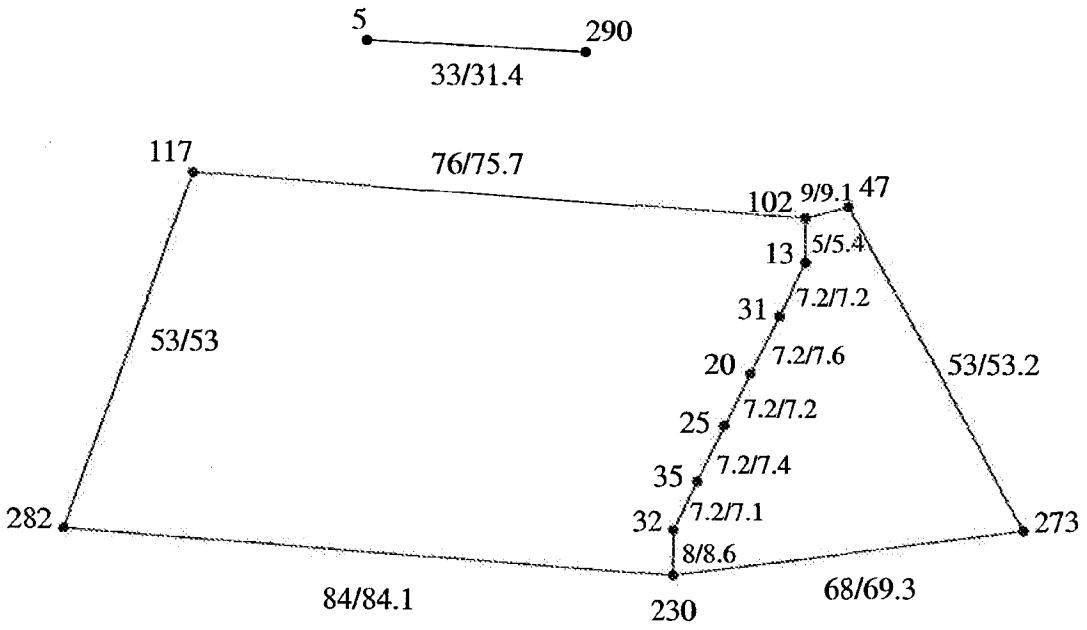
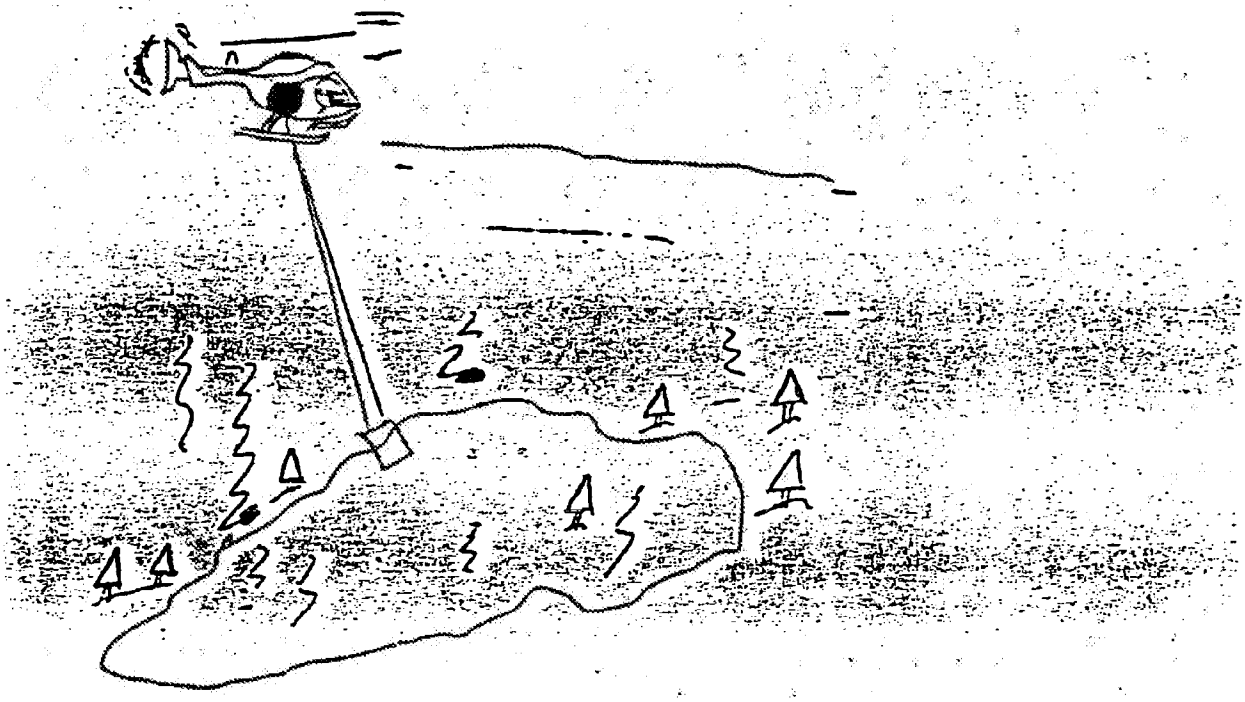


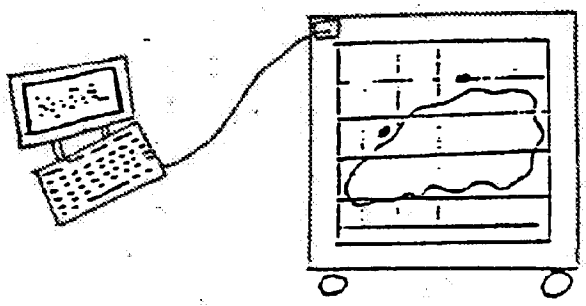
Figure 7.16: Comparison between measured and computed distances for the features in figure 7.15. The number before the slash is the measured distance, the one after is the computed distance. Lengths are in millimeters. Computed distances were scaled so that the computed distance between features 117 and 282 is the same as the measured distance.

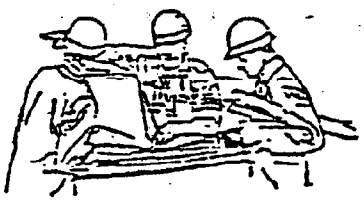
OFEK07659

FIRE MAPPING
with the
FIRE MOUSE TRAP
July 1986

USDA Forest Service
Advanced Electronics
Systems Development Group
Aviation and Fire Management
John Warren
Electronics Engineer







BEST AVAILABLE COPY

INTRODUCTION:

This report discusses the use and availability of the FIRE MOUSE TRAP (FMT)* system for mapping fires of any size from a helicopter or small fixed wing aircraft. The concept was first suggested in 1984.(1) It was first used operationally during the 1985 fire season by the State of Alaska, mounted on a T-28 aircraft.(2,3) It was used extensively in 1986, both in Alaska and the "lower 48", in R1, R4, and on BLM fires in Nevada. It has been used in subsequent years in Alaska, R5, R6, and R10, all of which have their own capability. It is available for use by the Forest Service or other agencies as a portable system which can be installed on any helicopter or light aircraft which is equipped with a compatible LORAN-C antenna. All other airborne equipment can be brought in and set up in about 30 minutes for initial operation, in whatever aircraft is available around the Incident Command Post (ICP). (The Alaska T-28, equipped with the FMT and crew can also be made available, subject to their state fire situation, to assist other agencies in Alaska or the "lower 48".)

FIRE MOUSE TRAP SYSTEM DESCRIPTION

This new approach to fire mapping uses a small Forward Looking InfraRed (FLIR) unit mounted on a helicopter (or small fixed wing aircraft) with a monitor in view of the pilot. The pilot uses the FLIR display as a guide to assist in flying around the outside edge of the fire perimeter. Visual observations are also used and a color video camera may be mounted beside the FLIR as an additional aid for viewing the fire perimeter. LORAN-C or a satellite positioning system, such as the Global Positioning System (GPS), periodically (every two or three seconds) updates the aircraft position in latitude and longitude. (NOTE: At this time the satellite positioning systems are not quite ready so LORAN-C is used to gather the latitude and longitude points.) Those position points are stored in a small, lap-size, personal computer (PC) which is used as the programmer-controller. Upon completion of the perimeter flight, the PC is taken to the ICP, connected to a pen plotter, and the perimeter is directly plotted, to scale, onto the maps being used at the fire or on overlays. There is no need for interpretation or distortion correction as is necessary for film imagery produced by the IR line scanners. Spot fires inside or outside the main fire perimeter are also stored and plotted. The FLIR units are used, primarily, only to identify the fire perimeter for the pilot, but the FLIR video is recorded on a standard VHS VCR for subsequent playback and review of any selected portion of the fire line as desired. The video will also provide much more detail of selected areas than is available from line scanner film imagery. The latitude and longitude coordinates are displayed on the FLIR video. Night flights could be made, (subject to approved FS night operational methods in use or developed.) The airborne system consists of a FLIR (such as the Inframetrics #445), a LORAN-C antenna and receiver, video caption unit, and a lap-top PC. A color TV camera could be added as an option. The ground system consists of a plotter, the same type of PC, and the VCR and video monitor for playback of the FLIR video.

*Flying InfraRed Enhanced Maneuverable Operational User Simple Electronic Tactical Reconnaisance And Patrol. A complex but "catching" acronym. Alaska called it TROLL for Thermal Recorded Observation and Loran Locating.

The system may also use an airborne transmitter and ground receiver to transmit the fire perimeter points back to the ICP as the helicopter or airplane is flying over it, if the time advantage is worth while. Note that a heliport is usually located in close proximity to ICPs giving a distinct advantage to physical delivery time compared to fixed wing. Within the next 5-10 years mobile (including airborne) satellite voice-grade communications will be in common use so transmission will be available anyway, probably without the need for any special equipment. Until the mobile satellite communications capability is available, transmission of the perimeter data to the ICP can be accomplished using a voice-grade radio and packet controller. The transmission system has been developed and tested but has seen only limited operational use.

ADVANTAGES:

The advantages over traditional IR line scanner mapping methods include availability, user control, flexibility, cost, timeliness of information, and use of system elements for other purposes. FLIR's can be used for other fire and non-fire uses, whether used in the FMT configuration or not. Chuck George has used FLIR's in Operational Retardant Effectiveness (ORE) studies and concluded that they could provide valuable information to fire managers during retardant drops on wildfires.(4) FLIR's have also been used for mop-up, prescribed burns, close-up fire line surveillance, and detailed quick look of selected areas. LORAN-C is useful as a navigation instrument for aircraft and was used by Region 4 in a flight following system for near real-time tracking of aircraft en-route or in remote areas.(5) The FMT has also been used for mapping other areas of interest such as insect or disease damage. Areas that can be seen visibly do not need to use the FLIR capability but the FMT provides a fast and accurate means for positively locating points or areas of any size. Law enforcement applications have been explored.

CONSIDERATIONS:

The FMT has many advantages, some mentioned above, for both fire and other applications. However it is limited for large area fire detection missions because of the smaller field of view than the line scanners. (For perimeter mapping they are not restricted by the size of the fire or other area of interest.) For smaller area detection or to augment visible detection methods they are very good. A major advantage is their ready availability and fast response time compared to the normal line scanner operations. The FMT's can be owned by the regions and used on contract helicopters under local control of the incident or the region. The FLIR's provide fire personnel with a capability for thermally viewing the perimeter or any area of interest showing hot spots and areas which cannot be seen visibly. At the same time they can store the locations for plotting and record the video, with location information and voice annotation for subsequent playback, review, and analysis. This is all accomplished by the region's own trained operators and does not require outside support and specially trained interpreters. The FMT is also very valuable for close-up looks at portions of the fire perimeter to determine whether control lines have been crossed or hot spots adequately suppressed.

COSTS:

Airborne:		
Inframetrics Model 445 FLIR*	$45,000.	
Monitor, VCR, Pwr.Sup., Integration*	2,000.	
Arnav Mod. 15 with RS232C (LORAN-C)*	1,500.	
Portable (lap-size) PC		2,500.
Video Caption Generator		3,800.
Color TV Camera (Optional)		2,000.
Basic system Total (Airborne)	$48,000.*	8,300.

*Items may be included in contract helicopter

Ground:	
Houston Instr. Mod DMP-56 Plotter	$ 6,000.
Portable PC	2,500.
VCR & Monitor	1,400.
Basic Total (Ground)	$ 9,900.
Total, exclusive of *items	18,200.
Total, including FLIR equipment and LORAN	66,200.

Training: Transportation (from Boise) and per diem for two people for 3-4 days.

IMPLEMENTATION:

Regions (or other units) procure above equipment with technical support for procurement from the F&AM Advanced Electronics Group (AEG) at Boise. Equipment will be received and acceptance tested by AEG at Boise lab. Equipment will then be delivered to Region and training provided. Region retains and operates equipment thereafter, year-round, under the control of the trained Regional operators. AEG provides technical support and training. FLIR units require an annual inspection/calibration at AEG lab in Boise. Contract helicopters with a FLIR capability may be available, eliminating the need for procurement and handling of the FLIR unit.

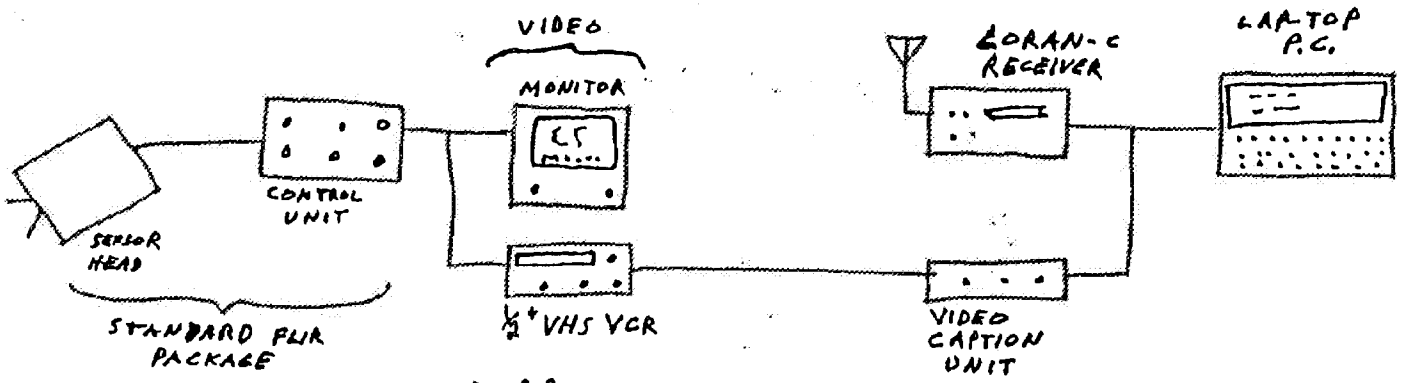
John Warren
Electronics Engineer
F&AM Advanced Electronics
208-389-2653 FTS-554-2653
DG-J.Warren:W02A

References:

1. "FIRE MOUSE TRAP", John R. Warren, October, 1984
2. "FIRE MOUSE TRAP/TROLL Prototype Test & Operations Report", John Warren & Ron Hanks, January, 1986
3. "Alaska Division of Forestry Goes TROLLing", Ron Hanks, John Warren, & Dennis Pendleton, Fire Management Notes, Vol. 47, No. 1
4. "An Operational Retardant Effectiveness Study", Charles W. George, Fire Management Notes, Volume 46, No. 2
5. "Intermountain Region Automated Flight Following System Test/Evaluation Project", Stanley E. Mc Grew, 19 November, 1984

BEST AVAILABLE COPY

FIRE MOUSE TRAP SYSTEM

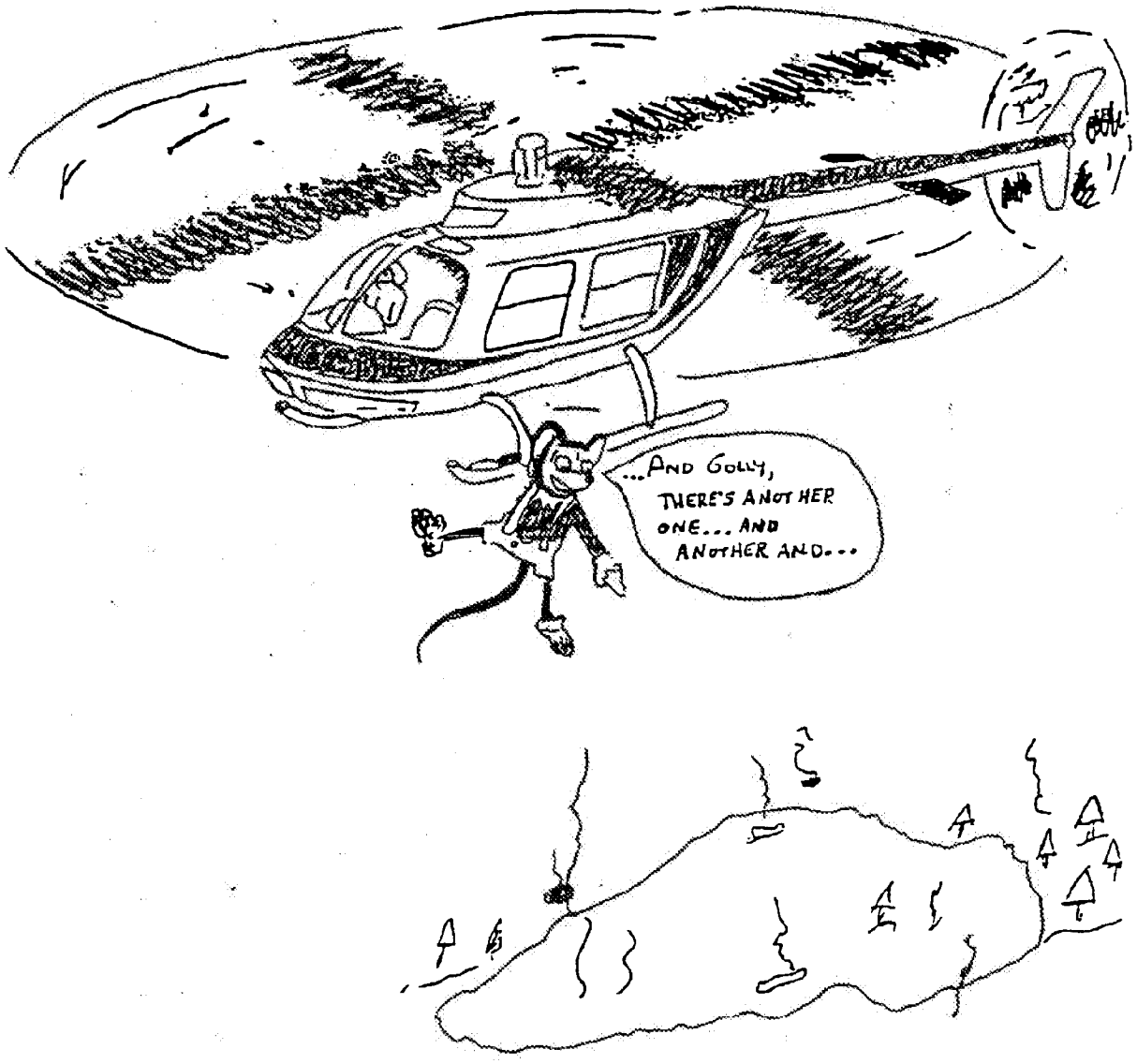


J.W.

FB001525

BEST AVAILABLE COPY

Mapping Fires with the FIRE MOUSE TRAP



Desktop Mapping with Personal Computers

R. Welch
Center for Remote Sensing and Mapping Science (CRMS), Department of Geography, University of Georgia, Athens, GA 30602

ABSTRACT: The Desktop Mapping System (DMS) is a low cost, powerful software package that facilitates image processing for photogrammetric, remote sensing, and GIS applications using off-the-shelf personal computers. Unique design features include the ability to conduct measurements from *monoscopic and stereoscopic* imagery in digital formats, and to undertake the compilation/revision of planimetric, thematic, and topographic map products. Terrain elevations can be derived from digital stereoscopic images by interactive procedures or fully automated stereocorrelation techniques. Accuracies of approximately ± 10 m in *X, Y,* and *Z*-terrain coordinates have been achieved with SPOT stereoimage data. The DMS also interfaces with computer-aided design (CAD) and geographic information system (GIS) software packages such as AutoCAD and ARC/INFO. It is anticipated that the DMS will make mapping oriented image processing and GIS technologies available to educators and scientists from diverse disciplines.

INTRODUCTION

DIGITAL IMAGE PROCESSING for use in remote sensing, photogrammetry, geographic information systems (GIS), and education has been constrained by the cost of hardware/software, complexity of available software packages, and limitations in hardware functionality and display technology. Over the last few years, for example, a number of personal computer (PC) software packages for image processing have been placed on the commercial market. However, only the more expensive packages (> $10,000) were oriented toward planimetric mapping and none provided the capability to derive terrain elevations from stereoimage data in digital formats or were truly compatible with existing GIS software. Consequently, a research project was initiated to develop a low cost, user friendly *mapping* software package for PCs with Intel 80286/80386 microprocessors. The following goals were established:

- Demonstrate the feasibility of using off-the-shelf PCs with *both monoscopic and stereoscopic* image data for planimetric, topographic, and thematic mapping tasks.
- Reduce the complexity of image processing and mapping tasks by featuring key operations in pull-down menus.
- Link raster image processing to vector mapping and GIS applications.
- Make mapping oriented image processing technologies available to educators and scientists concerned with problems in agriculture, cartography, ecology, forestry, geography, hydrology, etc.
- Provide a path for PC software developments that will eventually transfer remote sensing, photogrammetry, and GIS from highly specialized, costly technologies to a broad-based user community.

At the outset, three major problems were apparent: (1) the non-availability of digital image data in floppy disk formats; (2) the limitation imposed by 640 by 350 by 4-bit (16-color) enhanced graphic adapter (EGA) displays; and (3) the speed at which complex, notoriously slow mapping functions associated with geocoding, stereocorrelation, and three-dimensional (3-D) perspective view generation operate on large image data sets. Fortunately, the magnitude of these problems has been reduced by a combination of events. Satellite image data in floppy disk formats may be purchased from EOSAT and SPOT Image Corporation. Display technologies have evolved rapidly since the release of the IBM Professional Graphics Adapter (PGA, 640 by 480 by 256 colors) in 1984, and now include the Video Graphics Array (VGA, 640 by 480 by 16 colors) and enhancements and, most significantly, the IBM Display Adapter 8514/A (1024 by 768 by 256 colors) which is compatible with several 8514 class monitors. Of equal importance has been the release of PCs operating at clock speeds of 16 to 33 MHz, and the development of software designed to make use of efficient user interfaces (e.g., pull-down menus) and take advantage of display and speed enhancements. These advances in technology have enabled the development of the Desktop Mapping System (DMS)® (Welch, 1987).

The DMS was first exhibited in Baltimore, Maryland at the 1987 ASPRS-ACSM conference, where major commercial exhibitors and government agencies were attracted by the ability to quickly derive contours and spot heights using both interactive and automated techniques on a PC. In November 1988, a short course *Desktop Mapping with SPOT Image Data*, was sponsored by the Center for Remote Sensing and Mapping Science (CRMS), University of Georgia, and SPOT Image Corporation. This short course revealed that many individuals having limited skills with PCs, no photogrammetric background, and only cursory experience with digital image processing could, with a few hours of practice, measure *X, Y,* and *Z* terrain coordinates to an accuracy of ± 10 m (± 1 pixel). This accuracy is comparable to that achieved by skilled photogrammetrists with analytical plotters or very sophisticated computer systems (Konecny *et al.*, 1987; Sharpe, 1988).

In this paper, an effort is made to describe those image processing functions of the DMS which allow the preparation of planimetric, thematic, and topographic map products using an off-the-shelf PC in an office environment. However, while attention is given to hardware requirements and to the speed and functionality of the DMS for rectification, vector-on-raster overlay, merging of multiresolution data, and thematic classification, emphasis is placed on those unique aspects of the DMS which facilitate topographic mapping, three-dimensional terrain representation from stereoscopic image data, and integration of image processing and GIS functions. Only recently have three-dimensional mapping and integrated image processing/GIS applications on a PC been given serious consideration.

HARDWARE CONSIDERATIONS

The selection of a PC for digital image processing applications should be based on cost, performance, and display technology. Today, complete computer systems which operate under MS-DOS and utilize 80286/80386 microprocessor technology can be purchased for $2,000 to $10,000. Typical machines include the IBM PS/2 series (Model 30-286 and higher); Compaq 286 and 386 series; Dell 220, 310, and 325; and many others.

Processing speed is critical for computer intensive tasks such as geocoding (i.e., rectifying), automatic stereocorrelation, and perspective view generation. An 80386 machine operating at a clock speed of 20 to 25 MHz (e.g., Compaq 386-20 and 386-25; Dell 310 and 325) will have a 2× to 3× advantage in processing time over an 80286 machine (e.g., IBM PS/2 Model 60) operating

PHOTOGRAMMETRIC ENGINEERING AND REMOTE SENSING,
Vol. 55, No. 11, November 1989, pp. 1651–1662.

0099-1112/89/5511–1651$02.25/0
©1989 American Society for Photogrammetry
and Remote Sensing

at 10 MHz – assuming the required (80387/80287) math co-processors operate at equivalent speeds. This advantage becomes significant when rectifying or deriving elevations for large data sets (Figure 1). In order to take full advantage of inherent processing speeds, disk caching and a disk access of less than 30 milliseconds are desirable.

Recent improvements in display technology have removed significant impediments to low cost image processing. Initial development of the DMS was undertaken on an IBM PC/AT Professional Graphics System (6 MHz) with 640K of RAM. This development platform was subsequently replaced by an IBM PS/2 Model 60 (10 MHz) with 8514/A adapter and 8514 display, permitting either 640 by 480 or 1024 by 786 pixel resolution in 256 colors (from a 256K color palette). At these resolutions, the pixels are square (1:1 aspect ratio) giving equal scale in both the x and y directions, and fine enough to ensure smooth vector representation - important considerations for both mapping and GIS applications.

For planimetric mapping and thematic classification, the standard 640 by 480 by 16 colors VGA display of most PCs will provide an excellent black-and-white rendition of single band digital images and a very usable three-band color image. For topographic mapping from a stereopair of digital images, an 8-bit display is required to ensure perception of a smooth, continuous surface and permit the display of vector overlays.

The 256 colors required for stereoimage display at 640 by 480 or 1024 by 786 resolution can be realized with the IBM Display Adapter 8514/A used in conjunction with any of a number of IBM 8514 compatible displays that have recently entered the market (Rosch, 1989). However, the 8514/A adapter is designed for the IBM PS/2 line of computers featuring microchannel architecture. To achieve comparable display resolution with PC/ATs and most 80386 based machines (e.g., Compaq, Dell), a third-party product such as the new Enertronics Research, Inc. Aurora 1024 board with full 8514 compatibility can be installed. A comparison of 4-bit and 8-bit black-and-white and color images is presented in Plate 1.

PLANIMETRIC MAPPING AND MAP REVISION

Most mapping and GIS operations require that the image data be referenced to a standard rectangular coordinate system such as the Universal Transverse Mercator (UTM) or State Plane systems in common use throughout the United States (Snyder, 1982). In order to obtain correspondence between the image and map coordinate systems, a minimum of four ground control points (GCPs) located in both coordinate systems are used to rectify the image (Figure 2).

Map coordinates for the GCPs may be entered from the keyboard or digitized directly from a reference map with the DMS. The image locations of GCPs are determined by using the mouse to precisely position the on-screen cursor on a 2× or 4× smoothed enlargement of the GCP image location, providing image coordinates to the nearest 0.5 or 0.25 pixel, respectively (Figure 2a). Determination of image coordinates to a fraction of a pixel governs the accuracy to which the image can be geocoded-an important consideration for GIS applications (Welch *et al.*, 1985).

A least-squares solution of polynomial equations is then implemented to yield correction coefficients and to determine a root-mean-square error (RMSE) indicating the fit between the image and ground locations of control points (Figure 2b). Normally, an RMSE value of ± 0.3 to ± 1.0 pixel units can be obtained with SPOT and Landsat images. Application of the correction coefficients on a pixel-by-pixel basis yields a geocoded product, resampled (with cubic convolution, bilinear, or nearest neighbor algorithms) to a pixel dimension of the users choice (Figures 2c and 2d). On an 80386 machine operating at 20 MHz, rectification (with cubic convolution resampling) proceeds at a rate of about 2500 pixels per second, producing a 512 by 480 geocoded image or map file in approximately 1.5 minutes (see Figure 1).

By definition, a geocoded image will register to digital planimetric map files. However, *this registration also can be achieved without resampling the image file.* With the DMS, the correction coefficients discussed above are automatically applied to vector files digitized from corresponding maps, thus ensuring their registration as overlays to the original, unmodified raster image. All image coordinates transformed by the coefficient file are stored on disk as ground or map coordinates, facilitating their use for mapping and GIS applications. The above procedures are efficient and eliminate the need for pixel-by-pixel rectification. They also provide the necessary mechanism for registering pc ARC/INFO, USGS Digital Line Graph (DLG), and AutoCAD files to the image data.

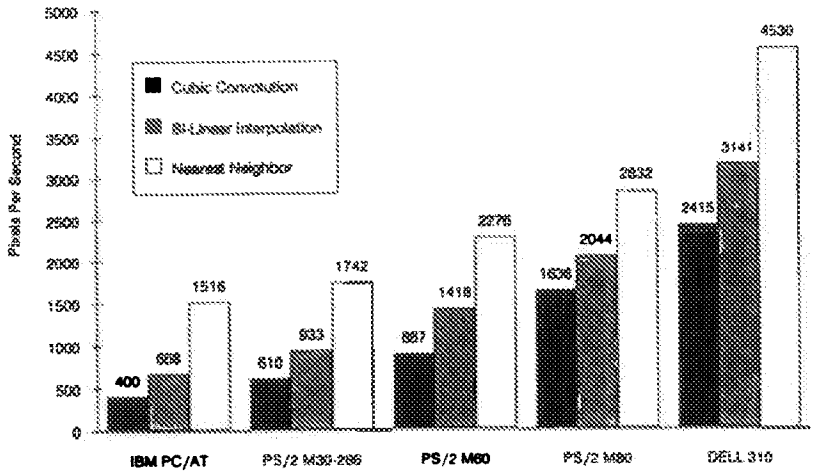


FIG. 1. DMS rectification rates on IBM PS/2 and Dell personal computers. All computers were equipped with factory installed hard disks and 80287 or 80387 math coprocessors. Processor speeds are 6 MHz (AT), 10 MHz (M30, M60), 16 MHz (M80), and 20 MHz (310).

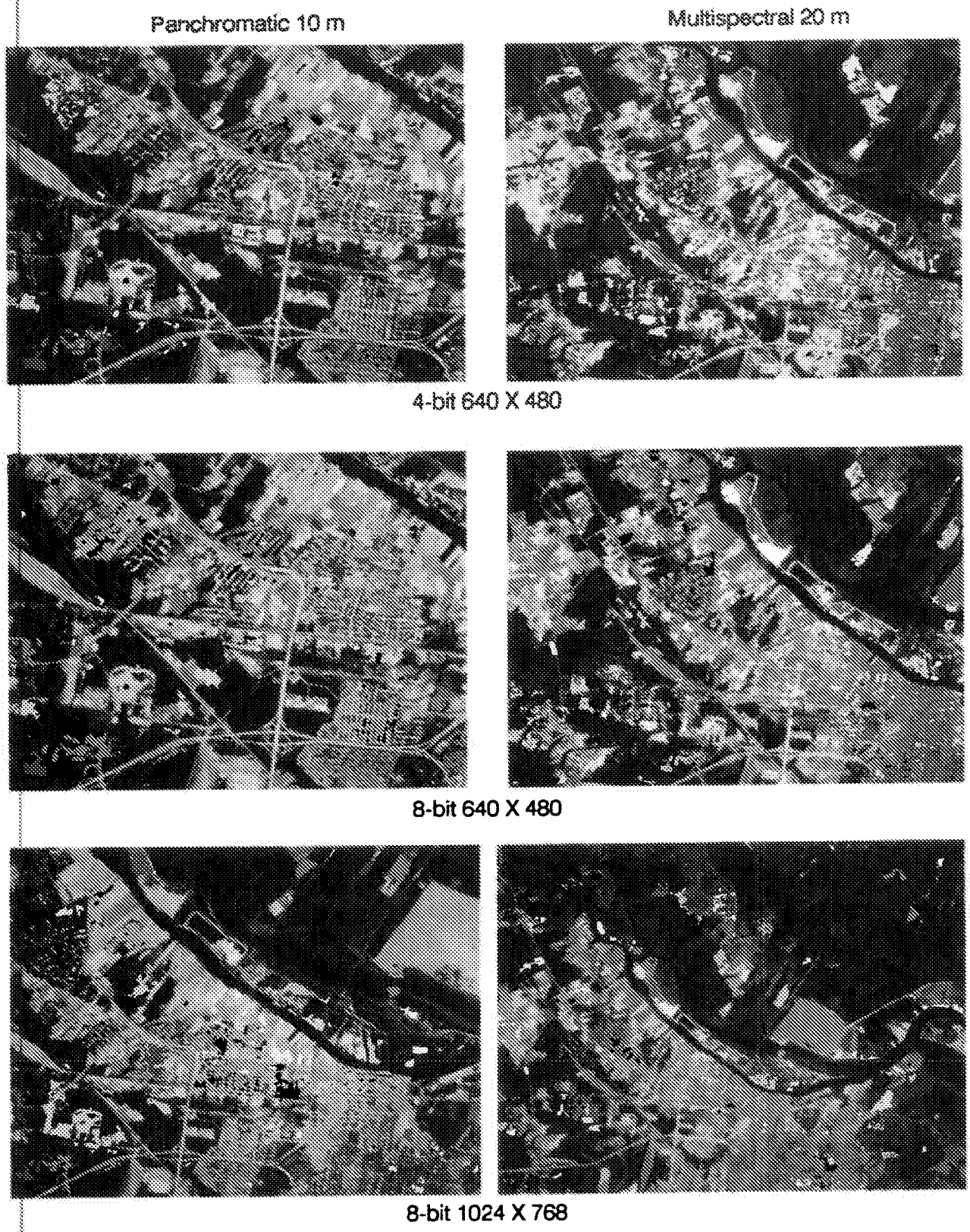
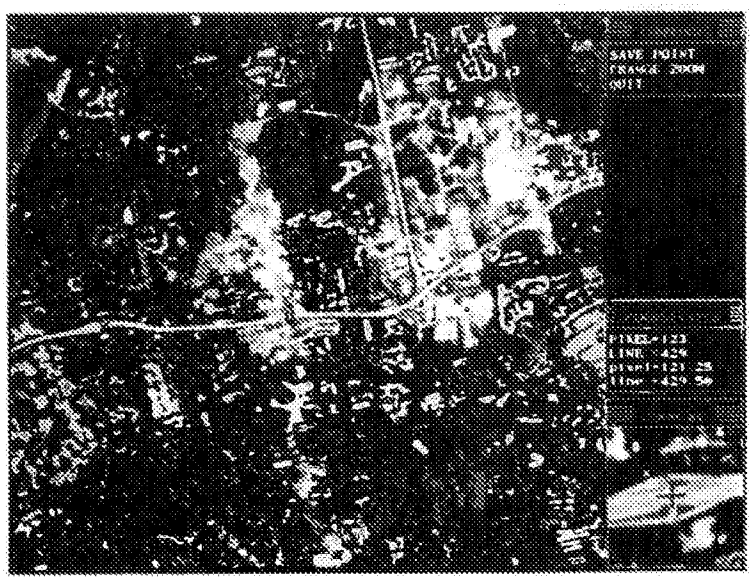


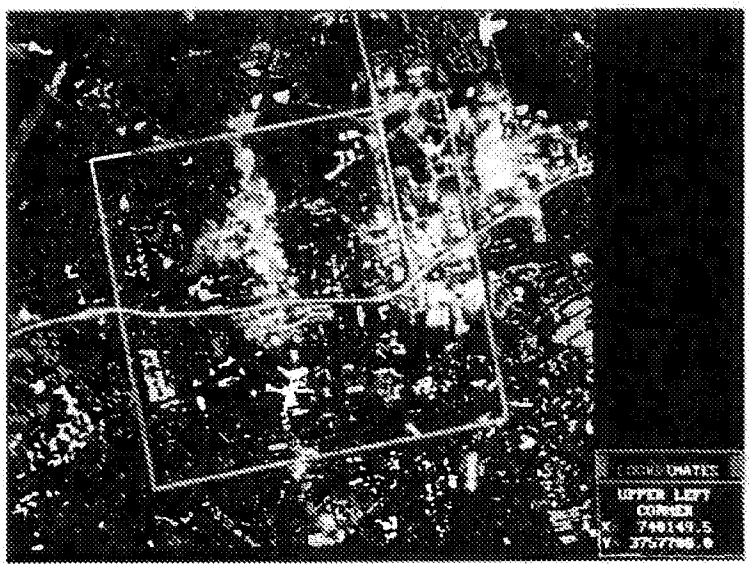
PLATE 1. Comparison of DMS 4-bit and 8-bit image displays of Savannah, Georgia. Original data are SPOT panchromatic (10-m) and multispectral (20-m) images.



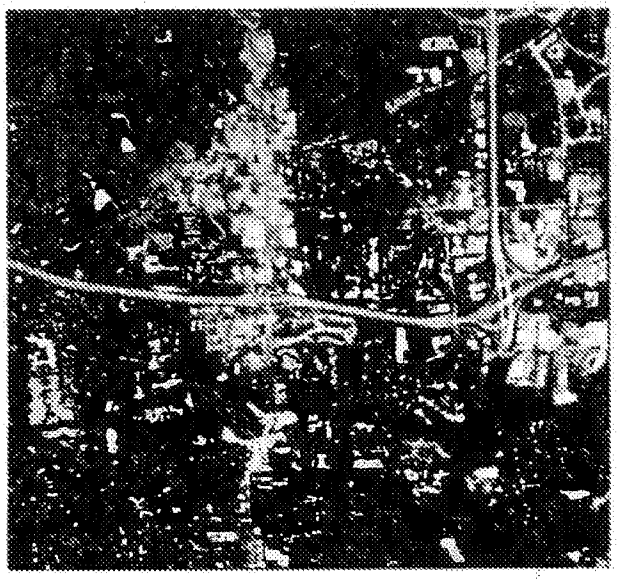
(a)

#	True X	True Y	Est X	Est Y	Error
1	742302	3755318	742301	3755314	3.62
2	743768	3754825	743770	3754830	5.44
3	746056	3758086	746054	3758085	2.09
4	739820	3758716	739821	3758722	6.39
5	739751	3755660	739750	3755661	1.51
6	739603	3756592	739600	3756589	4.08
7	741072	3757857	741075	3757851	6.24
			RMSExy (0.46 pixels)		4.56

(b)



(c)



(d)

FIG. 2. Steps in geocoding satellite image data. (a) SPOT panchromatic image (10 m) of Atlanta, Georgia with annotated control points displayed. Note enlargement window for refinement of control point location; (b) computation of rectification coefficients and residual planimetric error; (c) area to be rectified (in box); (d) geocoded image at 8-m pixel resolution.

MAP COMPILATION AND REVISION

Map compilation and revision from digital data sets require provision for overlay of existing vector files, enlargement or reduction of images, an ability to create vector files with attached attributes from raster image data, and a method for editing the vector files in digital format (Usery and Welch, 1989). In addition, because of the availability of digital image data at resolutions ranging from greater than 1000 m to less than 10 m recorded by a variety of electro-optical and electronic sensors (e.g., NOAA AVHRR; Landsat MSS, TM, SIR-B; SPOT HRV), it is important to be able to merge multisensor, multiresolution, multitemporal image files to create a composite image of improved resolution from which important map features can be extracted (Schowengerdt *et al.*, 1984; Chavez, 1986). With the DMS, image files are easily merged using an intensity-hue-saturation (IHS) algorithm (Welch and Ehlers, 1987).

The planimetric mapping capability of the DMS was used to revise a 1:12,000-scale utility map of a section of the Atlanta metropolitan area (Figure 3). A rectangular 6 by 5 km study area was defined on panchromatic and multispectral SPOT images

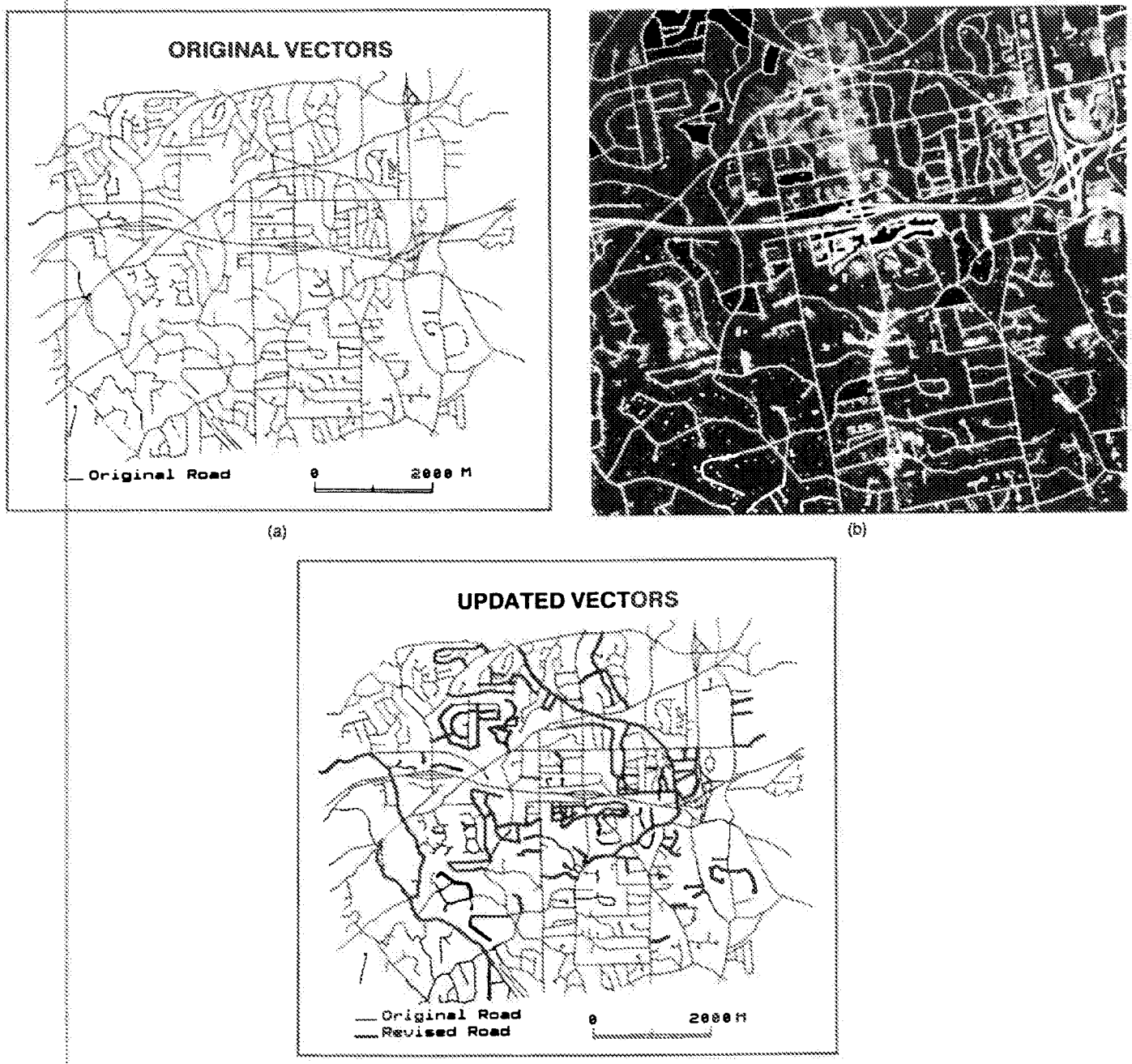


FIG. 3. Map revision with the DMS. (a) Vectors for Atlanta, Georgia digitized from existing map; (b) SPOT panchromatic image (10 m) with vector file as overlay; (c) revisions to vector file.

(Level 1B), and the panchromatic image rectified to the UTM coordinate system using GCPs digitized from USGS 1:24,000-scale topographic maps. In order to facilitate merging these data sets, the multispectral images were resampled to 10-m pixels using a cubic convolution algorithm.

The resampled multispectral images in combination with the SPOT panchromatic data were used to produce a composite IHS image of improved resolution suitable for revision tasks. Vectors digitized from the utility map (Figure 3a) were registered to the image using the overlay option of the DMS. New road features noted on the composite SPOT image were then added to the map file with the on-screen digitizing option (Figure 3b), and errors in the map file were revised (Figure 3c). Overall, the superior geometric quality of the SPOT images was noted and the 10-m resolution proved adequate to update the map file and correct for errors in street location and alignment.

THEMATIC MAPPING

The principles of thematic classification are well-documented (Jensen, 1986). With the DMS, a sequential approach to supervised classification is employed which permits automated classification procedures to be combined with interactive techniques, simulating a conventional photo-interpretation process. Classification is based on up to ten bands.

In practice, a pull-down menu defines the options and a legend for thematic classes is presented. Training sites are selected

for a given class, statistics generated, and a parallelepiped classification implemented by color coding the image pixels. This procedure is then repeated for each class until complete. It is possible to interrupt the classification in order to rectify mistakes by "unclassifying" features. Also, if desired, the boundaries of troublesome areas can be outlined and known classes overwritten. The unclassify and overwrite options provide considerable flexibility and when properly used ensure a classification of high accuracy. For a 512 by 480 image and four bands, a complete classification cycle (outline training sets, select the class name, and classify) requires about 30 seconds on a PC operating at 20 MHz. If required, vectors may be overlaid on the classified image using the planimetric mapping option.

TOPOGRAPHIC MAPPING AND TERRAIN REPRESENTATION

The DMS-Stereographic Module is the *first* PC software package that permits the interactive measurement of *Z*-terrain coordinates (contouring and spot heights) from stereoimage data in digital formats, generation of digital elevation models (DEMs) by automated stereocorrelation, creation of perspective terrain models, and the development of orthoimages. These capabilities are discussed in the following paragraphs.

Interactive Contouring

In order to contour a stereopair, it is necessary to perceive the terrain in three-dimensions. This can be accomplished through the use of anaglyph, polarizing, binocular, or liquid crystal shutter display techniques that ensure the left and right eyes view only the corresponding images of the stereopair. With the DMS, an anaglyph display technique is normally employed, requiring the user to wear eyeglasses with red (left) and blue (right) lenses. Although an anaglyph display may be considered an "old" technique, it can be implemented on standard color monitors without the addition of expensive image memory boards or special attachments. The intensity and illumination fall-off problems that have plagued traditional photogrammetric instruments are not experienced with a computer monitor. Thus, it is feasible to undertake mapping operations in a normally lit room. By taking advantage of the digital enhancement capabilities of the DMS, it is possible to quickly produce images of optimal contrast for stereo viewing.

An alternative approach to the anaglyph display of stereoscopic images involves the use of the new liquid crystal shutter technology as represented by the Tektronix SGS 430 and 620 systems. These shutters are controlled by a Stereoscopic Graphic Adapter card mounted in the PC and produce circularly polarized images at a frequency of 120 Hz which are viewed through polarizing glasses. The liquid crystal shutter display provides a comfortable, high resolution viewing environment, well suited for the display of all types of panchromatic and multispectral image data, including non-topographic images recorded by scanning electron microscopes (SEMs) and X-ray machines. Although the addition of the liquid crystal shutter significantly increases the cost of the hardware components, this cost is insignificant compared to that of digital stereoplotters now beginning to enter the market (Cogan *et al.*, 1988).

In practice, the two images of the stereopair are rectified to a common datum and one or more reference elevation points are identified. These reference points are used to "calibrate" the stereomodel. Elevations are measured by means of a floating dot, in precisely the same manner as with a conventional analog or analytical stereoplotter. However, the *Z*-motion is controlled with the arrow keys on the computer keyboard and planimetric motion is implemented with the mouse. If desired, the stereoimage can be enlarged or reduced up to 5× (in about 10 seconds); however, enlarging the digital image beyond 2× does not seem to facilitate contouring or heighting. The ability to *reduce* the scale of the displayed image is very useful when viewing mountainous terrain at base-to-height (*B/H*) ratios approaching 1.0. In these instances parallax too large to be visually perceived is also reduced, enabling the observer to obtain a clear, three-dimensional image.

The precision and ultimately the accuracy to which *Z*-coordinates can be determined is controlled by (1) the *B/H* ratio of the stereopair, (2) the pixel resolution, and (3) the stereoscopic acuity of the user or the sensitivity of the correlation technique. With satellite imagery, geometric quality is excellent due to the inherent stability of the satellite and the systematic corrections introduced to the data. Image deformations, at least for subscene-size datasets on the order of 1024 by 1024 pixels or less, do not appear to be a significant problem. Thus, the computer intensive, sophisticated analytical photogrammetric restitution techniques employed with aerial photographs are not required to achieve acceptable measurement accuracies with Landsat or SPOT images.

The theory of deriving *Z*-coordinates from satellite images in digital format has been a subject of considerable discussion (Welch and Marko, 1981; Welch, 1985; Rodriguez *et al.*, 1988). With satellite sensor systems such as the pointable HRVs of SPOT, the general equation for determining the *difference* in elevation (Δh) between two points is

$$\Delta h = \frac{H \cdot \Delta p}{B} = \frac{\Delta p}{\tan \alpha_1 + \tan \alpha_2}$$

where $\frac{H}{B}$ = the inverse of the *B/H* ratio. It is computed from the incidence angles (α) noted in the SPOT header records for the two scenes forming the stereopair. The *B/H* ratio is equal to $\tan \alpha_1 + \tan \alpha_2$

Δp = the difference in parallax between the two points

The Δh values when added to the known *Z*-coordinate for a control point or reference point in a screen-sized area, yield absolute elevations (*Z*) referenced to mean sea level. That is, assuming no deformation in the stereoimage:

$$Z = Z_{ref} + \Delta h$$

where Z_{ref} = the *Z*-coordinate for a reference point of known elevation. The pixel resolution establishes the measurement threshold for Δp.

Thus, for a stereopair of SPOT panchromatic images (10-m resolution) recorded at a *B/H* ratio of 1.0, a measurement error of ± 1 pixel will cause an equivalent error (± 10 m) in the *Z*-coordinate. Reduction of the *B/H* ratio will produce a proportionate increase in this error. Consequently, *B/H* ratios of about 1.0 are desirable for areas of flat to rolling terrain, whereas values of approximately 0.5 to 0.8 are better suited to mountainous regions where larger contour intervals are appropriate.

Tests of contouring and spot height accuracies with the DMS have produced excellent results. Terrain profiles developed from contours compiled with the DMS at a 50-m interval from SPOT panchromatic images (*B/H* = 0.57), and from a USGS topographic map (C.I. = 40 feet) of the same area, agreed to within ± 11 m and ± 15 m, respectively (Figure 4). Comparisons of elevations measured from SPOT panchromatic stereopairs having *B/H* ratios of 0.9 and 1.0 with elevations derived from topographic maps of 1:24,000- and 1:50,000-scale yielded RMSE$_z$ values of about ± 10 m. As map errors are included in these figures, it is evident the PC/DMS combination does provide heighting capabilities approaching those obtained with sophisticated analytical plotters or computer systems which are an order of magnitude more

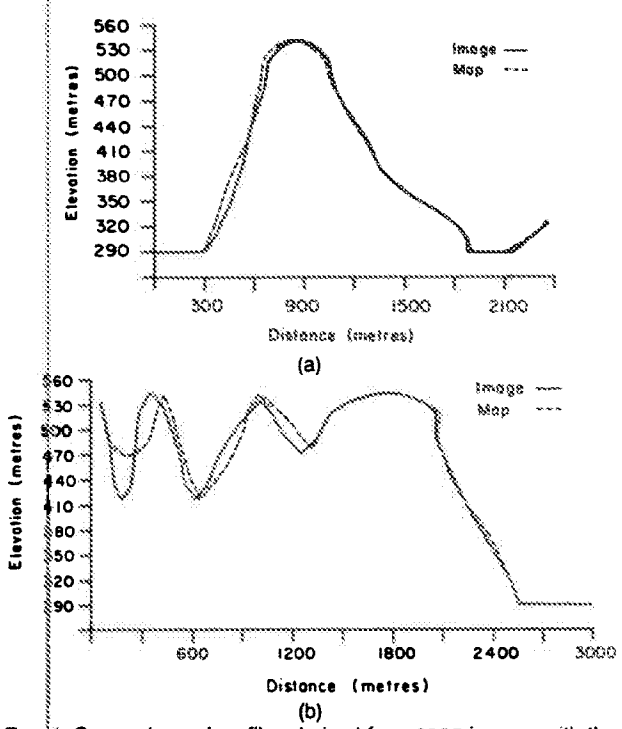


FIG. 4. Comparison of profiles derived from SPOT images with the DMS Stereographic Module and corresponding profiles taken from a USGS topographic map (C.I. = 40 feet). $RMSE_z$ values of ± 11 m and ± 15 m were obtained for profiles (a) and (b), respectively.

expensive (Gugan and Dowman, 1988). Of much greater significance, however, is the ability of the novice user to achieve acceptable measurement accuracies and to rapidly contour the terrain after only a few hours of practice.

The above approach also has been successfully used to develop contours from scanned aerial photographs (Figure 5). However, the tradeoffs between data volume, pixel resolution, measurement accuracy, and display resolution become a major problem when working from aerial photographic data in digital formats. For example, in order to capture the resolution of a stereopair of mapping photographs, it is necessary to scan them (or at least the stereomodel) at a pixel resolution of approximately 25 μm, creating a data set of about 85 Mbytes/photo or 68 Mbytes/stereomodel. With a stereopair of 1:80,000-scale aerial photographs scanned at 25-μm resolution (2 m on the ground), a 2- by 2-km patch of terrain will be visible on a 1024 by 1024 display. At 2-m resolution, heighting errors of about ± 3 to ± 5 m can be expected. Although the trend toward all digital photogrammetry is clear, it is equally evident that problems of data capture, storage, and display require attention.

STEREOCORRELATION

Stereocorrelation is a computational procedure utilized to automatically derive terrain elevations from digital images (Ackermann, 1984). When a stereopair of images rectified to a common datum are placed in register, the residual planimetric differences in the x-coordinates are assumed to result from relief displacement and can be determined by automatic correlation techniques (Ehlers and Welch, 1987). Differences in x-parallax may then be used to derive relative elevations or height differences, which when referenced to one or more GCPs of known elevation as described above, yield the absolute elevations required to form a DEM. The DEM is a fundamental requirement for the generation of contours, slopes, aspects, 3-D perspectives, and relief-corrected orthoimages. Recent experiments with stereoimages have confirmed the ability to achieve correlations to within ± 0.3 to ± 1.0 pixels (Rosenholm, 1986; Simard, 1988).

Stereocorrelation, however, is a *very* computer intensive task that until recently was viewed as suitable for only the most powerful minicomputer systems. With the DMS, stereocorrelation speeds of 30 to 60 pixels per second are routinely realized on a Dell 310 PC operating at 20 MHz (Figure 6). Thus, assuming the use of SPOT images of 10-m resolution, a grid of points at 50-m spacing can be computed for a 1024 by 1024 image in less than 25 minutes. Because stereocorrelation is undertaken as a batch

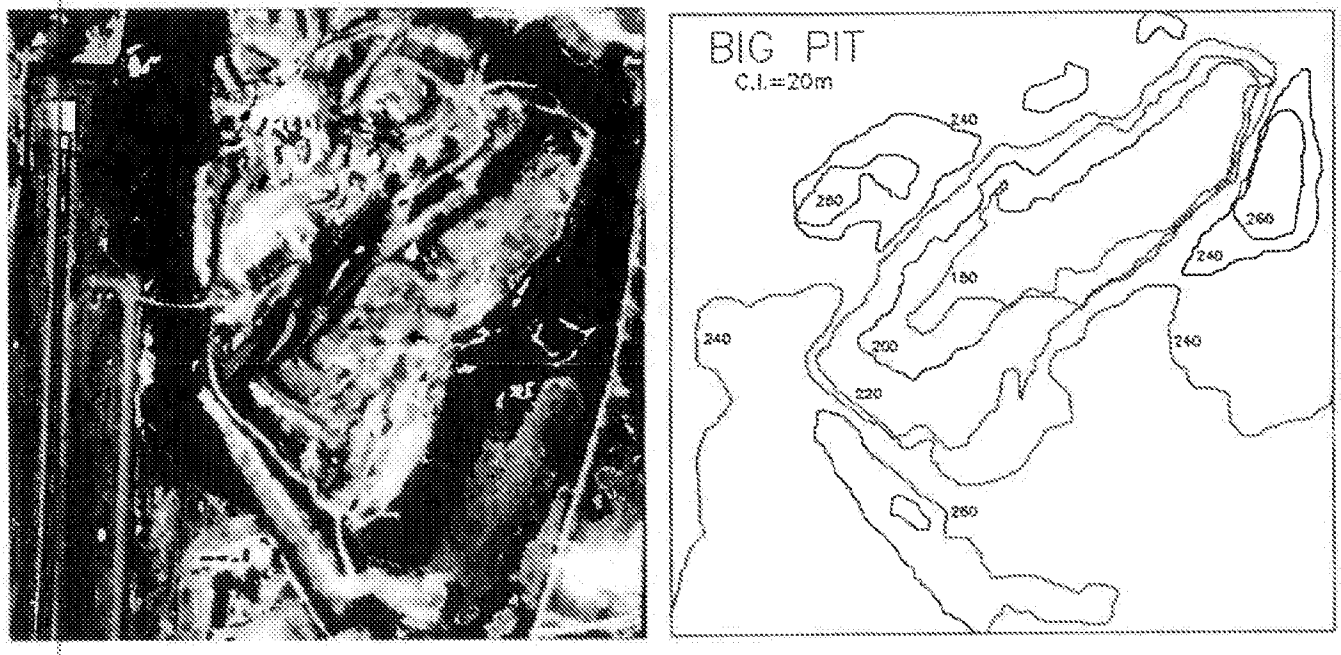


FIG. 5. (a) Section of an air photo digitized at 2.8 m pixel resolution, and (b) contours of a gravel pit (C.I. = 20 m) produced with the DMS.

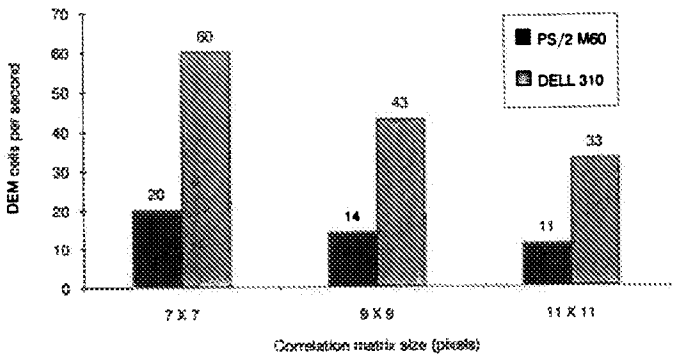


FIG. 6. Comparison of stereocorrelation rates for 80286 (IBM PS/2) and 80386 (Dell 310) computers.

job, the operator may, if desired, implement this task during off-peak hours. The completeness and accuracy of the DMS stereocorrelation will vary according to the selection of correlation matrix size, tonal and contrast similarities of the images forming the stereopair, terrain configuration, and *B*/*H* ratio. To date, completeness of correlation has averaged 80 percent or better and accuracies equivalent to ± 0.5 to ± 1.0 pixel are realized.

The DMS features a capability for interactively editing DEMs generated by the stereocorrelation option. A matrix of DEM "floating points" is superimposed on the stereoimage. The operator quickly scans the stereoimage, noting which points do not lie on the terrain surface. The elevations of these incorrectly correlated points may be adjusted with the mouse. Thus, the stereocorrelation editing option enables the user to take advantage of both automatic and interactive heighting capabilities.

Perspective Views

The ability to create a perspective view of the terrain and to drape digital numbers (DNs) or color values of the pixels on the perspective is of considerable interest to foresters, geographers, geologists, planners, and military intelligence specialists (Plate 2). Major drawbacks to generating terrain perspectives, however, include the volume of data to be manipulated, the time required to generate a display of adequate resolution, and the difficulty in establishing optimum vertical exaggeration, viewing angle, and azimuth. With the DMS, these problems are addressed by initially generating a coarse resolution wire frame or draped perspective at a cell size defined by the user. This coarse perspective is then rotated and tilted, and the vertical exaggeration is adjusted. Once the viewing parameters have been determined for the coarse resolution perspective, cell size is reduced to yield a high resolution perspective display. In this way, time consuming iterations of the display are reduced or eliminated. Comparisons of the rates at which fishnet perspectives (with and without hidden lines removed) can be generated on different hardware configurations are presented in Figure 7. It is interesting to note that direct comparisons for displaying the same DEM data sets as fishnet perspectives using the ARC/INFO TIN module operating on a Prime 2250 *minicomputer* and the DMS on a Dell 310 *PC*, show an approximate 20× speed advantage for the DMS/PC combination. Provided the DEM cell size corresponds to the image pixel dimension, the speeds at which draped perspectives are created will roughly correspond to those for the hidden lines removed column of Figure 7.

Orthoimages

Satellite images, like aerial photographs, suffer from displacement caused by terrain relief. The magnitude of relief displacement increases outward from the nadir and with pointable sensors, such as the SPOT HRVs oriented to ± 27 degrees east or west of the orbit track, relief displacements of greater than 50 pixels can occur in mountainous terrain, preventing the registration of planimetric and topographic features. In order to correct for relief displacements and ensure feature registration, terrain elevations must be known (Swann *et al.*, 1988).

With the DMS, a regular grid of terrain elevations can be derived directly by implementing on the PC the automated stereocorrelation option (or indirectly by first contouring the terrain or measuring the heights of the grid locations). Because the parallax at each pixel is known, the relief displacement relative to one image of the stereopair can be calculated and offsets introduced in the *x*-direction to place the pixels in their correct planimetric positions. The elevations required to generate the offsets also may be imported from USGS or DMA digital terrain data. Thus, it is possible to create orthoimages and image maps

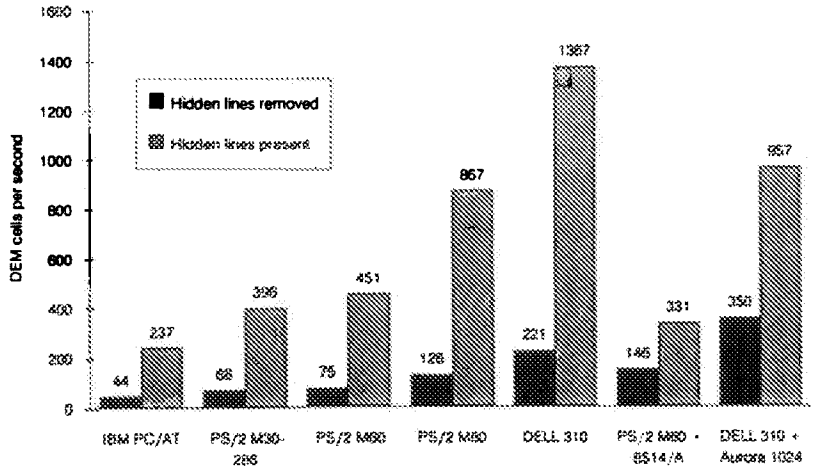


FIG. 7. Comparison of DMS rates (in DEM cells per second) for generation of perspective views with and without hidden lines removed. These rates include both calculation and display time. Except as noted, all computers were equipped with 80287 or 80387 math coprocessors and VGA boards.

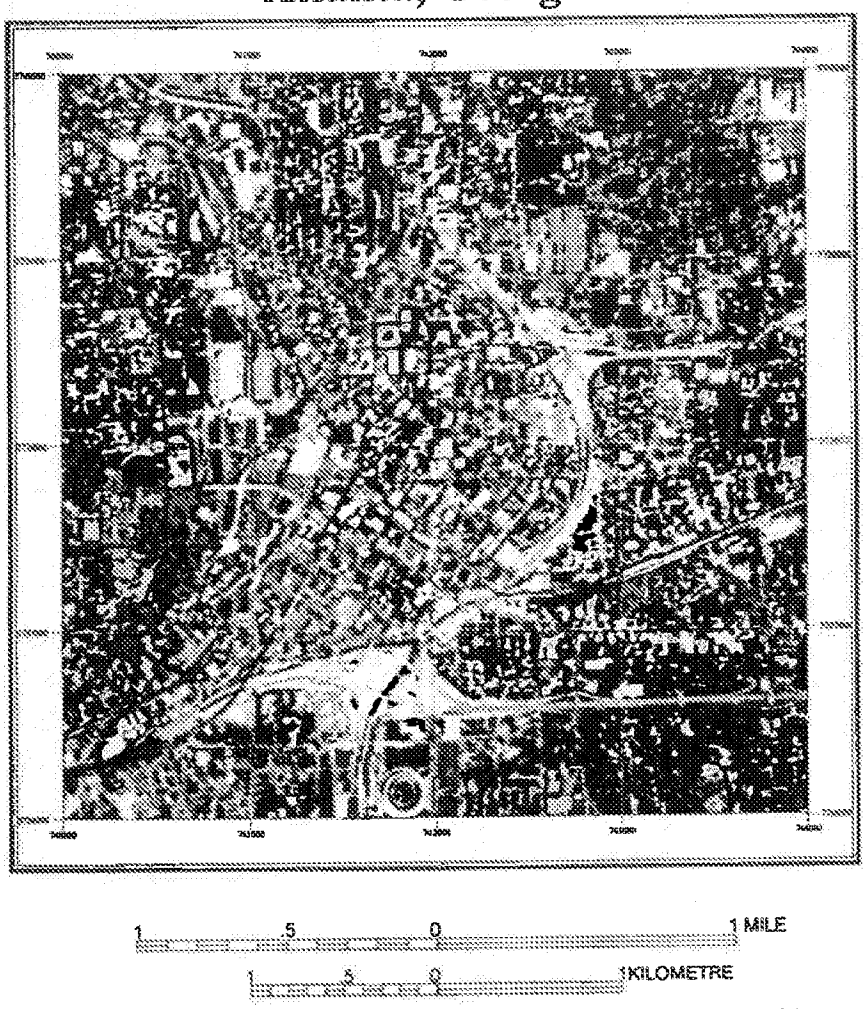


FIG. 8. Orthoimage generated with the DMS and SPOT panchromatic (10-m) data of Atlanta, Georgia.

of even the most rugged terrain that can serve as the reference layer for a GIS database (Figure 8).

INTERFACE BETWEEN IMAGE PROCESSING AND GIS

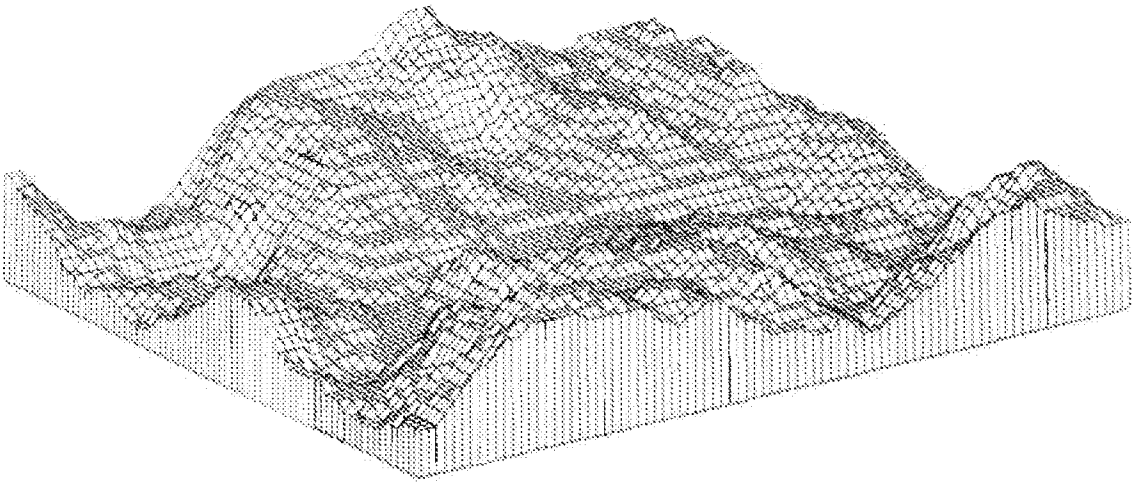
Today, emphasis is being placed on registering vector USGS Digital Line Graph, Bureau of Census TIGER, and GIS data files (e.g., ARC/INFO) with raster images for update or analysis. For such applications, the ability to read different data formats is important, as is the ability to place the vector files in exact registration with the image data. In this context, the DMS may be employed to create vector files that can be utilized with the ESRI ARC/INFO package resident on the same computer. Also, ARC/INFO files can be transported into the DMS environment for registration with digital image data (Welch, 1988). An example of the use of these capabilities to identify potential sites for small shopping centers in an urban/suburban setting is presented here.

A road net for the city of Athens, Georgia was digitized in vector format from USGS 1:24,000-scale topographic maps using the CAPTURE option within DMS. Because the topographic maps were about 15 years old, it was necessary to update the Athens vector file from a SPOT panchromatic image using the previously described revision techniques. A DMS conversion utility was then employed to transform the updated vector file to ARC/INFO format.

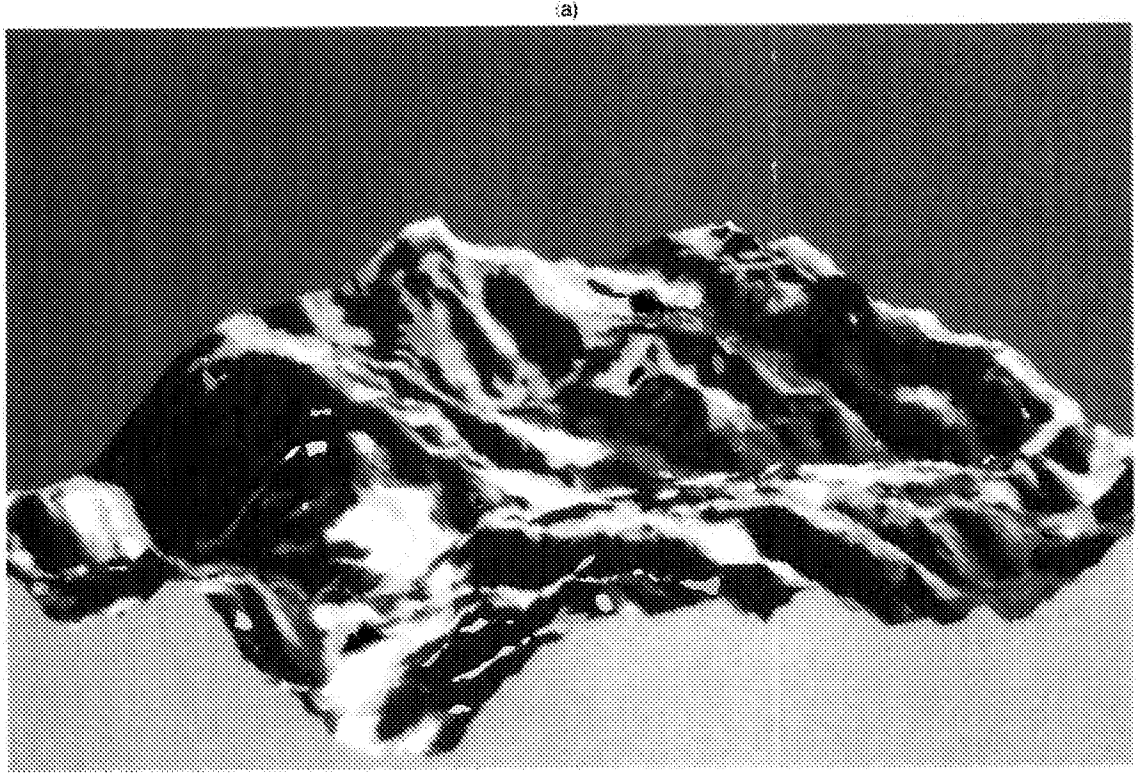
Within pc ARC/INFO — accessed by a few keystrokes — a coverage for the Athens road net was produced using the GENERATE command. Additional tasks undertaken with pc ARC/INFO included building the topology, adding attribute information, conducting a buffer analysis along major roads to create a 200-m wide zone within which shopping centers potentially could be located, and composing maps with ARCPLOT (Figures 9a and 9b). The UNGENERATE command was then employed to create an ASCII file of buffer coordinates which could be used within the DMS to overlay the buffers on the image data (Figure 9c). Once the buffers were superimposed on this image, it was possible to select and outline potential shopping center sites with the planimetric mapping option of the DMS. Of course, if required, other GIS coverages related to zoning, land prices, population density, market areas, and travel time also can be transferred from ARC/INFO to the DMS for registration with the image data.

CONCLUSION

The increased emphasis on the integration of image processing, photogrammetry, remote sensing, and GIS technologies

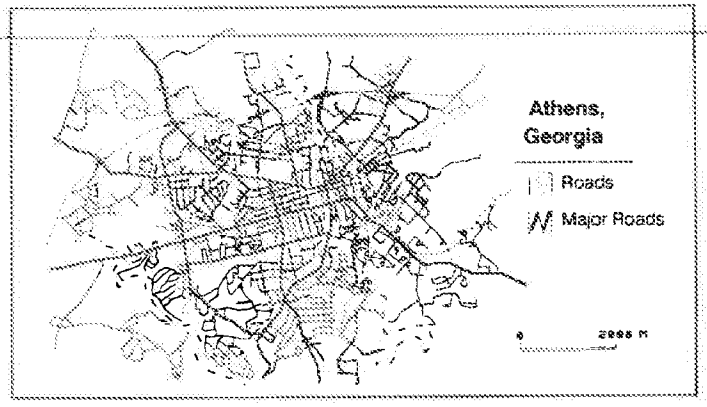


(a)

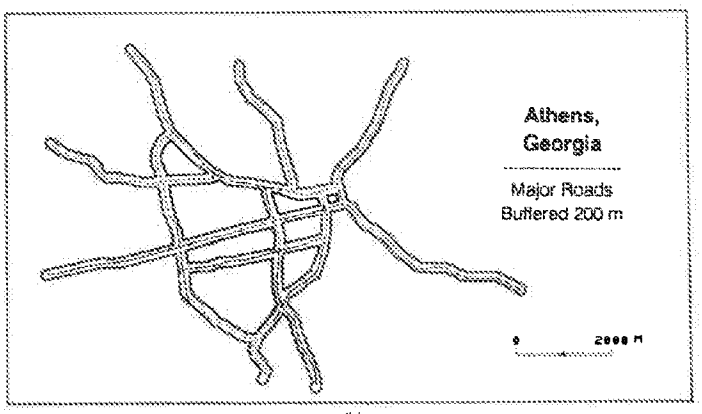


(b)

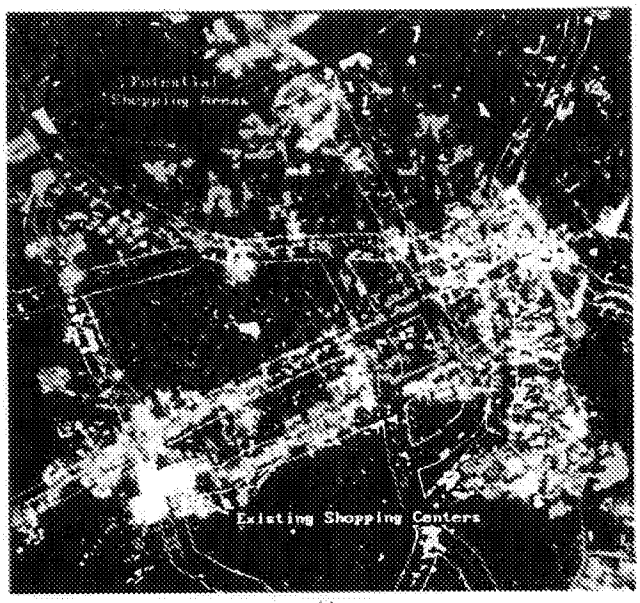
PLATE 2. (a) Wireframe perspective of DEM generated by automatic stereocorrelation from SPOT image data of north Georgia, and (b) multispectral Landsat TM image draped on the wireframe perspective.



(a)



(b)



(c)

FIG. 9. (a) Road map of Athens, Georgia created with pc ARC/INFO; (b) major roads buffered to indicate potential areas for the location of shopping centers; (c) buffers superimposed on a raw display of the SPOT panchromatic image (10 m) with existing and potential shopping center locations noted.

mirrors the growing demand for image and map data in digital formats. In this context, the DMS has been optimized to allow complex mapping tasks such as rectification, merging of multiresolution image data, interfacing raster image processing and vector GIS functions, thematic classification, and, particularly, the development of three-dimensional topographic data sets and orthoimages to be undertaken on off-the-shelf PCs in an office environment. Significantly, subpixel measurement accuracies in *X*, *Y*, and *Z* can be achieved by persons having only a few hours of training and little or no previous experience in photogrammetry and digital image processing. Results from investigations with SPOT stereodata, for example, have yielded RMSE values of ± 10 m and better depending on the quality and *B/H* ratio of the images. Computer intensive tasks such as rectification, automated stereocorrelation, and perspective view generation can be accomplished on 80386 PCs at speeds exceeding those realized on larger minicomputer systems.

It is anticipated that the continued evolution of PC and mapping software technology, coupled with low maintenance costs, will result in the transfer of many image processing, mapping, and GIS tasks from a specialized service industry to a broad-based user community. The DMS and similar software packages will facilitate this trend.

ACKNOWLEDGMENTS

The efforts of S. S. Fung, T. R. Jordan, D. Papacharalampos, and M. Remillard in converting a concept to an operational product are gratefully acknowledged. SPOT image data are copyrighted ((c) 1986) by the Centre National d'Etudes Spatiales, Toulouse, France and distributed in the United States by SPOT Image Corporation, Reston, Virginia. The DMS is now being marketed under license by ERDAS, Inc., Atlanta, Georgia.

REFERENCES

Ackermann, F., 1984. Digital Image Correlation: Performance and Potential Application in Photogrammetry. *Photogrammetric Record*, Vol. 11, No. 64, pp. 429–439.

Chavez, P. S., Jr., 1986. Digital Merging of Landsat TM and Digitized NHAP Data for 1:24,000-Scale Image Mapping. *Photogrammetric Engineering and Remote Sensing*, Vol. 52, No. 10, pp. 1637–1646.

Cogan, L., D. Gugan, D. Hunter, S. Lutz, and C. Peny, 1988. Kern DSP1 Digital Stereo Photogrammetric System. Paper presented at the XVI ISPRS Congress, Kyoto, Japan, July 1-10, 10 p.

Ehlers, M., and R. Welch, 1987. Stereocorrelation of Landsat TM Images. *Photogrammetric Engineering and Remote Sensing*, Vol. 53, No. 9, pp. 1231–1237.

Gugan, D. J., and I. J. Dowman, 1988. Topographic Mapping from SPOT Imagery. *Photogrammetric Engineering and Remote Sensing*, Vol. 54, No. 10, pp. 1409–1414.

Jensen, J. R., 1986. *Introductory Digital Image Processing*, Prentice-Hall, Englewood Cliffs, New Jersey, 379 p.

Konecny, G., E. Kruck, P. Lohmann, and H. Engel, 1987. Evaluation of SPOT Imagery on Analytical Photogrammetric Instruments. *Photogrammetric Engineering and Remote Sensing*, Vol. 53, No. 9, pp. 1223–1230.

Rodriguez, V., P. Gigord, A. C. De Gaujac, P. Munier, and G. Begni, 1988. Evaluation of the Stereoscopic Accuracy of the SPOT Satellite. *Photogrammetric Engineering and Remote Sensing*, Vol. 54, No. 2, pp. 217–221.

Rosch, W. L., 1989. Compromising Resolutions - 8514 Monitors Build on VGA. *PC Magazine*, Vol. 8, No. 3, pp. 195–232.

Rosenholm, D., 1986. Accuracy Improvement of Digital Matching for Evaluation of Digital Terrain Models. *Proceedings of the ISPRS Commission III Symposium*, Rovaniemi, Finland, IAPRS XXVI-3/2, pp. 573–587.

Schowengerdt, R., S. Park, and R. Gray, 1984. Topics in Two-Dimensional Sampling and Reconstructions of Images. *International Journal of Remote Sensing*, Vol. 5, No. 2, pp. 333–347.

Sharpe, B., 1988. Geometric Processing in MacDonald Dettwiler's MERIDIAN-GICS System. *Proceedings of the International Symposium on Topographic Applications of SPOT Data*, 13-14 October, Sherbrooke, Quebec, pp. 76–85.

Simard, R., 1988. L'Interet de L'Utilisation Du Systeme Cartospot Pour la Production de Cartes Topographiques. *Proceedings of the International Symposium on Topographic Applications of SPOT Data*, 13-14 October, Sherbrooke, Quebec, pp. 286–296.

Snyder, J. P., 1982. *Map Projections Used by the U.S. Geological Survey*, Geological Survey Bulletin 1532, U.S. Government Printing Office, Washington, D.C., 313 p.

Swann, R., D. Hawkins, A. Westwell-Roper, and W. Johnstone, 1988. The Potential for Automated Mapping from Geocoded Digital Image Data. *Photogrammetric Engineering and Remote Sensing*, Vol. 54, No. 2, pp. 187–193.

Usery, E. L., and R. Welch, 1989. A Raster Approach to Topographic Map Revision. *Photogrammetric Engineering and Remote Sensing*, Vol. 55, No. 1, pp. 55–59.

Welch, R., 1985. Cartographic Potential of SPOT Image Data. *Photogrammetric Engineering and Remote Sensing*, Vol. 51, No. 8, pp. 1085–1091.

———, 1987. Integration of Photogrammetric, Remote Sensing and Database Technologies for Mapping Applications. *Photogrammetric Record*, Vol. 12, No. 70, pp. 409–428.

———, 1988. Remote Sensing and GIS Data Integration. *Geographic Information Systems Seminar: Data Sharing - Myth or Reality*. Ministry of Natural Resources, Toronto, Ontario, pp. 138–145.

Welch, R., and M. Ehlers, 1987. Merging Multiresolution SPOT HRV and Landsat TM Data. *Photogrammetric Engineering and Remote Sensing*, Vol. 53, No. 3, pp. 301–303.

Welch, R., T. R. Jordan, and M. Ehlers, 1985. Comparative Evaluations of the Geodetic Accuracy and Cartographic Potential of Landsat-4/-5 TM Image Data. *Photogrammetric Engineering and Remote Sensing*, Vol. 51, No. 9, pp. 1249–1262.

Welch, R., and W. Marko, 1981. Cartographic Potential of a Spacecraft Line Array Camera System: Stereosat. *Photogrammetric Engineering and Remote Sensing*, Vol. 47, No. 8, pp. 1173–1185.

Introduction to GRASS 4

James Westervelt

June 11, 1991

OFEK07509

Contents

1 Introduction 1

2 What is GRASS? 1

2.1 GRASS is Public Domain . . . 1

2.2 GRASS is a Community of Users . . . 2

2.2.1 Inter-Agency Steering Committee . . . 2

2.2.2 Annual GRASS User Meetings . . . 3

2.2.3 GRASS Government Users . . . 3

2.2.4 Universities . . . 4

2.2.5 Commercial Firms . . . 4

2.3 GRASS is a Software Package . . . 4

2.3.1 GRASS is a Programming Language . . . 5

2.3.2 GRASS is Software for GIS Specialists . . . 6

2.3.3 GRASS is a Software Development Environment . . . 6

2.4 GRASS is Part of a Garden . . . 7

2.5 GRASS is a Sample Data Base . . . 7

3 GRASS Hardware Requirements 7

4 Why Does GRASS Exist? 9

4.1 Original Motivations . . . 9

4.2 UNIX Based GIS . . . 9

4.3 Easy to Distribute . . . 11

4.4 Market Stimulus . . . 11

4.5 Great for Sites With Talent . . . 11

4.6 Huge, Friendly User Community . . . 11

4.7 GRASS Versions and History . . . 12

5 Programs 12

6 GRASS Design and Implementation 15

7 GRASS Research and Development 17

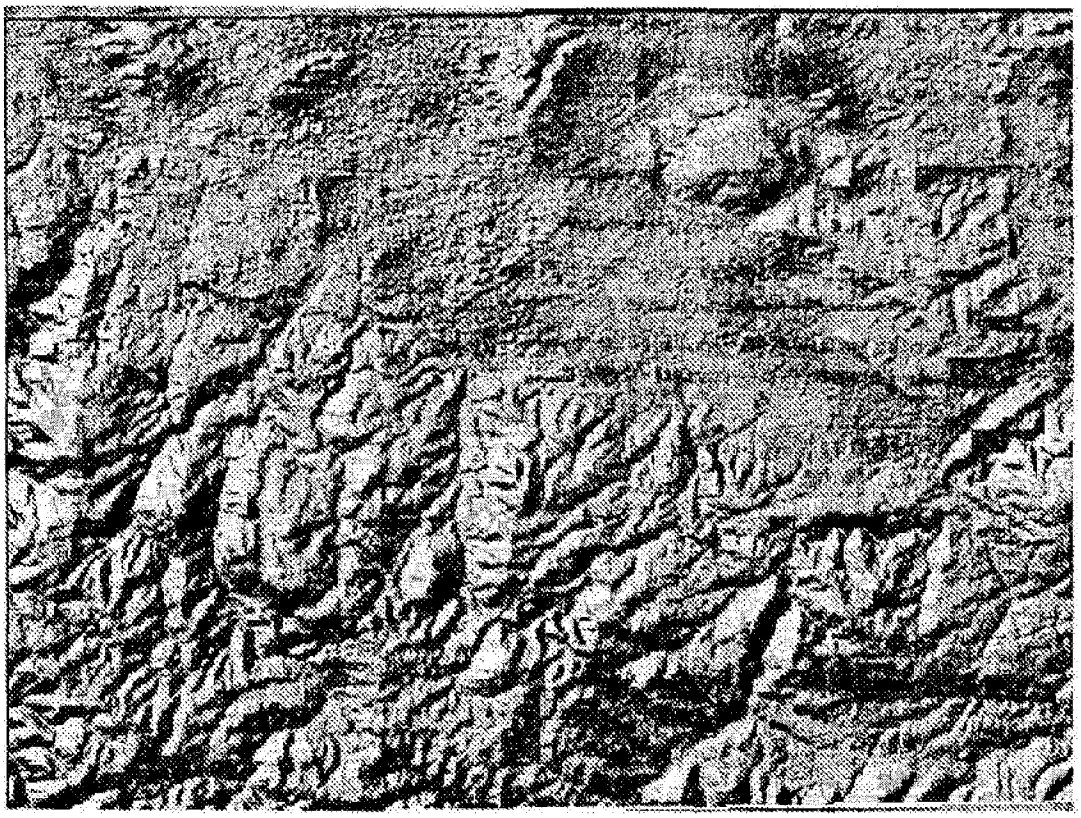
A GRASS Commands 19

B OVERHEADS 25

OFEK07510

Abstract

Welcome to GRASS, the Geographical Resources Analysis Support System. This document provides information on what GRASS is, where it comes from, and where to get more information. Basically, GRASS is a public domain raster geographical information system (GIS), vector GIS, image processing system, and graphics production system. It is used extensively at government offices, universities, and commercial organizations. It encompasses some 250 user programs, is written mostly in C for UNIX[1] machines, and contains more than 300,000 lines of software code. Overheads are provided to help the reader communicate GRASS to others.



Shade Relief Map of Spearfish - GRASS Sample Data Base

[1] UNIX is a trademark of ATT

OFEK07511

1 Introduction

This document introduces the reader to the public domain geographical information system GRAASS. Information on the capabilities of GRASS are matched with discussions on the ongoing development efforts, inter-agency cooperative programs, and the GRASS user community. Appendix A provides a brief overview of the primary GRASS programs as released in the summer of 1991. Appendix B provides some overheads that may be used in local GRASS briefings.

2 What is GRASS?

GRASS, more formally known as the Geographical Resources Analysis Support System, is fundamentally a geographical information system (GIS). The question, What is GRASS? can be answered in at least the following ways:

- GRASS is Public Domain
- GRASS is a Community of Users
- GRASS is a Programming Language
- GRASS is Software for GIS Specialists
- GRASS is Software for Image Processing
- GRASS is a Software Development Environment
- GRASS is Part of a Garden
- GRASS is a Sample Data Base

Each of these answers is discussed in the following sections.

2.1 GRASS is Public Domain

Many people come to GRASS with the lure of *free* software. GRASS, developed with United States taxpayer funds, is available to the public without charge. Users should however expected to encounter nominal charges for distribution, tapes, phone support, installation assistance, turn-key systems, documentation, etc.

Several commercial and university organizations are involved with porting GRASS to and supporting GRASS on various hardware platforms. For the latest information concerning GRASS status, distribution and support centers, and user mailing lists, contact the *GRASS Information Center*:

GRASS Information Center
U.S. Army CERL
P.O. Box 9005
Champaign, Illinois 61826-9005

(217) 373-7220

The *GRASS Information Center* can provide the following type of documents:

OFEK07512

General Information — Includes documents that introduce GRASS, describe the GRASS Inter-Agency Steering Committee's functions (see Section 2.2), and describes the various government, commercial, and government participants in GRASS.

GRASSCLIPPINGS — Place yourself on the mailing list for this page newsletter that is mailed several times a year.

Installing GRASS — Many documents describing hardware configurations, distribution and support sites, establishing return-on-investment estimates, and assistance in choosing the right system for you.

Educational Materials — Materials that you can use in briefings to describe GRASS to your co-workers.

GRASS Community Participation — This category includes documents that describe participation in the GRASS Steering Committee, the GRASSCLIPPINGS newsletter, the annual user meeting, and advertising possibilities.

System Development — For those sites interested in porting GRASS or creating new commands, there are many documents describing the GRASS programming environment.

Videos — Several videos which introduce GRASS and review some applications.

Advice — Advice on who to turn to for GRASS assistance.

2.2 GRASS is a Community of Users

Communities of GRASS users exist worldwide. Unlike user groups of commercial products, the GRASS user community members rely primarily on each other for support, system upgrades, and information. This process provides a wealth of "free" information and support for all members.

Figure 1 depicts the distribution of the GRASS user community based on a 1989 survey in which 500 sites responded.

2.2.1 Inter-Agency Steering Committee

GRASS is coordinated in large measure by the **GRASS Inter-Agency Steering Committee.** This not-for-profit organization meets 2–3 times a year for the purposes of coordinating GRASS community activities. Issues generally addressed include:

- Software design and development
- Software release schedules
- Inter-system integration issues
- User support issues
- Annual *GRASS User Meeting* arrangements
- Newsletter schedules and budget
- Inter-agency coordinations
- Commercialization issues

OFEK07513

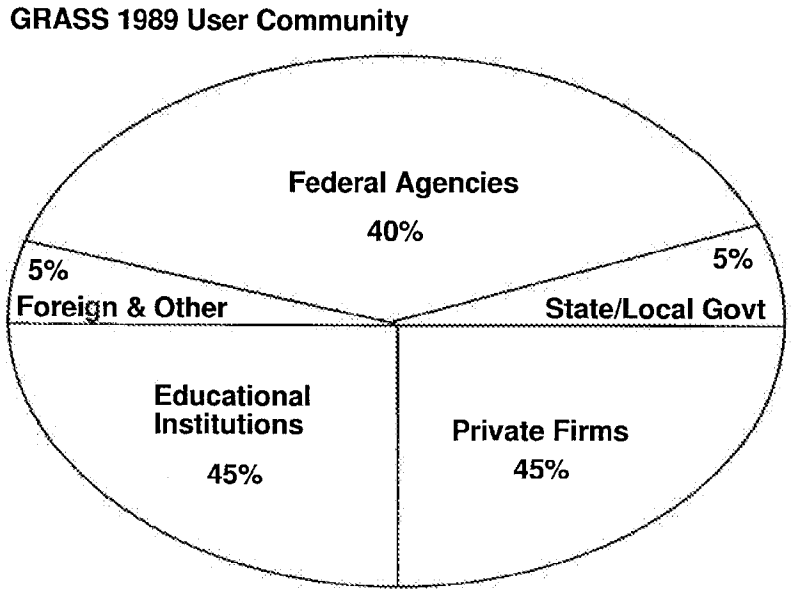


Figure 1: The GRASS User Community

The Steering Committee members represent GRASS users in many different Government agencies. As of Spring 1991, the agencies listed in table 1 had all participated in the GRASS Inter-Agency Steering Committee.

In addition to the representation of government groups, numerous universities and commercial groups have been involved as associate (non-voting) members.

2.2.2 Annual GRASS User Meetings

The GRASS user community is most visible each year when they gather together to present papers and participate in discussions ranging from GRASS fundamental design and development to experiences in applying GRASS to real-world problems. Meetings have been held annually since 1983; each meeting attracts 200-300 people who spend up to 5-days immersing themselves in the GRASS community. Meetings have been held in such exotic locations as Berkeley, California; Washington, D.C.; Champaign, Illinois (the birthplace of GRASS); Stennis Space Center (near New Orleans); Fort Hood, Texas; and Fort Lewis, Washington.

Annual GRASS user meetings have been held in Europe since 1990. Turnouts there suggest a long, healthy European user community. As of this writing plans are being considered for an Australian user meeting.

2.2.3 GRASS Government Users

The primary sources of funding for the design and development of GRASS has come from the largest government users of GRASS. The National Park Service and the Soil Conservation Service, in addition to the Army Corps of Engineers, has established GRASS support centers of expertise for GRASS within their agencies.

OFEK07514

U.S. Army Construction Engineering Research Lab	Champaign IL.
USDA, Soil Conservation Service	Washington DC.
National Park Service	Denver CO.
Bureau of Census	Washington DC.
Bureau of Land Management	Washington DC.
Department of Defense, Environmental Office	Alexandria VA.
Environmental Protection Agency, ERL-Corvallis	Corvallis OR.
NASA	Stennis Space Center MS.
NOAA	Boulder CO.
Navy, Naval Oceanographic Lab	Stennis Space Center MS.
U.S. Army Corps of Engineers	Washington DC.
U.S. Army Engineering and Housing Support Center	Ft. Belvoir VA.
U.S. Army Engineering Topographic Lab	Ft. Belvoir VA.
U.S. Geological Survey	Reston VA.

Table 1: Organizations involved with Guiding GRASS

2.2.4 Universities

GRASS was modeled in many ways after UNIX; a system whose original followers were graduate programs in computer science at numerous universities. GRASS similarly has found a firm and growing user community within numerous university departments including geography, geology, anthropology, regional planning, landscape architecture, archeology, and entymology. GRASS is taught at nearly 50 different Universities across the world today. The number grows yearly as GRASS offers a user environment for computer scientists as well as artistic landscape architects.

2.2.5 Commercial Firms

GRASS is being strongly embraced by many commercial entities. Many commercial firms that cannot afford commercial packages choose GRASS for the purpose of "getting into the GIS market." Many of the GRASS software distribution sites provide GRASS enhancements. The inexpensive nature of GRASS allows many potential GIS users to get experience with GRASS. This increases the number of people, firms, agencies, and universities that are familiar with the technology; this in turn broadens the commercial GIS marketplace.

2.3 GRASS is a Software Package

Yes, GRASS is a software package. This software package could only grow out of the type of user community described in the previous section. It is the user community which will drive GRASS design and development into the future.

Even at the software level, GRASS is different things to different people. Consider some of the statistics:

- Nearly 200 user programs
- Nearly 4000 software files
- More than 300,000 lines of C program code

OFEK07515

- Approximately 300 subroutines
- Programs written at about 15 different locations
- About 40 man-years of development time
- Distributed with several other public domain software packages
- Interfaced with numerous RDBMSs, expert systems, image processing systems

GRASS programs themselves are divided into the following groups:

Number	Programs that
40	Render images on monitors and paper
57	Manipulate raster maps
31	Manipulate vector maps
6	Manipulate sites maps
26	Manipulate multi-spectral imagery
16	Manage the data base
~20	Programs in alpha test
~20	Contributed programs
Numerous	"Related" Programs

2.3.1 GRASS is a Programming Language

Though GRASS, like most GISs, has a user community that operates the programs directly, GRASS has been conceived to be a programming language. UNIX itself is a programming language; it provides shells (like the Bourne shell (sh), the C-shell (csh) and the Korn-shell (ksh)). The shells provide programming flow control, and user input and output, and use other UNIX programs as subroutines. GRASS programs join the community of UNIX subroutines and, hence, enhance the power and flexibility of the UNIX operating system.

A growing community of end-users use shell scripts (UNIX macros) that contain GRASS programs as part of their main analysis functionality. In many cases the users of these scripts need know nothing about GRASS. Additionally, they need know nothing about other UNIX commands that may be embedded deep in the scripts.

To improve the possibilities of writing UNIX shell scripts, the GRASS design and development community is providing an application generator. This is a shell-script-like language that allows the script writer to communicate with the user through a graphical user interface on machines supporting X-windows. This program is called xgen; an X-windows based application generator.

What are the advantages of using a GIS as a programming language?

A GIS is hard to learn — Geographical information systems are powerful, general-purpose, and highly flexible software packages. Even a basic user must have significant knowledge of not only the GIS, but of the computer, the peripherals, the data bases being analyzed, the areas under analysis, and the requirements of the analysis. Most every GIS has been **developed as a scientific tool box**. They are generally not suitable for the casual or occasional user. If a user does progress through the learning curve to become proficient with a GIS, that user can be more effective if the GIS is a programming language. Using this language, software can be written for the local users who have limited analyses that are used repetitively. These local users need never be bothered with the scope and strength of the full-blown general purpose system.

OFEK07516

A GIS is Not a DSS — Decision Support Systems (DSS) in landscape planning, simulation, and analysis are best done if they approach a narrow problem. A GIS can play an integral role in the design and operation of a DSS in addition to graphical user interfaces, statistical packages, expert systems, report generators, etc. A GIS as a programming language allows the GIS expert user to generate decision support systems that are:

- Application specific
- Location specific
- User specific

Backend to User Interfaces — Numerous times users have suggested that GRASS be provided with various different types of front-ends: graphical user interfaces, expert systems, data base management systems, and natural language interfaces. With GRASS developed as a programming language, all of these types of interfaces are much easier to implement. As of this writing several such interfaces are under development at different sites.

Programming languages have long lives — User interfaces have relatively short lives. The recent fascination with 2-dimensional graphical user interfaces may give way to 3-dimensional interfaces, natural language interfaces, intelligent interfaces that "get to know the user", and holographic interfaces. Behind these interfaces can be the old tried-and-true systems. A GIS, stripped of its user interface, will command a much longer life than a GIS with a intimately integrated user interface. GRASS, fundamentally, is a command-line driven language devoid of any consequential interface. It is suitable as is to support numerous interfaces for years to come.

2.3.2 GRASS is Software for GIS Specialists

GRASS is most often viewed as software designed to do serious geographical data management, analysis, and display. Initially it was designed as a **raster-based GIS**. A co-developed **image processing package** was merged into GRASS early in its development because of the obvious utility in providing traditional GIS operations to image processing and vice-versa. GRASS always provided a vector approach to digitizing and data input. In recent years, this tradition has blossomed into a developing **vector-based GIS**. Chapter 5 provides a review of the GRASS 4.0 commands and displays the variety of capabilities offered.

2.3.3 GRASS is a Software Development Environment

At another level, GRASS is a software development environment for C programmers. To facilitate the design and development of new modules in GRASS, users at this level are provided with:

- Approximately 300 GRASS software subroutines that provide interface to the data and the user
- GRASS source code
- The document *GRASS 4.0 Programmer's Manual*
- Access to a community of GRASS Programmers

GRASS capabilities that have become part of the standard GRASS distribution have come from more than 15 different sites. Innumerable other sites have programmed local capabilities in GRASS.

OFEK07517

2.4 GRASS is Part of a Garden

GRASS grows in a "garden." In the process of using GRASS for, say, an Environmental Impact Statement, a user site may employ the capabilities of many other software systems. Some of these are public domain (or at least free) systems that are actually distributed with GRASS. Some of these include:

RIM	A relational data base management system out of the University of Washington, Seattle
MAPGEN	A cartographic output package for plotters developed by the USGS
GCTP	A coordinate translation package developed by the USGS
pbmplus	An image manipulation package developed by Jeff Poskanzer
xgen	A shell-script like language for generating X-windows interfaces

UNIX commands like awk, sed, grep, cat, csh, and sh round out a powerful programming environment in which these programs become the programmers subroutines. Other packages available on one's local system can provide yet more capabilities.

2.5 GRASS is a Sample Data Base

GRASS software is delivered with three sample data bases:

Spearfish — This famous data base (see Figure 2) was first developed by (or for) EROS Data Center. It became a member of the GRASS package and was greatly enhanced to provide more sample data layers. It is a complete data base that can be used to learn about GRASS.

Imagery — This data base provides several raw satellite and NHAP images for the Spearfish area which can be manipulated by users to generate new layers for Spearfish.

World — Portions of a larger data base used to study the earth. This data base demonstrates the format for a latitude-longitude data base as well as providing an environment for demonstrating GRASS's latitude-longitude capabilities.

3 GRASS Hardware Requirements

GRASS was designed and developed to operate under the UNIX operating system. It has been ported to numerous hardware environments supporting this operating system including:

- Sun computers (all)
- Concurrent workstations (formerly Masscomp)
- Intergraph Interpro workstation
- Silicon Graphics workstations
- Apple Macintosh (AUX)

OFEK07518

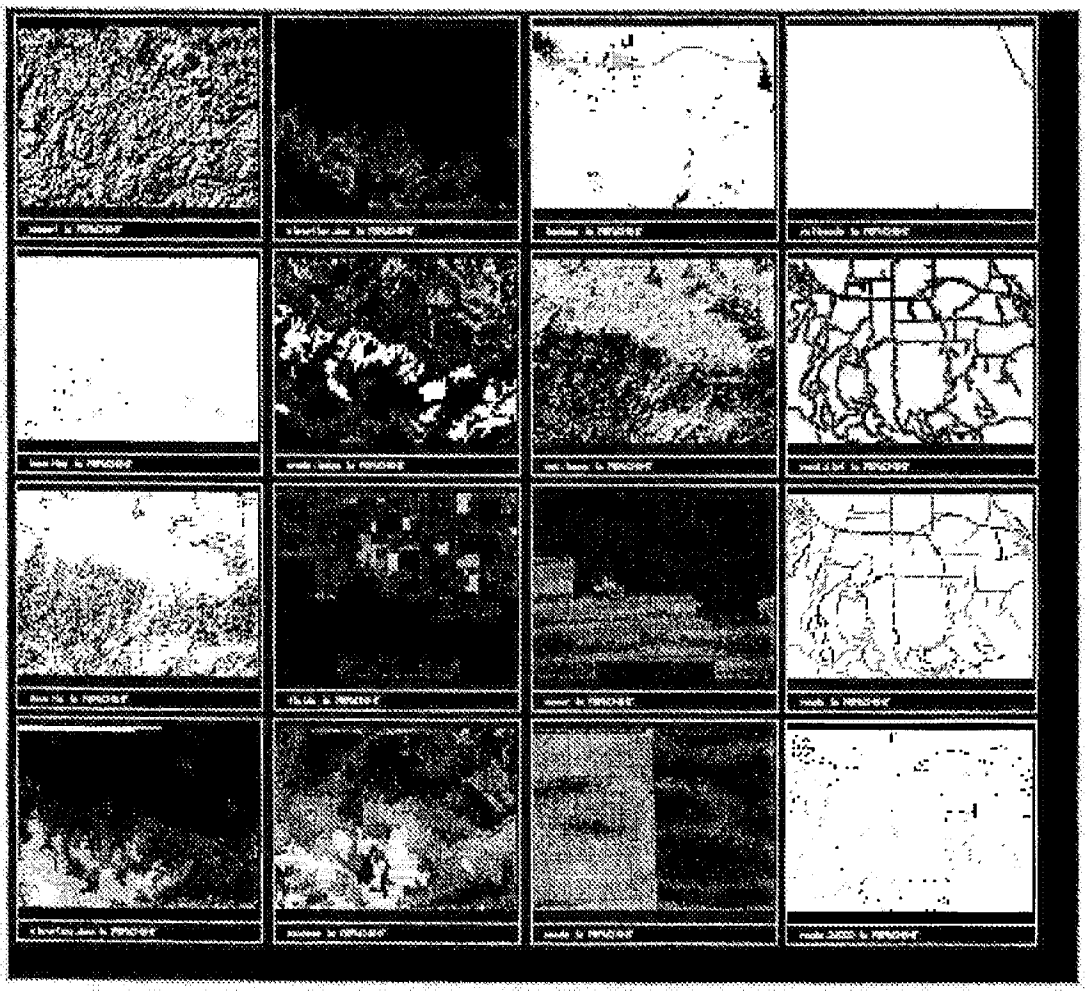


Figure 2: Sample maps from the Spearfish Data Base

OFEK07519

- PC 386's and 486's (with Microport or SCO UNIX)
- Digital Equipment Corporation (DEC) workstations
- Data General's Aviion workstation
- Apollo workstations
- Hewlett Packard 9000
- IBM PS-2 (AIX)
- IBM 6000 workstations
- Tektronix workstations
- AT&T 3B2 workstation

Each port is supported by a different software house and set of distributors. Contact the *GRASS Information Center* (see section 2.1) for the latest list of distributors and hardware configuration options.

4 Why Does GRASS Exist?

4.1 Original Motivations

GRASS was born in the early 80's to address needs at an Army environmental office at Fort Hood, Texas (See Table 2). Budgets were tight and talent was available. A VAX 11/780 computer was available (funded via other projects), but there were no UNIX based geographical information systems commercially available at the time. Graduate student programmers took over and created the beginnings of GRASS in the VAX's UNIX environment. When Sun Microcomputers offerred their first workstations with color monitors (Sun/1), GRASS development was moved to the workstation environment where it still thrives today.

4.2 UNIX Based GIS

GRASS was initially developed as an unnamed series of demonstrations operating on a Cromemco powered by a Z-80 cpu. Researchers at the Army Corps of Engineer's Construction Engineering Research Laboratory (CERL) were trying to demonstrate the concept of geographical information systems to the Corps. Enough funds were originally generated to do smalonly 1 pilot systems on available computers. The GRASS fore-runner was a small system running on a VAX 11/780 that powered black and white graphics terminals over 300-baud modems. This system was funded by the Environmental Office at Fort Hood, Texas and was called the Fort Hood Information System (FHIS). Other environmental offices became interested and the more general purpose GRASS was born. Funding was still insufficient to purchase standard geographical information systems available at that time. Members of the National Park Service that now employ GRASS warned CERL researchers against putting in the required 10 man-years of programming. But, CERL did not gather enough funds to purchase hardware to run available software. CERL had hardware and expertise to operate UNIX machines and did the initial GRASS work on a VAX running UNIX. Within a year the fledgling GRASS was ported to an early SUN-1. So far as was known, this was the first GIS to operate in UNIX.

OFEK07520

Year	Name	Additions to the System	Users
1982	FHIS	Single program, single location, raster database. Development and operation on UNIX based VAX 11/780. Digitizing on separate computer. Graphics on B/W monitor and B/W dot-matrix printer. User accessed remote via 1200 baud modem. Digitizing via polygon method.	Fort Hood, Texas
1983	IGIS	Multi-program accessed via menu, adapt to different data. SUN-1 microcomputer workstation. User operated on-site. Color display.	Fort McClellan, Alabama
1984	GRASS	Development on MASSCOMP MCS-560 and SUN-1. Digitizing via arc-node method. First color hardcopy output. 20 different programs.	Ft. Lewis, Central Washington University, National Guard Headquarters, data for 13 sites total.
1985	GRASS 1.0	First annual GRASS user group meeting - Fort Hood, Texas. First open distribution. Started inter-site electronic mail communication. Central Washington University offered first classes.	About 20 sites.
1986	GRASS 1.1	Run-length encoded raster files. Multi-byte grid-cell files supported by some programs. Image analysis as GRASS sub-system (runs only on MASSCOMP). Receives *Exemplary Systems in Government* from URISA. Interagency steering committee established.	Distribution to several dozen sites.
1987	GRASS 2.0	First programmer documentation. Some sites begin doing GRASS enhancements. GRASS distributed by Institute for Technology Development and DBA Systems. Rework of database. Adopt USGS digital line graph (DLG-3) format for vector data. Digitizing package for users. Ported to about seven different manufacturers machines. Army steering committee established.	Distribution to several hundred sites. Pilot tested by Soil Conservation Service. Adopted by National Parks Service.
1988	GRASS 3.0	Image analysis reworked into GRASS; runs on all GRASS machines. Raster files can contain from 1-4 bytes per cell. DLG dropped in favor of an internal vector format. Completely new digitizing package for user. Full assortment of command-line driven programs. Approximately 170 different programs.	Distribution to about 1000 sites.
1989	GRASS 3.1	Many new commands added. Significantly improved digitizing.	
1991	GRASS 4.0	This version realized the design goals set in 1986. Major additions include a standard command line parser for virtually all commands, substantial support for latitude-longitude based data, complete reorganization of command names, significantly better documentation, and performance enhancements.	Distribution to every household.

Table 2: GRASS History

OFEK07521

4.3 Easy to Distribute

A major strength of GRASS is that it is very easy to distribute. Anyone who wants to cut a tape or copy GRASS across the Internet may do so without violating copyright requirement. Sites developing software using GRASS libraries or programs can freely copy GRASS as much as desired. For this reason, government agencies and universities that support large user communities find GRASS especially attractive.

4.4 Market Stimulus

GRASS stimulates the GIS market in several ways.

- Provides basic research. GRASS is a scientific research and development environment where programs and algorithms with unproven market potential can be tested. Numerous journal articles have been published that discuss research done both with and on GRASS. Techniques proven in the GRASS environment may become adapted by the commercial GIS marketplace.
- Brings new users to the GIS marketplace. Many potential users are in situations where the purchase of a commercial GIS package is not possible. This can be due to a lack of funding, too much red-tape, unfamiliarity with the technology, or insufficient staffing to make a large purchase cost effective. An excellent public-domain system provides an alternative to such groups. As these sites get involved with the technology they most certainly will turn to the commercial marketplace to purchase data, computers, peripherals, expertise, and advice. GRASS facilitates a growing number of commercial vendors of hardware, software, and expertise.

4.5 Great for Sites With Talent

Sites that have more money than talent and man-power often find that the purchase of a commercial GIS provides them with an out-of-house support staff. Sites that have significant talent, but less purchasing power consider GRASS to be a wonderful option. There are several reasons for this. First, the purchase of a commercial GIS is often an initiates a long-term relationship with the GIS vendor. Talented sites generally underutilize such relationships which often take the form of phone support, on-site debugging, on-site classes and training, custom product design and development and the continual presence of a friendly assistant. Sites requiring only a powerful GIS environment will find GRASS an extremely attractive option.

4.6 Huge, Friendly User Community

In lieu of a single software vendor that provides all the services a GIS site might desire, GRASS comes with a huge, friendly user community. The community meets en-mass once a year to exchange ideas, software, and presentations. Recognizing their co-dependence, the group tends to be very helpful to those with questions. The commercial folks involved with GRASS are highly enthusiastic about the product and offer services at nominal charges. Numerous Universities and commercial training sites across the world offer GRASS classes at very low cost. Information on the user community and commercial offerings is maintained by the *GRASS Information Center*.

OFEK07522

4.7 GRASS Versions and History

GRASS can be appreciated through a cursory review of its history. It grew along with a user community new to GIS. A majority of its strength resides in its close development ties with such a user community. This development resulted in the history outlined in Table 2. GRASS 1.0 was in a class by itself. It was distinguished by a a user interface that allowed users to do something useful with the GIS in a very short time. This attracted a number of new users. It was also cited as one of the main reasons for being given the URISA ESIG Award[2].

The U.S. Army Corps of Engineer's research community awarded GRASS for it's excellence with the Army R&D Award.

Through the GRASS 4.0 release, GRASS software coordination, integration, testing, and distribution has been carried out by research staff at the Army Corps of Engineer's Construction Engineering Research Laboratory.

Beginning with GRASS 4.1, the GRASS Inter-Agency Software Coordination Center will be responsible for GRASS releases. This staff will likely be sited at USACERL. The office will be jointly funded by the major agencies doing GRASS system design and development.

5 Programs

This section introduces the GRASS 4.0 commands. For a very short listing and description of each command, refer to Appendix A on page 19. GRASS commands come in several flavors. Command names have the basic format: lower case letter, followed by a period (.), followed by a description string:

Command Prefix	Command Description
g.	General data (file) management commands
d.	Display (monitor) graphics
p.	Paint paper graphics
r.	Raster data manipulation and analysis
v.	Vector data manipulation and analysis
s.	Site data manipulation and analysis
i.	Imagery (multi-spectral) data manipulation and analysis
m.	Manipulation of external data

The naming convention was chosen to get a good balance in meeting the following objectives:

Non-conflict — Because GRASS commands are used in conjunction with other UNIX commands, it is important that GRASS commands not get confused with other programs. This requirement is met with the convention of prefixing each command with a letter and a period.

Separate raster, vector, etc. series — GRASS operations work with raster, vector, multi-spectral, and site data types. It is important that the user know what data type is being manipulated. It is also important that operation names be available for each data type. For example, by renaming the vector digitizing program from "digit" to "v.digit", there is room for a "r.digit" or "s.digit" program to be introduced in a later release.

[2]The Urban and Regional Information System Association's Exemplary Systems in Government (URISA ESIG) Award. This is presented annually to especially significant government developed software, and ws awarded to USACERL developers (Goran, Shapiro, and Westervelt) in 1987.

OFEK07523

Self-explanatory — Program names were chosen to be as self descriptive as possible without being verbose.

Easy to type — Names needed to be easy to type. The upper case letters of GRASS 3.0 were apparently harder for users (in general) to enter than the corresponding lower case and period combination.

The display commands (d.) manage the GRASS monitor. They manage the monitor operations and provide commands that render all data types on the display graphics monitor:

- 2-D display
- 3-D display (Figure 3)
- Profiles
- Histograms
- Pie Charts
- Graphs
- Screen dumps to hard copy

Raster analysis commands all begin with r. and are the oldest of GRASS data analysis commands. These operations provide the traditional raster GIS operation primitives:

- Overlay (boolean, weighted, cellophane, rule base)
- Full mathematical functions
- Filters
- Proximity analysis
- Measurements (length, area, volume, counts)
- Clustering
- Import/Export
- Line-of-sight
- Cost analysis
- Transformation to vector
- Rotation
- Patching
- Reclassification
- Network flow analysis
- Thinning
- Elevation transformations

OFEK07524

Perhaps the fastest developing set of GRASS capabilities is the vector GIS command set. Operations include the following:

- Digitizing
- Editing
- Labeling
- Measurements
- Import/Export
- Full topological linking
- Display
- Patching
- Transformation to raster
- Grid generation
- Contour labeling

Imagery commands form a powerful set of tools which manipulate multi-spectral images. GRASS users have made good use of Landsat, SPOT, and high-altitude NHAP images using this software. This suite of programs is continuing to grow and now contains:

- Tape handling for multiple formats
- Scene and sup-scene extraction
- Color enhancements
- Image registration
- Terrain correction
- Automated classification
- User directed classification
- Filtering
- Histograms
- Full integration with raster operations

Some geographical information can be stored as site data. The s. commands provide analysis capabilities for such data. These provide the following types of operations:

- Surface generation (interpolation)
- Statistical comparisons
- Reclassification
- Transformation to raster and vector

OFEK07525

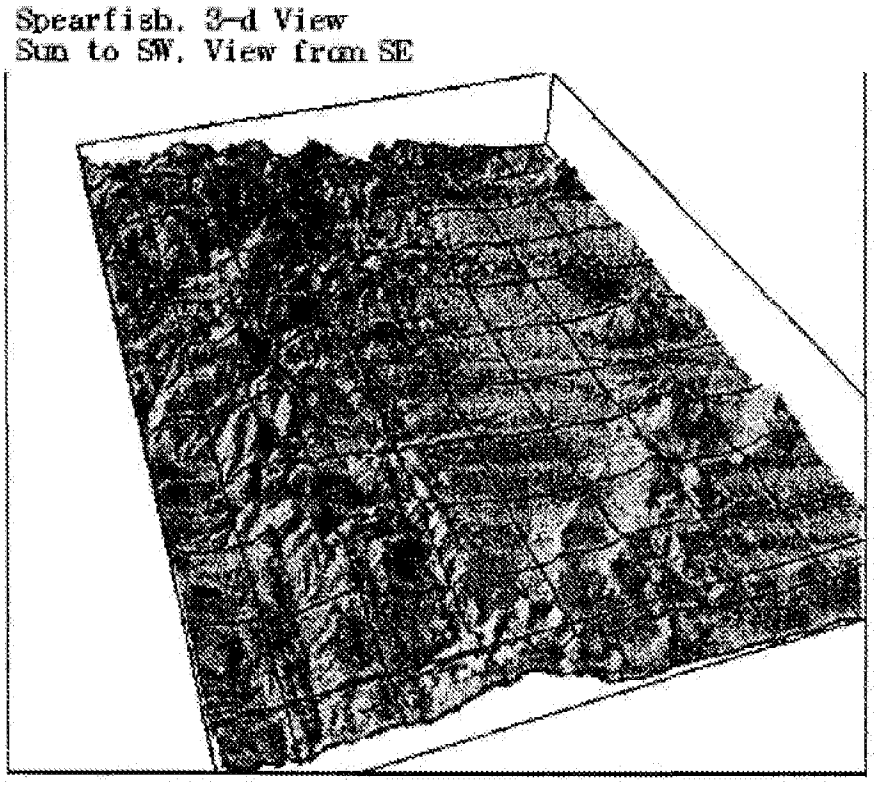


Figure 3: Sample 3-d Display

- Coordinate registration
- Data base searches and retrievals
- Proximity analysis
- Import/Export to the S statistical package

During the process of importing data into GRASS it is often necessary to resample data in various ways. The m. commands in provide mechanisms for doing some types of data resampling. These are most frequently used to assist in importing data into GRASS.

6 GRASS Design and Implementation

The design of GRASS has been quite successful because of sound guidelines established early in its development. This section looks at the key design and implementation policies currently embodied in GRASS and then looks at guidelines that may direct future work. First, a look at the current design:

UNIX and C — GRASS was to be developed for powerful UNIX workstations. The standard language on such machines was (and is) C.

OFEK07526

Modular design — GRASS demonstrates a highly modular design allowing easy module upgrades. There are hundreds of subroutines in about 10 basic libraries, which support almost 300 different programs.

Portable — GRASS development aimed at generating capabilities that would compile on a wide variety of UNIX workstations.

Workstations — Programs designed to run on individual color UNIX workstations.

Integrated GIS and image processing — Traditional image processing programs enhanced with traditional raster GIS functions (and vice-versa). GRASS is designed to provide both capabilities in a manner that uses the same subroutines and data bases interchangeably.

Integrated raster and vector — Some spatial operations are better performed in vector, others in raster. Most user communities require both.

Multiple user interfaces — Geographical information systems address the needs of a diverse community of users. It is very important that different interfaces be available to different users. GRASS is a powerful GIS for geographical information specialists (Section 2.3.2, page 6.) It is also a software development environment (Section 2.3.3, page 6). Lots of very easy user interfaces have been developed that are location, project, and user specific.

Mixed raster resolutions — GRASS may be unique in its ability to resample raster data at run-time into a user selected region and resolution. GRASS raster data bases are stored with their original resolution and map placement. Most all similar systems require that data be resampled into a fixed grid during the data import process. GRASS stores the raw data and resamples as needed.

Assorted temporary data storage formats — GRASS is a potpourri of analysis functions. Some access the data in a regular manner - grid-cell after grid-cell in row after row. Others require the simultaneous access of data spanning several rows of data (e.g. Satellite data resampling). Some access the data randomly within small regions (e.g. line-of-sight and proximity analyses). Some can be highly random. Methods exist to temporarily load the data into formats that make access of each approach efficient.

Future design and development guidelines will likely implement the following requirements. Studies are now underway to determine what should be implemented and how.

C++ — C++ has become a standard object-oriented programming language. This language offers easy access to capabilities that are inherently difficult in C. Future GRASS development must seriously consider C++ for the sake of improving program development.

Multiple-attributes — GRASS raster and vector files have the capability only to access single strings of information for each map entity. This is very limiting and has forced the user community to store multi-attribute information in RDBMSs operated in parallel with GRASS. This approach requires users to pay special attention to the management of two separate data areas. In some cases user communities have addressed this difficulty by gluing GRASS and RDBMSs together within shell scripts that maintain the integrity between information in the two systems.

Multiple map management — Some GRASS sites have developed data bases with hundreds and even thousands of digital maps. The management of such data needs to become better automated.

OFEK07527

Data access via network servers — GRASS was not initially designed to operate on networks. Though modifications have made such operation possible, GRASS must be thoroughly reviewed to more adequately function on networks. GRASS will likely be reworked so that software servers on machines with prodigious data storage parcel out data to GRASS systems running on local and remote workstations through UNIX sockets.

Efficient sub-map region queries — Individual GRASS data maps can be arbitrarily large. This is a problem, especially for programs that want to read in entire maps. Raster data needs to be accessible from these large maps without sacrificing efficiency.

Manage permissions — GRASS users are interested in sharing map data locations, maps, and map records. GRASS now allows only the owner of a data location write access to the location. A user can not run GRASS siumltaneously on different computers that share the GRASS data base. This must be relaxed.

Mix spatial and DBMS queries — GRASS provides a spatial analysis capability. RDBMSs provide query capabilities on map attribute information. Some queries, such as locating all sites withing 1 km of a sinuous road contain gold and silver, are best addressed if the spatial and RDBMS operations can occur simultaneously.

Floating point data — Currently only integer data in GRASS raster maps is possible (1, 2, 3, or 4 bytes). This must be relaxed to accommodate floats, doubles, structures, subroutine pointers, etc.

3-D data base — Future GRASS implementations will be called on to perform analyses on 3-D data bases.

7 GRASS Research and Development

GRASS is based on years of design and development, most of which was accomplished under research projects. Such research continues to evolve, resulting in the promise of more GRASS modules. Some of the projects planned for the next five years include the following:

X Interface — The UNIX community is standardizing their graphics efforts in a product called X-windows. This environment makes it possible to write portable code across a wide variety of UNIX hardware platforms providing sophisticated data visualization and user interfaces. Several efforts are underway to bring graphical user interfaces to GRASS.

Image Segmentation — New algorithms are being developed to identify homogeneous regions in images.

Raster editor — Two independent efforts are working toward a raster editing capability operating under X-windows.

Garden links — Numerous efforts are underway to link GRASS more closely with other systems.

Latitude-Longitude — Several significant research efforts will be undertaken to enable more of the GRASS capabilities to work directly with latitude-longitude data bases. Of particular interest will be modifications to allow digitizing of various projections.

Visualization — As real-time 3-D image rendering becomes more commonplace, the rapid rendering of GRASS data will become necessary.

OFEK07528

Floating-Point Data — The GRASS integer data bases (for raster) limit the modeling capabilities of GRASS. The data structures must be updated to provide for not only the storage of floating point values, but imaginary numbers, structures and arrays, rules, function pointers, etc.

Parallel processing — Within a very few years, parallel processing hardware will become standard equipment within workstations. GRASS can benefit dramatically from such equipment which will required re-thinking the data bases and the software.

Modeling — GRASS data bases can support modeling of information as it moves and changes across the landscape. Such operations require large amounts of processing time and will work best on future parallel processing environments.

Fundamental DBMS-GRASS links — Data base management software has been linked with GRASS in numerous configurations. It is appropriate however to re-think the internal management of GRASS data using object-oriented and relational data base technology.

Full vector GIS — GRASS must provide its user community with a more complete set of standard vector operations.

Neural Networks — Neural networks are being evaluated for incorporation into GRASS analyses. These might enable a user to train the computer to identify sites with similar features to known sites.

Automated Digitizing — The development of data continues to be the most expensive component of any working geographical information system. Users would like to minimize the cost of turning paper maps into digital data layers. Advances are being made in rendering scanned map images into vector representations. Associated R&D is looking at automatically labelling and aggregating features of scanned images.

Contouring — Mathematical solutions for efficiently generating elevation maps from sparse information are being investigated for inclusion in GRASS.

OFEK07529

A GRASS Commands

GENERAL GRASS DATA MANAGEMENT COMMANDS

g.access	Controls user access to the current GRASS mapset.
g.ask	Prompts the user for the names of GRASS data base files.
g.copy	Copies available data files in the user's current mapset search path and location to the appropriate element directories under the user's current mapset.
g.filename	Prints GRASS data base file names.
g.findfile	Searches for GRASS data base files and sets variables for the shell.
g.gisenv	Outputs the user's current GRASS variable settings.
g.help	GRASS help facility.
g.list	Lists available GRASS data base files of the specified data type to standard output.
g.manual	Accesses GRASS reference manual entries.
g.mapsets	Modifies the user's current mapset search path, affecting the user's access to data existing under the other GRASS mapsets in the current location.
g.region	Program to manage the boundary definitions for the geographic region.
g.remove	Remove data base element files from the user's current mapset.
g.rename	Rename data base element files in the user's current mapset.
g.version	Outputs the GRASS version number and date.

HARDCOPY GRAPHICS COMMANDS

p.chart	- Prints a color chart for the printer currently selected.
p.colors	- Allows the user to modify a color table for a raster map layer, assigning colors to the categories in the raster map layer based on printer color numbers (instead of red, green, blue percentages).
p.icons	- Allows the user to create and maintain icons which are used by the p.map command to depict sites.
p.labels	- Creates and modifies labels for hardcopy maps.
p.map	- Command language interface to color hardcopy and graphics monitor output.
p.screen	- Prints a graphics monitor display image file that has been saved by d.savescreen.
p.select	- Selects a device (printer) for GRASS hardcopy output. Outputs can also be previewed on the graphics display monitor.

DISPLAY GRAPHICS COMMANDS

d.3d	Three-dimensional raster map display program.
d.ask	Prompts the user to select a GRASS data base file from among files displayed in a menu on the graphics monitor.
d.colormode	Allows the user to establish whether a map will be displayed using its own color table or the fixed color table of the graphics monitor.
d.colors	Allows the user to interactively change the color table of a raster map layer displayed on the graphics monitor.
d.colortable	Display the color table associated with a raster map layer.

OFEK07530

d.display	Interactive program to display textual, symbolic, raster, vector, and site data in the active frame on the user's graphics monitor.
d.erase	Erases the active display frame on the graphics monitor.
d.font	Selects text fonts to be used for text display on the graphics monitor.
d.frame	Manages display frames on the graphics monitor.
d.geodesic	Displays a geodesic line, tracing the shortest distance between two geographic points along a great circle, in a latitude–longitude data set.
d.graph	Program for generating and displaying simple graphics to the graphics display monitor.
d.grid	Overlays a user-specified grid in the active display frame on the graphics monitor.
d.his	Produces and displays a raster map layer combining hue, intensity, and saturation (his) values from user-specified input raster map layers.
d.histogram	Plots a histogram in the form of a pie or bar chart for a user-specified raster file.
d.icons	Displays points, as icons, at user-defined locations in the active display frame on the graphics monitor.
d.label	Creates and places text labels in the active display frame on the graphics monitor.
d.labels	Create/edit GRASS label files for display on the graphics monitor.
d.legend	Displays a legend for a raster map layer in the active frame on the graphics monitor.
d.mapgraph	Generates and displays simple graphics on raster map layers drawn in the active graphics monitor display frame.
d.measure	Measures the lengths and areas of features drawn by the user in the active display frame on the graphics monitor.
d.menu	Creates and displays a menu within the active frame on the graphics monitor.
d.mon	Establishes and control use of a graphics display monitor.
d.paint.labels	Displays text labels formatted for use with GRASS paint (paint, p.map) output to the active frame on the graphics monitor.
d.points	Displays point graphics in the active frame on the graphics display monitor.
d.profile	Displays profiles of a user-specified raster map layer in the active frame on the user's graphics monitor.
d.rast	Displays and overlays raster map layers in the active display frame on the graphics monitor.
d.rgb	Allows multiple maps to be overlaid in the active display frame on the graphics monitor.
d.rhumbline	Displays the rhumbline joining two user-specified points in the active frame on the user's graphics monitor.
d.scale	Displays a map scale and north arrow relevant to a user's current geographic region setting in the active display frame on the graphics monitor.
d.sites	Displays site markers in the active display frame on the graphics monitor.
d.text	Draws text in the active display frame on the graphics monitor.
d.title	Outputs a title for a raster map layer in a form suitable for display by d.text.
d.vect	Displays GRASS vector data in the active frame on the

OFEK07531

	graphics monitor.
d.vect.dlg	Displays a vector USGS digital line graph (DLG-3) file in the active frame on the graphics monitor.
d.what.rast	Allows the user to interactively query the category contents of multiple raster map layers at user-specified locations within the current geographic region.
d.what.vect	Allows the user to interactively query the category contents of multiple (binary) vector map layers at user-selected locations within the current geographic region.
d.where	Identifies the geographic coordinates associated with point locations in the active frame on the graphics monitor.
d.zoom	Allows the user to change the current geographic region settings interactively, using a mouse.

RASTER DATA MANIPULATION COMMANDS

r.average	Finds the average of values in a values map within polygons of a user-specified base map.
r.basins.fill	Generates a raster map layer showing watershed sub–basins.
r.binfer	Bayesian expert system development function.
r.buffer	Creates a raster map layer showing buffer zones surrounding cells that contain non-zero category values.
r.cats	Prints category values and labels associated with user-specified raster map layers.
r.clump	Recategorizes data in a raster map layer by grouping cells that form physically discrete areas into unique categories.
r.coin	Tabulates the mutual occurrence (coincidence) of categories for two raster map layers.
r.colors	Creates/Modifies the color table associated with a raster map layer.
r.combine	Allows category values from several raster map layers to be combined.
r.compress	Compresses and decompresses raster files.
r.cost	Outputs a raster map layer showing the cumulative cost of moving between different geographic locations on an input raster map layer whose cell category values represent cost.
r.covar	Outputs a covariance/correlation matrix for user-specified raster map layer(s).
r.cross	Creates a cross product of the category values from multiple raster map layers.
r.describe	Prints terse list of category values found in a raster map layer.
r.drain	Traces a flow through an elevation model on a raster map layer.
r.grow	Generates an output raster map layer with contiguous areas grown by one cell (pixel).
r.in.ascii	Converts an ASCII text file into a raster map layer.
r.in.ll	Creates a raster file from data in latitude–longitude coordinates.
r.infer	Outputs a raster map layer whose category values represent the application of user-specified criteria (rules statements) to other raster map layers' category values.
r.info	Outputs basic information about a user-specified raster map layer.
r.line	Creates a new GRASS vector (digit) file by extracting linear features from a thinned raster file.

OFEK07532

r.los	Line-of-sight raster analysis program.
r.mapcalc	Raster map layer data calculator.
r.mask	Establishes/removes the current working mask.
r.mfilter	Raster file matrix filter.
r.neighbors	Makes each cell category value a function of the category values assigned to the cells around it, and stores new cell values in an output raster map layer.
r.out.ascii	Converts a raster map layer into an ASCII text file.
r.patch	Creates a composite raster map layer by using known category values from one (or more) map layer(s) to fill in areas of "no data" in another map layer.
r.poly	Extracts area edges from a raster map layer and converts data to vector format.
r.profile	Plots profiles of a GRASS raster map layer.
r.random	Creates a raster map layer and sites list containing randomly located sites.
r.reclass	Creates a new map layer whose category values are based upon the user's reclassification of categories in an existing raster map layer.
r.report	Reports statistics for raster map layers.
r.resample	GRASS raster map layer data resampling capability.
r.rescale	Rescales the range of category values in a raster map layer.
r.slope.aspect	Generates raster map layers of slope and aspect from a raster map layer of true elevation values.
r.stats	Generates area statistics for raster map layers.
r.support	Allows the user to create and/or modify raster map layer support files.
r.surf.contour	Surface generation program.
r.surf.idw	Surface generation program, from raster data.
r.thin	Thins non-zero cells that denote linear features in a raster file.
r.traj	Ballistic trajectory model.
r.transect	Provides transect information across a raster map.
r.volume	Sums cell values within clumps and calculates volumes and centroids of patches or clumps.
r.watershed	Watershed basin analysis program.
r.weight	Raster map overlay function.
r.what	Queries raster map layers on their category values and category labels.

VECTOR DATA MANIPULATION COMMANDS

v.cadlabel	Attaches labels to vector contour lines that have been imported to GRASS from DXF format.
v.digit	A menu-driven, highly interactive map development program used for vector digitizing, editing, labeling, and converting vector data to raster format.
v.import	Converts ASCII Digital Line Graph (DLG) files, binary DLG files, and ASCII vector files into binary vector files and creates the needed vector support files.
v.in.arc	Converts data in ARC/INFO format to GRASS's vector format, and stores output in the user's current GRASS mapset.
v.in.ascii	Converts ASCII vector map layers into binary vector map layers.

OFEK07533

v.in.dlg	Converts binary DLG (BDLG) file to binary vector (dig) file.
v.in.dxf	DXF format to GRASS vector format conversion program.
v.mkgrid	Creates a (binary) GRASS vector map of a user-defined grid.
v.mkquads	Creates a GRASS vector map layer and/or sites list and/or geographic region definition file for a USGS 7.5-minute quadrangle.
v.out.arc	Converts GRASS vector files to ARC/INFO's "Generate" file format.
v.out.ascii	Converts binary vector map layers into ASCII vector map layers.
v.out.dlg	Converts binary GRASS vector data to binary DLG-3 Optional format.
v.out.dxf	GRASS vector format to DXF format conversion program.
v.out.moss	Converts GRASS site, line, or area data into MOSS import format. (Data Export Program)
v.patch	Creates a new binary vector map layer by combining other binary vector map layers.
v.prune	Prunes points from binary GRASS vector data files.
v.spag	Processes a Spaghetti-digitized vector file.
v.stats	Displays information about a user-specified GRASS vector file.
v.support	Creates GRASS support files for (binary) GRASS vector data.
v.to.rast	Converts a map layer in (binary) GRASS vector format to GRASS raster format.
v.to.sites	Converts a GRASS vector file to a GRASS site-lists file.
v.transform	Transforms an ASCII vector map layer from one coordinate system into another coordinate system.
v.trim	Trims small spurs and removes excessive nodes from a GRASS vector (digit) file.

MULTISPECTRAL DATA MANIPULATION COMMANDS

i.build.blk	Interactive ortho-photo rectification program.
i.camera	An imagery function that establishes a camera reference file for an imagery group.
i.cca	Canonical components analysis (cca) program for image processing.
i.class	An imagery function that generates spectral signatures for an image by allowing the user to outline regions of interest. The resulting signature file can be used as input for i.maxlik or as a seed signature file for i.cluster.
i.cluster	An imagery function that generates spectral signatures for land cover types in an image using a clustering algorithm. The resulting signature file is used as input for i.maxlik.
i.colors	An imagery function that creates colors for imagery groups.
i.composite	An imagery function that creates a color composite image from three band files specified by the user.
i.fft	Fast Fourier Transform (FFT) for image processing.
i.grey.scale	An imagery function that assigns a histogram-contrast-stretched grey-scale color table to a raster map layer.
i.group	An imagery function that creates and edits groups and subgroups of (raster) imagery files.
i.his.rgb	Hue-intensity-saturation (his) to red-green-blue (rgb) raster map color transformation function.
i.ifft	Inverse Fast Fourier Transform (ifft) for image processing.
i.maxlik	An imagery function that classifies the cell spectral reflectances

OFEK07534

	in imagery data based on the spectral signature information generated in i.cluster.
i.mod.camera	An imagery function that creates or modifies entries in a camera reference file.
i.pca	Principal components analysis (pca) program for image processing.
i.points	An imagery function that enables the user to mark coordinate system points on an image to be rectified and then to input the coordinates of each point for creation of a coordinate transformation matrix. The transformation matrix is needed as input for the GRASS program i.rectify.
i.rectify	An imagery function that rectifies an image by computing a coordinate transformation for each cell (pixel) in the image using the transformation coefficient matrix created by the GRASS program i.points.
i.rectify.blk	An imagery function that ortho-rectifies an imagery group file.
i.rgb.his	Red-green-blue (rgb) to hue-intensity-saturation (his) function for image processing.
i.tape.mss	An imagery function that extracts Multispectral Scanner (MSS) imagery data from half-inch tape.
i.tape.mss.h	An imagery function that extracts header information from Landsat Multispectral Scanner (MSS) imagery data stored on half-inch tape.
i.tape.other	An imagery function that extracts scanned aerial imagery (NHAP, etc.) and SPOT imagery from half-inch magnetic tape.
i.tape.tm	An imagery function that extracts LANDSAT Thematic Mapper (TM) imagery from half-inch magnetic tape.
i.target	An imagery function that establishes a GRASS target LOCATION for an imagery group.
i.zc	Zero-crossing "edge detection" raster function for image processing.

SITE DATA MANIPULATION COMMANDS

s.db	RIM data base management/query interface for GRASS.
s.in.ascii	Converts a GRASS site-lists file in ASCII format to binary format.
s.menu	Accesses and manipulates GRASS sites data.
s.out.ascii	Converts a GRASS site-lists file in binary format to ASCII format.
s.surf.idw	Surface generation program, from sites data.

EXTERNAL DATA MANIPULATION COMMANDS

m.dem.extract	Extracts USGS Digital Elevation Model (DEM) data from 1/2-inch magnetic tape.
m.examine.tape	Provides a description of the files on a 1/2-inch magnetic tape.
m.ll2u	Converts geographic (latitude–longitude) coordinates to Universal Transverse Mercator (UTM) coordinates.
m.region.ll	Converts Universal Transverse Mercator (UTM) coordinates falling within the current geographic region from UTM coordinates to geographic (latitude/longitude) coordinates.
m.rot90	Rotates elevation data extracted by either m.dted.extract or m.dmaUSGSread.

OFEK07535

m.u2ll	Converts Universal Transverse Mercator (UTM) coordinates to geographic (latitude–longitude) coordinates.

B OVERHEADS

OFEK07536

RGB Videographics Report

McDonnell Douglas Integrates RGB Spectrum Systems in Helicopter Simulators

U.S. Army's Apache Training Facility Uses Sophisticated Scan Conversion, Video Windowing

RGB Spectrum's scan converters and video windowing products are key components in McDonnell Douglas' state-of-the-art helicopter training facility in Tempe, Arizona. The facility trains personnel in the operation of the U.S. Army's Apache helicopter.

The Apache uses various types of video and infrared (FLIR) signals, with tactical video overlaid by alphanumeric information relating to altitude, direction, etc. In the simulator, the student is seated in a replica of the Apache cockpit, with out-the-window views generated by an Evans and Sutherland graphics system.

"The RGB product family is the only way to make this system work."

-- Jeff Mordevance, McDonnell Douglas



The instructor's console from McDonnell-Douglas' Apache Crew Trainer. The system includes RGB/View™ and Watchdog™ video windowing products, and the RGB/Videolink scan converter for videotaping.

Continued, page 2....

Q FORMAT™ Revolutionary High-Res Recording System

INSIDE THIS ISSUE...

The World's First D-1 Scan Converter ..p. 2
User Profile: California's Intelligent Hwys..p. 3
Image Synchronizer for Simulation .....p. 4
Scan Conversion for Virtual Reality .....p. 4
User Profile: Network Monitoring .....p. 5
New Brochure For Large-Screen Solutions..p. 5

Videotape is the most cost-effective means of storing moving imagery. But ordinary scan conversion down to video resolution may not adequately convey the detailed imagery or small text often found on military situation displays and air traffic control consoles.

The Q Format™ system uses not one but multiple frames of video to represent each computer image. In this technique the computer image is split across a number of frames of video depending on the level of resolution required. For example, a complex 1280 x 1024 pixel image may be rendered over 4-6 video frames.

Continued, page 6...

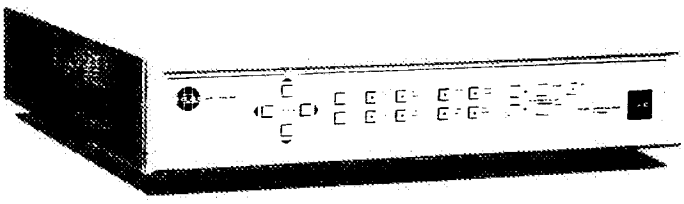
Published by RGB Spectrum • 950 Marina Village Parkway, Alameda CA 94501 • (510)814-7000 • © 1995 RGB Spectrum

SNEAK PREVIEW

Announcing the RGB/Videolink 1700 D-1: The World's First D-1 Scan Converter

The Soon-to-Ship RGB/Videolink 1700D-1 Outputs CCIR601 Digital Component Video as well as NTSC, PAL, S-Video, and Analog Component Video

A stand-out in RGB's new product arena is the RGB/Videolink® 1700D-1, the only scan converter in the world to ouput CCIR601 digital component video for D-1, Digital Betacam, and other digital component tape recorders. The 1700D-1 also ouputs broadcast quality NTSC and PAL composite video, S-Video, and analog component video. In addition, a double scan rate RGB signal at 31.5 kHz is available for projection.



The latest model in the RGB/Videolink line of video scan converters is the model 1700D-1, which is the only scan converter in the world capable of digital component video output.

The RGB/Videolink 1700D-1 accepts inputs from virtually any workstation or desktop computer. The model 1700D-1 automatically measures the horizontal and vertical frequencies of the input signal and sets up the parameters for the sharpest picture. It synchronizes to all computer signals with screen resolutions up to 1600 x 1200 pixels.

The RGB/Videolink 1700D-1 features a wide range, high quality, zoom. Typically, this is used to expand a portion of the image so it fills the video screen. It is also used to provide just the appropriate amount of underscan/overscan. The zoom is so smooth that it can provide a continuous pan and zoom effect while videotaping.

Other features include the ability to overlay video with computer-generated graphics. The model 1700D-1 offers a variety of alternatives, including both a linear luminance keyer and a chromakeyer, with overlays on either composite video or S-Video backgrounds.

The RGB/Videolink 1700D-1 is easy to use, with sophisticated front panel controls and on-screen menu-driven control. In addition, the system saves custom setups, with user definable smooth zoom presets always available on the front panel. And for remote control, an RS-232 port is provided.

McDonnell Douglas

....Continued from page 1

The instructor's console is arranged to display the same visuals, but in a more condensed and efficient format, with the inputs arranged in windows on the screen. The console consists of four monitors configured as a single display, so that windows moved off the edge of one screen appear on the next. RGB Spectrum's video windowing products reduce the number of screens the instructor needs to monitor, improving the instructor's focus of attention and reaction time.

Two video windowing systems are employed. The **RGB/View®** system, which displays real-time color video on a monitor, is used to show the out-the-window scenes. The video can be positioned, scaled, and overlaid with computer graphics. Also available are frame grabbing capabilities, a keyer for overlaying text and graphics on video, and software for control under X-Windows. The **Watchdog™**, which can display multiple monochrome video sources, is used to show the simulated FLIR.

In addition, an **RGB/Videolink®** scan converter is used to videotape the simulation. The RGB/Videolink transforms computer graphics to television format in real time, allowing the recording of the computer-generated imagery on a VCR. All the video feeds shown on the screen are recorded on a single tape, making record-keeping and evalution of student performance easy and efficient.

"The RGB product family is the only way to make this system work," according to Jeff Mordevanec, Lead Engineer for the operator instructor system. "Nothing else gave us the ability to work so well with both 1280 x 1024 computer signals and 875-line FLIR, plus videotape all the elements in sync."

CUSTOMER PROFILE

RGB/View Plays Lookout for California's "Smart Highways"

Video Windowing System Allows Live Viewing of Traffic Problems for Faster Response

The RGB/View video windowing system plays a key role in two major California cities' state-of-the-art traffic management systems. Both Irvine and Pasadena have recently implemented a high-tech approach to traffic management called Intelligent Vehicles Highway System, or IVHS.

In these "smart highway" systems, video cameras transmit live images from key locations around the city. Traffic engineers in a control room facility can control the direction and angle of the cameras, and see the live video images on their computer screens using the RGB/View system. This allows early detection of traffic congestion so traffic signals can be adjusted or emergency crews dispatched.

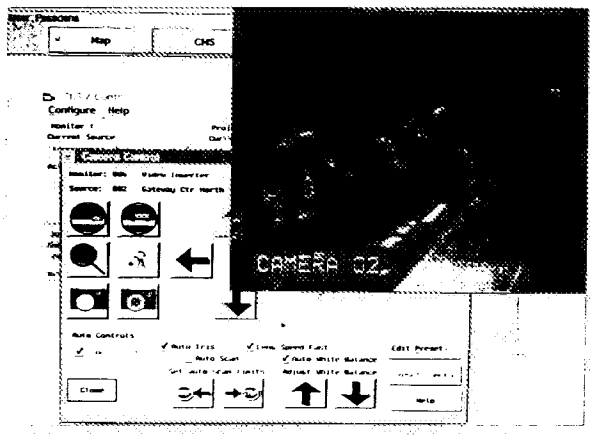
"Advanced traffic management takes advanced technology."

Lee Haffely, AudioVisions, Inc

Irvine's multi-modal network of freeways, streets, and transit systems has become a model for transportation planners across the country. At the heart of the system is the ITRAC facility (Irvine Traffic Response and Control Center), which monitors and manages traffic circulation throughout the city. Regional and city traffic grids can be intermixed with live traffic video, and using the RGB/View system, can be viewed by traffic engineers on both their computer monitors and a large-screen projection display.

The system, which started with video cameras at six key intersections, will ultimately have more than 80 cameras. Already, drivers experience less waiting time at signals and better traffic flow. The system's most important contribution long-term will be in accommodating expected increases in local traffic. Building new highways or physically widening older ones can take months and funding for such construction is scarce in California. It's much less time-consuming and expensive to use technology to improve conditions on existing streets.

According to Lee Haffely of AudioVisions, Inc., systems integrator for Irvine's ITRAC system, "Advanced traffic management takes advanced technology. We chose the RGB/View system for the video windowing part of the equation because not only does it provide very high quality for viewing, it places no burden on the host computer."



RGB/View® video windowing products allow one or more live video windows to be shown on a computer display. In Pasadena's system, live video of a freeway is overlaid on a screen that gives the operator control of the video camera ***(Photo courtesy JHK & Associates.)***

Another leader in managing traffic through technology is the city of Pasadena, whose Traffic Management Center is similar to Irvine's ITRAC. The Center is a sophisticated control room where traffic engineers use RGB/View systems to display live video feeds in windows on their monitors or on a large projection screen. By combining this real-time video with computerized city maps and other graphical information, technicians can respond quickly to traffic situations by controlling traffic signals or even communicating directly with motorists through local radio and message signs in strategic locations around the city.

"The RGB/View system is the best way we've found to integrate live video into computer displays to facilitate decision-making."

Serop Der-Boghossian, JHK & Associates

Pasadena is a growing city with many commuters and frequent special events that cause traffic backups. Using video as a part of a live traffic surveillance system allows engineers at the Traffic Management Center to respond more quickly, which means fewer congested streets, more efficient use of fuel, and improved air quality.

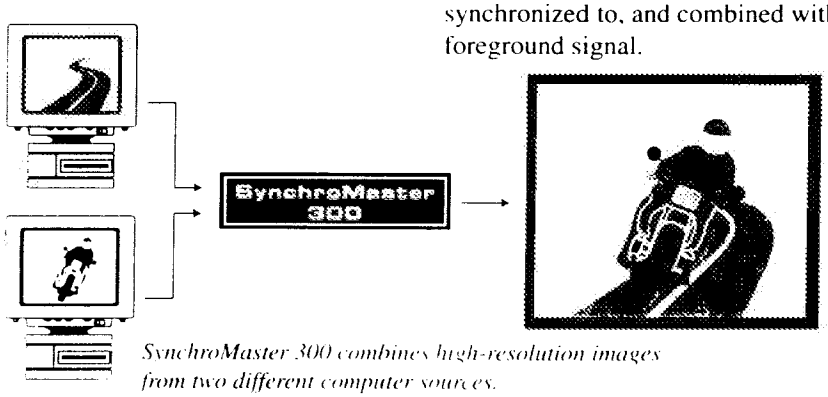
Says Serop Der-Boghossian of JHK & Associates, the systems manager for the Pasadena facility, "The RGB/View system is the best way we've found to integrate live video into computer displays to facilitate decision-making. A traffic engineer who can see a traffic problem developing in real time can respond much more quickly."

RGB Spectrum offers a full line of RGB/View video windowing systems. Various models allow the user to configure a system for showing multiple video inputs, with feeds from cameras, infrared devices (FLIR), and even other computers.

SynchroMaster 300 Is a Hit For Simulation and Training

The recently-introduced SynchroMaster™ 300 is generating a lot of interest in the simulation world. This image synchronizer combines images from two high-resolution computer sources into one composite image. The system enables more complex imagery than can be generated by a single workstation, an important advantage for real-time simulation systems.

For example, in a typical situation one workstation will generate the foreground and the other the background. The background signal is digitized and written to a 1280 x 1024 pixel frame buffer, synchronized to, and combined with the foreground signal.



SynchroMaster 300 combines high-resolution images from two different computer sources.

SynchroMaster 300 Features

- Autosync
- Combines asynchronous images
- Mixes interlaced and non-interlaced images
- Chroma Key, Linear Luminance Key, Weighted Sum
- Converts between interlaced and non-interlaced signals
- Operates with "field extend mode" simulators
- Automatic configuration for 3, 4, and 5-wire systems
- Control of all functions over RS-232 port
- Rear panel control
- Freeze frame



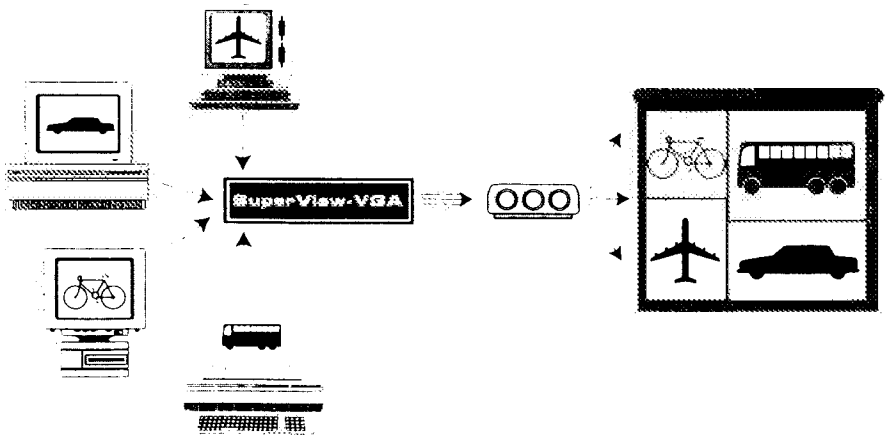
The Sim Eye™ HMD from Kaiser Electro-Optics, Inc. uses field sequential color signals. It can be connected to a computer or scene generator using RGB Spectrum's SynchroMaster™ 100. ***Photo courtesy of Kaiser Electro-Optics, Inc.***

Computer-in-Computer Windowing with SuperView VGA

The SuperView™ line of windowing products has expanded this year, and several models are now available. One unique and interesting version is the SuperView VGA, an advanced display system that combines up to four computer inputs on a single projector or large-screen monitor. It provides multi-image impact at a fraction of the cost of a multi-screen array.

SuperView VGA was developed for sophisticated audio-visual applications, such as multi-source presentations, show displays and exhibits, and control room

Continued, page 6



SuperView VGA lets you position four separate computer (or video) images anywhere on the screen for multi-image impact without the high cost of a traditional multi-projector system.

The "Other" SynchroMaster

The SynchroMaster 100 is a color field sequential scan converter that converts between color parallel and color serial signals. High end helmet-mounted displays often use miniature CRTs with

Continued, page 6....

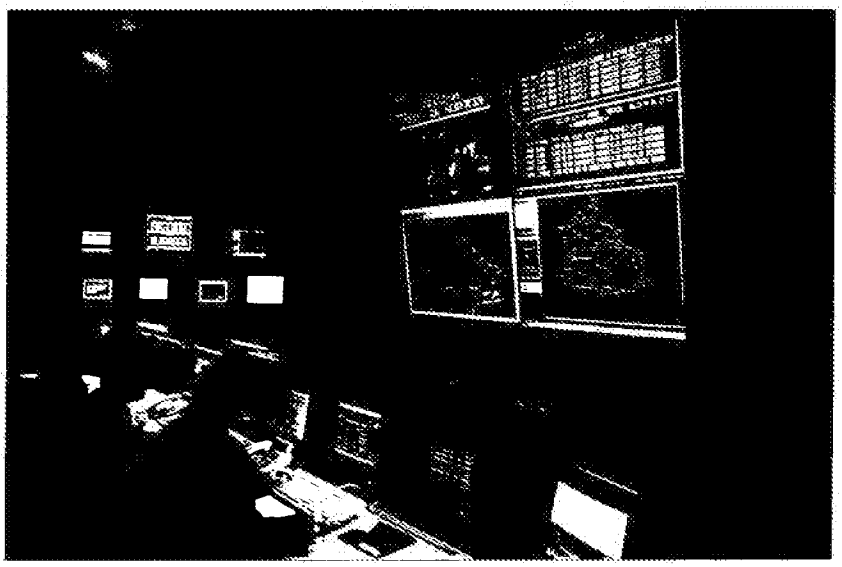
CUSTOMER PROFILE

Network Operation Centre Uses ComputerWall Multi-Screen Display

SHL Systemhouse Ltd. Provides Sophisticated Network Monitoring for Canada Post and Other Customers

RGB's ComputerWall multi-screen controller is part of SHL Systemhouse Ltd.'s Network Operation Centre in Ottawa, Canada. The Centre monitors and maintains a voice & data communications network for a variety of clients, including Canada Post, the Canadian postal service. The Network Operation Centre was designed and built by Tempest Management Corp., and the audio-visual systems were installed by AVspex Video Services, both of Ottawa.

The ComputerWall display is used to control a bank of four large-screen projectors. They can show four different computer sources or a single image split across the whole 4-screen array.



SHL Systemhouse Ltd.'s Network Operation Centre in Ottawa, Canada. Here, ComputerWall is used to control a bank of four large-screen projectors. The Network Operation Centre was designed and built by Tempest Management Corp. and the audio-visual systems were specified and installed by AVspex Video Services, both of Ottawa. ***Photo by W. McElligot Photography, courtesy of Tempest Management Corp., Ottawa, Canada.***

"Computerwall's installation was simple and straightforward and it works perfectly."

- Denis Levesque, SHL Systemhouse Ltd

In the Centre, intelligent systems using UNIX-based workstations collect and display information about the health of the network, which is comprised of over 60,000 devices including terminals, printers, personal computers, and telephones, providing connectivity to mini and mainframes, LANs, and telephony services across the country. If a failure or potential failure occurs, engineers in the Centre can react instantly, and in most cases avoid any compromise to the communications network.

The Centre operates 24 hours a day, 365 days a year, and at any given time there are eight to twelve people monitoring the network. The ComputerWall display system makes it easier for the group to see what's going on.

Having a high-quality multi-screen display also serves a marketing purpose: Potential customers who are touring the facility can easily see how SHL's system works, according to Denis Levesque, Manager of the Network Operation Centre.

"We've had no problems with ComputerWall," says Levesque. "Installation was simple and straightforward and it works perfectly. And aside from working well, it looks good."

ComputerWall, introduced in 1994, is a multi-screen processor that splits high resolution computer images across an array of projectors. The system is designed to create wall-sized, computer-based displays with the brightness and resolution required for control rooms, dispatch centers, and simulators.

New Brochure Tells Large-Screen Presentation Story

High-end projection systems may appear in many environments – control rooms, command centers, auditoriums, exhibit halls, and corporate board rooms. But wherever they're installed, these sophisticated display systems depend on high quality component products to tie them together with the input signal sources. RGB Spectrum is proud to offer such products, and has created a new brochure that details its innovative solutions.

Products include multi-screen and multi-image display controllers, high scan rate frame store synchronizers, video windowing systems, and video scan converters. The products described in the brochure can be used individually or in combination to form the most powerful large-screen and multi-screen presentation systems available. For a copy, call 510-814-7000 and ask for the Large Screen Presentation Products brochure.

Continued from page 1....

Q FORMAT™

The Q system uses standard video tape recorders. Applications include: (a) training, archiving and monitoring, wherever large quantities of pictorial data need to be stored and easily accessed; and, (b) transmission of high resolution computer images over ordinary video channels. For maximum flexibility, the recording (multiplex) unit and the playback (demultiplex) unit are available as separate modules. The QFormat products are expected to be available in the third quarter of 1995.



Multiplexor

The Q multiplexing unit outputs NTSC / PAL composite video and S-video, the latter preferred for videotaping, the former for video transmission. Other video formats are under development.



Demultiplexor

Stored or transmitted images are replayed through the demultiplexing unit onto a high resolution computer monitor. For convenience, the demultiplexor can share a monitor with a computer system and can be genlocked to it.

Superview VGA

Continued from page 4....

environments — any setting where multiple computer screens need to be displayed at full resolution.

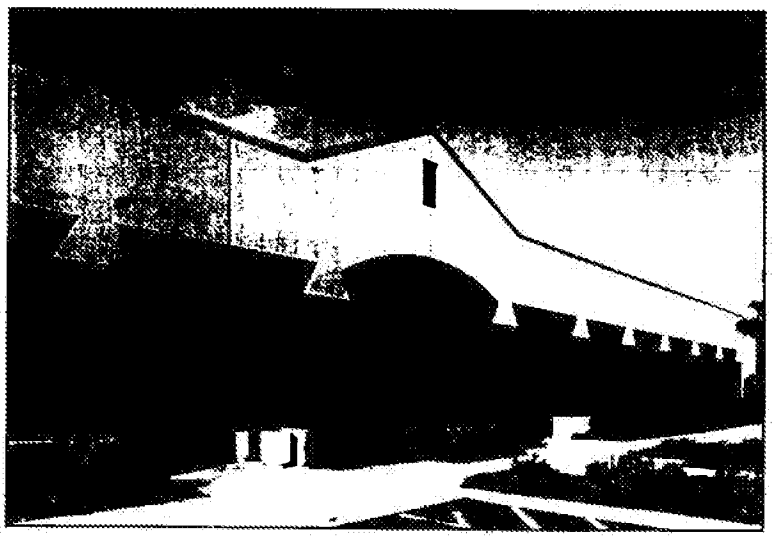
The system accepts a range of VGA inputs up to 800 x 600 pixels. The resolution of each image is preserved since SuperView "mosaics" the input images within a 1280 x 1024 pixel space rather than simply displaying each image at a reduced resolution. Optionally, video inputs are also accomodated.

SuperView VGA is an external standalone peripheral device, easily installed, and compatible with virtually all PCs and many other computers. Video functions can be controlled either from buttons on the easy-to-use front panel, or remotely via the RS-232 port.

SynchroMaster 100

Continued from page 4....

color shutters. These require RGB signals in serial, while computer display systems require RGB signals in parallel. To support both, the SynchroMaster 100 converts RGB signals bi-directionally.



RGB Spectrum's home is in Alameda, California, about 10 miles from San Francisco. Our address is:

RGB Spectrum
950 Marina Village Parkway
Alameda, CA 94501
Phone: (510)814-7000
Fax: (510) 814-7026
e-mail: sales@rgb.com

ComputerWall®

COMMAND CENTERS

CONTROL ROOMS

COMMUNICATIONS CENTERS

SIMULATION SYSTEMS

CONVENTION FACILITIES



ComputerWall Displays Computer Images Across Multiple Screens

ComputerWall is a multi-screen display controller designed for real-time, large format graphical presentations. It outputs bright, high resolution imagery easily seen even under high ambient light conditions.

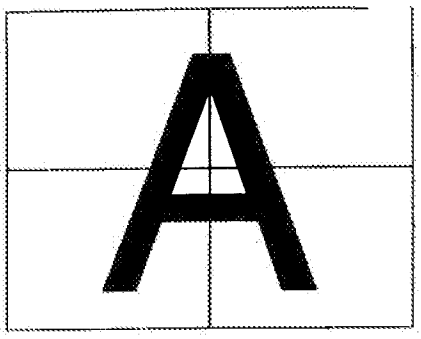
ComputerWall displays data, graphics and video on single screens or seamlessly across multiple screens. Data assessment and decision making are enhanced by ComputerWall's display of information from multiple sources. The system meets the growing need for real-time command and control in telecommunications, transportation, distribution, emergency, police and military operations.

ComputerWall is an extremely versatile and modular system, making it the ideal choice for both new installations and upgrades of existing facilities. It provides maximum flexibility to the end user or systems integrator. It supports variable size display configurations, video and computer inputs up to 1280 x 1024 pixels, *and* a wide variety of projection devices. ComputerWall can be used directly with any software or SCADA system.

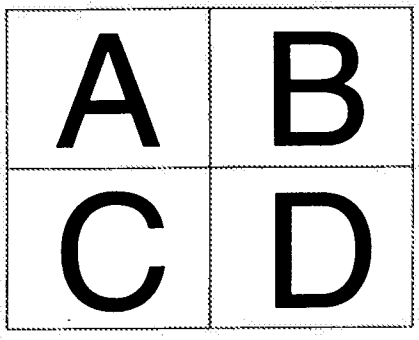
ComputerWall easily connects to the RGB analog outputs of workstations. Its "plug and play" autosync front end ensures that the input computer image is exactly duplicated (at identical resolution), on the display wall.

The result is a wall-sized multi-screen display of unsurpassed brightness and resolution.

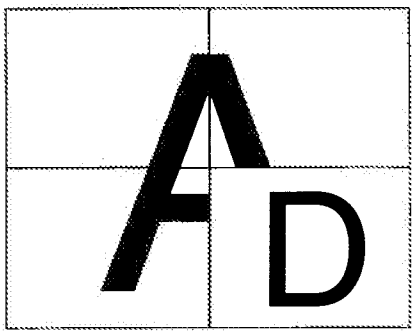
RGB SPECTRUM



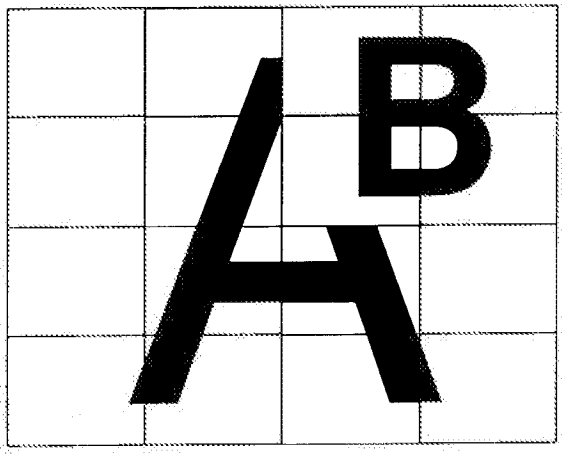
Split Mode
Display an image split across the array



Bypass Mode
Display non-split, passed-through images on individual screens



Split and Bypass Modes
Display split and bypassed images simultaneously



4x4 Configuration
Display split or bypassed images across sixteen screens

The ComputerWall processor splits computer images into quadrants for display across a 2x2 array of four projectors or monitors. Multiple processors can be combined to support larger arrays.

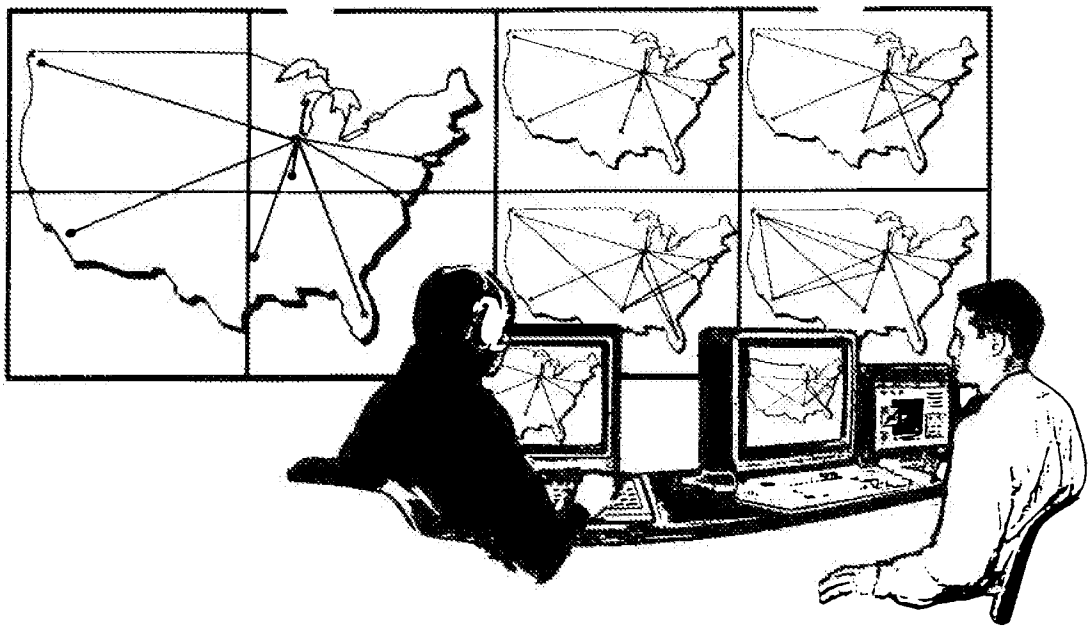
Two models are available. The basic **ComputerWall** accepts two inputs from computers and can display either as a split image. **ComputerWall *Plus*** features a built-in matrix routing switcher with six inputs.

ComputerWall

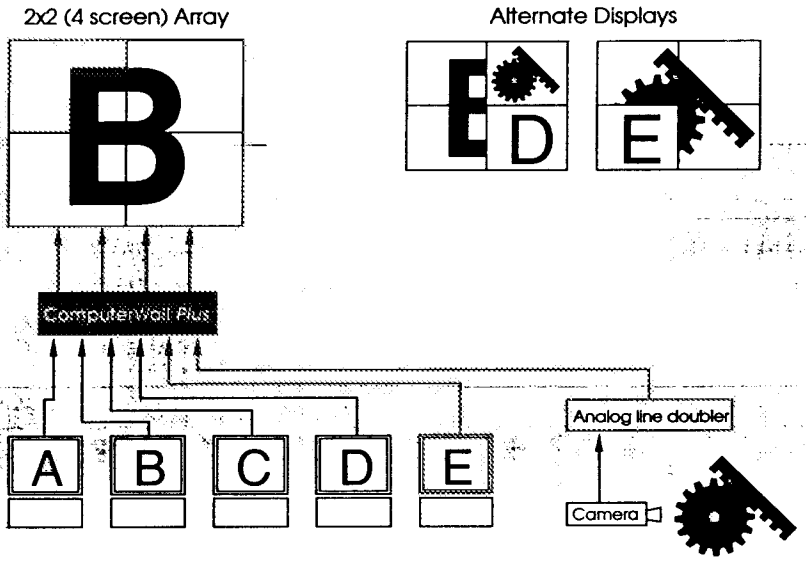
- Accepts high-resolution analog computer signals
  - Connects directly to the RGB monitor port
  - Simple hardware installation
  - Compatible with all software
- Automatically synchronizes to input signals from workstations or PCs up to 1280 x 1024 pixels
- Extremely high image quality
  - Splits all computer imagery, including text, graphics, animation and digitized video
  - Full 24-bit internal image processing
  - Advanced interpolation smoothes magnified images
- Accepts NTSC (or PAL) analog video via optional line doubler
- Two output modes
  - Non-Interlaced: Output scan rate identical to that of the computer source, yielding the highest image quality
  - Interlaced: Output scan rate half that of the computer source, allowing use of less-expensive display devices
- Expandable to many possible configurations
  - ComputerWall processors can be combined to provide 16-way splits on a 4x4 display array
- Mullion control: inter-screen spacing (bezel) compensation
- Freeze frame
- Remote control of all functions via RS-232 serial port

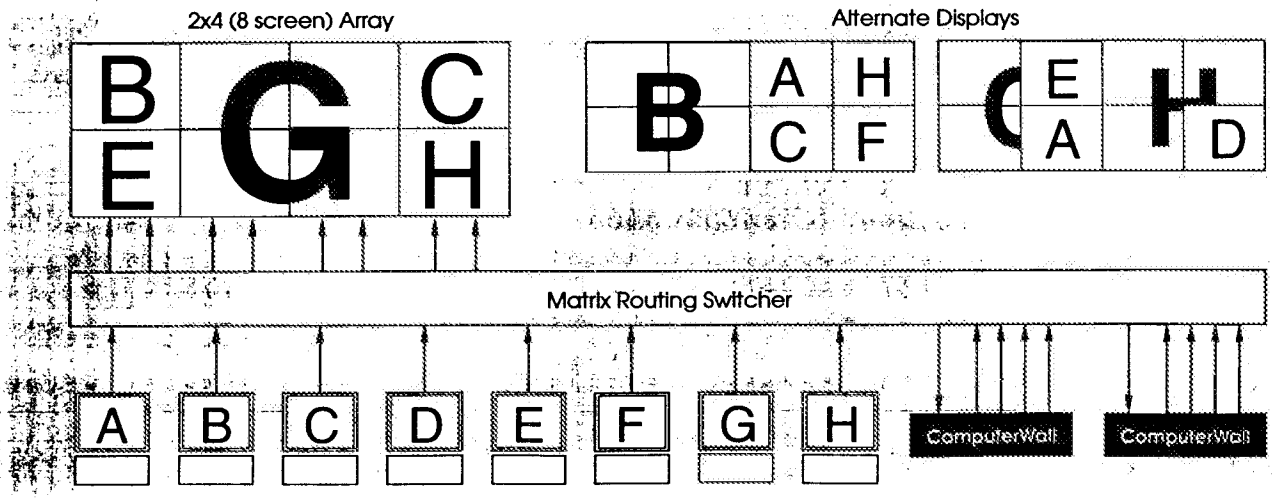
ComputerWall *Plus*

- All features of the basic ComputerWall system
- Built-in, six-input routing switcher
  - Select from among six sources (up to 1280x1024 pixels each)
  - Display four quadrants of a split image or non-split pass-through images, or a combination
- Output signals can be blanked during switching to eliminate undesirable transition effects
- Choice of remote or manual control via front panel pushbuttons



Sample ComputerWall Configurations





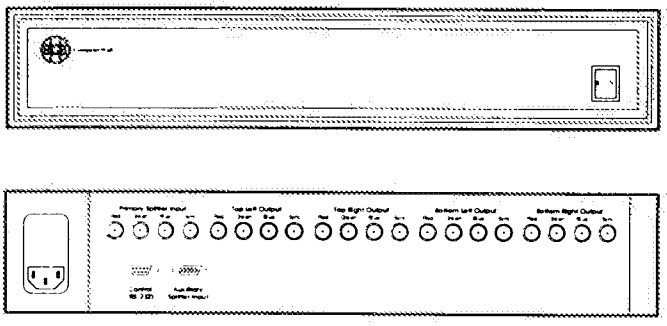
Technical Specifications

Video Input	
Video format	Non-interlaced (NTSC/PAL video with optional line doubler)
Resolution	640 x 480 to 1280 x 1024
Horizontal rate	to 80 kHz
Vertical rate	45 Hz to 76 Hz
Amplitude	0.7 to 1.0 Volt p-p; white positive
Input impedance	75 Ω
Sync amplitude	1 Volt to 5 Volt (75Ω)
Connectors	BNC (Sync on green or separate composite sync) 15 pin HD D-sub (3, 4 or 5 wire); VGA pinout
Video Output	
Resolution	Identical to input
Amplitude	Identical to input
Scan rate	Identical to input (non-interlaced) or half of input scan rate (interlaced)
Output impedance	75 Ω
Connectors	BNC
Control Input	
RS-232 port (1200, 2400, 4800, 9600 baud, echo or no-echo)	
Mechanical	
Size	17.5" x 3.5" x 18.5" (rack-mountable)
Weight	20 lbs.
Power	100 Watts

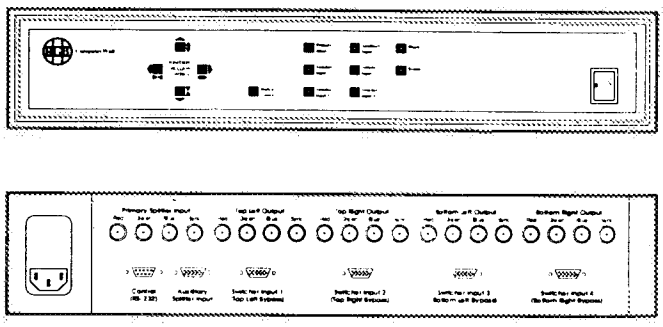
Specifications subject to change without notice
Made in the USA

© 1995 RGB Spectrum

ComputerWall



ComputerWall *Plus*



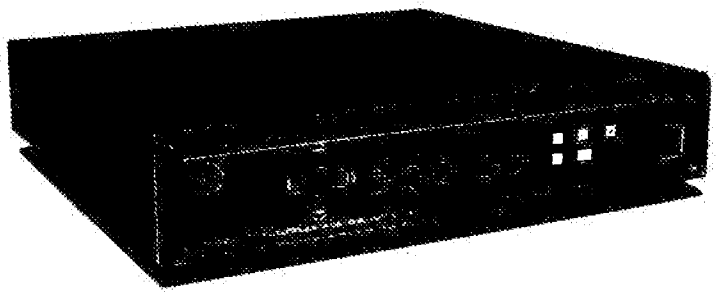
SPECTRUM

950 Marina Village Pkwy
Alameda, CA 94501
TEL (510) 814-7000
FAX (510) 814-7026

THE FIRST SCAN CONVERTER WITH DIGITAL VIDEO OUTPUT

We designed our new RGB/Videolink scan converter with the widest range of outputs available, including CCIR601 digital component video. Now anything you create on a computer can be recorded in D-1, Digital Betacam or other digital video formats.

And, even if you aren't ready for digital video, a unique combination of quality and features makes the RGB/Videolink 1700D-1 the right choice for all your scan conversion applications.



INTRODUCING . . .
THE RGB/VIDEOLINK® 1700D-1

Autosync to all computers

Up to 1600 x 1200 pixel input

Flicker elimination

Smooth zoom

D-1 digital video

NTSC *and* PAL, S-Video, component analog video

Front panel buttons, on-screen menus and RS-232 control

Simple external connections

The RGB/Videolink 1700D-1 transforms computer signals to broadcast video format in real time. Computer-generated images can be recorded on videotape, or displayed on video projectors, teleconferencing systems, and composite monitors.

The model 1700D-1 automatically synchronizes to all computer signals up to 1600 x 1200 pixels. This includes virtually all desktop computers and workstations, from Sun, DEC, HP, IBM, Silicon Graphics, and others.

In addition to NTSC/PAL, S-Video, component analog video (Betacam/MII), and CCIR601 digital video (D-1 Digital Betacam) outputs for recording, a double scan rate RGB signal at 31.5 kHz is available for projection.

State-of-the-art digital signal processing (DSP) circuitry eliminates interlace flicker in the output image. Even thin horizontal lines appear stable; twenty-four levels of filtering offer you the best choice between image sharpness and flicker elimination.

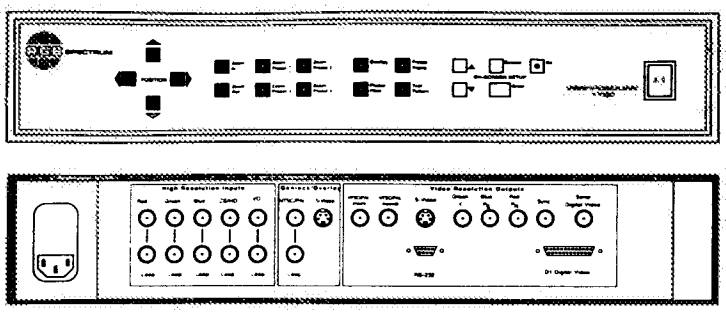
A powerful zoom function lets you scale a portion of the image to fill the video screen and provides just the right amount of underscan/overscan adjustment. The operation is so smooth that it allows continuous pan and zoom effects while videotaping.

The model 1700D-1 also gives you the ability to overlay computer-generated graphics on video using either a built-in linear luminance keyer or a chroma keyer, on composite video or S-Video backgrounds.

Control over so many sophisticated features has never been this easy. Front panel and on screen menu-driven controls put all functions at your fingertips. An RS-232 port is provided for remote control. Custom setups are saved in non-volatile storage, with user-definable zoom presets available on the front panel.

Simply stated, the RGB/Videolink 1700D-1 is the finest scan converter in the world.

RGB SPECTRUM
a visual communications company



Specifications subject to change without notice
Patent Pending
©1995 RGB Spectrum

Computer Input Signals

Type:	Red, Green and Blue analog video
Interlace:	1:1, 2:1
Amplitude:	0.5 V to 1.0 V peak-peak (black level to white level)
Pedestal:	0 to 120 mV
Impedance:	Bridging
Connectors:	BNCs with loop through
Video Polarity	Positive
Resolution:	320 x 200 to 1600 x 1200
Scan Rate:	5 kHz to 140 kHz
Sync Type:	Sync on green, separate composite sync or separate horizontal drive and vertical drive
Sync on green	200 mV to 400 mV
Separate sync	1.0 V to 5.0 V, polarity negative/positive

Video Outputs

Composite	Differential phase	< 2 degrees
	Differential gain	< 2%
	K2T	< 1%
	KPB	< 2%
	Connector	BNC
	Output Level	1.234 V for 100% color bars
	Adjustment range	0.7 V to 1.4 V p-p
	Number of outputs	Two (one with overlay)
CAV	Broadcast RGB scan rate	15.734 kHz, 29.97 Hz / 15.625 kHz, 25 Hz
	Y, PB, PR scan rate	15.734 kHz, 29.97 Hz / 15.625 kHz, 25 Hz
	Double rate RGB scan rate	31.469 kHz, 59.94 Hz / 31.25 kHz, 50 Hz
Digital	10 bit CCIR601 (RP125 /EBU Tech. 3267-E) parallel and serial	
S-Video	Standard S-Video levels on a four pin mini-DIN connector	

Genlock Broadcast quality genlock with timing controlled through the serial port or on-screen sdisplay. S-Video, composite 9NTSC/PAL), black burst

Overlay/ Superimpose Linear luminance keyer *and* linear chroma keyer. NTSC/PAL or S-Video

Visual Controls
Zoom 70% - 250%
Pan
Aspect ratio
Overscan/underscan adjustment
Flicker filter - 24 levels
Fade to black
Freeze frame

Serial Communications

Physical:	9 pin D-sub
Configuration	Software switched between DCE and DTE
Data:	8 bits, 1 start, 1 stop / 7 bits, 1 start, 2 stop / parity optional
Echo:	User selectable
Baud rate:	300, 1200, 2400, 4800, 9600, 19200, 38400

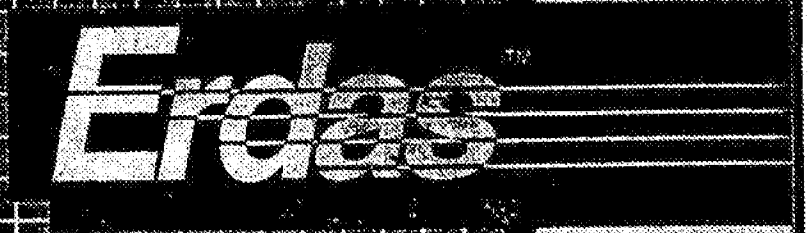
Physical

Dimensions:	17.5 (w) x 14.0 (d) x 3.5 (h)
Weight:	18 lbs
Power:	AC 90-132V or AC 180-264V 100W

Control
On screen menu display
RS-232 ser al port
Front panel

RGB SPECTRUM
950 Marina Village Parkway
Alameda, California 94501
TEL (510) 814-7000
FAX (510) 814-7026

Field Guide



Version 7.4, January 1990

OFEK07537

Image Data From Aircraft

Image data can also be acquired from multispectral scanners aboard aircraft rather than satellites. This can be useful if you cannot wait for the next satellite pass over a particular area, or you desire a specific spatial or spectral resolution that cannot be attained with the satellites.

This type of data acquisition can also be beneficial in the event of a natural or man-made disaster, because there is more control over when and where the data are gathered.

Image Data From Scanning Cameras

Besides satellite data, hardcopy maps and photographs can be incorporated into the ERDAS system through the use of a scanning camera or video digitizer.

In ERDAS, **scanning** refers to the transfer of analog data, such as photographs, maps, or another viewable image, into a digital (raster) format.

Scanning vs. Remote Sensing

Scanning is remote sensing in a manner of speaking, but "remote sensing" is usually reserved for satellite or aerial data collection. The scanned object is usually a map, picture or other representation of the earth, but it could be anything you wanted to incorporate into your data base.

Once an image is scanned, it is stored in a LAN file and can be retrieved, displayed, enhanced, and analyzed just as any other remotely sensed data.

Video Digitizing

Video digitizing involves digitizing a frame of analog video camera input. An analog-to-digital converter, known as a **frame grabber**, digitizes the data and stores it in the memory of the digitizer. Memory is then read by the host computer and the digital information is stored in a LAN file.

Video digitizing is dependent upon the resolution of video camera which is defined as 512 x 480. It cannot be improved over this value.

Use VIDDIG (Image Scanning) to video digitize an image.

Eikonix Scanning

Eikonix scanning involves the use of a camera mounted above a moveable stage. The map, photograph, transparency, or other object to be scanned is placed on the stage and the detector within the camera moves to record the image, transferring it from analog to digital data.

OFEK07538

Advantages

Eikonix scanning allows you to create a 4096 x 4096 digital image, and Eikonix images have better color fidelity than video digitized images.

You control:

- exposure level,
- focus accuracy,
- scanning dimensions, and
- scanning color.

You can create single or multiband images in color or black-and-white. The image you create is saved to a LAN file, and then can be displayed on the display screen, or output to hardcopy.

Downsampling

Downsampling is the skipping of pixels during the display of the scanning process.

If you send the scanned image to the display screen or to a printer, the number of pixels must often be downsampled to account for the discrepancy in the resolution of the camera and the resolution of your display device or printer. The camera can scan a up to a 4096 x 4096 area, but your display may only be able to display a 1024 x 1024 or 512 x 512 area.

Use ESCAN (Image Scanning) to scan an image with the Eikonix camera.

Radiometric Correction

There are several errors that are manifested in the data due to the sensor system. Below are some common problems and how to remedy them.

❑ These errors are usually already corrected in data you receive from EOSAT or SPOT.

Line Dropout

Line dropout occurs when a detector either completely fails to function, or becomes temporarily overloaded during a scan (like the effect of a camera flash on your retina). The result is a line or partial line of data with higher data file values, creating a horizontal streak until the detector(s) recover, if they recover.

Line dropout is usually corrected by replacing the bad line with a line of estimated data file values, based on the lines above and below it.

Use BADLIN (Core) to correct line dropout in LAN files.

OFEK07539

Striping

Banding or **striping** will occur if a detector goes out of adjustment - that is, it provides readings consistently greater than or less than the other detectors for the same band over the same ground cover.

Some Landsat 1, 2 and 3 data have striping every sixth line, due to improper calibration of some of the 24 detectors that are used by the MSS. The stripes are not constant data values, nor is there a constant error factor or bias. The differing response of the errant detector is a complex function of the data value sensed.

To help to eliminate the stripes, six histograms are computed - one for every 6th line, starting at line 1, line 2, etc. to line 6. These six histograms are averaged. Then, a lookup table is computed for each of the six histograms, which is used to map every pixel in the corresponding set of lines to approximate the average histogram.

Use DESTRIP (Core) to correct striping on Landsat 1, 2 and 3 data. DESTRIP is not a general-use destriping program - it corrects only one specific error in one type of data.

Skew

As a satellite orbits the earth from north to south or south to north, the earth rotates beneath it such that the position of the satellite relative to the earth moves westward. Therefore, each line of data represents terrain that is slightly west of the data in the previous line. This condition is called **skew**.

Landsat data sets gathered prior to 1979 are provided only in the EROS X format, which does not correct skew. Later data sets are in the EROS EDIPS format, which does correct skew.

Use DESKEW (Core) to correct skew in Landsat 1, 2, or 3 data gathered prior to 1979. DESKEW is not a general use deskewing program - it corrects only one specific error in one type of data.

OFEK07540

Chapter 7
Rectification

Definitions

Raw, remotely sensed image data, gathered by a satellite or aircraft, is a representation of the irregular surface of the earth. Even images of flat areas are distorted by the earth's curve. This chapter covers the processes of geometrically correcting an image, so that it can be represented on a planar surface, or so that it conforms to other images.

Map Projections and Coordinates

A **map projection system** is any system designed to represent the surface of a sphere or spheroid (such as the earth) on a plane. There are a number of different map projection methods. Since flattening a sphere to a plane causes distortions to the surface, each map projection system compromises accuracy between certain properties, such as conservation of distance, angle or area.



The properties of map projections and of particular map projection systems are discussed in "Appendix D: Map Projections."

There are a number of **map coordinate systems** for determining location on an image. These coordinate systems conform to a grid, and are expressed as X,Y (column, row) pairs of numbers. Each map projection system is associated with a map coordinate system.

Rectification

Rectification is the process of projecting the data onto a plane, and making it conform to a map projection system. In many cases, the image must also be oriented so that the north direction corresponds to the top of the image.

In the rectification process, the grid of the raw data must be projected onto a new grid. **Resampling** is the process of extrapolating data values for the pixels on the new grid from the values of the source pixels.



Latitude/Longitude is a map coordinate system that is not associated with a map projection. Lat/Lon expresses locations in the terms of a sphere, not of a plane. Therefore, an image is not usually "rectified" to Lat/Lon.

Registration

In many cases, images of one scene that are collected from different sources must be used together. To be able to compare separate images pixel by pixel, the pixel grids of each image must conform to the others in the data base. The tools for rectifying image data are used to transform disparate images to the same coordinate system.

Registration is the process of making image data conform to another image. A map coordinate system is not necessarily involved.

OFEK07541

Georeferencing

Georeferencing refers to the process of assigning map coordinates to image data. The image data may not need to be rectified - it may already be projected onto the desired plane, but not yet be referenced to the proper coordinate system.

Rectification, by definition, involves georeferencing, since all map projection systems are associated with map coordinates. Image-to-image registration involves georeferencing only if the reference image is already georeferenced.

Georeferencing, by itself, only involves changing the map coordinate information in the image file. The grid of the image does not change.

Geocoded Data

Geocoded data are images that have been rectified to a particular map projection and pixel size, and have had radiometric corrections applied. Image data can be purchased that is already geocoded. It is only necessary to rectify geocoded data if it must conform to a different projection system, or be registered to other data.

When To Rectify

Rectification is necessary in cases where the pixel grid of the image must be changed to fit a map projection system or a reference image.

There are several reasons for rectifying image data:

- for scene-to-scene comparisons of individual pixels in applications such as change detection or thermal inertia mapping (day and night image comparison),
- for developing GIS data bases for GIS modeling,
- for identifying training samples according to map coordinates,
- for creating photomaps,
- to overlay an image with ARC/INFO vectors,
- for comparing images at different scales,
- for mosaicking images, or
- any other applications in which precise geographic locations must be identified.

OFEK07542

When to Georeference Only

Rectification is not necessary if there is no distortion in the image. For example, if an image file is produced by scanning or digitizing a paper map that is in the desired projection system, then that image is already planar, and does not require rectification unless there is some skew or rotation of the image.

Scanning and digitizing produce images that are planar, but do not contain any map coordinate information. The image needs only to be georeferenced, which is a much simpler process than rectification.

Use MAPTAC (Image Scanning) to georeference a scanned image.

Disadvantages of Rectification

During the process of rectification, the data file values of rectified pixels must be resampled, to fit into a new grid of pixel rows and columns. Although the algorithms for calculating these values are highly reliable, some spectral integrity of the data can be lost during rectification. If map coordinates or map units are not needed in your application, then it may be wiser not to rectify your image. An unrectified image is more spectrally correct than a rectified image.

Classification

If you are classifying your image, it is recommended that you do so before you rectify, for the same reasons. The classification will be more accurate if the original data file values are used in the algorithms. Another benefit is that a GIS file has only one band to rectify, instead of the multiple bands of a LAN file.

GIS Files

Only the nearest neighbor and GIS aggregation resampling methods are appropriate for GIS files, which may be a drawback in some applications. (See below for an explanation of the available resampling methods.)

OFEK07543

Steps in Rectifying Image Data

❑ Registration and rectification involve the same set of procedures. Throughout this documentation, any reference to rectification also applies to image-to-image registration.

An image can be rectified either temporarily, on the display device, or permanently, with the changes stored to a new output file.

Display

Use IFX (Core) to rectify an image on the display device. Only linear (1st-order) transformations are possible on the display.

Disk

Rectification of a data file involves:

- rearranging the pixels of the image onto a new grid, which conforms to a plane in the new map projection and coordinate system, and
- inserting new information to the header of the file, such as the upper left corner map coordinates, and the area represented by each pixel.

Usually, rectification is the conversion of data file coordinates to some other grid and coordinate system, called a **reference system**.

Rectifying or registering image data on disk involves the following general steps, regardless of your application.

1) Locate ground control points, with GCP (Image Processing). (Ground control points can also be generated with PROGCP (Image Processing) for converting from one map projection system to another.)

2) Compute and test a transformation matrix with COORDN (Image Processing). (LRECTIFY (Image Processing) also allows you to create a 1st-order transformation matrix.)

3) Create an output image file, with the new coordinate information in the header. The pixels must be resampled to conform to the new grid. Use LRECTIFY or NRECTIFY (Image Processing).

These steps are explained in detail under the headings below.

OFEK07544

Ground Control Points

Ground control points (GCPs) are specific pixels in image data for which the output map coordinates (or other output coordinates) are known.

GCPs consist of two x,y pairs of coordinates:

- **source coordinates**, which are usually data file coordinates, and
- **reference coordinates**, the coordinates of the map or reference image to which the source image is being registered.

The **rectified coordinates** of the image are extrapolated from the ground control points. Ideally, the rectified coordinates for the ground control points are exactly equal to the reference coordinates. Since there is often some error tolerated in the rectification, this is not always the case.

☞ The term "map coordinates" is sometimes used loosely, to apply to reference coordinates and rectified coordinates. These coordinates are not limited to map coordinates. For example, in image-to-image registration, map coordinates are not necessary.

Entering Ground Control Points

Accurate ground control points are essential to an accurate rectification. From the ground control points, the rectified coordinates for all other points in the image are extrapolated. Many GCPs should be located throughout the scene. The more dispersed the GCPs are, the more reliable the rectification.

GCPs for large-scale imagery might include the intersection of two roads, airport runways, utility corridors, towers, or buildings. For small-scale imagery, larger features such as urban areas, water features or geologic features may be used.

The source and reference coordinates of the ground control points may be entered in the following ways.

- They may be known *a priori*, and entered at the keyboard.
- The pointing device may be used to select a pixel from an image that is on the display screen. This method can be used to enter either source coordinates or reference coordinates.
- To register an image to a hardcopy map, a digitizing tablet may be used. (Information on the use and setup of a digitizing tablet is discussed in "Chapter 2: Vector Data.")

These coordinates are stored in a ground control point file (GCP file) with the extension GCP.

Use GCP (Image Processing) to enter ground control points.

OFEK07545

Orders of Transformation

Polynomial equations are used to convert source coordinates to rectified coordinates. Depending upon the distortion in the imagery, the number of GCPs, and their locations relative to one another, complex polynomial equations may be required to express the needed transformation. The complexity of the polynomial is known as the **order** of the polynomial. The order is simply the highest exponent used in the polynomial.

The **order of transformation** is the order of the polynomial used in the transformation. ERDAS allows 1st- through 10th-order transformations. Usually, 1st-order or 2nd-order transformations are used.

⇨ **A discussion of polynomials and their orders is included in "Appendix A: Math Topics."**

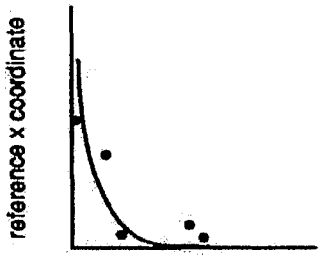
Transformation Matrix

A **transformation matrix** is computed from the GCPs. The matrix consists of coefficients which are used in polynomial equations to convert the coordinates. The size of the matrix depends upon the order of transformation.

The goal, in calculating the coefficients for the transformation, is to find the polynomial equations for which there is the least possible amount of error when they are used to transform source coordinates of the GCPs into the reference coordinates. It is not always possible to derive coefficients which produce no error.

For example, these GCPs are plotted on a graph, and compared to the curve that is expressed by a polynomial:

Polynomial Curve vs. GCPs



Every GCP influences the coefficients, even if there is not a "perfect fit" of every GCP to the polynomial that the coefficients represent. The distance between the GCP reference coordinate and the curve is called RMS error, which is discussed below.

The **least squares regression** method is used to calculate the transformation matrix from the GCPs. This method would be discussed in a statistics textbook.

OFEK07546

Georeferencing

Georeferencing is the process of updating a file header with new map coordinate information. This involves redefining:

- the map coordinate of the upper left corner of the image, and
- the cell size (the area represented by each pixel).

Georeferencing is usually needed for files created by scanning or digitizing, which are generated in the proper map projection, but do not contain the map coordinate information.

FIXHED (Core) is the most straightforward way to georeference an image. FIXHED allows you to change the header of the file to include the new georeferencing data. Similarly, MAKEFIL (Core) creates an empty, georeferenced file, that can be written to with other programs.

Use MAPTAC (Image Scanning) to georeference scanned or digitized images that do not require rectification. MAPTAC converts known Lat/Lon coordinates that you specify into the desired coordinate system (which should correspond to the projection system used on the scanned map), and updates the image file header.

Use DIGUTIL (Core) to convert a DIG file from data file (or data base) coordinates to map coordinates or back again.

OFEK07547

Projection Files

Several ERDAS programs make use of a **projection file** (PRO extension). This file contains parameters that are specific to the map projection used in an image or vector (DIG) file.

The programs that use PRO files ask a set of questions that are specific to the map projection/coordinate system being used. The responses to these prompts are stored in the PRO file.

The PRO file is used...

- to convert coordinates from one map coordinate system to another.
- to provide default parameters for the projections calculations in ERDAS programs, whenever a PRO file has already been generated for a data file.
- to provide Lat/Lon coordinates for the image, regardless of the map coordinate system to which the file is georeferenced.

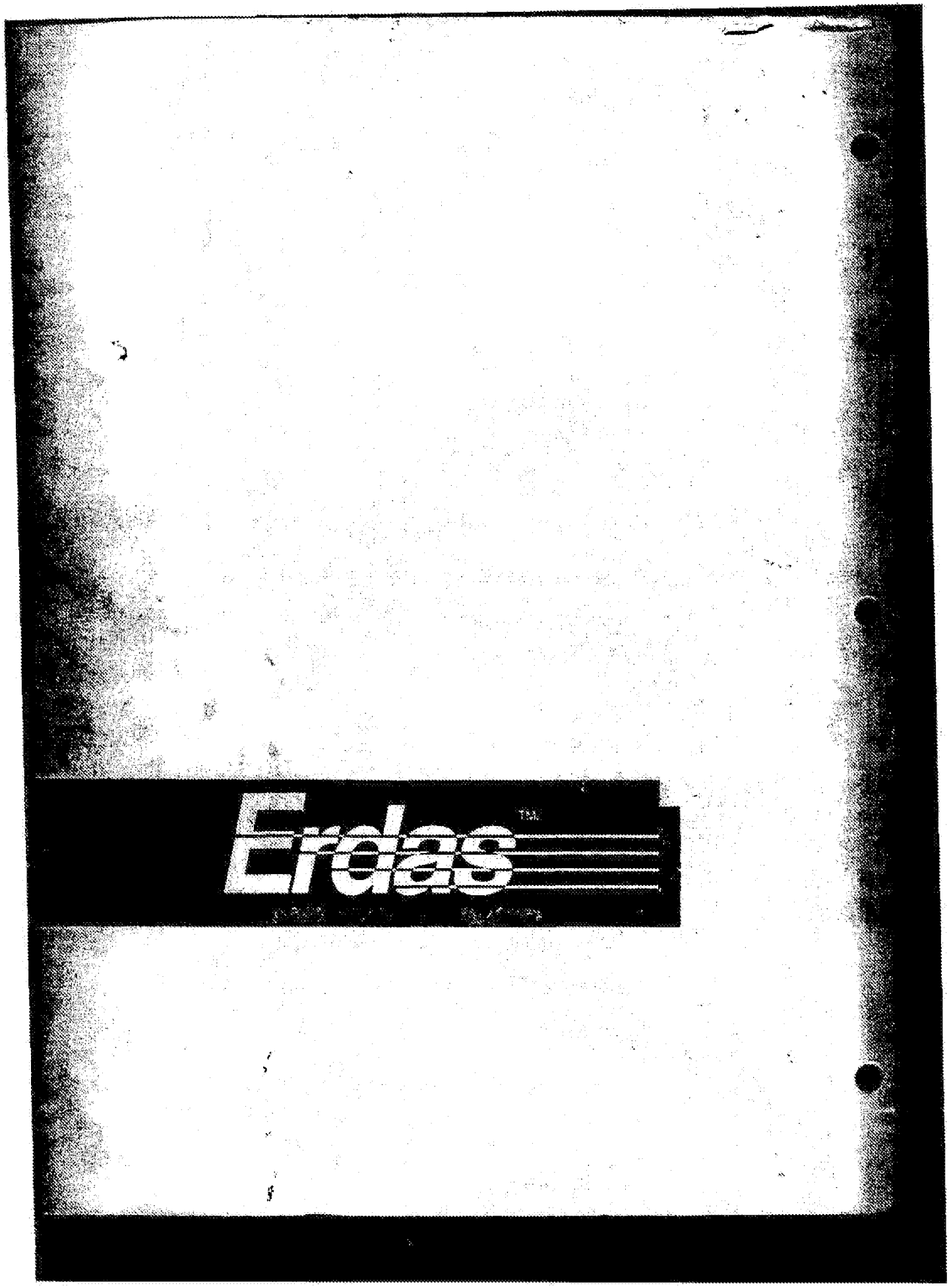


The prompts used for entering PRO file parameters are documented in "Appendix D: Map Projections" of this manual.



The format of the PRO file is documented in "Appendix B: ERDAS File Formats & Extensions."

OFEK07548



OFEK07549

IMAGE MEASUREMENT AND AERIAL PHOTOGRAPHY

MAGAZINE FOR ALL BRANCHES OF PHOTOGRAMMETRY AND ITS FRINGE AREAS

Organ of the German Photogrammetry Association (Regd. Assn)
Editor Kurt Slawik, Berlin Wilmersdorf, Hildegardsrasse 5

With acceptance and publication of manuscripts, the sole right for copying and translating is transferred to the publisher	Reprinting is only permitted with the permission of the magazine management and with a brief source reference. Liability is not accepted for rejected manuscripts

1958 Berlin-Wilmersdorf, 1 March 1958. No. 1

Contents: Mechanical Radial Triangulation with Convergent Photos, P.1/ Gotthardt; Comparative measurements with Stereotop and AeroProjector Multiplex, P. 8/Weimann; Sectional Drawings with Planigraphs, P.12, Wirths, the Application of Aerial Photo Measuremenet in the Production of Cadaster Cards in North-Rhine-Westphalen, P. 21, /Hasse/Nowatzky, RE: The Conjunction of Successive P, P. 29/Dressler, Aerial Photo and Cards Exhibition in Berlin, P. 30/Repots {P. 32. Book Reviews P. 38hotographs

MECHANICAL RADIAL TRIANGULATION WITH CONVERGENT PHOTOS

By Dipl-Ing. G Konecny, Munich.

1. General.

Control point determinations are significant for photogrammetric evaluations. Due to the high costs of control point determination, however, efforts are being made to replace the more precise geodetic determination methods with more economic photo triangulation. In small-scale areas, radial triangulation has not lost its significance for quickly determining the horizontal control points.

In recent years convergent photogrammetry has gained fresh momentum due to its more favorable surface performance. Since 1951 the U.S. Geological Survey has used several 15/23 wide angle chambers with a convergence angle of 40^0 for production of cards on a scale of 1: 24 000. Park Aerial Surveys and AMS have also used convergent wide angle photos for high altitude aerial flights.

For European photogrammetric problems, the convergent photo with the Zeiss-Aerotopograph normal angle, dual chamber 2 X RMK 21 / 18 might be

OFEK07589

applicable. Dr. Brucklacher (1) gives a brief description of the possibility of radial triangulation with convergent photos.

During a two year USA stay in 1955, the author was engaged in applying mechanical radial triangulation methods to convergent wide angle photos at a convergence angle of $40^0 = 2v$. These involved tests with the picture slot method and with metal templets. However, the considerations were also valid for numerical radial triangulation, whose use had long diminished.

In radial triangulation, angles in the photo are compared with angles in nature. In doing so, 3 specific points can be used as radial centers [2]:

1, The main point *(M)*

2. The nadir-point *(N)*

(3) The focal point *(F)* (the angle-faithful point).

If v =0 (i.e. in the case of an exactly perpendicular photo), all three points converge in one point and all angles measured in it between rays in the picture and in nature are equal. Usually, however, the picture angle will undergo distortions due to picture inclination and unevenness on the site. According to Fagergolg [3] the radial distortions in the picture for approximately vertical photos are:

For the main point: $d\alpha = \frac{v^2}{4} \sin 2\alpha - v \frac{\Delta Z}{R} \cos \alpha,$

For the nadir point: $d\alpha = \frac{v^2}{4} \sin 2\alpha,$

For the focal point : $d\alpha = -\frac{v}{2} \cdot \frac{\Delta Z}{R} \cos \alpha,$

Legend:

v = inclination

a Angle of the ray counted from the inclination axis

Δz = Difference in height between the end points of a ray

R = Length of the ray.

In practice, the nadir and focal point are usually not precisely definable due to lack of knowledge of the exact inclination; - in vertical pictures , therefore,

OFEK07590

particularly, however, due to the secure possibility of transmitting the points - one uses approximately radial centers at prominent picture points in the proximity of the ideal position. According to Fagerholm, the formulae provided would thus still need to be supplemented if the actual radial center was at a distance of ξ alongside the inclination axis and *Δ (not legible)* perpendicular to it; namely by the expressions ;

$$+\left(\frac{\nu}{2}\sin 2\alpha - \frac{\Delta Z}{R}\cos\alpha\right)\Delta\nu - \left(\nu\sin^2\alpha - \frac{\Delta Z}{R}\sin\alpha\right)\xi.$$

From this it emerges that nadir- point triangulation is more favorable when there are large land height differences and focal point triangulation takes precedence for large picture inclinations.

R. Foerstener (4) made a graphic representation giving an overview of the direction errors of main point-, nadir- point and focal point triangulation. His publication also contains the deduction of the complicated, strong (**strongly simplified?**)relationships of the direction errors which, in the perpendicular case (*v* up to 5°), can be transmitted by series development in the above-mentioned, greatly simplified form.

The strict formula for focal point triangulation is noted here for interest:

$$\operatorname{tg} d\alpha = \frac{\frac{\Delta Z}{h}\cos\alpha\left[\sin\alpha\,(1-\cos\nu) - \frac{f}{R}\operatorname{tg}\frac{\nu}{2}\right] + \left[\operatorname{tg}\frac{\nu}{2} - \operatorname{tg}\frac{(\nu-\Delta\nu)}{2}\right]}{\left(1-\frac{\Delta Z}{h}\right) + \frac{\Delta Z}{h}\sin\alpha\left[\sin\alpha\,(1-\cos\nu) - \frac{f}{R}\operatorname{tg}\frac{\nu}{2}\right] - \left[\operatorname{tg}\frac{\nu}{2} - \operatorname{tg}\frac{(\nu-\Delta\nu)}{2}\right]}$$

$$\frac{\left[\sin\alpha\cdot\sin\nu - \frac{f}{R}\frac{\Delta Z}{h}\cos\nu\right] - \operatorname{tg}\xi\cdot\sin\alpha\left[\sin\alpha\cdot\sin\nu - \frac{f}{R}\cdot\frac{\Delta Z}{h}\right]}{\left[\sin\nu\cdot\cos^2\alpha - \frac{f}{R}\cdot\frac{\Delta Z}{h}\sin\alpha\cdot\cos\nu\right] + \operatorname{tg}\xi\cdot\cos\alpha\left[\sin\alpha\cdot\sin\nu - \frac{f}{R}\cdot\frac{\Delta Z}{h}\right]}$$

F= focal distance and h = flight altitude

2. Focal Point Triangulation.

A comparison of the formulae shows that a radial center, which - depending on inclination and uneven topographies - causes the least number of errors,

OFEK07591

will lie somewhere between nadir-point and focal point. When the strict formulae are evaluated, a range of $0.1 > \frac{\Delta Z}{h} > 0$ emerges in which focal point triangulation will be more favorable than nadir-point triangulation. This always applies to high-altitude flying, as well as for level and medium-hilly land.

Contact copies of convergent photos can consequently be used directly for radial triangulation without special aids, as long as one knows the convergence angle and thereby (approximately) the inclination angle.

The focal points lie vertically to the inclination axis at a distance of $f \cdot \mathrm{tg} \frac{v}{2}$ from the main point of the picture, approximately in flight direction or contrarily. They can be easily constructed on a transparent templet and thus transmitted onto the photos, likewise the selection and transmission of other external connection points. The further transmission of focal points from photo to photo occurs stereoscopically, as do the selection and transmission of external connection points. Although with convergence photos stereoscopic viewing without compensation through enlargement is subject to strong compulsion, and will only be possible in the point's immediate surroundings, stereoscopic point transmission is possible after some practice, especially when one uses inclined photo carriers in conjunction with a mirror stereoscope.

The following diagrams serve to explain the network image:

OFEK07592

Diagram 1 Focal Point Triangulation

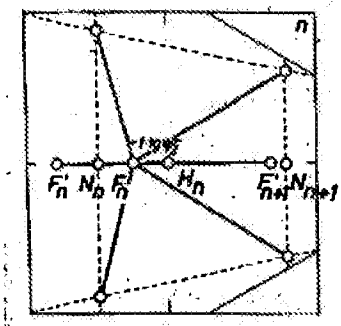


Diagram 1a.Convergent Photo

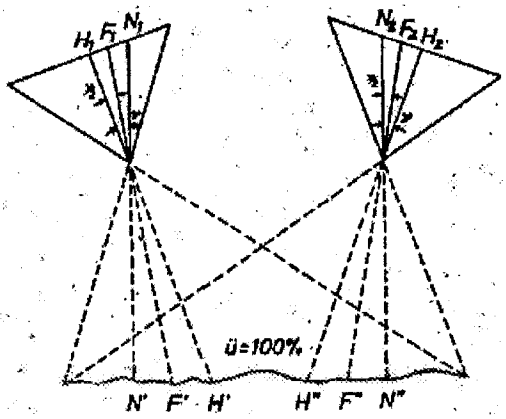


Diagram 1b. Geometric Interrelationships

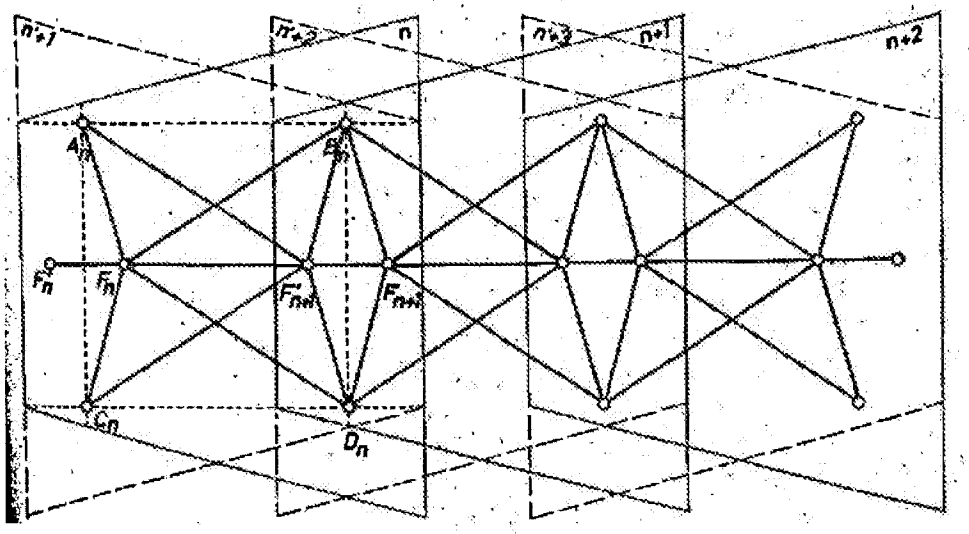


Diagram 1 c. Focal Point Network

In Focal Point *Fn,* 6 directions result according to points *An, Bn, F`n+1, Dn, C(illegible) and F1n,* permitting a very rigid triangulation network to be constructed.

Due to the network's rigidity, the focal point method in mechanical radial triangulation- which in today's practice is used almost exclusively - is only possible without disturbing gapings when the direction errors remain small.

Theoretical directional deviations must therefore at least be sufficiently precise to enable a radial point to be determined and transmitted. If we assume a

OFEK07593

value of 0.3 mm for this precision at the end point of a ray, then in the most unfavorable case we receive – at a fixed $v = 20^0$ - a value of

$\frac{\Delta z}{h} = 11^o/_{oo}$.

The focal point *of* the triangle can consequently be executed when $\frac{\Delta z}{h} = 11^o/_{oo}$ remains.

Care must be taken to keep ξ and Δv as small as possible, since the errors they cause are several times the number of errors conditioned by nadir-point and topography. It is therefore recommended that the focal points themselves be used as radial centers, even if they are not prominent points in the photo. Their transmission must be carried out with particular meticulousness.

3. Nadir-Point Triangulation with Distorted Pictures or Rays

To reduce the disadvantages that accompany focal point triangulation, an approximated distortion of the photos (by half the convergence angle) can be performed. The nadir-point of the copy point then corresponds to the directional fields of a regular main point triangulation. The only difference lies in the fact that each nadir point has two appended pictures of the dual chamber. In each of the two pictures, the pictures are each determined according to 5 points. Two of the rays in the inclination axis are then identical in both pictures. This results in an expanded form of a lozenge (rhombus).

OFEK07594

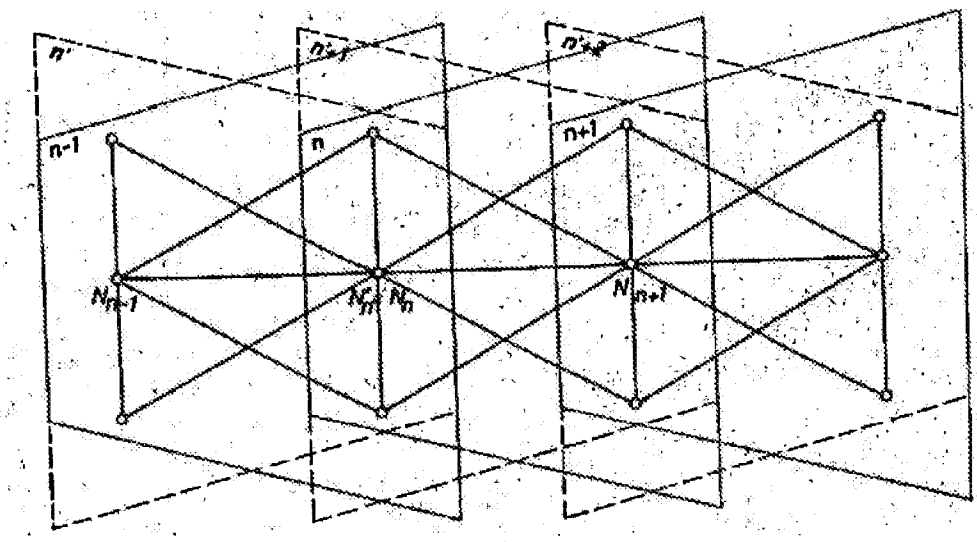


Diagram 2. Nadir-Point Triangulation

If $\xi = 0^{0,}$ the directional distortion can be fully ignored· For ξ = (illegible) and with 0.3 mm distortion at the end point of the ray at $v = 200$, one obtains a limit of $\frac{\Delta z}{h} < 11.3/_{oo}$. Here, too, therefore, it advisable to use nadir - points attained with a templet instead of other nearby prominent points so that ξ can be kept small.

Distortion can occur in different ways. The simplest is photographically, by means of a distortion device in accordance with data for settings [5]. Of the European devices, the Zeiss SEG 1 and the WILD E 2 are well suited for 40^0 convergent pictures because of their large inclination areas. Naturally, distortion can be limited to the rays themselves by means of suitable methods It can, for example, be graphically [5] executed.

A mechanical distortion of rays takes place in the RS radial sector of a Zeiss Aerotopograph. As a universal instrument for radial triangulation it possesses a device to adjust *v* picture inclinations up to 22.5^0 and to correct all rays for the adjusted *v* in the nadir- point. The advantage of using the radial secator is that a radial point triangulation can be executed directly with contact copies.

OFEK07595

4.Stereotemplet Triangulation

If one also expands the concept of radial triangulation so that angles in the stereo model are included with those in nature, then the stereotemplet method introduced by the National Geographic Survey belongs in the area under consideration [6].

The method is based on the {observation /fact/ assumption?} that in a relative and an almost absolutely-oriented model, the radial displacements between the orthogonal projections of any balancing-out of any yardsticks are practically ineffective. The method was therefore employed mainly for balancing yardsticks of aerotriangulation blocks [7].

In the case of radial triangulation, however, no height information is used. For the use of the stereotemplet method therefore, an approximate horizontalization of the model, roughly like running water, suffices. Knowledge of the yardstick is therefore immaterial. The model's horizontalization precision will usually increase with the altitude at which the pictures are taken.

The choice of radial center is optional, since the model represents a true image of nature. To achieve a more favorable scale compensation, one selects two diagonally-facing radial centers (Diagram 3).

Naturally, an arrangement as in nadir-point triangulation is also possible and is recommended , especially in the case of several picture strips. (Diagram 3)

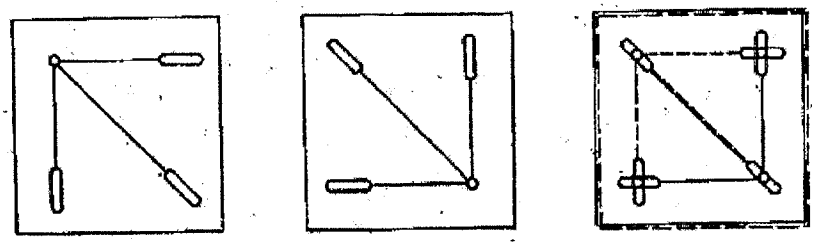


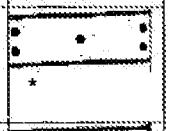
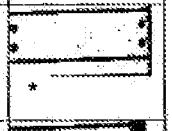
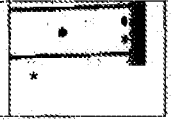
Diagram 3. Stereotemplet

OFEK07596

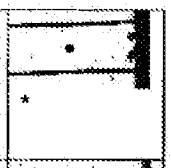
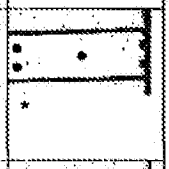
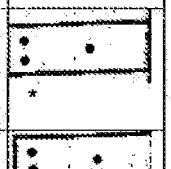
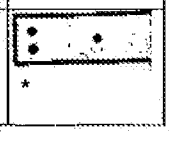
The templets into which holes and slots are stamped later, can be attained with the aid of any stereo evaluation device for convergent photos. Manufacturing of the templet might be most profitable in Device 2 arrangement (Kelsh plotter with pantograph, multiplex, twinplex).

Comparison of the Different Procedures

The three procedures described were tested in practice on a photographic flight at 10,000 m. altitude. The radial triangulation consisted of 2 strips, each with 8 models of 100% overlap, photographed with a 40^0 · 2 X 15 / 23 Mark Hurd convergency chamber with Metrogon objectives. In a 25 X 100 km test area, 42 fixed-point positions were known. Of these, 4 or 5 fixed points, respectively, were used to adjust the **formation/assembly**, the rest served as control points. Contact detachments and distorted pictures were available on a scale of 1:50 000. As triangulation scale, 1:50 000 was selected.
The results are briefly summarized below:

					Maximal	Median	Systematic Share	Fixed Point Division
		Δx_d mm	Δy_d mm	Δx_{dm} m	$y\Delta_{dm}$ m	Δx_{dm} m	Δy_{dmm}	
Metal Templet methods	Focal point triangulation	49	32	26	15	13	1	
	Focal point triangulation	49	30	25	15	11	1	
	Nadir-point triangulation	121	101	53	31	29	16	
	Nadir-point triangulation	49	82	30	27	6	1	

OFEK07597

Photo slot methods	Focal point triangulation with simple photographic templet image	32	18	12	11	4	2	
	Nadir- point triangulation with simple photographic templet image	37	29	20	17	5	1	
	Nadir-point triangulation with radial secator	18	21	8	7	0	5	
	Stereotemplets	16	19	5	7	0	5	

A glance at the overview shows immediately that the results with metal templets appear unusable in comparison with picture slot methods. The errors are apparently caused by torsion of the metal arms and by rotations of the individual arms against one another when Lazy Dazy templets are screwed together. The relationship of the precision of the metal templet method to the picture slot method reflects the results for vertical photos published by Fagerholm in [3].

In the case of nadir point triangulations, one recognizes the strong dependence of the (illegible) fixed **point hanging up** of the **formation/assembly**. Only after 5 fixed points have been used does the (illegible) acquire adequate stability. In contrast, the focal triangulation network is more rigid, thus providing better results; the external " illegible" there are determined by 4 rays, compared with only 3 rays in nadir-point triangulation.

When carried out with a simple template image, both focal point- and nadir point triangulation, are at a disadvantage compared with nadir point triangulation by means of secator. The reason is the lack of precision in transmission and punching of the triangulation points, which Fagerholm had already viewed as a principal source of errors in mechanical radial

OFEK07598

triangulation. In the case of a radial secator, this is reduced by viewing the photo through a magnifying glass during punching.

In the end, where the ground is level, the stereotemplet method demonstrates the fewest theoretical errors. There are no transmission errors, since the radial points in the model are adjusted, and strongly reduced to templet dimensions by means of a pantograph or coordinatograph. In practice, only errors arising from punch imprecision have an effect, and the radial secator reduces these. Thus the results of stereotemplet methods and nadir point triangulation using a radial secator should be viewed as of equal value.

The time requirement for the various procedures was as follows:

Focal point triangulations		
using simple devices	36 photos	10 hours
Nadir point triangulations		
using simple devices	36 photos	9 hours +
		4-8 hours with distortions
Nadir point triangulation		
With radial secator	36 photos	6 hours
Sterotemplet methods	16 models	20 hours

In the writer's opinion, it is clear that a generally-valid quantitative comparison of methods based on the available photographic material is not possible. Likewise, the question of propagation of the most systematic or pseudo-systematic radial triangulation errors can only be clarified through a wider selection of photographic material. He was able, however, to determine in what manner the individual methods were suited for radial triangulation. Similarly, the consistency in the size of errors in vertical- and convergent photos leads one to assume that that it is not the theoretical errors but rather those of the mechanical triangulation that are decisive in mechanical radial triangulation.

OFEK07599

Gotthardt, Comparative Measurements with Stereotop and Aeroprojector [BuL (IMAGE MEASUREMENT AND AERIAL PHOTOGRAPHY)] 1958 No. (Illegible)

Written Material

[1] W. Brucklacher: Aspects of the Use of a Convergence Chamber 2 X RMK 21/18 of a Zeiss Aerotopograph.

[2] R. Finsterwalder : Photogrammetry, P. 256-259.

[3] Fagerholm. See German version.

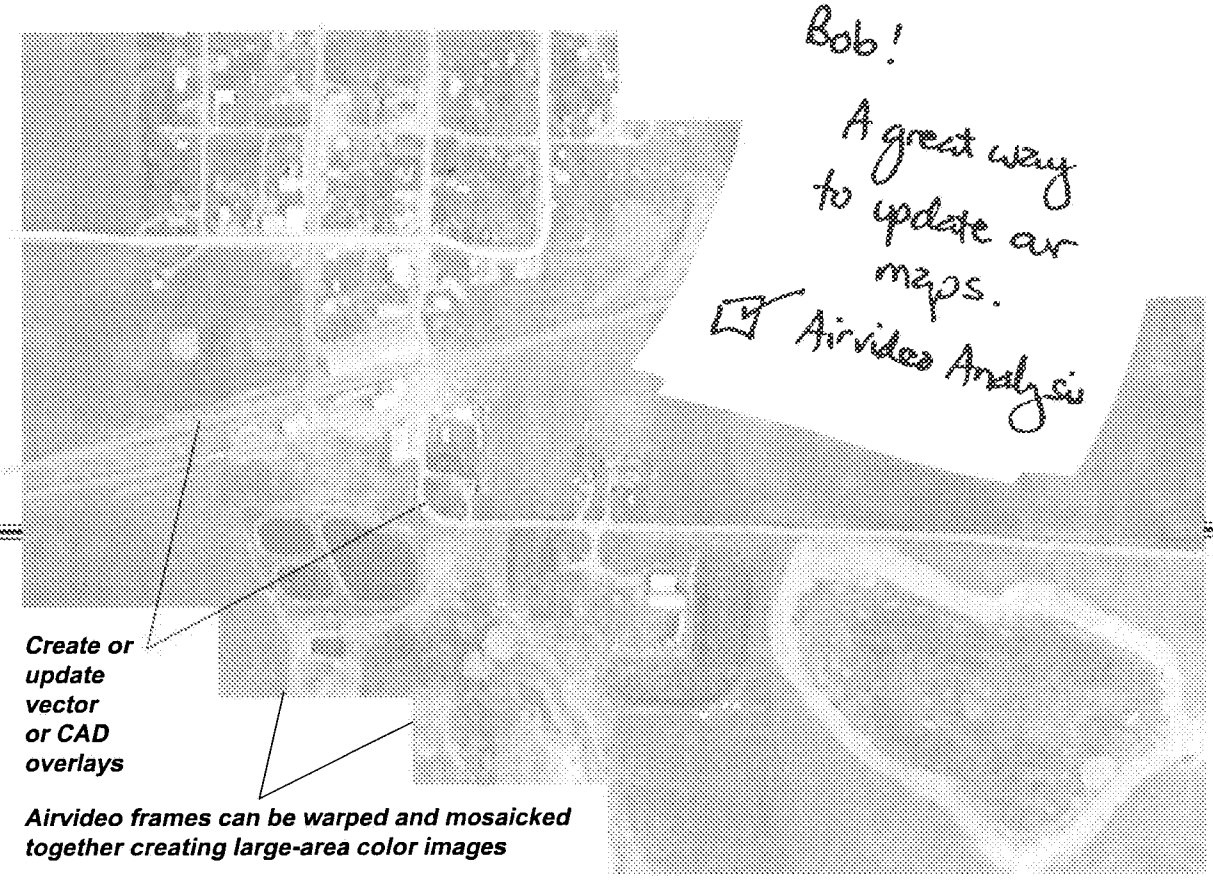
[4] R. Foerstner. Aerial Photo Tendencies to Err Directionally in Radial Triangulation. Stuttgart, 1948.

[5]. (See German version). Pages 768 – 771.

[6]. C.H. Davey Ditto. Page 707.

[7] M.B. Scher. Ditto. Pages 655 to 664.

OFEK07600



Create or update vector or CAD overlays

Airvideo frames can be warped and mosaicked together creating large-area color images

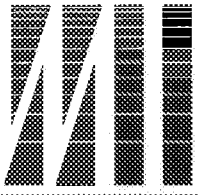
Airvideo Analysis

You need a system that can take advantage of the inexpensive images that can be quickly gathered by airvideo. With the integrated video capture process in the Map and Image Processing System (MIPS™) from MicroImages, Inc., you can fly over your site and bring the images into your computer as soon as you land. MIPS directly supports the capture of color, infrared, or black and white video from any source: live, broadcast, or tape.

Once you capture the desired frames, you can trace CAD or vector interpretations directly on the images, or use the unique, interactive Feature Mapping process to create or update CAD or vector files. Though Feature Mapping also works with airphoto and multiband satellite images, it was specifically designed for airvideo. With Feature Mapping, you select sample pixels of a known feature type, and the process automatically finds matching pixels across the entire image. The process then allows marking and measurement of these features and their immediate conversion to vector or CAD formats. You can assemble the CAD or vector materials into maps, use them in other processes, or export them to other application software.

Add georeference control from GPS positional data saved with the airvideo frames, or by adding your own georeferenced vector or CAD materials and tying common features together with snap lines. Construct a large-area coverage map from airvideo frames by using the mosaic process to assemble a chain or block of frames. Your airvideo can be used to create fully annotated large-format color maps and posters with vector and CAD overlays for presentation and reference.

Airvideo Analysis. Another good reason to check out the unique power of the **Map and Image Processing System** from **MicroImages, Inc.** It's the one system you need for your multiple-layer, multiple-source raster, vector, CAD, and database materials. **FAX (402) 477-9559 or write for your information kit today.**



MicroImages, Inc.

201 North 8th Street
Lincoln, Nebraska 68508-1347 USA
™

Mosaic-Based 3D Scene Representation and Rendering

Zhigang Zhu
Department of Computer Science
City College of New York, New York, NY 10031
zhu@cs.ccny.cuny.edu

Allen R. Hanson
Department of Computer Science
University of Massachusetts Amherst, MA 01003
hanson@cs.umass.edu

Abstract - **In this paper we address the problem of fusing images from many video cameras or a moving video camera. The captured images have obvious motion parallax, but they will be aligned and integrated into a few mosaics with a large field-of-view (FOV) that preserve 3D information. We have developed a geometric representation that can re-organize the original perspective images into a set of parallel projections with different oblique viewing angles. In addition to providing a wide field of view, mosaics with various oblique views well represent occlusion regions that cannot be seen in a usual nadir view. Stereo pair(s) can be formed from a pair of mosaics with different oblique viewing angles and thus image-based 3D viewing can be achieved. This representation can be used as both an advanced video interface and a pre-processing step for 3D reconstruction.**

Keywords – stereo mosaics; image-based rendering; visual representation;

I. INTRODUCTION

A 2D panoramic mosaic of a 3D scene generated from video from a translating camera has the geometry of multiple viewpoints [1,2], but it only preserves information from a single viewing direction. Three-dimensional (3D) structure and surface information from other viewing directions of the original video is lost in such a representation. A digital elevation map (DEM) generated from aerial photometry consists of a sampled array of elevations (depths) for a number of ground positions at regularly spaced intervals [3]. It usually only has a nadir viewing direction, hence the surfaces from other viewing directions cannot be represented. However, in some applications such as surveillance and security inspection, a scene or an object (e.g. a vehicle) needs to be observed from many viewing directions to reveal anomalies hidden in unusual views. Stereo panoramas [4,5] have been presented as a mechanism for obtaining the "best" 3D information from an off-center rotating camera. In the case of a translating camera, various layered representations [6-8] have been proposed to represent both 3D information and occlusions, but such representations need 3D reconstructions.

This paper presents an approach for fusing images from many spatially distributed video cameras or a moving video camera into a few mosaiced images that preserve 3D information. In both cases, a virtual 2D array of cameras with FOV overlaps is formed to generate complete coverage of a scene (or an object). Note that many viewing directions are already included in the original camera views. This property has been used in the X-slit mosaics with non-parallel rays [9] for image-based rendering. In this paper we propose a representation that can re-organize the original perspective images into a set of parallel projections with different oblique viewing angles (in both the x and the y directions of the 2D images). Mosaics with 2D oblique parallel projections are a unified representation for our previous work on parallel-perspective stereo mosaics [11,12] and multi-camera mosaics [13,14]. Such representations provide a wide field of view, optimal 3D information for stereo viewing and reconstruction, and the capability to represent occlusions. This paper is organized as follows. In addition to the description and discussions of the unified presentation in Sections II and III, we also present a general ray interpolation method in Section IV, and a mosaic-based 3D rendering method in Section V. Experimental results are given in Section VI for two important applications – aerial video surveillance and under vehicle inspection. Section VII is a brief summary.

II. 2D OBLIQUE PARALLEL PROJECTION

A normal perspective camera has a single viewpoint, which means all the light rays pass through a common nodal point. On the other hand, an orthogonal image with parallel projections in both the x and y directions has all the rays parallel to each other. Imagining that we have a sensor with parallel projections, we could turn the sensor to capture images with different *oblique* angles (including both nadir and oblique angles) in both the x and y directions. Thus we can create many pairs of parallel stereo images, each with two different oblique angles, and observe surfaces occluded in a nadir view.

Fig. 1 shows the parallel stereo in a 1D case, where two oblique angles β_1 and β_2 are chosen. The depth of a point can be calculated as

$$Z = \frac{B}{\tan\beta_2 - \tan\beta_1} \qquad (1)$$

where β_1 is β_2 are the angles of the two viewing directions, respectively, and B is the adaptive baseline between the two viewpoints that is proportional to the displacement of the corresponding points in the stereo mosaics. It has been shown by others [10] and by us [11, 12] that parallel stereo is

0-7803-9134-9/05/$20.00 ©2005 IEEE

superior to both conventional perspective stereo and to the recently developed multi-perspective stereo with concentric mosaics for 3D reconstruction (e.g., in [5]). The adaptive baseline inherent in the parallel-perspective geometry permits depth accuracy independent of absolute depth in theory [10,11] and as a linear function of depth in stereo mosaics generated from perspective image sequences [12]. In contrast, the depth error of perspective stereo and the concentric stereo is proportional to the square of depth.

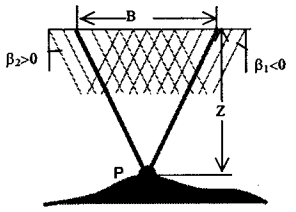


Fig. 1. Depth from parallel stereo with multiple viewpoints: 1D case.

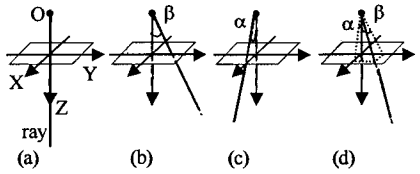


Fig. 2. Parallel projections with two oblique angles α and β (in the x and y directions).

We can make two extensions to this parallel stereo. First, we can select various oblique angles for constructing multiple parallel projections. By doing so we can observe various degrees of occlusions and can construct stereo pairs with different depth resolution via the selection of different pairs of oblique angles. Second, we can extend this 1D parallel projection to 2D (Fig. 2): we can obtain a mosaiced image that has a nadir view (Fig. 2a), oblique angle(s) only in one direction (Fig. 2b and c) or in both the x and the y directions (Fig. 2d).

III. 2D (VIRTUAL) ARRAY OF CAMERAS

It is impractical to use a single sensor to capture orthogonal images with full parallel projections in both x and y dimensions for a large scene, and with various oblique directions. However there are least three practical ways of generating images with oblique parallel projections using existing sensors: a 2D sensor array of many spatially distributed cameras (Fig. 3a), a "scanner" with a 1D array of cameras (Fig. 3b), and a single perspective camera that moves in 2D (Fig. 3c).

With a 2D array of many perspective cameras (Fig. 3a), we first assume that the optical axes of all the cameras point in the same directions (into the paper in Fig 3a), and the viewpoints of all cameras are on a single plane perpendicular to their optical axes. Then we can reorganize the perspective images into mosaiced images with any oblique viewing angles by extracting rays from the original perspective images with the same viewing directions, one ray from each image. If the camera array is dense enough, then we can generate densely mosaiced images.

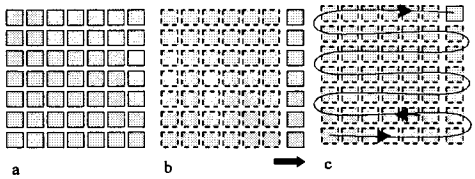


Fig. 3. Parallel mosaics from 2D bed of cameras. (a) 2D array; (b) 1D scan array and (c) a single scan camera.

If we only have a 1D linear array of perspective cameras (Fig. 3b), we can "scan" the camera array over the scene to synthesize a virtual 2D camera array. Then we can still generate stereo mosaic pairs with oblique parallel projections, given that we can accurately control the translation of the camera array. We have actually used this approach in an Under Vehicle Inspection System (UVIS) [13, 14, 18].

Even if we just use a single camera, we can still generate a 2D virtual bed of cameras by moving the camera in two dimensions, along a "2D scan" path shown in Fig. 3c. This is the case for aerial video mosaics [11, 12, 15, 17].

IV. PRISM: VIDEO MOSAICING ALGORITHM

In real applications, there are two challenging issues. The first problem is camera orientation estimation (calibration). In our previous study on an aerial video application, we used external orientation instruments, i.e., GPS, INS and a laser profiler, to ease the problem of camera orientation estimation [11, 12]. In this paper, we assume that the extrinsic and intrinsic camera parameters are known at each camera location. The second problem is to generate dense parallel mosaics with a sparse, uneven, camera array, and for a complicated 3D scene. To solve this problem, we have proposed a Parallel Ray Interpolation for Stereo Mosaics (PRISM) approach [11]. While the PRISM algorithm was originally designed to generate parallel-perspective stereo mosaics (parallel projection in one direction and perspective projection in the other), the core idea of *ray interpolation* can be used for generating a mosaic with full parallel projection at any oblique angle.

Fig. 4 shows how the PRISM works for 1D images. The 1D camera has two axes – the optical axis (Z) and the Y-axis. Given the known camera orientation at each camera location, one ray with a given oblique angle β can be chosen from the image at each camera location to contribute to the parallel mosaic with this oblique angle β. The oblique angle is defined against the direction perpendicular to the *mosaicing direction*, which is the dominant direction of the camera path (Fig. 4). But the problem is that the "mosaiced" image with only those existing rays will be sparse and uneven since the camera array are usually not regular and very dense. Therefore *interpolated* parallel rays between a pair of existing parallel rays (from two neighboring images) are generated by performing local

matching between these two images. The assumption is that we can find at least two images to generate the parallel ray. Such an interpolated ray is shown in Fig 4, where Ray I is interpolated from Image A and Image B.

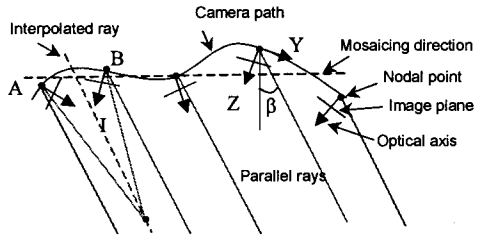


Fig. 4. Ray interpolation for parallel mosaicing from an camera array.

The extension of this approach to 2D images is straightforward, and a region triangulation strategy similar to that in [11] can be applied here to deal with 2D cases. One important issue here is the selection of neighborhood images for ray interpolation. For example, with a 1D scan sequence of a single camera, it is hard to generate full parallel projection in the X direction, which is perpendicular to the motion of the camera, since the interpolated parallel rays far off the center of the images in the x direction have to use rays with rather different oblique angles in the original perspective images.

V. Stereo Viewing and 3D Reconstruction

Parallel mosaics with various oblique angles represent scenes from the corresponding viewing angles with parallel rays and with wide fields of view. There are two obvious applications of such representation. First, a human can perceive the 3D scene from a pair of mosaics with different oblique angles (e.g. using polarized glasses) without any 3D recovery. If we have mosaics with various oblique angles in both the x and the y direction, we can generate a virtual fly/walk-through by noting that (1) the translation in the *xy* plane can be simulated by shifting the current displayed mosaic pair, (2) the rotations around the X and the Y axes can be simulated by selecting different pairs of mosaics with different oblique angles, and (3) the rotation around the optical axis only needs to rotate the pair of mosaics in their image planes. The visual disparities can also be controlled by changing the angles between the two mosaics for stereo viewing.

Second, for 3D recovery, matches are only performed on a pair of mosaics, not on individual video frames. Stereo mosaic methods also solve the baseline versus field-of-view (FOV) dilemma efficiently by extending the FOV in the directions of mosaicing – in both the *x* and *y* directions. More importantly, the parallel stereo mosaics have optimal/adaptive baselines for all the points, which leads to uniform depth resolution in theory and linear depth resolution in practice. For 3D reconstruction, epipolar geometry is rather simple due to the full parallel projections in the mosaic pair.

VI. Experimental Examples

A. *Video Mosaics from Aerial Video*

In theory, with a camera undergoing an ideal 1D translation and a nadir view direction, two spatio-temporal images can be generated by extracting two columns of pixels at the front and rear edges of each frame in motion (Fig. 5). The mosaic images thus generated are *parallel-perspective*, with parallel projection in the motion direction and perspective projection in the other. In our aerial video environmental monitoring application, a single camera is mounted in a small aircraft undergoing 6 DOF motion, together with a GPS, INS and laser profiler to measure the moving camera locations and the distance to the terrain [11, 12]. So we generate seamless stereo parallel-perspective video mosaic strips from image sequences with a 1D scan path but with a rather general motion model, using the proposed parallel ray interpolation for stereo mosaicing (PRISM) approach [11]. In the PRISM approach for large-scale 3D scene modeling, the computation is efficiently distributed in three steps: camera pose estimation via the external measurement units, image mosaicing via ray interpolation, and 3D reconstruction from a pair of stereo mosaics [11, 12, 15].

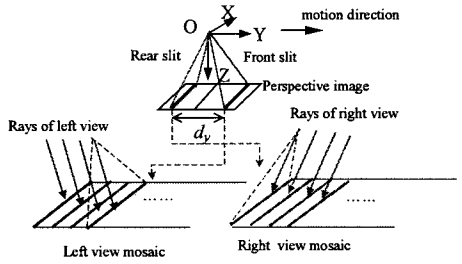


Fig. 5. Parallel-perspective stereo mosaics with a 1D camera scan path

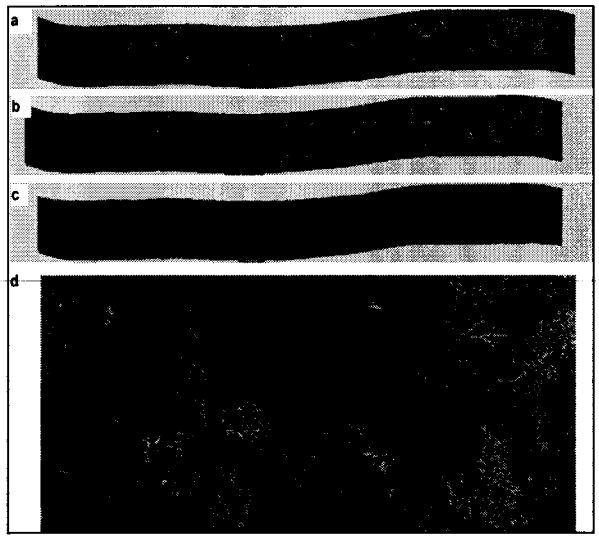


Fig. 6. Stereo mosaics and 3D reconstruction of a 166-frame telephoto video sequence.

Fig. 6 shows a real example of stereo mosaics (with two y-oblique angles) generated from a telephoto camera and 3D recovery for a forest scene in Amazon rain forest. The average height of the airplane is $H = 385$ m, and the distance between the two slit windows is selected as 160 pixels (in the y direction) with images of 720 (x) * 480 (y) pixels. The image resolution is about 7.65 pixels/meter. The depth map (Fig. 6c) generated from the stereo mosaics (Fig. 6 a and b) was obtained by using a hierarchical sub-pixel dense correlation method [16], where the range of depth variations of the forest scene (from a stereo fixation plane) is from -24.0 m (tree canopy) to 24.0 m (the ground). Even before any 3D recovery, a human observer can perceive the 3D scene with a stereo pair using a pair of red/blue stereo glasses (Fig. 6d).

Multiple oblique parallel-perspective mosaics generated in a similar way can be used for image-based rendering as discussed in Section 4. A mosaic-based fly-through demo may be found at [17], which uses 9 oblique mosaics generated from a real video sequence of the UMass campus. This demo shows *motion parallax, occlusion and moving objects* in multiple parallel-perspective mosaics. We note that the rendering shows parallel-perspective rather than true perspective perception. A true perspective fly-through will be enabled by 3D reconstruction from the multiple mosaics.

B. Video Mosaics for Under-Vehicle Inspection

As one of the real applications of full parallel stereo mosaics, we have generated an approximate version of mosaics with full parallel projections from a virtual bed of 2D camera arrays by driving a car over a 1D array of cameras in an under-vehicle inspection system (UVIS) [13, 14, 18]. UVIS is a system designed for security checkpoints such as those at borders, embassies, large sporting events, etc. It is an example of generating mosaics from very short-range video so a 2D virtual array of camera is necessary for full coverage of the vehicle undercarriage.

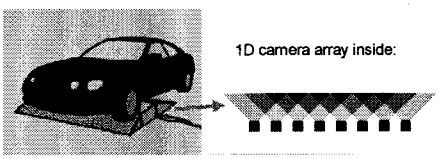


Fig. 7. 1D camera array for under-vehicle inspection [13, 14]



Fig. 8. Full parallel projection mosaics with a bed of 2D array of cameras

Fig. 7 illustrates the system setup where an array of cameras is housed in a platform. When a car drives over the platform, several mosaics with different oblique angles of the underside of a car are created. The mosaics can then be viewed by an inspector to thoroughly examine the underside of the vehicle from different angles. Fig. 8 shows such a mosaic generated from four overlapping image sequences taken by four moving cameras side by side simulating the motion of the vehicle. A PPT demo of five oblique parallel views of the mosaics can be found at [18] where different "occluded" regions under a pipe in the center can be observed by switching to different mosaics.

VII. CONCLUSIONS

This paper presents an approach of fusing images from many video cameras or a moving video camera with external orientation data into a few mosaiced images with oblique parallel projections. In both cases, a virtual 2D array of cameras with FOV overlaps is formed to generate the whole coverage of a scene (or an object). The proposed representation provides wide FOV, preserves optimal 3D information, and represents occlusions. This representation can be used as both an advanced video interface for surveillance or a pre-processing step for 3D reconstruction.

ACKNOWLEDGMENT

This work is supported by NSF EIA- 9726401, AFRL Grants FA8650-05-1-1853 and F33615-03-1-63-83, and by funding from New York Institute for Advanced Studies and from Atlantic Coast Technologies, Inc.

REFERENCES

[1].J Y Zheng and S Tsuji, Panoramic representation for route recognition by a mobile robot, IJCV, 9(1), 1992: 55-76

[2]. S Peleg, B Rousso, A Rav-Akha, A. Zomet, Mosaicing on adaptive manifolds, *PAMI*, 22(10), Oct 2000: 1144-1154.

[3].USGS DEM, http://data.geocomm.com/dem/

[4]. S Peleg, M Ben-Ezra and Y Pritch, OmniStereo: panoramic stereo imaging, *PAMI*, March 2001:279-290.

[5].H-Y Shum and R Szeliski, Stereo reconstruction from multiperspective panoramas, *ICCV'99*: 14-21.

[6].S Baker, R Szeliski and P Anandan, A layered approach to stereo reconstruction. *CVPR'98:* 434-441

[7].J Shade, S Gortler, L He. and R Szeliski, Layered depth image. *SIGGRAPH'98:* 231-242

[8].Z Zhu and A R Hanson, LAMP: 3D Layered, Adaptive-resolution and Multi-perspective Panorama - a New Scene Representation, CVIU 96(3), Dec 2004: 294-326.

[9].A Zomet, D Feldman, S Peleg, D Weinshall, Mosaicing new views: crossed-slits projection, *PAMI* 25(6), June 2003.

[10].J Chai and H-Y Shum, Parallel projections for stereo reconstruction, CVPR'00: II 493-500.

[11].Z Zhu, E M Riseman, A Hanson, Generalized Parallel-Perspective Stereo Mosaics from Airborne Videos, PAMI 26(2), Feb 2004:226-237.

[12].Z Zhu, A R Hanson, H Schultz and E M Riseman, Generation and error characteristics of parallel-perspective stereo mosaics from real video. In *Video Registration*, M. Shah and R. Kumar (Eds.), Kluwer, 2003: 72-105.

[13].P Dickson, J Li, Z Zhu, A R Hanson, E M Riseman, H Sabrin, H Schultz and G Whitten, Mosaic generation for under-vehicle inspection. *WACV'02*:251-256

[14].http://vis-www.cs.umass.edu/projects/uvis/index.html

[15].http://www-cs.engr.ccny.cuny.edu/~zhu/StereoMosaic.html

[16].H Schultz, Terrain reconstruction from widely separated images, SPIE 2486, April 1995: 113-123.

[17].http://www-cs.engr.ccny.cuny.edu/~zhu/CampusVirtualFly.avi

[18].http://www-cs.engr.ccny.cuny.edu/~zhu/mosaic4uvis.html

DIRECT POSITIONING AND ORIENTATION SYSTEMS HOW DO THEY WORK? WHAT IS THE ATTAINABLE ACCURACY?

Mohamed M.R. Mostafa, Research Scientist, Airborne Applications
Joseph Hutton, Product Manager, Airborne Applications
APPLANIX Corporation, 85 Leek Cr., Richmond Hill
Ontario, Canada L4B 3B3
Mmostafa@Applanix.com
Jhutton@aplanix.com

ABSTRACT

This paper describes how position and orientation measurement systems are used to directly georeference airborne imagery data, and presents the accuracies that are attainable for the final mapping products. The Applanix Position and Orientation System for Airborne Vehicles (POS/AV^{TM}) has been used successfully since 1994 to georeference airborne data collected from multispectral and hyperspectral scanners, LIDAR's, and film and digital cameras. The POS/ AV^{TM} uses integrated inertial/GPS technology to directly compute the position and orientation of the airborne sensor with respect to the local mapping frame. A description of the POS/AV^{TM} system is given, along with an overview of the sensors used and the theory behind the integrated inertial/GPS processing. An error analysis for the airborne direct georeferencing technique is then presented. Firstly, theoretical analysis is used to determine the attainable positioning accuracy of ground objects using only camera position, attitude, and image data, without ground control. Besides theoretical error analysis, a practical error analysis was done to present actual results using only the POS data plus digital imagery without ground control except for QA/QC. The results show that the use of POS/AV enables a variety of mapping products to be generated from airborne navigation and imagery data without the use of ground control.

INTRODUCTION

A direct georeferencing (DG) system provides the ability to directly relate the data collected by a remote sensing system to the Earth, by accurately measuring the geographic position and orientation of the sensor without the use of traditional ground-based measurements. Examples of where DG systems are used in the airborne mapping industry include: scanning laser systems or LIDAR such as the Optech ALTM, Interferrometric Synthetic Aperture Radar systems (InSAR) such as that produced by the Aero-sensing, multispectral and hyperspectral scanners such as the ITRES CASI, the new state-of-the-art digital line scanners systems such as the LH Systems ADS40, and more increasingly small format digital cameras and traditional film cameras such as the Leica RC30 and TOP RMK. The current state-of –the-art direct georeferencing systems such as the Applanix POS/AV^{TM} use carrier phase differential GPS measurements integrated with an Inertial Measurement Unit (IMU). This paper gives an overview of how the systems work, and investigates what ground accuracy is attainable for typical applications such as mapping with a digital camera. This is supported through theoretical and practical results.

DESCRIPTION OF THE POS/AV^{TM} DIRECT GEOREFERENCING SYSTEM

The Applanix POS/AV^{TM} direct georeferencing system (see Figure 1) is comprised of four main components: an IMU, a dual frequency low-noise GPS receiver, a computer system (PCS) and a post-processing software suite called POSPac^{TM}. The heart of the system however is the Integrated Inertial Navigation software that is implemented both in real-time on the PCS and in postmission using the POSPac^{TM} software. In this software the GPS measurements are used to aid the inertial navigation solution produced by integrating the IMU outputs to produced a blended position and orientation solution that retains the dynamic accuracy of the inertial navigation solution but has the absolute accuracy of the GPS.

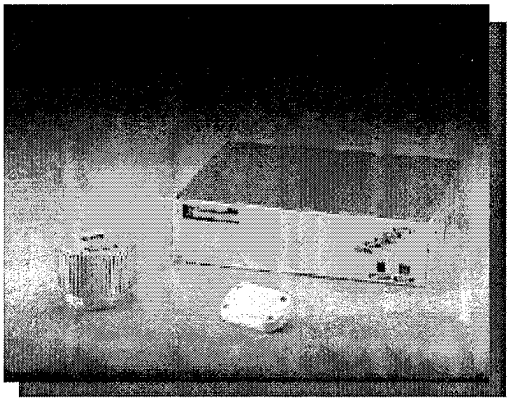


Figure 1. The POS/AV™ System

Inertial Measurement Unit (IMU)

An IMU is comprised of triads of accelerometers and gyros, digitization circuitry and a CPU that performs signal conditioning and temperature compensation. The compensated accelerometer and gyro data are output as incremental velocities and angular rates via a serial interface to the PCS typically at rates of 200 to 1000Hz. The PCS then integrates the accelerations and angular rates in a so-called "Strapdown" inertial navigator to produce position, velocity and orientation of the IMU geographically referenced to the earth. Rigidly mounting the IMU to a remote sensor thus means the inertial navigator produces position, velocity and orientation of the sensor itself. To ensure maximum accuracy, the IMU's must be relatively small and lightweight so that they can be mounted as close to the sensor's reference point (perspective center) as possible. This ensures there is no flexure between the IMU and sensor, as shown in Figure 2. Typical high-quality IMU's use force rebalance accelerometers and either Fiber Optic Gyros (FOG), Ring Laser Gyros (RLG), Dry Tuned Gyros (DTG). New gyro technologies such as MicroElectroMechanical Systems (MEMS) are just now becoming available but it will take a few years until they reach the performance level required for direct georeferencing. The primary requirements on gyros for direct georeferencing is size, bias drift, and noise. While the RLG technology produces the best performing gyro by far, their size precludes them from being used in many airborne applications. At the moment the DTG has the smallest noise for its size, although recent signal processing advances are now being used to reduce the noise in FOG's to levels sufficient for some of the higher accuracy DG applications. The POS/AV™ systems use IMU's containing both FOG and DTG technology.

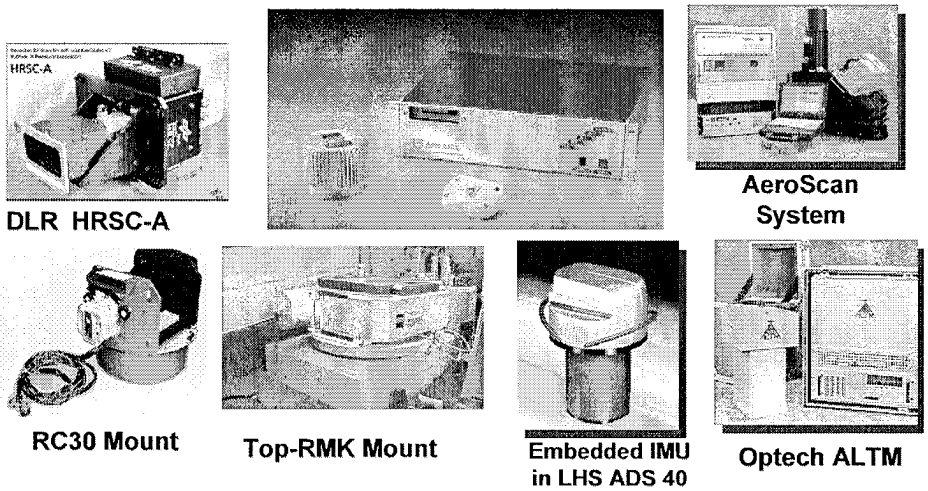


Figure 2. IMU Installation on Different Airborne Sensors

GPS Receiver

The GPS system is comprised of a constellation of satellites and a remote receiver that uses range measurements to the satellites and triangulation techniques to compute the position of the receiver's antenna. Carrier phase differential GPS is an advanced technique that combines the phase data from two receivers so as to eliminate all significant errors except the integer ambiguities in the number of wavelengths between the receivers (both base and rover) and each satellite. Redundant phase observations from 5 or more satellites provide the information to resolve the ambiguities, thus translating each satellite's estimated phase cycles into precise range measurement. A high precision satellite-to-receiver range measurements allow the computation of the baseline (interstation) vector between the receivers and hence the position of the remote receiver to decimeter or better accuracy. POS/AV™ uses an embedded low noise dual frequency GPS receiver that provides phase and range data to the processing software.

POS Computer System (PCS)

The POS Computer system or PCS contains the GPS receiver, a mass storage system that writes data to a removable PC Card flash disk, and a computer that runs the real-time integrated navigation software. The real-time navigation solution is used as input to flight management systems and to point and control stabilized mounts. The PCS is also used to precisely time-tag external sensor data.

POSPac™ Post-processing Software

The POSPac™ post-processing software is used to compute an optimal integrated inertial navigation solution by processing the raw IMU and GPS data collected from the POS/AV™ during the flight, along with GPS observables recorded form base station receiver(s). It computes a carrier phase GPS solution and then blends it with the inertial data using forward and reverse time processing. When using the POS/AV™ in a photogrammetric application, as a final step a module called POSEO is used to compute the exterior orientation of each image at the moment of exposure.

HOW THE POS/AV™ DIRECT GEOREFERENCING SYSTEM WORKS

The key component of the POS/AV™ system is the Integrated Inertial Navigation (IIN) software. This software runs in real-time on the PCS and in post-processing in the POSPac™ software suite, and performs the integration of the inertial data from the IMU with the data from the GPS receiver. The functional architecture of the software is given in Figure 3. The software consists of the following components:

- Strapdown inertial navigator
- Kalman filter
- Closed-loop error controller
- Smoother (POSPac™ only)
- Feed forward error controller (POSPac™ only)
- In-flight Alignment

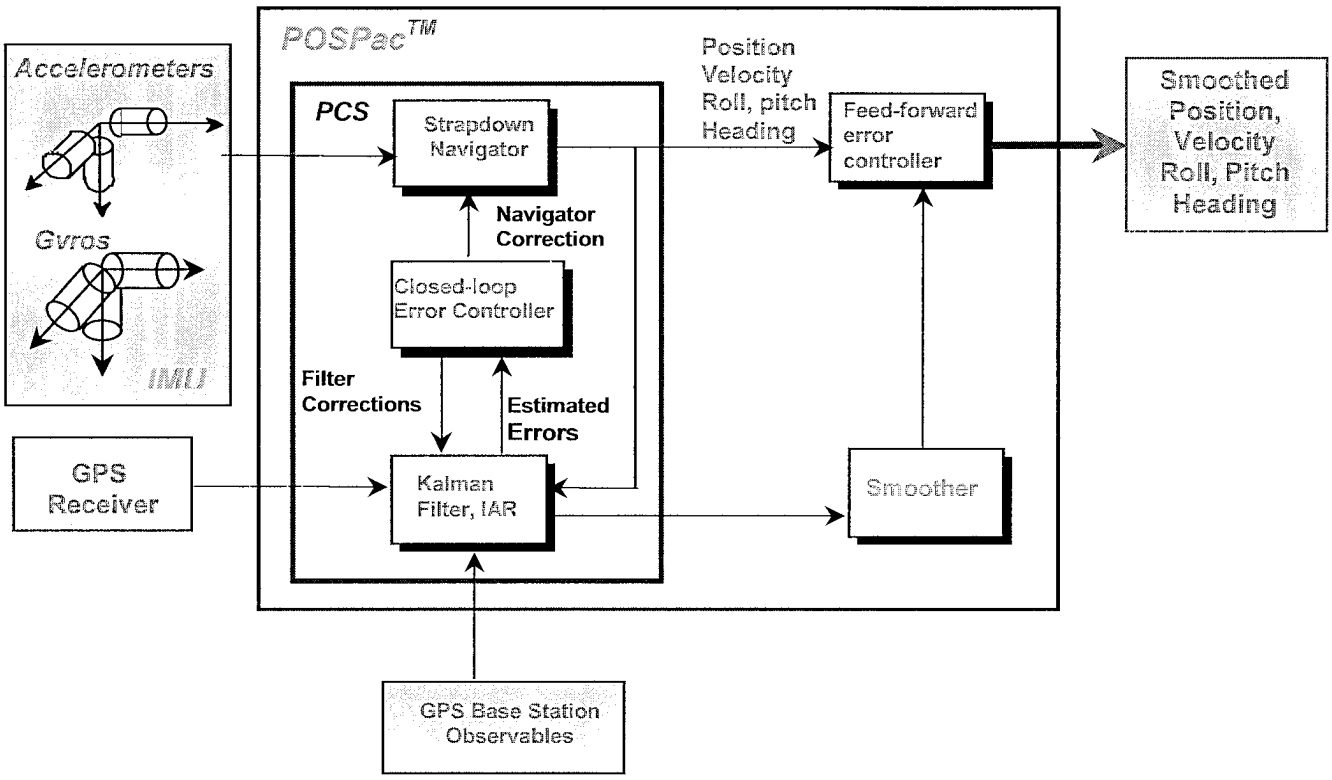


Figure 3. Closed-Loop GPS-Aided Inertial Navigation

Strapdown Navigator

The strapdown inertial navigator solves Newton's equations of motion on the rotating earth by integrating acceleration and angular rates sensed by the IMU. In order to do this, the inertial navigator must first be initialized with known position and velocity from the GPS, and aligned with respect to the true vertical and true North. Alignment with respect to the vertical is referred to as *leveling,* while alignment with respect to North is referred to as *heading alignment*. Once aligned the inertial navigator has established a local-level mathematical frame of reference called the navigation frame, whose heading is known with respect to North, and to which the orientation of the IMU is known, as shown in Figure 4.

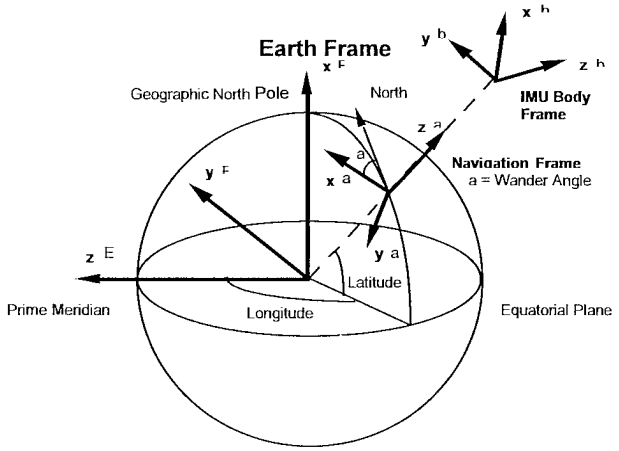


Figure 4. Frames of References Used in Inertial Navigation

After removing the rotation rate of the Earth that (computed as a function of position), the navigator integrates the incremental angles from the IMU to continuously compute the change in orientation of the IMU with respect to the navigation frame. It then uses the orientations to resolve the incremental velocities from the accelerometers into the local-level navigation frame, which it then integrates to compute the position change of the navigation frame over the Earth. Note that this means any error in the orientation will directly contribute to a position error on the Earth. The solution it produces is dynamically very accurate; however, since the inertial navigator uses an integration process, any errors in the accelerometers and gyros will integrate into slowly growing position, velocity and orientation errors. GPS is an ideal aiding sensor for an inertial navigator since its positional errors are complementary to the inertial navigation errors in the sense that they are spectrally separate: the GPS position and velocity errors are bounded and noisy, while the inertial navigator errors grow unbounded but are essentially noise free. The GPS can thus be used to estimate and correct the errors in the inertial navigation solution.

Kalman Filter

In order to use the GPS to estimate the errors in the inertial navigator, a Kalman Filter is used. The Kalman Filter implements a linearized and discretized set of differential equations that model the inertial navigator errors and the IMU sensor errors that drive them. Differences between the position from the inertial navigator and the position from the GPS are processed in the Kalman filter (typically at 1 Hz), to estimate the slowly growing position error in the inertial navigator. Since this error is a function of both errors in the orientation and errors in the inertial sensors, (as modeled by the differential equations in the Kalman filter), observing the inertial position errors means the orientation errors and IMU sensor errors can also be implicitly estimated.

Closed-Loop Error Controller

The closed-loop error control algorithm is used to apply resets to the inertial navigator using the Kalman filter-estimated parameters. Estimates of the inertial sensor errors are also applied to the IMU-measured raw incremental angles and velocities before they are integrated, which has the same effect as calibrating the sensors. The resultant integrated inertial navigation solution has its position and velocity directly regulated to the absolute accuracy of the GPS position and velocity, and its orientation accuracy indirectly improved by the calibration of the inertial sensor errors. This is the solution that is computed and output by the PCS in real-time.

Smoother

The Smoother is a module that computes the optimal estimates of the inertial navigator and IMU sensor errors, by processing the data backwards in time and then combining it with the estimates from the forward in time Kalman filter. The resultant error estimates are based upon all available information from the past and future, and hence are more accurate. The Smoother is implemented only in the POSPac^{TM} software.

Feed-forward Error Controller

The Feed-forward Error Control module uses the optimal error estimates from the Smoother and applies them to the integrated inertial navigation solution at the IMU rate, thus generating what is referred to a the smoothed best estimate of trajectory (SBET). The Feed-forward error controller is only used in the POSPac^{TM} software after the smoother is run.

In-Flight Alignment

An important feature of the POS/AV^{TM} system is its ability to align itself (establish initial navigation frame, see above) in the air. The alignment process is comprised of 3 stages: i) Coarse Leveling, ii) Coarse Heading Alignment, and iii) Fine Heading Alignment. Coarse Leveling uses a first-order low-pass filter on the accelerometer data to observe the mean gravity signal in each accelerometer, from which the approximate roll and pitch of the IMU are determined to within 1 to 2 degrees error (see Figure 5).

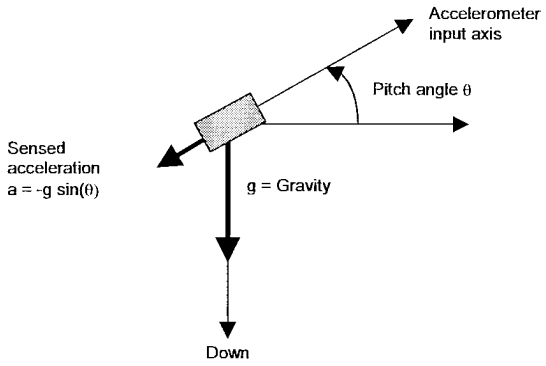


Figure 5. Coarse Leveling Using Accelerometers

At this point, Coarse Heading Alignment is started which uses a Kalman filter error model to describe the initial 180 deg uncertainty in heading. The heading error of the navigation frame will cause the incorrect Earth rate to be removed from the gyro measurements during the integration process, causing an orientation error. This in turn will integrate into a velocity and position error. If the gyros errors are small enough, the position and velocity error due to the misresolved Earth rate can be detected in the differences with the GPS, and hence the heading error will be estimated by the Kalman filter (so-called gyrocompassing). However, since the gyros themselves can have biases anywhere from 0.5 to 20 deg/hr, usually the error due to the misresolved Earth rate is only sufficient to observe the heading error down to a few degrees at best. Fortunately the heading error also causes the accelerations of the IMU to be misresolved in the navigation frame, which then integrate into very large position and velocity errors that are observable against the GPS measurements. This allows the Kalman filter to estimate the heading error to fractions of a degree, and as soon as Coarse Leveling is completed a single turn will complete the heading alignment. Once the Coarse Heading Alignment Kalman filter estimates the heading error to less than 10 degrees, the software changes to Fine Heading Alignment, which uses a small-angle error model Kalman filter to continuously estimate and refine the heading error.

ACCURACY OBTAINABLE FROM POS/AV™

Positional Accuracy

With proper mission planning, careful flight operations to minimize satellite loss of lock, and multiple base station deployment to ensure the maximum baseline separation between the remote and base receivers are within 10 - 50 km, position accuracies in the range of 5 to 30 cm RMS are achievable using post-processed carrier phase Differential GPS. Most of the position error is due to residual propagation delays caused by the ionosphere, which are low frequency in nature and cannot be removed by blending with the inertial data. This means the absolute accuracy of the POS/AV™ smoothed navigation position from POSPac™ will also typically be 5 to 30 cm RMS.

Orientation Accuracy

The orientation accuracy of the POS/AV™ smoothed navigation solution is described best in terms of *absolute accuracy* and *relative accuracy*. The *absolute accuracy* is the total RMS error including mean, while the *relative accuracy* describes the high frequency sample-to-sample error. It is convenient to do this since in most cases the orientation error is comprised of a slow varying signal with almost no noise, and in some applications it is the accuracy of the change in orientation that is most important (such as that in a digital line scanner). The relative accuracy of the roll, pitch and heading is a function of the gyro noise and residual gyro bias after smoothing.

Roll and Pitch Accuracy

The absolute roll and pitch accuracy of the POS/AV™ smoothed navigation solution is a function of the residual error in estimating the accelerometer biases after smoothing. Errors in the roll and pitch will cause gravity to be misresolved, causing apparent horizontal accelerations that integrate into ramping velocity and quadratic position errors when compared to GPS. However an accelerometer bias will also produce the same error signature, so the

Kalman filter will only be able to estimate the roll and pitch error down to the level where the misresolved gravity cancels out the accelerometer biases.

Heading Accuracy

As described above in the In-Air Alignment section, the heading error is observed primarily through accelerations. During straight-and-level flight with little or no accelerations, the heading error will grow at a rate defined by the gyro noise and residual gyro bias. As soon as a significant acceleration is experienced, the heading error will be observed and the error reset (see Figure 6). The smoother will then extrapolate the reset backwards in time to reduce the overall error (see Figure 7). Hence in order to maintain heading accuracy to the maximum level, it is important that a maneuver be performed periodically (usually every 10 to 30 minutes, depending upon the quality of the IMU, which is typically not a problem for aerial survey missions).

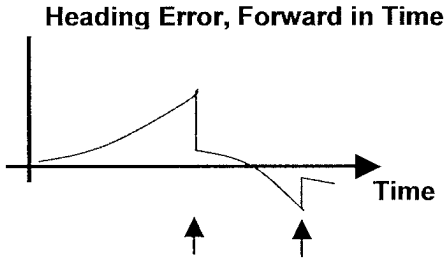


Figure 6. Heading Error Improvement after maneuvers (Forward Solution)

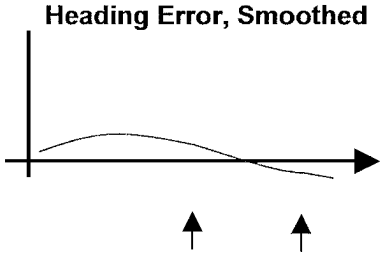


Figure 7. Heading Error Improvement after maneuvers (Smoothed)

The post-processed *absolute* accuracy for each POS/AV™ model is given in Table 1, for a typical survey mission profile including turns every 10 minutes or so. The post-processed relative orientation accuracy for each POS/AV™ model is given in Table 2.

Table 1. Post-processed POS/AV™ Absolute Accuracy

Parameter Accuracy (RMS)	*POS/AV™ 210*	*POS/AV™ 310*	*POS/AV™ 410*	*POS/AV™ 510*
Position (m)	0.05 –0.30	0.05 –0.30	0.05 –0.30	0.05 –0.30
Velocity (m/s)	0.010	0.010	0.005	0.005
Roll & Pitch (deg)	0.040	0.013	0.008	0.005
Heading (deg)	0.080	0.035	0.015	0.008

Table 2, Post-processed POS/AV™ Relative Orientation Accuracy

Parameter Accuracy	*POS/AV™ 210*	*POS/AV™ 310*	*POS/AV™ 410*	*POS/AV™ 510*
Random Noise (deg/sqrt(hr))	0.20	0.15	0.07	< 0.01
Residual Bias (deg/hr), 1 sigma	0.75	0.5	0.5	0.1

DIRECT GEOREFERENCING OF DIGITAL IMAGES USING POS/AV™

Direct digital image georeferencing using POS implies the direct measurement of position and orientation of each single image frame or scan line at the moment of data acquisition. In principal, this allows immediate map production using the photogrammetric unit (either a stereopair of images, or a single image+DEM). Ultimately, this approach totally bypasses the aerotriangulation step with no ground control point requirement, except for Q/A and Q/C. Figure 8 shows the georeferencing concept.

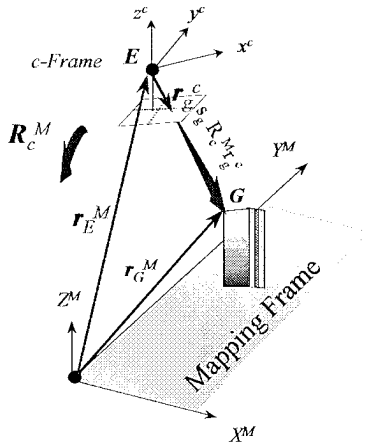


Figure 8. Image Georeferencing

In this context, a brief description on the subject is presented and the obtainable accuracy is introduced using theoretical and practical analysis. Certain Calibration aspects have to be dealt with to ensure successful map production with no aerotriangulation or ground control. Therefore, calibration will be briefly highlighted.

Digital Orthophoto Production Data Flow

As shown in Figure 9, a typical Orthophoto production project includes calibration, navigation data processing and image data processing. The calibration consists of imaging sensor calibration (e.g., a digital camera), boresight calibration, and lever arm calibration. The Earth-Fixed Earth-Centered (ECEF) position and orientation angles derived by POS/AV™, as shown in Figure 3, are compensated for the boresight and lever arm calibration parameters The trajectory parameters are then interpolated at the recorded camera events and transformed into the required local mapping frame (M-frame) using POSEO™. If the calibration parameters are not available, POSEO™ solves for them using the navigation and image data. This yields the exterior orientation (EO) parameters of each single image frame or scan line coordinatized in the local mapping frame (X, Y, Z, ω, ϕ, and κ). In a Softcopy, image data and exterior orientation data are processed either in single image mode or in stereo mode to produce ortho mosaics using either available DEMs or produced DEMs from stereo imagery, respectively.

Ground Accuracy From Theoretical Analysis

The necessary error models have been developed for two different cases of orthophoto production, namely, using either a single digital image or an image stereopair. Some assumptions have been made to account for different practical aspects. As an example of these theoretical studies, a specific case was studied which involved a digital camera of a 3k x 2K CCD chip and a 28 mm lens. This example is presented due to the availability of a real airborne data set to back up the theoretical analysis. Figure 10 depicts the horizontal DRMS theoretical accuracy (in left panel) and the height accuracy (in right panel) when using a stereo model of digital images for different Ground Sample Distance (GSD) when using POS/AV™ 210, 310, 410, and 510, respectively. Figure 11depicts the horizontal DRMS theoretical accuracy using a single digital image and 1 foot accuracy DEM (in left panel) and the horizontal DRMS theoretical accuracy using a 10 feet DEM (in right panel). Note that Figures 10 and 11 show the accuracy at image/model edge to represent worst case scenario. In practice, however, image points will not all be at image or model edge.

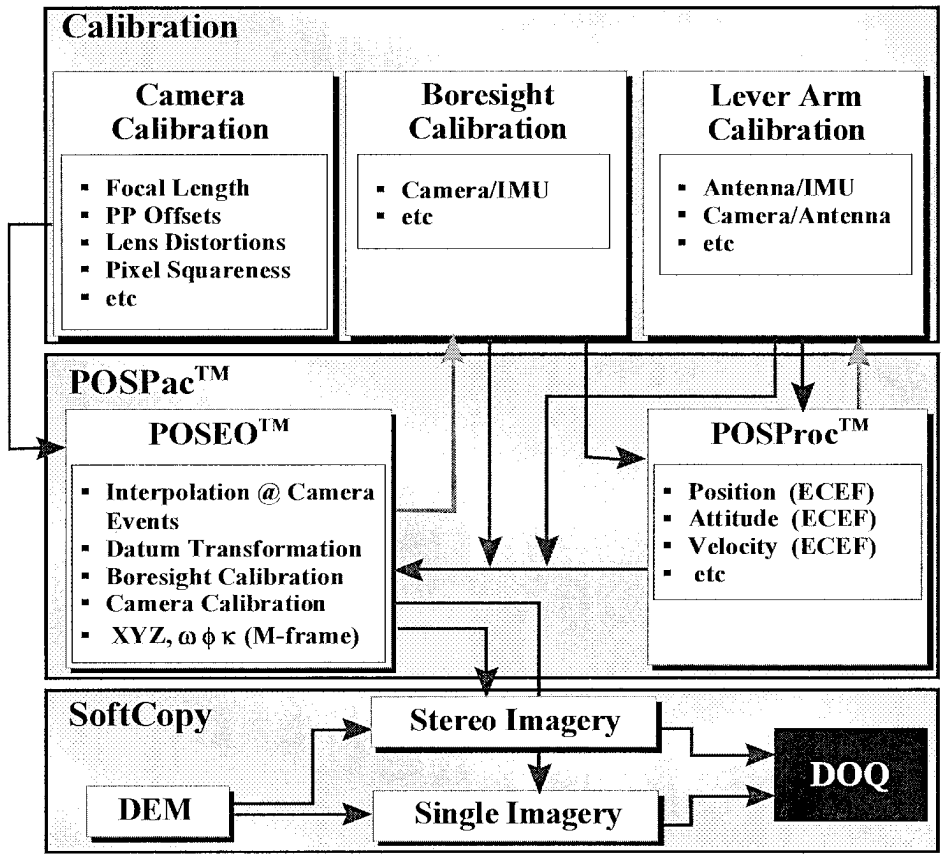


Figure 9. Digital Orthophoto Production Data Flow

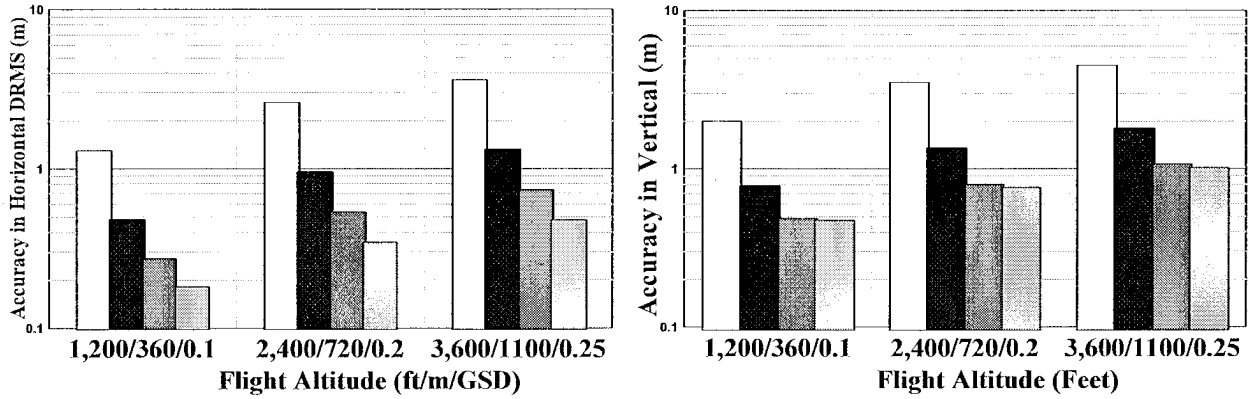


Figure 10. Ground Horizontal Accuracy (Left) and Height Accuracy (Right) Using a Stereo Model For a 3k x 2k Digital Camera Equipped with a 28 mm Lens

Ground Accuracy From Practical Analysis

A flight test data was collected using POS/AV 410 and a digital frame camera of 3k x 2k and 28 mm lens. The digital camera was calibrated to compute the focal length, the principal point offsets, and the lens distortion parameters. Boresight calibration took place to determine the misalignment angles between the IMU body frame and the image coordinate frame. The lever arms were calibrated using POSEO™ utilizing the measured lever arms

between the GPS antenna, the IMU center, and the camera lens perspective center. The airborne navigation data was processed in POSPac™.

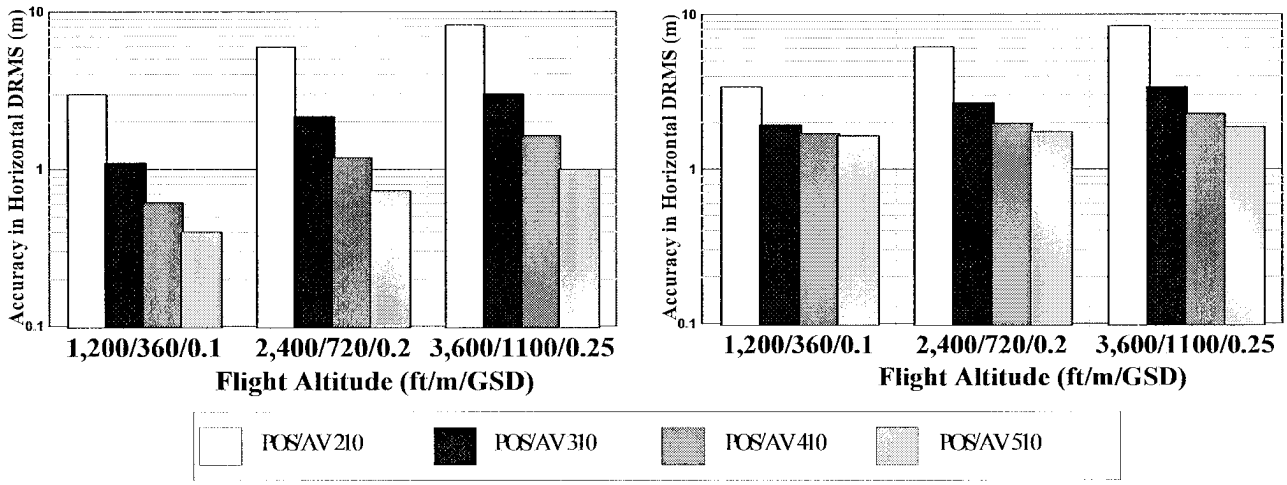


Figure 11. Ground Horizontal Accuracy Using a Single Digital Image + DEM For a 3k x 2k Digital Camera Equipped with a 28 mm Lens for a 1 ft DEM Accuracy (left) and for a 10 feet DEM Accuracy (right)

The image data together with POS data were used to compute the coordinates of the ground control points that appeared in different stereo models. A total of 20 models have been analyzed to account for different point location in the model. The POS-derived ground coordinates were then compared to the land-surveyed ones. The results are shown in Table 3.

SUMMARY AND OUTLOOK

In this paper, a brief description of direct georeferencing systems has been introduced through Applanix's POS systems. The basic concepts of inertial GPS integration have been described, along with the accuracy that can be achieved using such techniques.. Then the ground accuracy using POS integrated with a digital frame camera was analyzed. The results show that direct georeferencing can be used to obtain digital orthophotos to an accuracy that can meet many mapping or remote sensing requirements.

Ongoing research and analysis at Applanix include defining a standard procedure for quality control for fault detection and repair including but not limited to: boresight calibration residual errors, residual y-parallax, camera calibration errors.

Table 3. Ground Point Accuracy Derived by POS Compared to GCP Surveyed Reference

Model ID	*Easting (m)*	*Northing (m)*	*Horizontal (m)*	*Height (m)*
1	-0.08	0.10	0.13	-0.59
2	0.07	-0.10	0.12	-0.11
3	0.13	0.09	0.16	0.88
4	0.38	-0.18	0.42	-0.02
5	-0.24	0.01	0.24	0.71
6	-0.18	-0.32	0.37	-0.40
7	0.19	-0.08	0.20	0.00
8	-0.07	0.07	0.10	-0.45
9	-0.25	-0.05	0.25	0.34
10	0.06	0.20	0.21	-0.15
11	0.28	-0.10	0.30	0.28
12	0.13	-0.37	0.39	0.39
13	0.35	-0.20	0.40	-0.05
14	0.09	0.17	0.19	0.52
15	0.34	-0.02	0.34	1.34
16	-0.06	0.06	0.09	0.30
17	-0.21	0.15	0.25	-0.01
18	-0.04	-0.34	0.34	0.53
19	0.21	-0.10	0.24	0.03
20	-0.20	-0.11	0.23	-0.64
		Statistical Summary		
Min	-0.25	-0.37	0.09	-0.64
Max	0.38	0.20	0.42	1.34
Mean	0.04	-0.06	0.25	0.15
Std	0.21	0.17	0.10	0.50
RMS	0.21	0.18	0.27	0.52

REFERENCES

ASCE, 1996. Photogrammetric Mapping - Technical Engineering and Design Guides as Adapted from The US Army Corps of Engineers, No. 14, American Society of Civil Engineers Press.

FGDC, 1998, Geospatial Positioning Accuracy Standards, FGDC-STD-007.3-1998, Part 3: National Standard for Spatial Data Accuracy (NSSDA).

Fraser, C.S., 1997. Digital Camera Self Calibration, ISPRS Journal of Photogrammetry & Remote Sensing, 52(1997): 149-159.

Hutton, J., Savina, T., and Lithopoulos, L., 1997. Photogrammetric Applications of Applanix's Position and Orientation System (POS). ASPRS/MAPPS Softcopy Conference, Arlington, Virginia, July 27 - 30.

Merchant, D.C., 1982. Analytical Photogrammetry - Theory and Practice, Part II, Department of Geodetic Science and Surveying, The Ohio State University.

Moffit, F., and E.M. Mikhail, 1980. Photogrammetry, Harper and Row, Inc., New York, 648 p.

Mostafa, M.M.R., J. Hutton, and E. Lithopoulos, 2001. Direct Georeferencing of Frame Imagery - An Error Budget. Proceedings, The Third International Mobile Mapping Symposium, Cairo, Egypt, January 3-5.

Mostafa, M.M.R. and K.P. Schwarz, 2000. A Multi-Sensor System for Airborne Image Capture and Georeferencing. PE&RS, 66 (12): 1417-1424.

Reid, D.B., E. Lithopoulos, and J. Hutton, 1998. Position and Orientation System for Direct Georeferencing (POS/DG), Proceedings, Institute of Navigation 54th Annual Meeting, Denver, Colorado, USA, June 1-3, pp. 445-449.

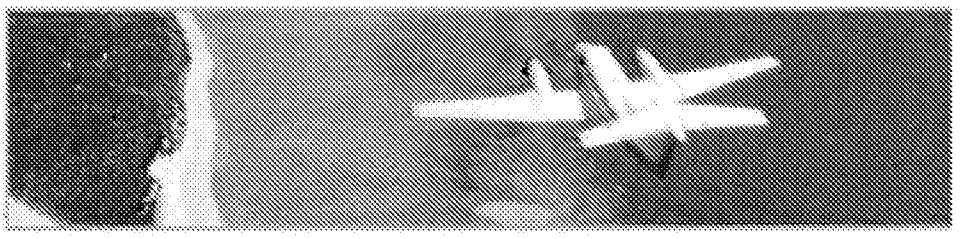
Scherzinger, B., 1997. A Position and Orientation Post-Processing Software Package for Inertial/GPS Integration (POSProc). Proceedings of the International Symposium on Kinematic Systems in Geodesy, Geomatics and Navigation (KISS 97), Banff, Canada, June 1997.

Schwarz, K.P., M.A. Chapman, M.E. Cannon, and P. Gong, 1993. An Integrated INS/GPS Approach to the Georeferencing of Remotely Sensed Data, PE& RS, 59(11): 1167-1674.

APPLANIX

POS AV

position & orientation system for airborne vehicles



POS AV - Airborne Vehicles

The Next Generation **- The POS AV is specifically designed for direct georeferencing of airborne sensor data. By integrating precision GPS with inertial technology, POS AV enables geospatial projects to be completed more efficiently, effectively, and economically. Supported by Applanix industry expertise and technological innovation, POS AV is engineered for aerial cameras, scanning lasers, imaging scanners, synthetic aperture radar, and LIDAR technology.**

DIRECT GEOREFERENCING

Compact, reliable, and a revolution in airborne surveying and mapping, directly georeferenced sensor data is generated with:

- An accurate solution for all motion variables
- Precise, image-specific Exterior Orientation parameters
- No requirement for aerotriangulation
- No requirement for a complete ground control survey (check points only required)

INCREASED PRODUCTIVITY AND ACCURACY

The next generation POS AV system is easily integrated with today's airborne sensors. Combined with the system's ability to geometrically correct and geographically encode sensor data, POS AV allows for:

- Increased savings in operational costs
- Increased savings in time
- Increased productivity
- Increased accuracy

UPGRADE STRATEGIES

A convenient upgrade path is available for current customers, including:

- IMU compatibility
- GPS card replacement
- Upgraded communications interface

Global Customer Support is available 24/7 with:

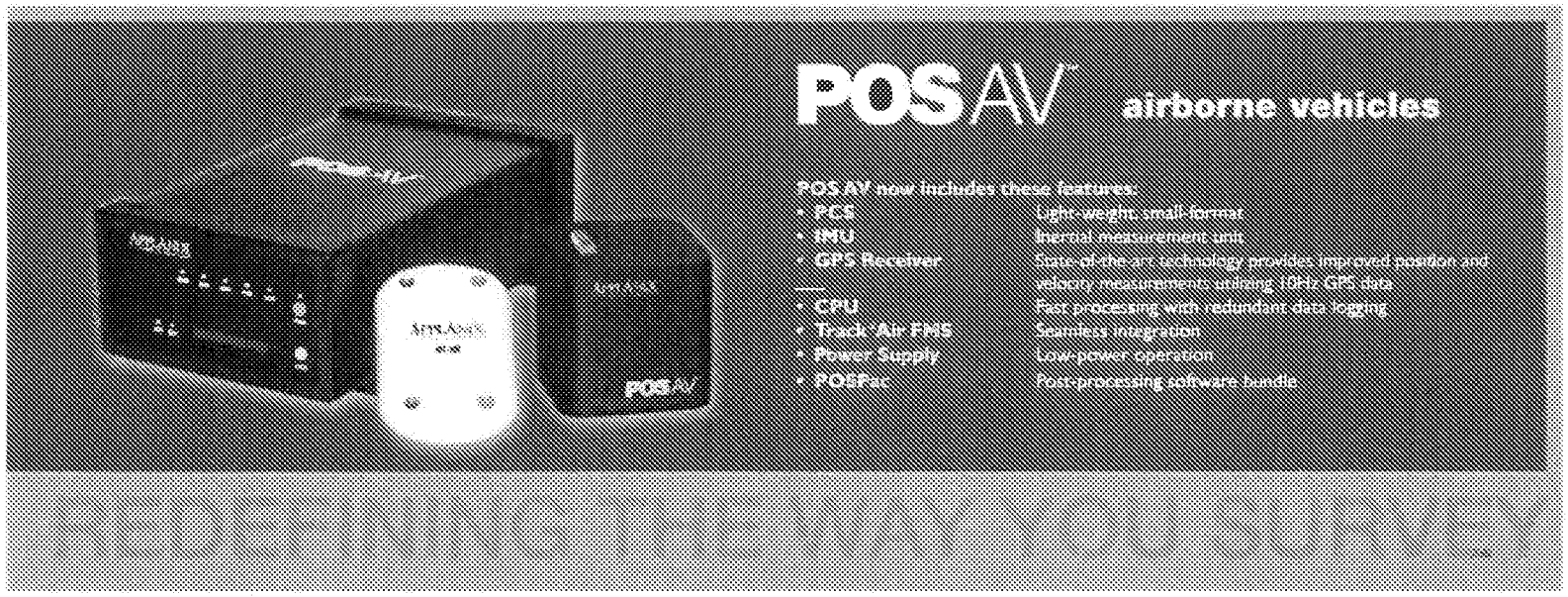
- Maintenance programs
- Integration support
- Extended warranties
- Full upgrade path
- Scalable options

STRENGTH BUILT ON EXPERIENCE

Applanix' engineering expertise and innovative technology solutions drive the largest user community in the airborne sensor market.

Applanix has priority access to state-of-the-art GPS technology, as part of the Trimble family's extensive experience and industry awareness.

Applanix' continued leading-edge status and dedicated customer service is assured.


POSAV
airborne vehicles
POS AV now includes these features:
• PCS
Light-weight, small-format
• IMU
Inertial measurement unit
• GPS Receiver
State-of-the-art technology provides improved position and velocity measurement, utilizing 10Hz GPS data
• CPU
Fast processing with redundant data logging
• Trask-Air FMS
Seamless integration
• Power Supply
Low-power operation
• POSPac
Post-processing software bundle
POS AV

Film Camera Applications

Client: AeroMap

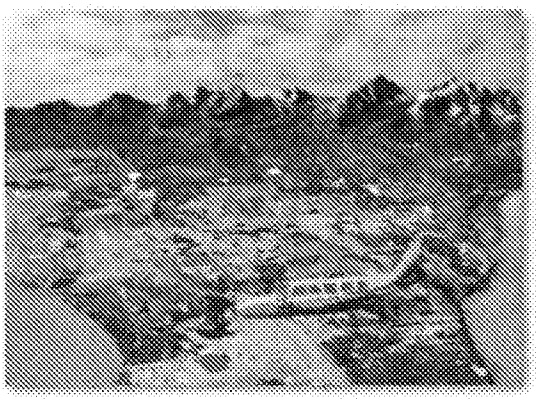
Film Camera Overview

Producing 23cm square, high-resolution color, color infrared, and B&W photography, aerial film cameras have been a standard within the industry for many years. Stable and robust, and now fitted with FMC, gyro-stabilized mounts, and various navigation and GPS subsystems, aerial film cameras are an efficient and complete photographic unit.

AeroMap U.S. is a division of Aero-Metric Inc., one of the largest photogrammetric companies in the United States. AeroMap is based in Anchorage, Alaska, and is a full-service Geographic Information and Mapping Sciences firm, with expertise in all areas of aerial survey, airborne remote sensing, and satellite image processing. AeroMap's clients include government agencies and private sector organizations which use airborne imagery for various applications, from environmental monitoring to engineering design work.

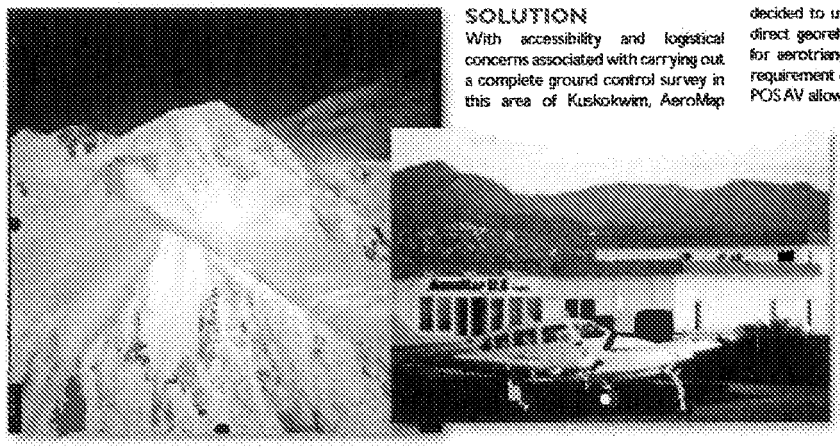
CHALLENGE

Faced with limited good flying weather and the rugged Alaskan environment, AeroMap was tasked with capturing color aerial photography for the Federal Bureau of Indian Affairs. The Class II Orthophotography project involved generating images for approximately 500 native allotments in the Calista Native Lands area of western Alaska. The allotments were scattered throughout the region, and could be as far apart as 200 miles or share a common boundary, and vary in size between 20 and 150 acres. "It was a difficult assignment in which to capture the images efficiently, so precise coordination was required," Dean Cimmiyotti explained. "As the orthophotos would be used to assess the timber stands in each allotment, positional accuracy was an important consideration, particularly as vector data was to be overlaid to show the individual property limits."



Film Camera Applications

Client: AeroMap



SOLUTION

With accessibility and logistical concerns associated with carrying out a complete ground control survey in this area of Kuskokwim, AeroMap decided to use their POS AV system to generate direct georeferenced imagery, eliminate the need for aerotriangulation, and easily meet the Class II requirement of 5' horizontal positioning. "Using the POS AV allowed us to fly single lines with as few as 3 or 4 images per allotment. To verify the accuracy of the georeferenced data we used a minimum amount of ground control as a QC check," said Cimmiyotti, "and it exceeded our expectations."

> "The POS AV system enabled us to complete this project very cost effectively because we could georeference our aerial imagery without surveying multiple ground control points."
>
> Dave Cimmiyotti, Project Manager, AeroMap U.S.

RESULT

The final georeferenced imagery was used to generate a Digital Elevation Model, which allowed the orthophotos to be produced quickly. Digital vector data, provided by the Bureau of Land Management, was then accurately overlaid to illustrate the individual allotment boundaries. Since incorporating the POS AV system into its workflow, AeroMap has found that increased productivity and additional accuracy are readily attainable under the difficult conditions encountered in Alaska, streamlining their airborne surveys into a precise and efficient operation.

Digital Frame Camera Applications

Client: 3001 Inc.

Digital Frame Camera Overview

Designed around CCD (Charged Coupled Device) imaging elements to ensure rigid image geometry, a digital frame camera has radiometric pixel resolution to generate standard perspective, high-resolution digital imagery. Producing four color channels in red, green, blue, and near-infrared, products can now be undertaken in low light conditions with excellent results.

3001 Inc. is an international spatial data corporation with offices located across the United States. Its geospatial expertise has been utilized in numerous projects throughout the Americas, providing technological leadership and innovative solutions to the engineering, surveying and geomatics community, with a dedicated team of aerial survey, GIS and photogrammetry professionals. Using leading-edge technology 3001 Inc. continues to harness the power of geospatial information in an everchanging world.



CHALLENGE

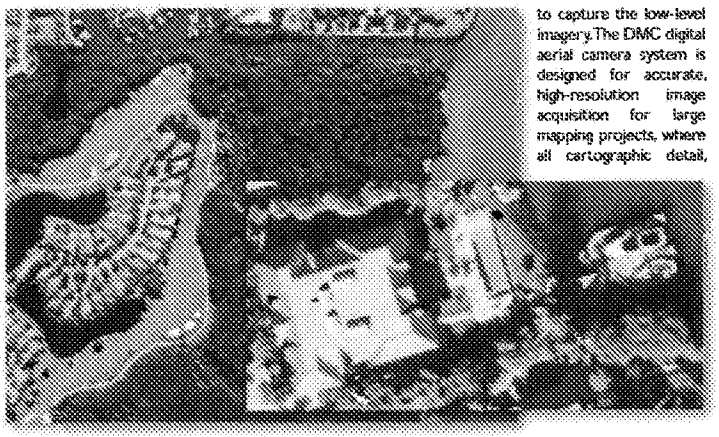
In December 2003, the company was tasked with providing a series of high resolution color digital images of Collier County in southwest Florida, as part of an on-going GIS update program involving digital orthophotography, stereocompilation, and planimetric mapping. Collier County is bordered on the west by the Gulf of Mexico, and five other counties to the north, east, and south. This portion of the project covered approximately 800 square miles of varied terrain, including large areas of swamp found along the coastal regions of western Florida. The digital imagery would be used to generate digital orthophotos and photogrammetric mapping data using stereoscopic image coverage. The final orthorectified imagery and vector mapping data would be input into the county's GIS system and accessible through the Collier County Property Appraiser's web site.

SOLUTION

To meet the project's specific requirements, 3001 Inc. used their Z/I Imaging DMC (Digital Mapping Camera) equipped with an Applanix POS AV integrated inertial position and orientation system,

Digital Frame Camera Applications

Client: 3001 Inc.



to capture the low-level imagery. The DMC digital aerial camera system is designed for accurate, high-resolution image acquisition for large mapping projects, where all cartographic detail, such as vegetation, transportation networks, hydrography, and buildings, can be clearly defined. It provides excellent visibility in areas of shadow and generates a bright, sharp image, ideal for this type of application.

RESULT

Within two weeks the flying portion of the project was completed, and image processing and data capture started. Flown at an altitude of 4500', the color digital imagery generated a 0.45' pixel size and a final delivery accuracy of 0.5' for the orthophotos. The company found the POS AV system enabled them to attain a tighter aerotriangulation result by utilizing its direct georeferencing capability in areas where image tie point matching was particularly difficult.

Greg Horrall explained. "There were areas along the coast that were completely covered in [illegible]. Identifiable ground features, such as small islands, were few and far between, so we took advantage of the POS AV direct georeferencing capability. By taking the exterior orientation parameters for the images covering those areas, and using them as part of the aerotriangulation adjustment, we were able to achieve a much more accurate result."

> "The POS AV system enabled us generate a more cost effective aerotriangulation adjustment in areas where it was most needed."
>
> Greg Horrall, Aerial Photogrammetric Specialist, 3001 Inc.

Using the POS AV-equipped DMC system, 3001 Inc. successfully completed the Collier County project, and provided positionally-accurate and highly-detailed digital imagery, ideally suited to the orthophotography and data update requirements.

LIDAR Applications

Client: MD Atlantic

LIDAR Overview

Light Detection And Ranging is the technology behind LIDAR, a system that uses rapid, high-intensity laser light, for the acquisition of Digital Terrain related information. It is a very effective tool for generating accurate topographic data over large areas of homogenous terrain.

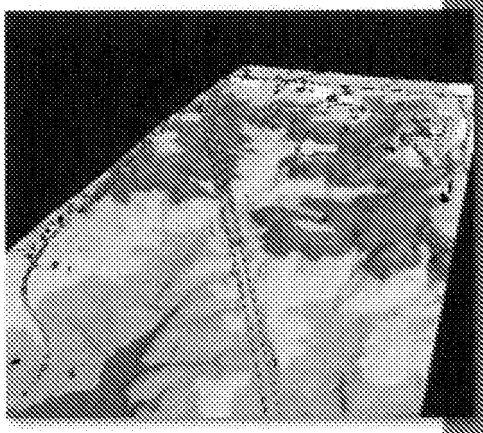
MD Atlantic Technologies is a leading supplier of geospatial information, digital aerial photography, photogrammetric mapping, airborne LIDAR data, and GIS database information. The organization provides geographic and spatial solutions to state and federal agencies, municipal governments, and the private sector. With a team of highly skilled professionals, MD Atlantic maintains its position as a leading-edge company at the forefront of the geospatial industry.

CHALLENGE

MD Atlantic was asked to undertake an extensive mapping project of Montgomery County, Alabama. A comprehensive dataset of geographic information was to be incorporated into the county's GIS system as part of its expanding GIS program. Planimetric and topographic data was required for an area covering approximately 790 square miles of rolling terrain, to include transportation networks, hydrographic features, and urban structures for all towns and cities, including Montgomery, the state capital. Color orthophotography was required together with a DTM (Digital Terrain Model), which would accurately define the topography of the county, and be used to generate 2' contour information.

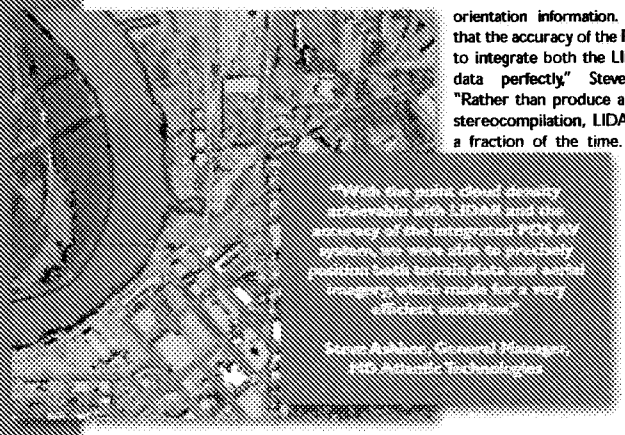
SOLUTION

To effectively complete the project, MD Atlantic's solution was to use two types of sensors to capture the information, an Optech 1210 LIDAR system, and a Leica RC30 aerial camera. Both technologies use integrated POS AV systems to generate sensor-specific position and



LIDAR Applications

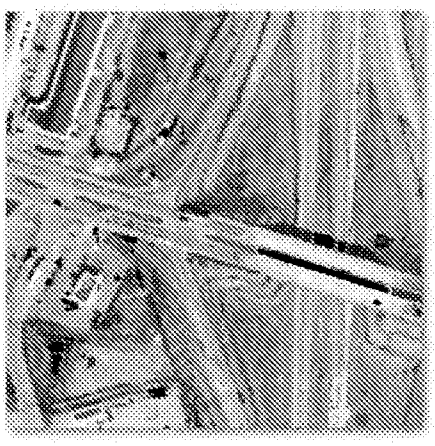
Client: MD Atlantic



orientation information. "We were confident that the accuracy of the POS AV would allow us to integrate both the LIDAR and the mapping data perfectly," Steve Ashbee explained. "Rather than produce a complete DTM using stereocompilation, LIDAR will generate it in a fraction of the time. We then supplement the LIDAR mass point data with breaklines, road edge and hydrographic features captured photogrammetrically from the aerial photo, to produce a very accurate and true depiction of the terrain."

RESULT

Flying at an altitude of 3,280' the elevation data was acquired very quickly, with overlapping parallel swaths generating accurate XYZ point cloud information ready for mission post-processing. The terrain data was easily integrated into the project workflow and the required contour information generated. Although the LIDAR data was captured independently of the aerial photography, the accuracy of the POS AV on both systems ensured the datasets were compatible, allowing the development of a highly accurate topographic model from which 2' contour information was developed.



Synthetic Aperture Radar Applications

Client: Orbisat

Synthetic Aperture Radar (SAR) remote sensing provides high resolution imagery using the long range, all-weather, day/night capabilities of radar and its ability to penetrate vegetation and soil surfaces. Airborne and satellite SAR systems are used for a wide variety of applications.

Orbisat da Amazônia is a leader in the application of Remote Sensing technology for use in mapping, geomatics, and geospatial information gathering. The company's expertise lies in its use of Interferometric Synthetic Aperture Radar (InSAR), which provides fast, accurate, and cost-effective solutions for the professional and scientific communities engaged in activities such as urban and regional planning, environmental analysis, and resource exploration and mapping.

CHALLENGE

The CartoSUR II project was established in Venezuela in 2003 as a national cartographic venture to acquire radar-based mapping data covering approximately 1/3 of the entire country. Located at the northernmost end of South America, Venezuela has a total area of 912,050 km². Included in the CartoSUR II project area was the state of Bolivar, which contains some of the oldest land forms in South America. The rugged mountains, steep cliffs, and plateaus, rise to over 3000 m in places, and contain one of the highest waterfalls in the world, Angel Falls. The terrain gradually flattens out and drops down to the Delta Amacuro on the east coast. Densely covered with forest and scored with tributaries of the Rio Orinoco, this whole region is often under thick cloud cover, and as such can be a very difficult area to map effectively.

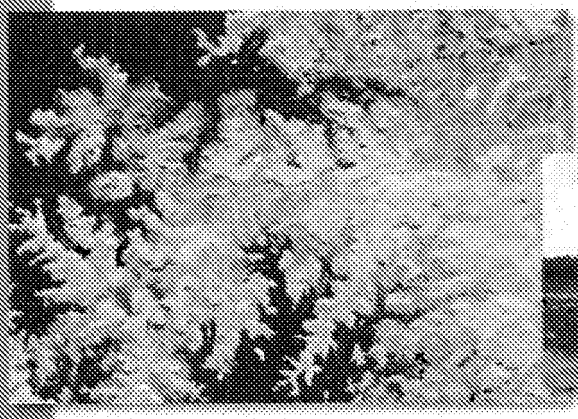
SOLUTION

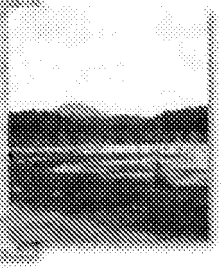
Orbisat immediately saw the solution to generating accurate cartographic data for this type of environment. The InSAR technology, with its all-weather operational capability, is unaffected by cloud, rain, poor visibility, and ground vegetation, and can very quickly produce accurate, detailed imagery, including digital terrain models. Installed aboard a Gulfstream Aerocommander aircraft, OrbiSAR-1 simultaneously uses two radar bands



Synthetic Aperture Radar Applications

Client: Orbisat





to generate image data, a result of the unique response of terrain and cultural targets to radar frequencies. The X-band reflects off surface objects such as trees, and buildings etc., to produce a Digital Surface Model, and the P-band reflects below the vegetation and produces a Digital Terrain Model.

RESULT

Within three months of starting the airborne operation, and 700hrs of air time, all image acquisition was completed. Flying at an altitude of 23,000', and using a dual pass for P-band interferometry with an 80 m baseline, the 3D imaging data was generated and made ready for processing. Dieter Leubeck, Project Manager, Orbisat, explained. "As well as providing position and orientation information for the radar imagery, the POS AV system also generates a real-time navigation solution that is incredibly accurate. We can fly a 120 km line and stay within a 1m horizontal variance quite easily. These attributes make the OrbiSAR-1 system extremely effective in undertaking radar mapping projects, and it's the POS AV that provides the spatial orientation accuracy." Final data delivery to the Geographical Institute of Venezuela Simon Bolivar (IGVSB) totaled 518 map sheets at a scale of 1:50,000, and covered an area of more than 263,000 km². Contour information was illustrated on the X-band orthoimage maps, and digital terrain model and full polarimetric P-band image data was made available for the complete project.

EarthData is a leader in the airborne imaging, mapping, and Geographic Information Systems (GIS) field. Its fleet of specially configured survey aircraft collects a variety of information about the Earth's surface, using aerial cameras and various types of airborne sensors. The company transforms the data into customized mapping and GIS products and services. For close to 50 years, EarthData's clients have used this geospatial information for design infrastructure, terrain modeling, transportation engineering and environmental research, to better understand the Earth and its resources.

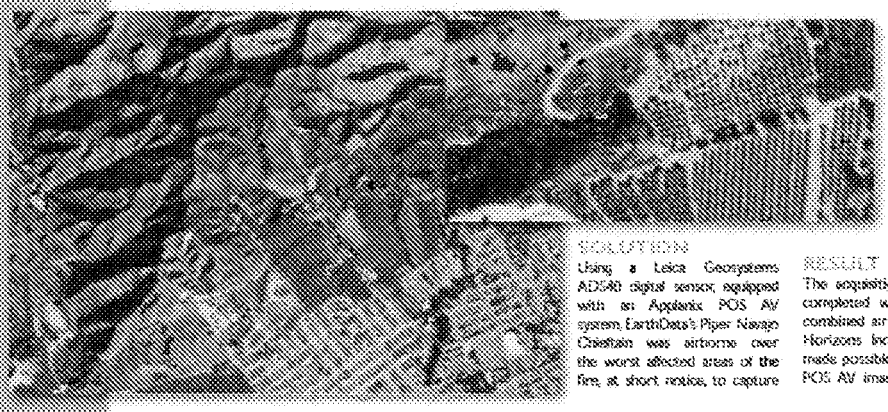
CHALLENGE

In October 2003, the State of California suffered one of the most devastating wildfires in its history. It caused extensive damage to property and the environment and posed a potential threat to the state's energy systems, which included transmission lines, major natural gas pipelines, and various oil refineries located in the immediate area. The fires were spread across more than 300,000 acres of land, with states of emergency being declared in Los Angeles, San Diego, Ventura and San Bernardino counties, where the authorities were battling fires on 10 separate fronts. EarthData, working in conjunction with ESRI and Horizons Inc., was tasked with generating accurate and detailed aerial imagery of the affected areas, to enable damage analysis to begin, in support of rapid response and recovery efforts.



Digital Scanner Applications

Client: EarthData



SOLUTION

Using a Leica Geosystems ADS40 digital sensor, equipped with an Applanix POS AV system, EarthData's Piper Navajo Chieftain was airborne over the worst affected areas of the fire, at short notice, to capture color-infrared imagery. Mitch Jorden, EarthData's project manager, explains, "The POS AV system integrates very well with our airborne sensors, and its direct georeferencing capability is a big plus, especially for emergency response operations such as this one, where there is no time to carry out ground control surveys. Accurate georeferenced digital images can be generated very quickly with this system."

RESULT

The acquisition of detailed digital imagery was completed within 14 days, as a result of the combined airborne operations of EarthData and Horizons Inc. The quick data turnaround was made possible with the ADS40 digital system and POS AV image georeferencing attributes, which together prove a very efficient combination. In total 3,143 square miles of severely burned terrain were captured and processed. With the image acquisition complete, state and local authorities were able to access the data immediately for use in damage assessment and recovery. Image analysis experts at ESRI used the digital orthophotography and corresponding DTM data to map the fire-damaged environment, and analyze the drainage patterns as a precaution against the potential risk of mudslides now that ground cover vegetation had been destroyed.

Direct Georeferencing Advantages

Direct Georeferencing is the direct measurement of image exterior orientation parameters, using a POS (Position & Orientation) system to enhance the functionality of an imaging sensor, such as an aerial camera (digital or film-based), multi-spectral or hyper-spectral scanner, or LIDAR. The POS serves as the georeferencing component and the sensor as the imaging component.

Raw positioning data generated by the POS, are processed together with camera (sensor) location measurements, to calculate accurate position and orientation values for each image. These are referred to as Exterior Orientation parameters.

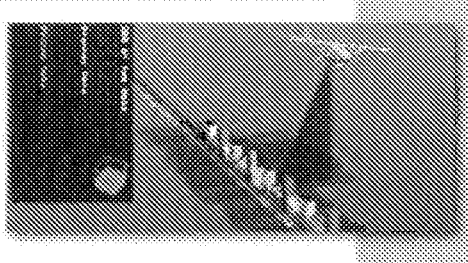
The Exterior Orientation parameters, together with the digital imagery, are input into a digital photogrammetric workstation, and data capture or image orthorectification performed.

THE ADVANTAGES OF DIRECT GEOREFERENCING:

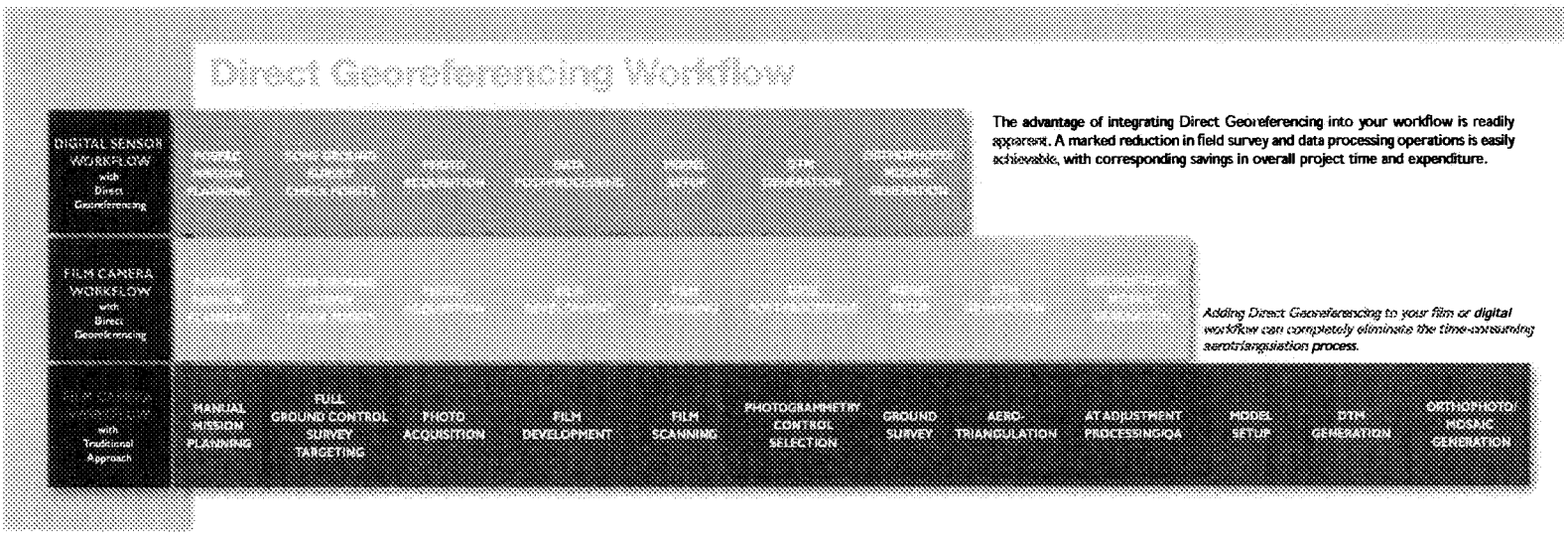
- The requirement for project wide tie-point matching and aerotriangulation (AT) can be drastically reduced or eliminated completely, resulting in enormous savings in data acquisition and processing time
- Limited ground control may be required only for quality control check point purposes, eliminating the need for a full ground survey
- Data workflow and quality control are streamlined and automatic
- Tight project deadlines are more achievable by eliminating extensive ground survey, and AT preparation/processing tasks

POS ASSISTED DIRECT GEOREFERENCING ALLOWS FOR:

- *Stereo Model Mapping* – typical photogrammetric model setup using a stereopair of photos or digital frame images used to determine 3D object point coordinates
  Advantages: reduction in time and cost – eg: projects involving medium-scale forested areas where point matching is difficult, georeferenced processing time is drastically reduced
- ***Single Photo Orthorectification*** – making use of currently available DTM data to generate accurate ground object position for digital orthophotos
  Advantage: stereo coverage unnecessary, fewer photos required, corresponding reduction in film/ scanning costs, short project turnaround times achievable



In addition to improving the productivity of more traditional aerial mapping applications, Direct Georeferencing is ideally suited to situations where ground control is simply not available, such as inhospitable environments, or in developing countries where ground surveys may be limited. It is also ideal for rapid mapping applications where ground control is not needed – in emergency situations such as forest fires and floods, or where environmental disasters have occurred, such as oil or chemical spills.


Direct Georeferencing Workflow
DIGITAL SENSOR WORKFLOW with Direct Georeferencing
FILM CAMERA WORKFLOW with Direct Georeferencing
FILM CAMERA WORKFLOW with Traditional Approach
MANUAL MISSION PLANNING
FULL GROUND CONTROL SURVEY TARGETING
PHOTO ACQUISITION
FILM DEVELOPMENT
FILM SCANNING
PHOTOGRAMMETRY CONTROL SELECTION
GROUND SURVEY
AERO TRIANGULATION
AT ADJUSTMENT PROCESSING/QA
MODEL SETUP
DTM GENERATION
ORTHOPHOTO MOSAIC GENERATION
The advantage of integrating Direct Georeferencing into your workflow is readily apparent. A marked reduction in field survey and data processing operations is easily achievable, with corresponding savings in overall project time and expenditure.
Adding Direct Georeferencing to your film or digital workflow can completely eliminate the time-consuming aerotriangulation process.

System Specifications

1. Performance - POS AV Absolute Accuracy Specifications (RMS):

	C/A GPS	DGPS	RTK	Post-Processed
	Model 310			
Position (m)	4.0 - 6.0	0.5 - 2	0.1 - 0.3	0.05 - 0.3
Velocity (m/s)	0.05	0.05	0.01	0.005
Roll & Pitch (deg)	0.02	0.02	0.02	0.015
True Heading[1] (deg)	0.10	0.08	0.07	0.035
	Model 410			
Position (m)	4.0 - 6.0	0.5 - 2	0.1 - 0.3	0.05 - 0.3
Velocity (m/s)	0.05	0.05	0.01	0.005
Roll & Pitch (deg)	0.015	0.015	0.015	0.008
True Heading[1] (deg)	0.08	0.05	0.04	0.015
	Model 510			
Position (m)	4.0 - 6.0	0.5 - 2	0.1 - 0.3	0.05 - 0.3
Velocity (m/s)	0.05	0.05	0.01	0.005
Roll & Pitch (deg)	0.008	0.008	0.008	0.005
True Heading[1] (deg)	0.07	0.05	0.04	0.008
	Model 610			
Position (m)	4.0 - 6.0	0.5 - 2.0	0.1 - 0.3	0.05 - 0.3
Velocity (m/s)	0.03	0.03	0.01	0.005
Roll & Pitch (deg)	0.005	0.005	0.005	0.0025[2]
True Heading[1] (deg)	0.030	0.030	0.020	0.0050

POS AV Relative Accuracy Specifications:

	Model 310	Model 410	Model 510	Model 610
Noise (deg/sec/√hr)[1]	0.15	0.07	0.02	0.005
Drift (deg/hr)[1]	0.5	0.5	0.1	< 0.01[3]

[1] *Typical random profile, root RMS error*
[2] *Attitude will drift as the vertical reference error defined by absolute accuracy in the table above*
[3] *Max remote local gravity model as shown full accuracy*
[4] *Drift (deg/hr), 1 sigma*

2. Sensors

	Model 310	Model 410	Model 510	Model 610
IMU	300 Hz High performance MEMS quartz gyros, accelerometers	300 Hz High performance MEMS quartz gyros, accelerometers	200 Hz High performance FOG gyros, silicon accelerometers	200 Hz High performance RLG gyros, quartz accelerometers
GPS	12 channel dual frequency (L1/L2), low noise, DGPS ready, 10 Hz raw data	12 channel dual frequency (L1/L2), low noise, DGPS ready, 10 Hz raw data	12 channel dual frequency (L1/L2), low noise, DGPS ready, 10 Hz raw data	12 channel dual frequency (L1/L2), low noise, DGPS ready, 10 Hz raw data

3. Physical - All Models PCS:

Temp Range:	-20 deg C to +55 deg C (Operational)
Size:	279 L x 165 W x 91 H mm (11.0L x 6.5 W x 3.6 H inches)
Weight:	3.90 kg
Power:	20-34 Volts DC - 30 W Max

System Specifications

Physical - IMU:

Model 310		Model 610	
Temp. Range:	-40 deg C to +71 deg C (Operational)	Temp. Range:	-40 deg C to +71 deg C (Operational)
Size:	105.4 L x 105.4 W x 106.8 H mm (4.15 L x 4.15 W x 4.21 H inches)	Size:	105.4 L x 105.4 W x 106.8 H mm (4.15 L x 4.15 W x 4.21 H inches)
Weight:	1.7 kg (with top-hat and plate)	Weight:	1.7 kg (with top-hat and plate)
Power:	20-34 Volts DC 48 W Max (supplied by PCS)	Power:	20-34 Volts DC 48 W Max (supplied by PCS)
Model 510		**Model 610**	
Temp. Range:	-54 deg C to +71 deg C (Operational)	Temp. Range:	-40 deg C to +70 deg C (Operational)
Size:	97 D x 86 H mm (3.8 D x 3.4 H inches)	Size:	163 L x 165 W x 163 H mm (6.4 L x 6.5 W x 6.4 H inches)
Weight:	1.00 kg (with top-hat and plate)	Weight:	14.49 kg
Power:	20-34 Volts DC 20 W Max (supplied by PCS)	Power:	20-34 Volts DC 28 W Max (supplied by PCS)

4. I/O

Ethernet (100 base-T)

Parameters	Time tag, status, position, attitude, velocity, track and speed, dynamics, performance metrics, raw IMU data (IMU rate), raw GPS data (10Hz)
Display Port	Low rate (1 Hz) UDP protocol output
Control Port	TCP/IP input for system commands
Primary Port	Real-time (up to IMU rate) TCP/IP protocol output
Secondary Port	Buffered TCP/IP protocol output for data logging to external device

Logging

Parameters	Time tag, status, position, attitude, velocity, track and speed, dynamics, performance metrics, raw IMU data (IMU rate), raw GPS data (10Hz)
Media	External Removable 1 Gbyte Flash Disk (2 supplied), Internal Embedded 1 Gbyte Flash Disk for redundant logging

RS232 NMEA ASCII Output

Parameters	NMEA Standard ASCII messages: Position ($INGGA), Heading ($INHDT), Track and Speed ($INVTG), Statistics ($INGST)
Rate	Up to 50 Hz (user selectable)

RS232 High Rate Binary Output

Parameters	User selectable binary messages: Time, position, attitude, speed, track, PAV30 output, Yaw Drift Correction,
Rate	Up to IMU rate (user selectable)

RS232 Input Interfaces

Parameter	Gimbal encoder input, AUX GPS Input (RTK, NavCom Starfire, OmniStar HP), RTCM104 DGPS Corrections Input
Rate	1 Hz to IMU rate

Other I/O

1PPS	1 pulse-per-second Time Sync output, normally high, active low pulse
Event Input (2)	Two time mark of external events. TTL pulses > 1 msec width, max rate 100 Hz.

5. User Supplied Equipment

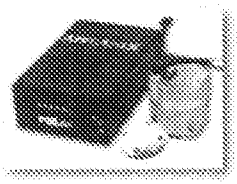
PC for POS Controller (Required for configuration)

- Pentium 90 processor (minimum)
- 16 MB RAM, 1 MB free disk space
- Ethernet adapter (RJ45 100 base-T)
- Windows 98/2000/NT/XP

PC for POSPac Post-processing Software

- Pentium III 800Mhz or equivalent (minimum)
- 256 MB RAM, 400 MB free disk space
- USB Port (for Security Key)
- Windows 2000/XP

OEM System Specifications



The POS AV system has been successfully integrated with a number of original equipment manufacturers producing various types of sensors for the aerial survey and remote sensing industry.

The OEM version of the new POS AV has been designed with OEM requirements in mind, and contains the following features to allow for a more flexible installation and operation process:

- Light weight, smaller format
- Remote power ON/OFF capability
- Non-removable PC card for internal data logging, or logging over the Ethernet to save power
- Designed to be used with OEM custom-manufactured cable systems

1. Physical

Temp. Range:	POS	-20 deg C. to +60 deg C
Size:	POS	239 L x 158 W x 82 H mm (9.4 L x 6.2 W x 3.2 H inches)
Weight:	POS	2.54 kg
Power:	20 - 34	Volts DC
	POS	25 W, Max (not including IMU)

2. General - Sensors

IMU	GPS
Model dependant	12 channel dual frequency (L1/L2), low noise, DGPS ready, 10 Hz raw data

3. I/O

Ethernet (100 base-T)

Parameters	Time tag, status, position, attitude, velocity, track and speed dynamics, performance metrics, raw IMU data (IMU rate), raw GPS data (10Hz)
Display Port	Low rate (1 Hz) UDP protocol output
Control Port	TCP/IP input for system commands
Primary Port	Real-time (up to IMU rate) TCP/IP protocol output
Secondary Port	Buffered TCP/IP protocol output for data logging to external device

Logging

Parameters	Time tag, status, position, attitude, velocity, track and speed, dynamics, performance metrics, raw IMU data (IMU rate), raw GPS data (10Hz)
Media	Embedded 1 Gbyte Flash Disk

RS232 NMEA ASCII Output

Parameters	NMEA Standard ASCII messages: Position ($INGGA), Heading ($INHDT), Track and Speed ($INVTG), Statistics ($INGST)
Rate	Up to 50 Hz (user selectable)

OEM System Specifications

RS232 High Rate Binary Output

Parameters	User selectable binary messages: Time, position, attitude, speed, track, PAV30 output, Yaw Drift Correction
Rate	Up to IMU rate (user selectable)

RS232 Input Interfaces

Parameter	Gimbal encoder input, AUX GPS input (RTK, NavCom Starfire, OmniStar HP), RTCM104 DGPS Corrections Input
Rate	1 Hz to IMU rate

Other I/O

1PPS	1 pulse-per-second Time Sync output, normally high, active low pulse
Event Input (2)	Time mark of external events. TTL pulses > 1 msec width, max rate 100 Hz
Remote Power	ON/OFF control via remote signal

4. User Supplied Equipment

PC for POS Controller (Required for configuration)

- Pentium 90 processor (minimum)
- 16 MB RAM, 1 MB free disk space
- Ethernet adapter (RJ45 10G base T)
- Windows 98/2000/NT/XP

PC for POSPac Post-processing Software

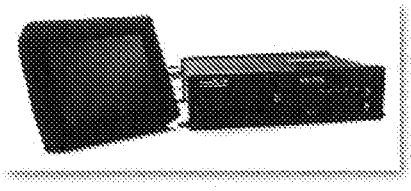
- Pentium III 800Mhz or equivalent (minimum)
- 256 MB RAM, 400 MB free disk space
- USB Port (For Security Key)
- Windows 2000/XP

POSTrack V5 Specifications

POSTrack
One Compact Solution

Combining the precision of POS AV Direct Georeferencing with the versatility of the Track'air XTRACK Flight Management System

POSTrack is the first fully integrated, real-time direct georeferencing and flight management system designed for the airborne geospatial community.
Purpose-built to reduce the costs associated with the preparation and implementation of airborne surveys, POSTrack minimizes mission planning and operational workload. Utilizing a combination of specifically developed software and hardware tools, the system combines the best of both technologies with all the functionality necessary to simplify and streamline today's aerial survey and remote sensing operations.



POSTrack incorporates the latest integrated inertial/GPS direct georeferencing technology from Applanix, with the Flight Management System (FMS) expertise of Track'air, the industry's leading FMS manufacturer. Unlike other IMU/GPS/FMS configurations, which utilize independent components for in-flight task automation and mission planning, POSTrack is engineered as a single system, compact, convenient, and easily installed on all types of aircraft without a complicated network of cables and connectors.

Compact, Simplified Cockpit Configuration
Configured to control and trigger various airborne sensors in addition to handling the GPS/IMU functions, POSTrack will ensure the highest levels of precision are maintained. The XTRACK component monitors the real-time position and orientation of the sensors computed by the POS AV, then instructs the system when to perform certain tasks. The in-flight automation enables exact flight path guidance and accurate sensor positioning, which translates into optimized airtime over the target area for the most economical and efficient mission capability.

With sensor-compatible interfaces, mission status display, flat panel pilot screen, and planning and reporting software, POSTrack is the ideal system for single-pilot or pilot/navigator crew configurations who want a streamlined, cost-effective airborne operation.

Complete Upgrade Path
As with all Applanix products, POSTrack has a clear upgrade path to ensure the system provides the best results and continued service.

POSTrack V5 Specifications

1. Physical

Computer System

Temp. Range:	-20 deg C to +55 deg C
Size:	279 L x 330 W x 91 H mm
Weight:	5.9 kg

Pilot Touch Screen Display

Temp. Range:	-10 deg C to +50 deg C
Size:	45 L x 215 W x 175 H mm
Weight:	1.34 kg
Power:	20 - 34 Volts DC, 110 W, Max (including IMU, GPS, pilot display)

2. I/O

Ethernet (100 base-T)

Parameters	Time tag, status, position, attitude, velocity,track and speed,dynamics, performance metrics, raw IMU data (200 - 300Hz), raw GPS data (10Hz)
Display Port Low rate	(1 Hz) UDP protocol output
Control Port	TCP/IP input for system commands
Primary Port	Real-time (up to 300 Hz) TCP/IP protocol output
Secondary Port	Buffered TCP/IP protocol output for data logging to external device

Logging

Parameters	Time tag, status, position, attitude, velocity, track and speed, dynamics, performance metrics, raw IMU data (200 - 300 Hz), raw GPS data (10Hz)
Media	External: Removable 1 Gbyte Flash Disk (2 supplied), Internal: Embedded 1 Gbyte Flash Disk for redundant logging

RS232 NMEA ASCII Output

Parameters	NMEA Standard ASCII messages: Position ($IHGGA), Heading ($IHHDT), Track and Speed ($IHVTG), Statistics ($INGST) Rate: Up to 50 Hz (user selectable)

RS232 High Rate Binary Output

Parameters	User selectable binary messages: Time, position, attitude, speed, track, PAV30 output, Yaw Drift Correction,
Rate	Up to 200 Hz (user selectable)

RS232 Input Interfaces

Parameter	Gimbal encoder input, AUX GPS Input, (RTK, NavCom Starfire, OmniStar HP), RTCM104 DGPS Corrections Input
Rate	1 to 200 Hz

Other I/O

1PPS	1 pulse-per-second Time Sync output, normally high, active low pulse
Event Input (2)	Time mark of external events TTL pulses > 1 usec width, max rate 100 Hz

4. Sensor Interfaces

3-axis Mount

Drift Correction	TAS (analog/ RS232), PAV30 (RS232), GSM3000(RS232) DSS Azimuth Mount (RS232)
Levelling Control	PAV30 (RS232), GSM3000 (RS232)
Gimbal Encoder	TAS (RS232), PAV30 (RS232), GSM3000 (RS232) DSS Azimuth Mount (RS232)
Stab. Control	GSM3000 (RS232)

Frame Cameras

Triggering/MEP	RC20/30, TOP RMK, LMK 2000,Vexcel UltraCam Generic
Data Interface	RC20/30 (RC20 w/o data annotation), TOP RMK, Vexcel UltraCam LMK2000 (requires additional interface module) Generic

LIDAR

Logging On/Off	ALS40/50, Riegl Q240

5. User Supplied Equipment

PC for POSPac Post-processing Software:

- Pentium III 800Mhz or equivalent (minimum)
- 256 MB RAM, 400 MB free disk space
- USB Port (For Security Key)
- Windows 2000/XP

Ground Accuracy from Directly Georeferenced Imagery

Investigating the accuracy of GPS/Inertial/Photogrammetry

By Dr. Mohamed Mostafa, Mr. Joseph Hutton, Mr. Erik Lithopoulos, Applanix Corporation

Reduction of the time and cost involved in photogrammetric mapping has been the subject of extensive research over the past two decades. The development of GPS-assisted aerotriangulation with minimal ground control was one of the important results of this research. The drawback of this technique is the lack of measuring image orientation information and, thus, "blocks" of images are always needed for solving for each photo's orientation in 3D space.

The Applanix's POS/AV™ system integrates GPS data with an Inertial Measurement Unit (IMU), which allows for measuring the camera exposure station position and image orientation angles for each single photo. Therefore, mapping may be done using a directly georeferenced photo steoreopair as the mapping element. This ultimately eliminates the aerotriangulation step from the mapping process. Using the POS/AV™ system, results in flexible configurations of imaging that may be used as image strips or small image blocks - a very common resource in mapping and forestry applications. In contrast, such applications cannot be attained when using GPS-assisted aerotriangulation, unless special GCP distribution is implemented, since image blocks with some geometry strength are always needed to compute image orientation.

This solution ultimately eliminates the aerotriangulation step

The POS/AV™ system has been widely used with most airborne imaging sensors. These include multispectral and hyperspectral scanners, LIDARs, Synthetic Aperture Radar (SAR), along with film and digital cameras. In this paper, a summary of a theoretical/practical study is presented. These investigations were carried out to evaluate the accuracy of positioning ground objects when using the POS/AV™ in conjunction with a frame digital or film camera. The accuracy specifications for the family of POS/AV™ systems are listed in Table 1.

Single Photo Case

In traditional photogrammetric mapping, the determination of the 3D position components of a ground object is done using photo stereopairs. This is the tried and tested way, to compute the point-based scale factor using the so-called 3D space intersection concept. However, if the scale is provided for each image point by an extra piece of measurement

Parameter Accuracy (RMS)	POS/AV™ 210	POS/AV™ 310	POS/AV™ 410	POS/AV™ 510
Position (m)	0.05 - 0.30	0.05 - 0.30	0.05 - 0.30	0.05 - 0.30
Velocity (m/s)	0.010	0.010	0.005	0.005
Roll & Pitch (Deg)	0.040	0.013	0.008	0.005
True Heading (Deg)	0.080	0.035	0.015	0.008

Table 1: Post-processed POS/AV navigation parameter accuracy

Published in GIM International Vol.14 N.12 December 2000

such as a laser range, processing a single photo would be faster and more cost-effective (although maybe less accurate).

Another possibility for processing single photos is by using an available Digital Elevation Model (DEM) of the mapped area. In this case, the computation of the height component of the ground object 3D position is mainly driven by the DEM and the 3D space intersection is done between one image and the DEM. This approach is an attractive option - especially for applications wherein the available or specially created DEM can be used along with digitally acquired images to produce digital orthophotos in a short time frame.

Typical DEM sources include existing topographic maps, aerial photography, and more recently LIDAR In the study at hand, this approach is simulated using error propagation techniques to analyse the theoretical accuracy of ground object positioning with the different POS/AV™ models. Figure 1 shows the ground point accuracy in horizontal (DRMS) for different POS/AV™ models and image scales. A 9" x 9" format camera, equipped with a 6" lens is used in this simulation. Image precision is taken as 5 mm. To emphasize the exterior orientation accuracy effect on ground positioning accuracy, the errors due to camera calibration, boresight calibration, and DEM are not considered.

Stereo Model Case

This case represents the classical 'model set-up' scenario, where a pair of photos or digital frame images can be used to determine the 3D object point coordinates using the space intersection concept. By using the

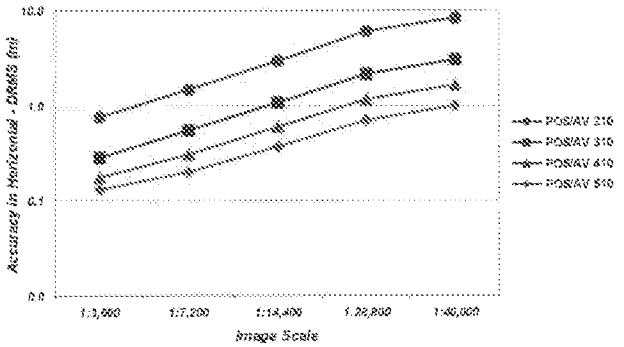


Figure 1: Ground horizontal accuracy (DRMS) - The Single Photo + DEM Case

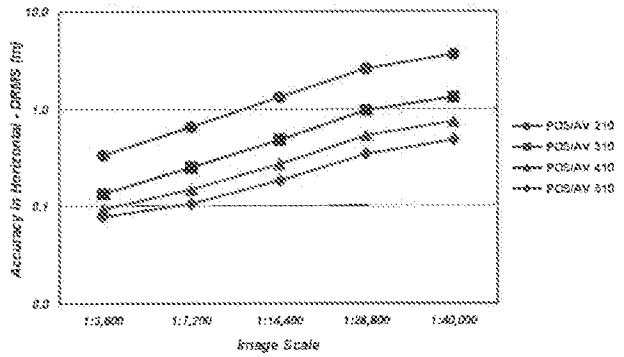


Figure 2: Ground horizontal accuracy (DRMS) - The Model Case

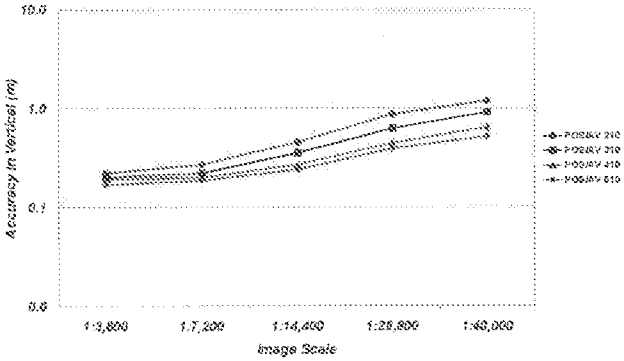


Figure 3: Ground object height accuracy - The Model Case

POS/AV™ data, the aerotriangulation step is bypassed. This results in immediate map production from the raw image data and post-processed POS/AV™ data. The result is a significant reduction in the time and cost for the mapping process. Using the standard error propagation techniques, the effect of GPS/IMU accuracy on ground positioning accuracy is studied. Figure 2 shows the ground point accuracy in horizontal (DRMS) for different POS/AV™ systems and for different image scales. Again, a 9" x 9" format camera equipped with a 6" lens and a 5 mm image precision is used in this simulation. To emphasize the exterior orientation accuracy effect on ground positioning accuracy, the errors due to camera calibration, and boresight calibration, are not considered in this study. Figure 3 shows the ground point height accuracy for different POS/AV™ systems and for different image scales.

In the stereo model case, the use of the entry-level POS/AV™ 210 and POS/AV™ 310 models would result in satisfying ground positioning accuracy for some applications. However, they may also produce a non-satisfactory y-parallax in the model that would make stereovision more difficult than if using a higher end system such as the POS/AV™ 410 or POS/AV™ 510. There is an ongoing study at Applanix, to provide the necessary knowledge for multi-sensor system design purposes.

As previously mentioned, some calibration issues have not been considered in the study presented herein. Two calibration parameters are important, namely, camera calibration and boresight calibration. The former is the determination of the camera interior geometry (principal point offsets and focal length) as well as lens distortion parameters, which are lab-calibrated. The latter is the orientation offset between the image coordinate system and the IMU coordinates system (which is done using a target ground field). Residual errors of these two calibration parameter sets should be kept to a minimum - usually by checking them on a regular basis, especially for the boresight.

Flight data was analyzed to confront the theoretical studies

Error Analysis of Flight Data

A flight data set was analyzed to confirm the theoretical studies presented in the aforementioned sections. HJW of Oakland, California, provided the image data, the precisely surveyed GCPs, and the GPS-assisted aerotriangulation reference. The Applanix POS/AV™ 510 system was used in this flight together with a Zeiss RMK Top camera. A 1: 6000 medium scale, four-strip flight (flown in opposite direction with minimum banking angles to avoid GPS cycle slips) resulted in a block of 4 strips of 11 images each (a 44-image block). A total of 27 well-distributed GCPs were included in the block. Using the POSPac™ post-processing package, a smoothed best estimate of the trajectory was produced. Then, the interpolated camera exposure station positions and image orientation angles at the moment of exposure were extracted for each photo from the trajectory coordinatized in the US state plane mapping frame using the POSEO™ package.

Comparing the camera station

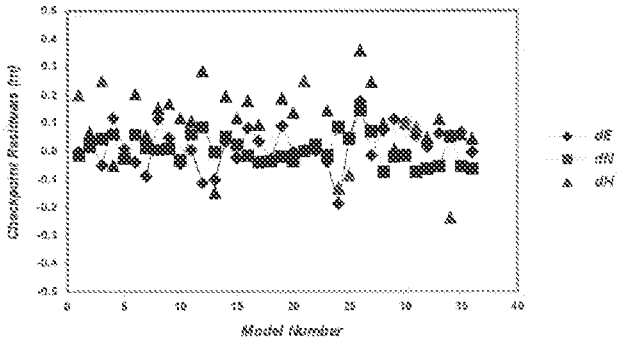


Figure 4: On-the-ground accuracy computed by comparing the coordinates derived from POS/AV 410 with the coordinates derived from land surveying

positions and image orientation produced independently by aerotriangulation and by the POS/AV™510, verified the POS/AV™ 510 system specifications listed in Table 1. The boresight was computed from processing the block without GCPs. The available GCPs were used as checkpoints. In this way the effect of boresight is canceled from the data, so that the practical error analysis could be compared to the theoretical one.

To determine the absolute accuracy of the direct georeferencing approach without GCPs, 36 models were processed individually using only one image point (with known ground coordinates) per model. In each model, the exterior orientation data derived by POS/AV™ were used along with the image point coordinates on both model photos, to determine the conjugate ground point position using the space intersection concept. The determined ground coordinates were then compared to the reference land-surveyed values. The checkpoint residuals are shown in Figure 4, while their statistics are depicted in Table 2. It is obvious from the checkpoint residuals that the accuracy of direct georeferencing using POS/AV™ 510 is similar to the theoretical accuracy presented in Figures 2 and 3 for the model case.

Min	-0.19	-0.08	-0.24
Max	0.18	0.14	0.36
Mean	*0.02*	*0.01*	*0.09*
Std. Dev.	0.07	0.05	0.13
RMS	0.08	0.05	0.16

Table 2: Statistics of checkpoint residuals

Conclusions

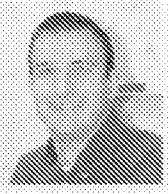
In this paper, a theoretical and a practical error analysis have been presented. The main objective of the theoretical error analysis is to present the POS/AV™ system accuracies in mapping terms. This has been done under variant conditions, for the different POS/AV™ systems, for various image scales and with dissimilar data acquisition/processing scenarios. The practical error analysis confirmed the validity of the theoretical one. The theoretical accuracy plots presented herein can be used for designing a multi-sensor system for data acquisition, such as a LIDAR/Digital camera system.

Acknowledgement

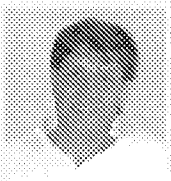
HJW, Oakland, California, is gratefully acknowledged for providing image data, precise GCP data, and AT reference for the analysis presented here.



Dr. Mohamed Mostafa obtained a Ph.D. in Geomatics Engineering from The University of Calgary in 1999. He is responsible for R&D in Airborne Applications at Applanix. He has worked extensively in the area of kinematic Geodesy and digital Photogrammetry.



Mr. Joseph Hutton obtained a Master of Applied Science in Aerospace Control from the University of Toronto in 1991. He has been with Applanix since 1991 as Product Manager if Airborne Applications. He has worked extensively in the area of inertial/GPS sensor integration for airborne survey and mapping applications



Mr. Erik Lithopoulos obtained a Master of Applied Science in Electrical Engineering from the University of Toronto in 1981. He is responsible for exploring and developing new markets for Applanix's GPS/Inertial products and technology. He has been with the company since 1991 as Manager of Business Development.

APPLANIX

Airborne Direct Georeferencing of Frame Imagery: An Error Budget

Mohamed M.R. Mostafa, Joseph Hutton, and Erik Lithopoulos
APPLANIX Corporation
85 Leek Cr., Richmond Hill
Ontario, Canada L4B 3B3
Phone: (905) 709-4600
E-mail: MMostafa@applanix.com

ABSTRACT

This paper presents an error analysis for the airborne direct georeferencing technique, where integrated GPS/IMU positioning and navigation systems are used in conjunction with aerial cameras for airborne mapping. The technical specifications for the Applanix POS/AV^{TM} family of airborne positioning and attitude determination systems are used in this study. Two cases are discussed herein, namely the standard stereo model case and the single photo case.

The first example is based upon standard map production - where the aerotriangulation step is ultimately bypassed when using the direct exterior orientation information, measured by the POS/AV^{TM} systems during image data acquisition. The second case is not as widely used, yet provides a more economical alternative. In this example, single photos are processed together with the available DEMs to produce orthorectified quads/images.

The effect of exterior orientation parameter accuracy on the ground point positioning accuracy is discussed in some detail. In addition to the theoretical analysis, an error breakdown is performed to an airborne set of data where the POS/AV^{TM} 510 system was used to directly georeference or to aid the georeferencing of the aerial frame imagery.

Finally, a comparison between the theoretical and practical investigations is presented. The results show that the use of POS/AV enables a variety of mapping products to be generated from airborne navigation and imagery data using ground control only for Q/A purposes.

Key words: Direct Georeferencing, Photogrammetry, Multi-Sensor Systems, GPS/INS.

1. INTRODUCTION

Image direct georeferencing is one of the most important topics currently considered in the photogrammetric mapping industry. Ultimately, the aerotriangulation step can be bypassed when using direct measurements for the exterior orientation parameters of each single image at the moment of camera exposure. Direct georeferencing therefore enables a variety of mapping products to be generated from airborne navigation and imagery data with minimal ground control, mainly used for Q/A.

The achievable, on-the-ground accuracy, of direct georeferencing is studied theoretically for specific applications such as low-cost digital camera systems for small scale mapping (c.f., Mostafa and Schwarz, 1999); or for quality digital cameras used in large scale mapping (c.f., Grejner-Brzezinska, 2000). A number of practical studies were also done for performance analysis purposes (c.f., Cramer et al, 1997; Lechner and Lahmann, 1995; Mostafa et al, 1998; Reid et al, 1998; and Škaloud et al, 1996).

Each of the aforementioned authors studied a specific scenario that implied specific digital/film image acquisition sensor and different GPS/Inertial integrated system configuration. Although, it gives quite a wide background on the subject, the common ground in these studies is the concept, rather than the achievable results, when using standard equipment to apply such a model.

In this paper, a summary of the results of theoretical and practical investigations is presented. The objective for conducting such investigations is to analyze the effect of the exterior orientation parameter accuracy on the ground object positioning accuracy, using standard sensors such as the Applanix POS/AV^{TM} systems and an aerial film camera with 9" x 9" format coupled to a 6" lens cone - such as that of the Zeiss or Leica products.

First, a summary of the theoretical error propagation results are presented. This is followed with an example of practical flight data. The presentation is therefore intended to show the *typically* achievable accuracies using theoretical and practical investigations and thus, the mathematical treatment is avoided.

2. THEORETICAL ANALYSIS

The standard error propagation technique is used to derive the ground object 3D positioning accuracy as a function of the exterior orientation parameter accuracy. Two cases are presented here.

In the first instance - referred to as The Single Photo Case – the result is a single directly georeferenced photo, that is used along with an available Digital Elevation Model (DEM). This produces an orthorectified image.

The second illustration - referred to as The Model Case - illustrates the typical photogrammetric photo stereo model that is used to do the mapping.

2.1. The Single Photo Case

The determination of ground object position using a single photo is currently done for two reasons. First, this approach makes use of the currently available quality DEMs - especially, those derived by LIDAR. Second, this approach provides a shorter turn-around-time to produce digital orthophotos - making use of the available POS/AV™ derived exterior orientation elements for each single photo.

In traditional photogrammetric mapping, the determination of the 3D position components of a ground object is done using photo stereopairs. This is executed in this way in order to compute the point-based scale factor, using the so-called 3D space intersection concept. However, if the scale factor is provided for each image point by an extra piece of measurement such as a laser range, processing a single photo would be faster and more cost-effective. The other possibility to process single photos is to use an available DEM of the mapped area.

In this model, the computation of the height component of the ground object 3D position is mainly driven by the DEM. Put another way, the image-based 3D space intersection is not needed anymore since the intersection occurs between image ray and the corresponding ground elevation.

To analyze the ground object positioning accuracy, a number of factors have to be considered. These factors are:

1. Exterior orientation accuracy;
2. Image coordinate measurement accuracy;
3. Calibration accuracy;
4. DEM accuracy.

The accuracy of the exterior orientation comes from post-processed accuracy specifications listed in Table 1 for the POS/AV™ 210, 310, 410, and 510, respectively. The POS/AV™ post-processed solutions are generated by the software package POSPac™. The GPS accuracy is assumed to be 0.10 m in the horizontal and 0.15 m in the vertical. Image coordinate measurement accuracy is taken as 5 μm.

The calibration of an integrated imaging/navigation system comes from the combination of individual sensor calibration and overall system calibration. The sensor calibration required for the camera is done in a lab environment, while the inertial sensor errors are calibrated in a closed-loop fashion using an optimal Kalman filter/smoother implemented by the POSPac™ package. The overall system calibration includes the antenna/camera/IMU lever arms and the IMU/camera boresight. In the investigations presented here, these are considered error-free. DEMs can typically be obtained from government organizations such as The US Geological Survey (USGS) or produced using LIDAR. In the simulation presented here, a 0.3 m, DEM accuracy derived by LIDAR, is assumed.

Figure 1 shows the horizontal accuracy (DRMS) of ground positioning for the family of POS/AV™ systems using different image scales. Note that the vertical axis of Figure 1 is logarithmic.

Table 1. Post-Processed POS/AV™ Navigation Parameter Accuracy

Parameter Accuracy (RMS)	POS/AV™ 210	POS/AV™ 310	POS/AV™ 410	POS/AV™ 510
Position (m)	0.05 - 0.30	0.05 - 0.30	0.05 - 0.30	0.05 - 0.30
Velocity (m/s)	0.01	0.01	0.005	0.005
Roll & Pitch (Deg)	0.04	0.013	0.008	0.005
True Heading (Deg)	0.08	0.035	0.015	0.008

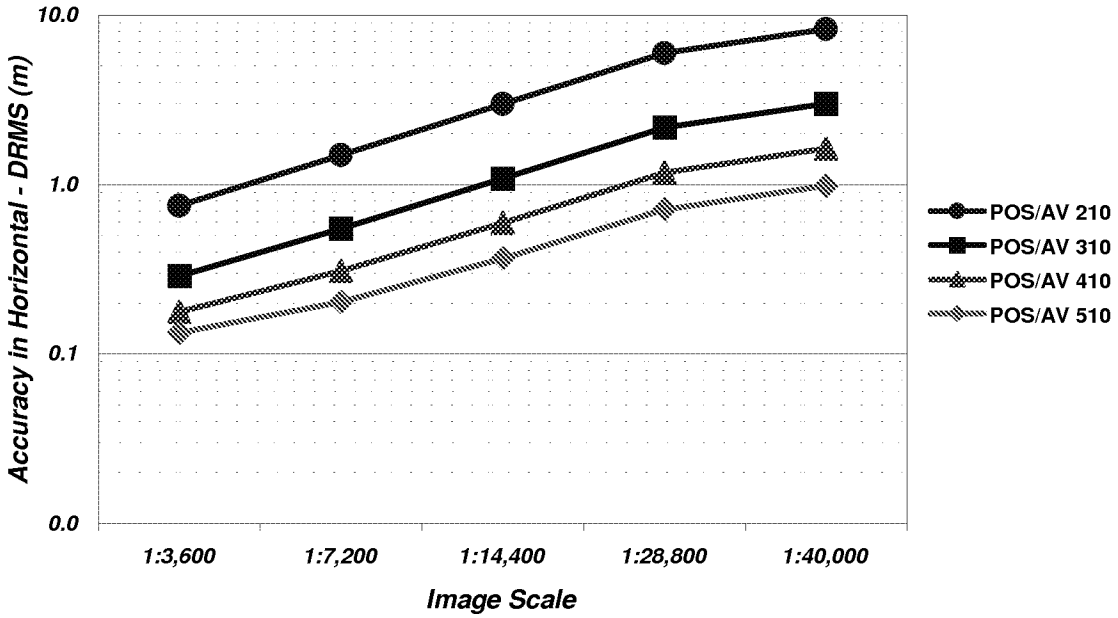


Figure 1. Ground Horizontal Precision (DRMS) – The Single Photo Case
0.3 m DEM Accuracy, 6" Lens Cone

A more detailed insight into the effect of exterior orientation accuracy on ground positioning accuracy can be attained, by isolating the error contributions for the individual positioning and attitude components. Therefore, the exterior orientation parameters are divided into 5 components, namely horizontal positioning accuracy (GPS-Hal), vertical positioning accuracy (GPS-Val) and the three attitude angles, namely roll, pitch and yaw (which represent the aircraft roll, pitch and yaw, respectively). The effect of each of these components on the ground positioning precision (S_Y) in the Y-component (across track) for the POS/AV™ 510, is demonstrated in Figures 2, 3, 4, 5, and 6, for image scales 1: 3,600, 1: 7,200, 1: 14,400, 1: 28,800, and 1: 40,000, respectively.

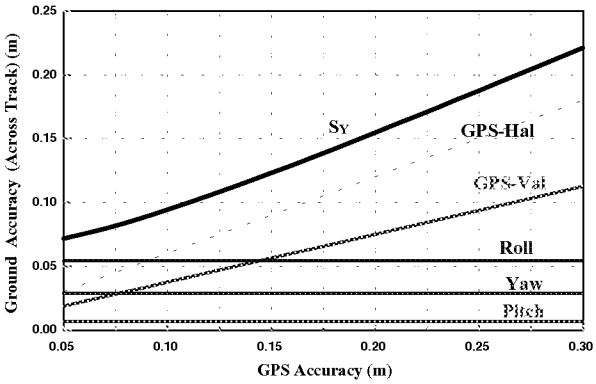


Figure 2. Ground Accuracy for 1:3,600 Photo Scale Vs. 3D GPS Accuracy Using POS/AV™ 510

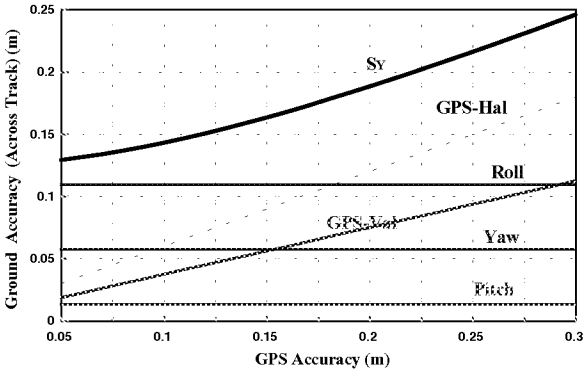


Figure 3. Ground Accuracy for 1:7,200 Photo Scale Vs. 3D GPS Accuracy Using POS/AV™ 510

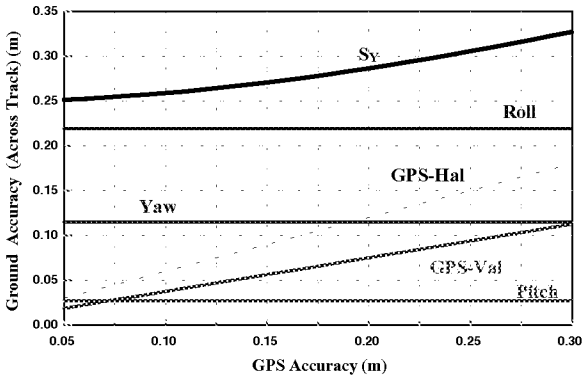


Figure 4. Ground Accuracy for 1:14,400 Photo Scale Vs. 3D GPS Accuracy Using POS/AV™ 510

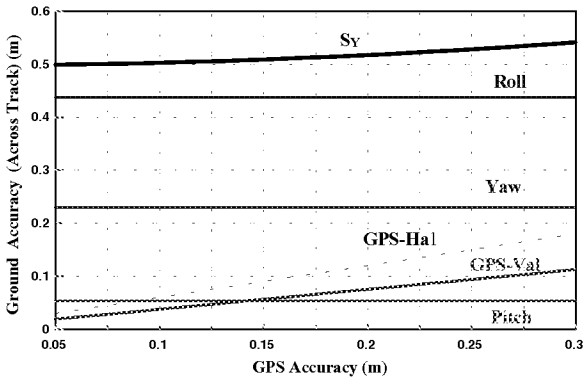


Figure 5. Ground Accuracy for 1:28,800 Photo Scale Vs. 3D GPS Accuracy Using POS/AV™ 510

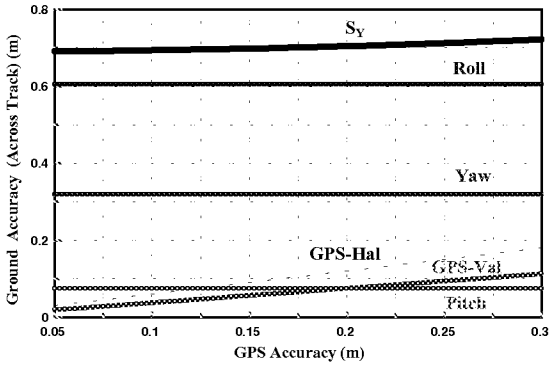


Figure 6. Ground Accuracy for 1:40,000 Photo Scale Vs. 3D GPS Accuracy Using POS/AV™ 510

Note that the accuracy of ground objects is mainly affected by the GPS accuracy for larger photo scales. Conversely, it is the attitude accuracy that influences the accuracy on the ground for the smaller photo scale. Consequently, the deterioration of the ground positioning precision is more for larger photo scale than for smaller photo scales - especially when the GPS accuracy deteriorates.

If the GPS accuracy deteriorates from 0.05 m to 0.3 m, the ground object positioning precision is more affected for larger photo scales than for smaller photo scales. For example, Table 2 shows the ground point positioning accuracy deterioration factor for different photo scales. This factor is computed by dividing the ground object positioning accuracy corresponding to GPS accuracy of 0.3 m by that corresponding to GPS accuracy of 0.05 m. It is obvious that the larger the photo scale, the more dominant the effect of the GPS positioning accuracy on the ground precision.

Table 2. Ground Accuracy Deterioration Due to GPS Accuracy Deterioration

POS/AV System	Image Scale	Across Track Ground Precision (S_Y)		Accuracy Deterioration Factor
		0.05 m (1Φ) GPS Accuracy	0.30 m (1Φ) GPS Accuracy	
POS/AV™ 510	1:3,600	0.07	0.22	**3.14**
	1:7,200	0.13	0.25	1.92
	1:14,400	0.25	0.33	1.32
	1:28,800	0.5	0.54	1.08
	1:40,000	0.69	0.72	1.04

2.2. The Model Case

This case represents the classical 'model set-up' scenario - a pair of photos or digital frame images can be used to determine the 3D object point coordinates using the space intersection concept. Using POS/AV™ data, the aerotriangulation step is bypassed. This results in immediate map production from raw image data and post-processed POS/AV™ data. Such an approach significantly reduces the time and cost of the mapping process.

Using the standard error propagation technique, the effect of exterior orientation accuracy on ground positioning accuracy is studied. The same assumptions made in Section 2.1 are made here. Figure 7 shows the ground point accuracy in horizontal (DRMS) for different POS/AV™ systems and for different image scales. Figure 8 shows the ground point height accuracy for different POS/AV™ systems and for different image scales.

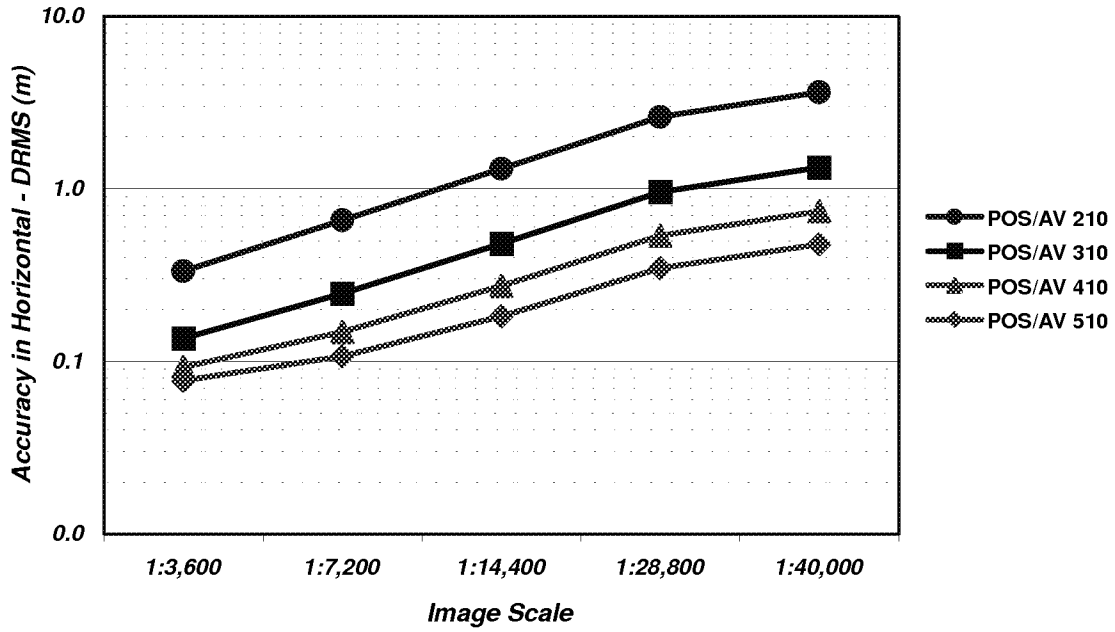


Figure 7. Ground Horizontal Accuracy (DRMS) - The Model Case - 6" Lens Cone

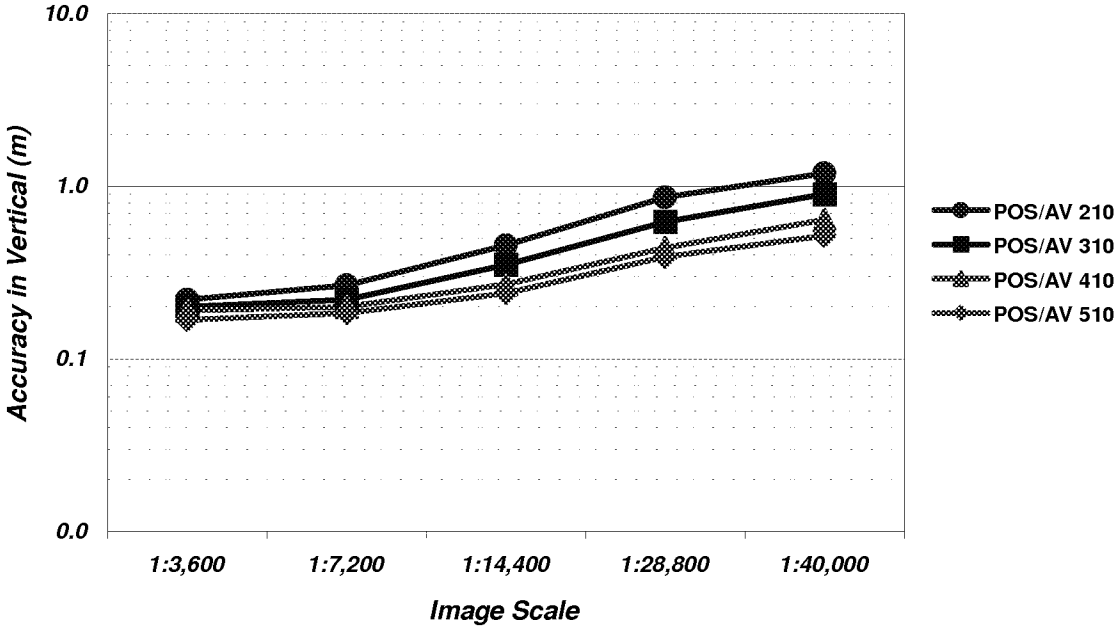


Figure 8. Ground Object Height Accuracy (RMS) - The Model Case - 6" Lens Cone

In the model case, the POS/AV^{TM} 210 and POS/AV^{TM} 310 satisfy the ground positioning accuracy for some applications. However, they may produce a non-satisfactory y-parallax in the model that would make stereovision more difficult than that when using a POS/AV^{TM} 410 or POS/AV^{TM} 510. This topic is the subject of an ongoing study at Applanix.